Eimeria falciformis Infection of Mouse Cells Identifies Host Determinants of Parasite Development

Dissertation

zur Erlangung des akademischen Grades

doctor rerum naturalium

(Dr. rer. nat.)

im Fach Biologie

eingereicht an der

Mathematisch-Naturwissenschaftlichen Fakultät I

der Humboldt-Universität zu Berlin

von Diplom-Biologin Manuela Schmid

Präsident der Humboldt-Universität zu Berlin

Prof. Dr. Jan-Hendrik Olbertz

Dekan der Mathematisch-Naturwissenschaftlichen Fakultät I

Prof. Stefan Hecht, PhD

Gutachter/in:

1. Prof. Dr. Richard Lucius
2. Prof. Dr. Kai Matuschewski
3. Prof. Dr. Susanne Hartmann

Tag der mündlichen Prüfung: 26.06.2014

Acknowledgements

First, I would like to thank my supervisor Dr. Nishith Gupta for his continuous guidance and motivation during my thesis.

I am also very thankful to Prof. Richard Lucius for his support and for the opportunity to perform my doctoral project at the Department of Molecular Parasitology.

I would like to express my deepest gratitude to my former colleagues. Especially, I would like to thank Grit, Vera, Anne, Simone, Jörg and Emanuel for their scientific and technical support, and also for creating a wonderful working environment. Special thanks also to Gabi Drescher and Dr. Maik Lehmann for their research assistance with electron microscopy. Furthermore a dziękuję bardzo to Emilia for her never-ending moral support during our coffee breaks. Thanks to all of you. I will never forget this time!

I would also like to acknowledge the contribution of the collaborators to this work. I thank Dr. Hans-Joachim Mollenkopf and Ina Wagner at the MPI for Infection Biology for their technical supervision towards the microarray experiments. Special thanks to Prof. Kai Matuschewski, Carolin Nahar and Manuel Rauch for the opportunity to gain the insight into another research field. I also thank Prof. Christoph Loddenkemper and Simone Spieckermann for their contributions to immunohistochemical work.

Moreover, I would also like to thank Prof. Richard Lucius, Prof. Susanne Hartmann and Prof. Kai Matuschewski for agreeing to review this thesis and Prof. Ann Ehrenhofer-Murray and Prof. Benedikt Kaufer for being part of my dissertation committee.

I am deeply grateful to the organizers of the MDC-PhD program and to the ZIBI graduate school for the financial and scientific support. It was a real pleasure to be part of these institutions.

Finally, I would like to thank my family. First and foremost, I would like to thank my mother for taking care of my little princess. This thesis would not have been possible without your help!

Abstract

Eimeria falciformis is a highly host- and tissue-specific parasite of murine caecum epithelium. Its monoxenous life cycle in a well-investigated host makes it an excellent model to examine parasite-host interactions during all apicomplexan stages. To identify the host determinants of the parasite infection, this work involved the comparative *in vitro* and *in vivo* analyses of mouse gene modulation by *E. falciformis* and experimental validation. Besides, gene expression studies of *T. gondii*-infected cells were used for comparative purposes.

The *in vitro* microarray data suggest the modulation of 1239 and 1145 transcripts during an *E. falciformis* and *T. gondii* infection of YAMC cells, respectively. Cluster analyses indicate these genes to be involved in multiple biological processes including gene expression, cell signaling and immune response. The immediate early transcription factor FBJ osteosarcoma oncogene (c-FOS) was induced upon early as well as during late *E. falciformis* and *T. gondii* infection. C-FOS is part of the activator protein 1 (AP-1) complex, which controls the transcription of genes involved in pro-inflammatory responses, cell proliferation, apoptosis and differentiation. We show that infection of c-FOS-deficient mouse cells results in an impaired development of *Eimeria* and *T. gondii*, highlighting an exploitation of the host transcription factor by apicomplexan parasites.

Our *ex vivo* gene expression analyses using the parasite mouse caecum cells revealed the modulation of 206 and 2297 transcripts within 24 h and 144 h of natural *Eimeria* infection, respectively. The most prominent mouse genes induced during the onset of asexual and sexual parasite cycle include IFN-γ-regulated factors *e.g.*, immunity-related GTPases, guanylate-binding proteins, chemokines and several enzymes of the kynurenine pathway including indoleamine 2,3-dioxygenase 1 (IDO1). IDO1 mRNA, induced 36- and 51-fold at 24 and 144 h post-infection, was one of the most up-regulated epithelial transcripts. IDO1 is the first and rate-limiting enzyme of tryptophan catabolism in the kynurenine pathway. Induction of IDO1 supposedly depletes tryptophan in host cells, which is proposed to inhibit the *in vitro* growth of pathogens auxotrophic for this essential amino acid. We show that *E. falciformis* induces IDO1 in the epithelial cells in an IFN-γ-dependent manner, and the enzyme expression remains induced during the entire infection of the parasite. The absence or inhibition of IDO1, or of two downstream enzymes of the kynurenine pathway in the mouse impairs parasite growth. Likewise, the oocyst output was impaired in IFN-γR$^{-/-}$ mice. The reduced parasite yield is not due to a lack of an immunosuppressive effect of IDO1 in the parasitized IDO1$^{-/-}$ or

inhibitor-treated mice because they exhibit a normal Th1 and IFN-γ response. Noticeably, the parasite development was entirely rescued by xanthurenic acid, a by-product of tryptophan catabolism. These data demonstrate contrasting roles of IFN-γ signaling and a conceptual subversion of the host defense (IFN-γ, IDO1) by an intracellular pathogen for progression of its natural life cycle.

Zusammenfassung

Eimeria falciformis ist ein Wirts- und Gewebe-spezifischer Parasit, welcher das Blinddarmepithel der Maus befällt. Aufgrund des monoxenen Lebenszyklus in einem exzellent-erforschten Wirt, bietet sich *E. falciformis* als Modellorganismus an, um Wirts-Parasit-Interaktionen in verschiedenen Stadien der Entwicklung von Apicomplexa-Parasiten zu untersuchen. Im Rahmen dieser Arbeit wurden Genexpressionsanalysen bei *E. falciformis*-infizierten Zellen und Mäusen durchgeführt, um wichtige Wirtsfaktoren der Infektion zu identifizieren. Zudem wurden für vergleichende Zwecke Transkriptomanalysen bei *T. gondii*-infizierten Zellen vorgenommen.

Nach Auswertung der Microarray-Daten infizierter Wirtszellen (YAMC, *in vitro*) zeigte sich, dass eine Infektion mit *E. falciformis* oder *T. gondii* die Expression von 1239 bzw. 1145 Transkripten änderte. Alle regulierten Gene wurden in funktionellen Klassen zusammengefasst und beinhalten Gruppen, deren Transkripte eine wichtige Rolle in der Genexpression, Kommunikation zwischen Zellen und der Immunantwort spielen. Besonders bemerkenswert ist die erhöhte Expression des Transkriptionsfaktors c-FOS (FBJ osteosarcoma oncogene) während der Infektion mit *E. falciformis* als auch *T. gondii*. C-FOS ist ein Bestandteil des AP-1 (activator protein 1) Komplexes, welcher die Transkription zahlreicher Gene der Immunantwort, Proliferation, Differenzierung und Apoptosis steuert. Unsere Ergebnisse zeigen, dass die Entwicklung von *E. falciformis* und *T. gondii* in c-FOS$^{-/-}$ Zellen beeinträchtigt ist. Diese Beobachtung betont eine mögliche Ausbeutung des Transkriptionsfaktors des Wirtes durch die Apicomplexa-Parasiten.

Eine Infektion der Maus mit *E. falciformis* für 24 bzw. 144 Stunden (*ex vivo*) betraf die Expression von 206 bzw. 2297 Transkripten. Darunter befinden sich einige Gene, welche durch IFN-γ reguliert werden (z.B. Guanylat-bindende Proteine und Chemokine). Auch das Enzym Indoleamine 2,3-dioxygenase (IDO1) wird IFN-γ abhängig exprimiert und war in den infizierten Zellen induziert (36- bzw. 51-fach nach 24 und 144 Stunden). IDO1 ist ein Enzym des Kynurenin-Stoffwechselweges, und katalysiert die erste und geschwindigkeits-bestimmende Reaktion des Tryptophan-Abbaus. Aufgrund des IDO1-induzierten Katabolismus der essentiellen Aminosäure wurde beschrieben, dass die Expression von IDO1 auf das Wachstum auxotropher Pathogene *in vitro* schädigend wirkt. Wir zeigen in dieser Studie, dass in den *E. falciformis*-infizierten Epithelzellen IDO1 IFN-γ abhängig induziert wird. Das Enzym wird darüber hinaus während des gesamten parasitären Lebenszyklus

exprimiert. Das Wachstum des Parasiten war zudem beeinträchtigt in IDO1$^{-/-}$ Mäusen sowie in Mäusen, in welchen IDO1 als auch zwei weiterer Enzyme des Kynurenin Stoffwechselweges pharmakologisch inhibiert wurden. Diese Mäuse zeigten eine normale Th1 und IFN-γ Antwort, womit ein immun-supprimierender Effekt von IDO1 nahezu ausgeschlossen werden kann. Bemerkenswerterweise konnte das Parasitenwachstum in IDO1$^{-/-}$ Mäusen durch Gabe von Xanthurensäure, welche ein Nebenprodukt des Tryptophan-Abbaus ist, auf Wildtyp-Niveau angehoben werden. Diese Daten demonstrieren, dass sich der intrazelluläre Parasit *E. falciformis* die wirtseigenen Verteidigungsmechanismen (IFN-γ, IDO1) für seine eigene Entwicklung zu Nutze macht.

Table of Contents

List of Abbreviations

AP-1	Activator protein 1
CD	Cluster of differentiation
DIC	Differential interference contrast
CLR	C-type lectin receptor
C_t	Threshold cycle
DAPI	4’,6-diamidino-2-phenylindole
DC	Dendritic cell
DHFR-TS	Dihydrofolate reductase thymidylate synthase
DMEM	Dulbecco’s modified eagle medium
EGR	Early growth response
FCS	Fetal calf serum
FOS	FBJ (Finkel–Biskis–Jinkins) osteosarcoma oncogenes
GPI	Glycosylphosphatidylinositol
HAAO	3-hydroxyanthranilate dioxygenase
HFF	Human foreskin fibroblast
HPF	High power field
IDO	Indoleamine 2,3-dioxygenase
IFN-γ	Interferon gamma
IHC	Immunohistochemistry
IL	Interleukin
iNOS	Inducible nitric oxide synthase
i.p.	intraperitoneal
IPA	Ingenuity pathway analyses
IRG	Immunity-related GTPase
JAK	Janus kinase
JUN	Jun oncogene
KAT	Kynurenine aminotransferase
KMO	Kynurenine 3-hydroxylase
KYNU	Kynureninase
MAPK	Mitogen-activated protein kinase
MLN	Mesenteric lymph node
MODE-K	Murine duodenal epithelial cell clone K

MOI	Multiplicity of infection
1-MT	1-methyl tryptophan
NaOCl	Sodium hypochloride
NF-κB	Nuclear factor kappa B
NLR	(NOD)-like receptor
NK	Natural killer
NO	Nitric oxide
NOD	Nucleotide-binding oligomerization domain
ORF	Open reading frame
PAMP	Pathogen-associated molecular patterns
p. i.	Post-infection
PRR	Pattern recognition receptor
PV	Parasitophorous vacuole
PVM	Parasitophorous vacuole membrane
qPCR	Quantitative PCR
RBC	Red blood cells
RFP	Red fluorescent protein
Ro61-8048	3,4-dimethoxy-N-[4-(3-nitrophenyl)thiazol-2-yl]-benzenesulfonamide
ROP	Rhoptry protein
RPMI 1640	Roswell Park Memorial Institute medium 1640
rRNA	Ribosomal RNA
RT	Room temperature
SEM	Standard error of the mean
(S)-ESBA	((S)-(4-Ethylsulfonyl)benzoylalanine hydrochloride
SOZ	Sporulated oocyst
STAT	Signal-transducer and activator of transcription protein
TCA	Tricarboxylic acid cycle
TGF-β	Transforming growth factor beta
Th	Helper T cell
TLR	Toll-like receptor
TNF-α	Tumor necrosis factor alpha
U	Units
VERO	Green Monkey kidney cell line
wt	Wild type

XA	Xanthurenic acid
YAMC	Young adult mouse colonic epithelial cell
YFP	Yellow fluorescent protein

1. Introduction

1.1 Apicomplexan parasites

The protozoan phylum apicomplexa consists of more than 5000 species (1), mostly all of which are obligate intracellular parasites. The phylum includes several pathogens of clinical and veterinary importance, such as *Toxoplasma*, *Plasmodium*, *Cryptosporidium*, *Eimeria*, *Babesia*, *Theileria* and *Sarcocystis*. The apicomplexan parasites are classified by a similar fashion of replication and share common morphological features (Fig. 1).

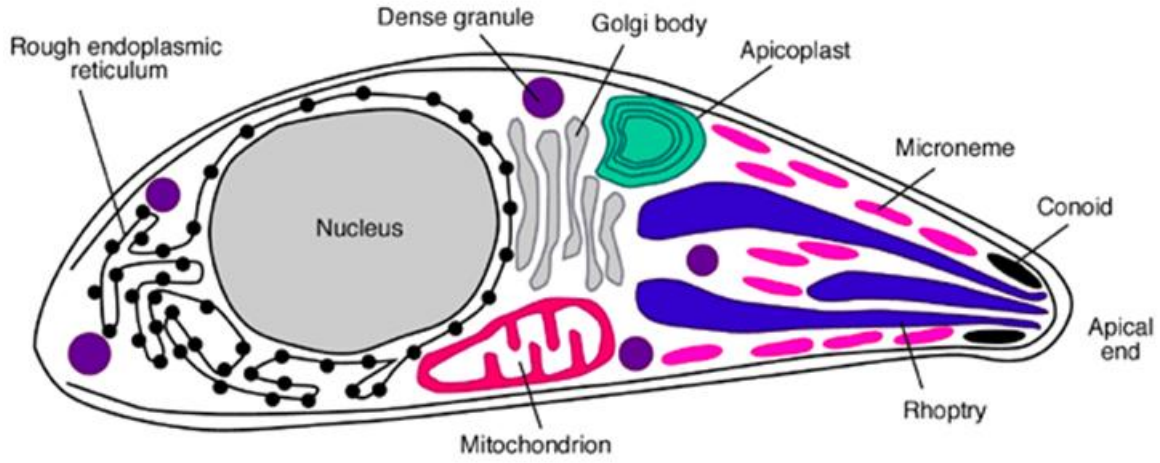

Fig. 1: Morphology of apicomplexan parasites. The archetypical eukaryotic organelles nucleus, Golgi body, endoplasmic reticulum, mitochondrion and apicoplast are displayed. The three secretory organelles, micronemes, rhoptries and dense granules are responsible for successful invasion and formation of the parasitophorous vacuole. The picture is adapted from (2)

The anatomical hallmark of these unicellular organisms is the apical complex at their anterior end, a structure composed of unique secretory (micronemes, rhoptries) and structural elements (apical polar ring, conoid). During the active process of host cell invasion, the contents of the secretory organelles are released (3), form a moving junction and lead to the formation of the parasitophorous vacuole (PV) (4). The cone-shaped conoid (5), not present in *Plasmodium* and *Theileria* (6), is surrounded by polar rings composed of microtubules and is thought to mechanically support the invasion process (7). Furthermore, contents of the rhoptries together with the dense granules are capable to reprogram host cell functions (8). Another distinctive feature of most apicomplexan parasites is the presence of the apicoplast, even if not present in *Cryptosporidium* (9), a parasite which eventually secondarily lost this plastid. The apicoplast is a specialized non-photosynthetic chloroplast relict involved in the synthesis of fatty acid, isoprenoids and heme (10). It is derived by secondary endosymbiosis of red alga (11).

This study focuses on exploring interactions between *Eimeria falciformis* and its host, the mouse. Two other apicomplexan parasites, *T. gondii* and *P. berghei*, were used for comparative purpose. Therefore, all these parasites are introduced below.

1.1.1 The genus *Eimeria*

1.1.1.1 Veterinary importance

Parasites of the genus *Eimeria* infect several animals including chicken, rabbits, goats, sheep and cattle. These parasites cause coccidiosis in the infected animals, which is a disease of the intestinal tract leading to hemorrhagic diarrhea, reduced food and water uptake, lethargy and eventually to death. Especially in the poultry industry, *Eimeria* infections impose the loss of more than 1 billion US dollars per year (12) for treatment, prevention and prophylaxis. Several vaccination strategies to prevent or attenuate the infection in chickens are available. Because infections with small doses of parasites generate only a mild coccidiosis with subsequent species-specific immunity to re-infection (13, 14), young chicken can be infected with a small dosage of *Eimeria* oocysts (15). Furthermore, vaccines containing attenuated strains of the seven chicken-infecting parasite species have been developed and applied to protect against infection (16). Other efforts include immunization with irradiation-killed parasites (17) and the use of monoclonal antibodies against selected *Eimeria* proteins (18). However, the use of anticoccidial drugs in the diet is still favored, because of more expensive vaccination treatments (19).

1.1.1.2 Parasite culture and manipulation

The main problem in the field of *Eimeria* research is the lack of an efficient *in vitro* culture system. *Eimeria* parasites successfully invade primary as well as immortal cell lines *in vitro*; however, the *in vitro* development is interrupted during the asexual stages. Although the entire life cycle of *E. tenella* could be reproduced using primary kidney cells of chickens (PCKC), the development and oocyst yield are extremely limited (20). Furthermore, oocysts were only occasionally obtained by infection of bovine fetal gastrointestinal cells (BFGC) with *E. bovis*, an *Eimeria* species of cattle. Among the murine *Eimeria* species, *E. falciformis* has been shown to invade different cell types including MODE-K (21), HFFs and VERO cells (22). Culture in these cell lines allowed only a minor development into schizonts of the first or second generation with no progression to the sexual stages. Also the rat parasite, *E. nieschulzi*, can be cultured *in vitro* up to the second merozoite generation in VERO or IEC6 (rat intestinal

epithelial cells) cells (23). Similar results were obtained with *E. vermiformis* infection of bovine kidney cells (24). Hence, the lack of an efficient *in vitro* culture complicates the development of genetic manipulation tools. A transfection system has been developed for *E. tenella* with successful expression of a bacterial reporter gene, β-galactosidase (25), as well as fluorescent proteins, YFP and RFP (26). In both cases, the transfected sporozoites developed only into schizonts of the first generation with merozoites still expressing the foreign proteins. Shi *et al.* were able to further develop a transfection system with parasites expressing the YFP as a reporter gene in all life cycle stages *in vitro* including fluorescent oocysts (27). However, propagation of fluorescent oocysts in chickens was not successful. Finally Clark *et al.* (2008) reported the establishment of stably transfected *E. tenella* parasites (28). The transfected sporozoites harbored plasmids containing a fluorescence marker (YFP) and dihydrofolate reductase thymidylate synthase from *T. gondii* (*Tg*DHFR-TS), which confers resistance to pyrimethamine. The transfected sporozoites were inoculated into the ileocaecal opening of chickens *via* the cloaca, pyrimethamine was applied in the diet and oocysts from the feces were collected. YFP-positive oocysts were sorted by FACS and propagated, which resulted in more than 95% fluorescent oocysts after five to six passages in chickens (28, 29). In the experiments carried out in rodent *Eimeria* species *e.g.*, *E. nieschulzi* and *E. falciformis*, the regulatory sequences of *E. tenella* were used to drive expression of the reporter gene (22, 23). Reporter genes were successfully expressed *in vitro* up to the second merozoite generation in *E. nieschulzi* and the application of transfected sporozoites to rats, resulted in YFP-expressing oocysts (23). Similar results were obtained in experiments with the murine parasite, *E. falciformis*. Rectally applied YFP and DHFR-TS co-expressing sporozoites led to the excretion of fluorescent oocysts, even though with much poor oocyst yield (22).

1.1.1.3 The life cycle of *Eimeria falciformis*

The model organism used in this study, *E. falciformis*, is a parasite exclusively infecting the mouse (Fig. 2). Its monoxenous life cycle initiates with the ingestion of sporulated oocysts, harboring 4 sporocysts each with 2 sporozoites. Enzymatic activities in the stomach and the small intestine lead to the digestion of the oocyst and sporocyst walls and the release of the sporozoites (30). These infective stages specifically invade the crypt epithelial cells of the caecum and the upper half of the colon (31, 32), round up to form trophozoites, which develop into schizonts and merozoites of the first generation. Merozoites infect neighboring epithelial cells for additional rounds of asexual development (schizogony). The development of sexual stages (gamogony), micro- and macrogametocytes, occurs after three to four cycles

of schizogony. The sexual stages fuse to form the diploid zygote, which differentiates into an unsporulated oocyst. After a prepatent period of 6 to 7 days, oocysts are shed with the feces predominantly between the day 8 and 10. The unsporulated oocysts sporulate to form infectious oocysts within 3 to 5 days (31, 32). The symptoms of an *E. falciformis* infection *e.g.*, weight loss, are most prominent on the peak days of oocyst shedding. Once the infection is retracted, the animals recover completely and develop a life-long immunity against the parasite (33). The severity of pathology depends on the number of inoculated oocysts (34) and varies amongst different mouse strains (35).

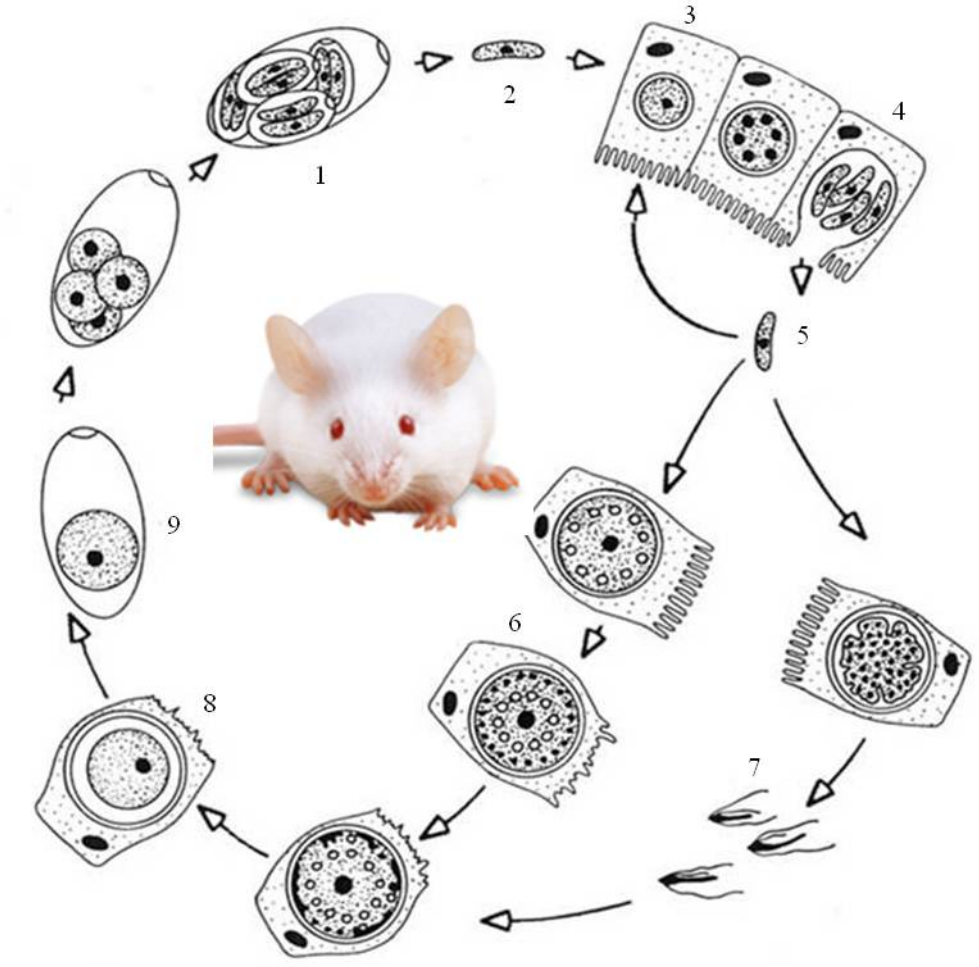

Fig. 2: The life cycle of *E. falciformis*. The ingestions of the sporulated oocysts (1) results in the release of sporozoites (2), which invade intestinal epithelial cells of the caecum and form trophozoites (3). Several rounds of asexual replication produce schizonts (4) harboring merozoites (5). Following 3-4 rounds of schizogony, merozoites (5) develop into macro- (6) and microgametes (7) which fuse to form the zygote (8). The unsporulated oocysts (9) are shed into the environment, where sporulation takes place. Figure is adapted from (36)

The site of *E. falciformis* development resembles to *E. tenella* infection of chicken. Thus, *E. falciformis* can be used as a model to study avian coccidiosis. Moreover, the life cycle of *E.*

falciformis in a well established host organism makes this parasite a decent model for investigating the *in vivo* parasite-host interaction.

1.1.2 *Toxoplasma gondii* and *Plasmodium berghei*

1.1.2.1 The biology of *Toxoplasma gondii*

Unlike other apicomplexans, *T. gondii* can invade and replicate within every nucleated cell. Thus, *T. gondii* is considered one of the most successful parasites on earth (37). Its life cycle includes an asexual phase in the intermediate hosts, which can be any warm-blooded animal, and a sexual reproduction in one of any feline species (Fig. 3). An infection begins with the ingestion of sporulated oocysts harboring two sporocysts, each with four sporozoites. Upon ingestion, sporozoites form tachyzoites, which cause tissue lysis and disseminate throughout the body. Tachyzoites then differentiate into bradyzoites, slow replicating forms, which persist in cysts. The sexual phase starts with the ingestion of an infected intermediate host by a cat. Bradyzoites are released from tissue cysts and invade epithelial cells of the gut followed by the production of merozoites, which differentiate into micro- and macrogametocytes. A fusion of the micro- and macrogametes produce zygotes and then unsporulated oocysts. Sporulation initiates after shedding of the oocysts into the environment. Humans get infected by oral ingestion of either oocysts by contaminated food, or meat harboring the tissue cysts. The global sero-prevalence varies across the world with around 23% in the USA (38) and 20-80% in Europe (39). The disease toxoplasmosis, caused by the rapidly replicating tachyzoites, is often asymptomatic or produces mild flu-like symptoms. In many cases however, a reactivation of bradyzoites within the tissue cysts especially in the brain in immune-compromised humans (*e.g.* AIDS) can lead to death. Also the pregnant women acquiring a primary infection may transmit the parasites to the developing fetus leading to abortion or cognitive deficits in neonates.

The asexual forms of *T. gondii* can be propagated *in vitro*. Moreover, the parasite is accessible to gene manipulation (40) using a variety of selection markers (41, 42). Thus, *T. gondii* have become a widely used model organism to study the biology of apicomplexan parasites and free living protozoans (43).

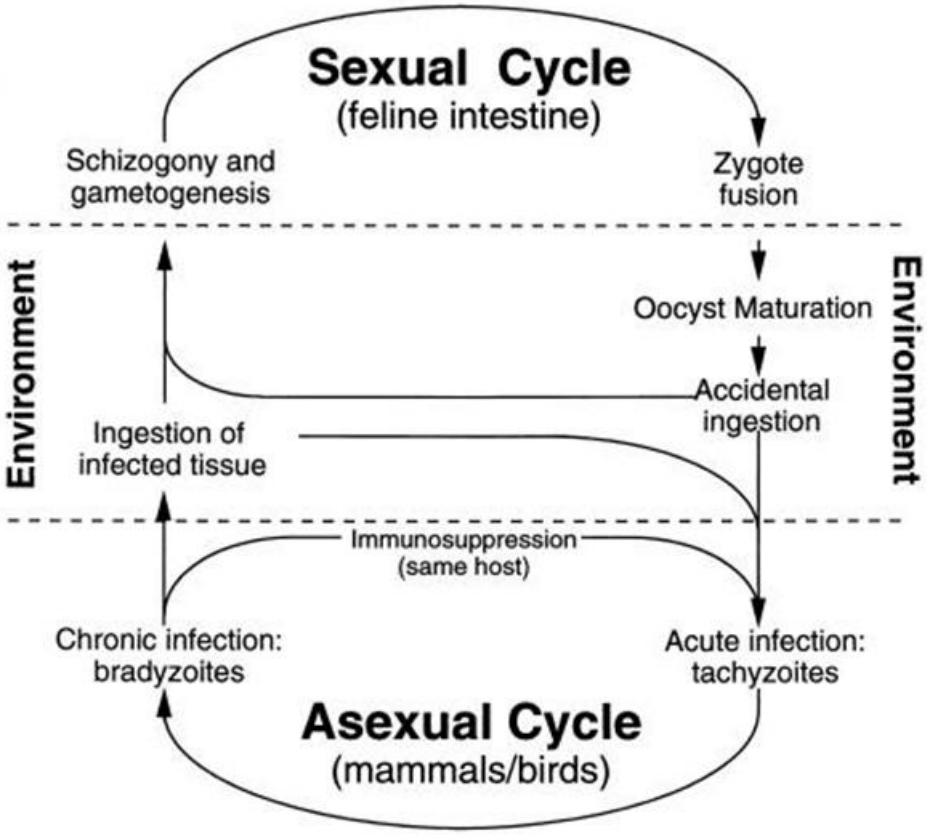

Fig. 3: Schematic life cycle of *T. gondii.* Asexual replication is initiated by ingestion of oocysts in the warm-blooded animals. Upon immune stress, the fast-replicating tachyzoites form tissue-dwelling dormant bradyzoites. The sexual cycle occurring in the feline host is initiated by ingestion of parasite-infected animals. Figure is adapted from (44)

1.1.2.2 The biology of *Plasmodium* spp.

Five common *Plasmodium* spp. cause malaria in humans (*P. falciparum*, *P. malariae*, *P. knowlesi*, *P. vivax*, *P. ovale*), and are responsible for about a million deaths per year, mostly of children under 5 years (45). The invertebrate hosts, female mosquitoes, transmit the sporozoites to intermediate vertebrate hosts *via* the blood meal, which initiates the asexual part of the life cycle of *Plasmodium* spp. (Fig. 4). The majority of sporozoites reach the liver, where they infect hepatocytes and produce merozoites, which invade erythrocytes. Subsequent generations of merozoites are released into the blood stream (46). Concurrent with the release of merozoites, the ruptures of the parasitized red blood cells cause malaria symptoms. A fraction of merozoites develop into micro- and macro-gametocytes. Gametocytes enter its mosquito host during the blood meal and develop into gametes in the mosquito mid-gut.

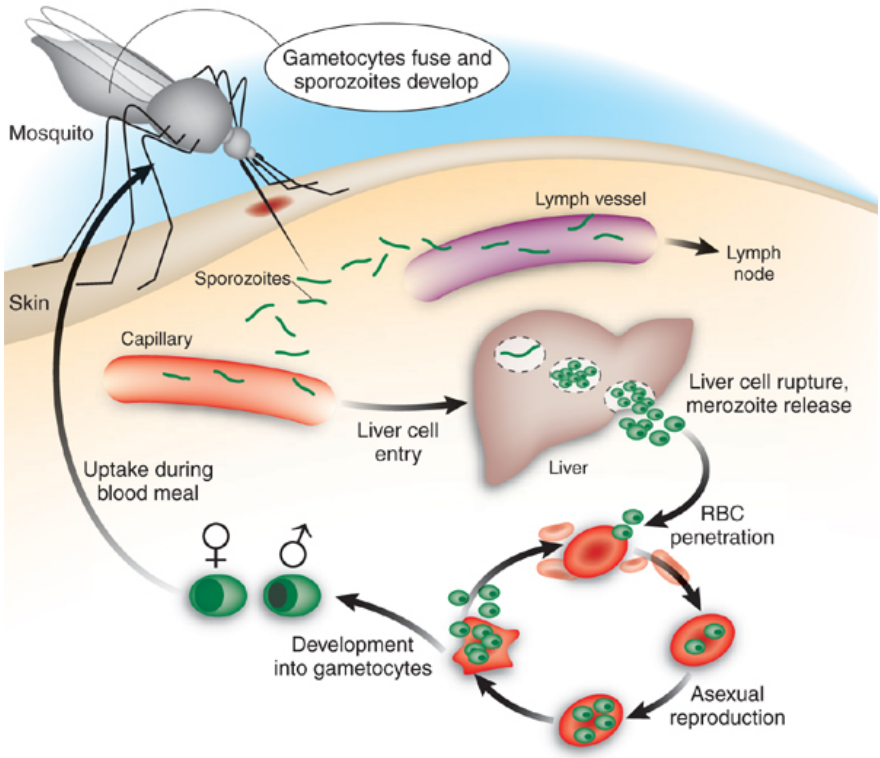

Fig. 4: The life cycle of *Plasmodium* spp. Once sporozoites are injected into the vertebrate host, the asexual reproduction takes place. Sporozoites invade hepatocytes and initiate schizogony and form merozoites. The merozoites invade and multiply in red blood cells (RBC). They can either infect new RBC or develop further into gametocytes, which are taken up of a female mosquito during the blood meal. The sexual development takes place in the insect host. Figure is adapted from (47)

Gametogenesis is induced by a reduced temperature in the mid-gut (48) in conjunction with an mosquito-derived gametocyte-activating factor, xanthurenic acid (49). Following fertilization, the diploid zygotes differentiate into motile ookinetes, which migrate through the mid-gut epithelium. Ookinetes then form oocysts outside the mid-gut, and eventually produce sporozoites to complete the life cycle.

The blood stages of *P. falciparum* can be continuously propagated *in vitro*, whereas *P. berghei* needs to be passaged *in vivo* (50). Techniques for transient as well as stable transfections of the blood stages by using resistance marker (51) are available. However, in comparison to *T. gondii*, transfection efficiency in *Plasmodium* spp. (52) is less due to difficulty to target the parasite within the red blood cell (53). Moreover, the A/T-rich genome is unstable in *E. coli* and hindered the production of transforming constructs (54, 55). The use of rodent *Plasmodium* spp. *e.g.*, *P. berghei* and *P. yoelli*, is mostly limited to study the asexual development of the parasite.

1.2 Host-parasite interactions

Infection of host cells and tissues by different pathogens inflict a variety of molecular and morphological changes. Affected categories include the modulated gene expression, immune response, apoptosis, morphology and metabolism of the host cell. These categories are described below with an emphasis on the diseases caused by apicomplexan parasites.

1.2.1 Gene expression

Parasite infection results in a massive modulation of the host transcriptome, which is the basis for visible effects in the host response. Blader *et al.* nicely described that host genes, modulated in response to *T. gondii* infection can be divided into 3 classes: 1) genes involved in host defense, 2) genes beneficial for the parasite development and 3) genes affected as a consequence of the other two classes (56).

The transcription of several genes functioning in most biological categories is regulated by transcription or activation of transcription factors. One prominent transcription factor is the NF-κB family (Fig. 5), consisting of p50 (NF-κB_1), p52 (NF-κB_2), RelA, RelB and c-Rel subunits. NF- κB/Rel is normally bound to its inhibitors (IκBs) and thus inactive. External stimuli, such as pattern recognition receptors (PRRs; see below), cause phosphorylation of the serine residues in the IκB subunits leading to its proteasomal degradation and activation of NF-κB. The active heterodimer translocates into the nucleus and initiates the transcription of genes involved in cell growth, apoptosis and immune responses (57). The NF-κB family of transcription factors is active during infection with various pathogens (58). RelB is important to control the infection by regulating components of the innate as well as adaptive immunity (59). The absence of RelB increases the susceptibility to *T. gondii* infection due to reduced NK cell activities and T-cell derived IFN-γ levels. Moreover, NF-κB_2-deficient mice show an increased apoptosis of T lymphocytes and an elevated mortality during the chronic phase of *T. gondii* (60). Besides the role of NF-κB in conferring host resistance to infection, its activation is also beneficial for the parasite. For example, the transcription of several anti-apoptotic genes by NF-κB is induced in *T. gondii*-infected fibroblasts, which enhance parasite survival (61). The anti-apoptotic machinery mediated by NF-κB signaling is also described to facilitate survival and propagation of *C. parvum* in epithelial cells (62).

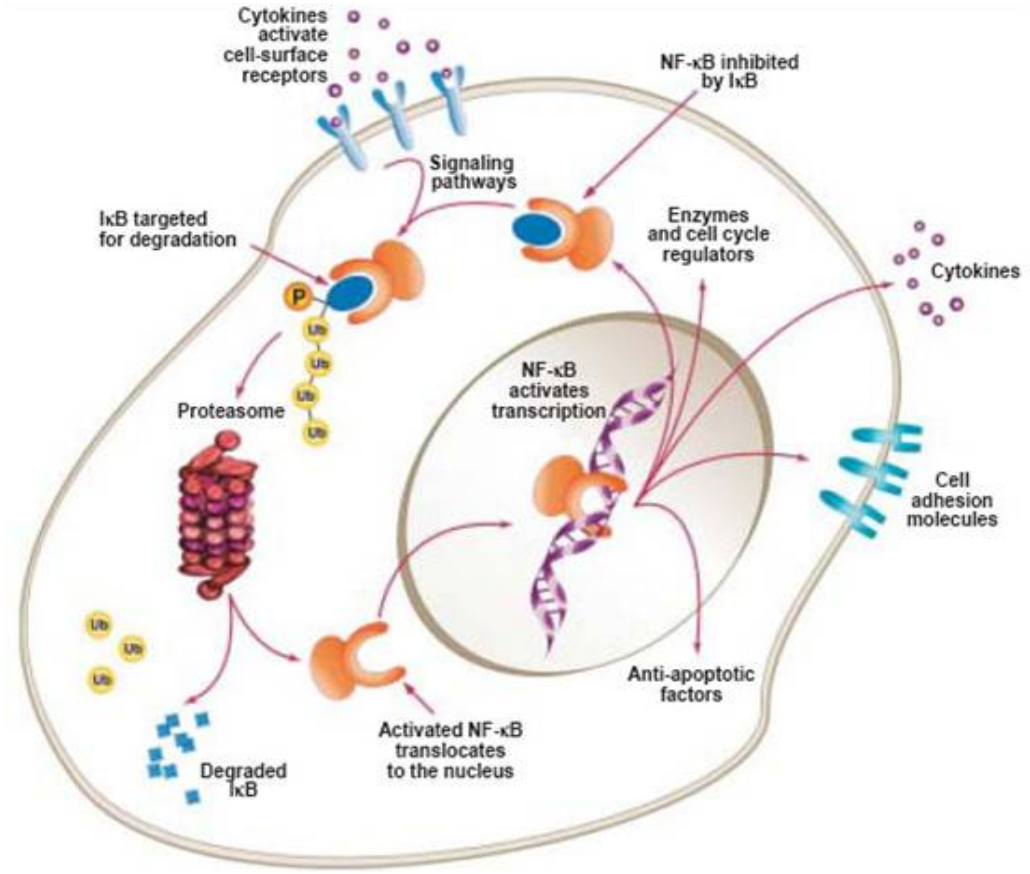

Fig. 5: The activation and roles of NF-κb. Several signals sensed by pattern recognition receptors activate a cascade resulting in phosphorylation and degradation of the inhibitory subunit of NF-κb (IκB). NF-κb translocates into the nucleus and activates the transcription of cytokines, adhesion molecules and anti-apoptotic factors. Figure is taken from (63)

Studies on *T. gondii*-infected macrophages however, have also demonstrated a parasite-mediated interference with NF-κB translocation into the nucleus (Fig. 6) (64). Similarly, a surface protein of the rodent malaria parasites (circumsporozoite protein) blocks the nuclear translocation of NF-κB in hepatocytes resulting in a diminished pro-inflammatory response and enhanced parasite development (65). On the other hand, infections with *P. falciparum* cause activation of NF-κB in the host vascular endothelium and an increased ICAM-1 expression (66). An elevated expression of the adhesion molecule ICAM-1 is involved in sequestration of infected red blood cells in endothelium to escape clearance in the spleen and underlies the fatal outcome of cerebral malaria.

Other transcriptions factors, which are part of the immediate early response include the AP-1 complex and EGR family. These are involved in activating genes that regulate cell survival, growth and differentiation (67, 68). The EGR family consisting of EGR1-4 is a group of zinc-finger binding transcription factors. The AP-1 complex consists of members of the JUN (c-JUN, JUNB, JUND) and FOS (cFOS, FOSB, FRA1 and FRA2) family. Dimerization is

necessary for a successful binding to the DNA motif and distinct partner combinations confer different transcriptional activity (69-71). Members of the AP-1 complex and the EGR family are up-regulated in *T. gondii*-infected cells (56). Activation mediates the transcription of several target genes, which might favor the host or the parasite. Interestingly, EGR2 was induced by rhoptry discharge in *T. gondii*-infected cell, which may promote the parasite development (72).

Another prominent example is the STAT family, which consists of seven members (STAT1-4, STAT5a, STAT5b, STAT6) activated in response to cytokines. The family regulates the transcriptional response for cell differentiation, growth, survival and immune response. The phosphorylation of STAT members, mediated by cytokine-activated Janus kinases, lead to their dimerization, nuclear translocation and transcription of the target genes (73). For instance, IFN-γ causes the activation of STAT1 followed by transcription of IFN-γ stimulated genes (Fig.7). In a murine *T. gondii* model, the absence of STAT1 increased the mortality (74, 75) and likewise, $STAT1^{-/-}$ mice were more susceptible to *C. parvum* infection (76). Whereas activation of STAT1 however is important for the host defense, the activity of STAT3 and STAT6 promotes *T. gondii* development (Fig. 6). The sustained STAT3/6 phosphorylation is mediated by ROP16 (77, 78).

1.2.2 Pattern-recognition receptors and apicomplexan parasites

Infection of host cells by pathogens results in a sequence of events leading to the onset of an immune response, which is at least in part triggered by engagement of pattern-recognition receptors (PRRs). PRRs, such as Toll-like receptors (TLRs), Nucleotide-oligomerization domain (NOD)-like receptors (NLRs), and C-type lectin receptors (CLRs), are activated by foreign molecules and initiate the innate defense (79). Binding of specific ligands to the TLRs lead to a signaling cascade and activation of interferon response element (IRFs), nuclear factor-κB (NF-κB) and/or mitogen-activated protein kinase (MAPK) signaling pathways (80-82). The subsequent transcription of several chemokines and cytokines is induced, either directly by NF-κB and IRFs (type I interferons) or *via* MAPK-mediated activation of the transcription factor AP-1 (83-85). Likewise, activation of the intracellular NLRs (NOD1 and NOD2) or the CLRs result in NF-κB- and MAPK-mediated transcription of several pro-inflammatory cytokines (86-88). Some NLRs are also part of the inflammasome, which is involved in processing of pro-IL1β and pro-IL18 to their active forms by caspase-1 (89). The expression of IL1 and IL18 is also stimulated by CLR engagement among others (90).

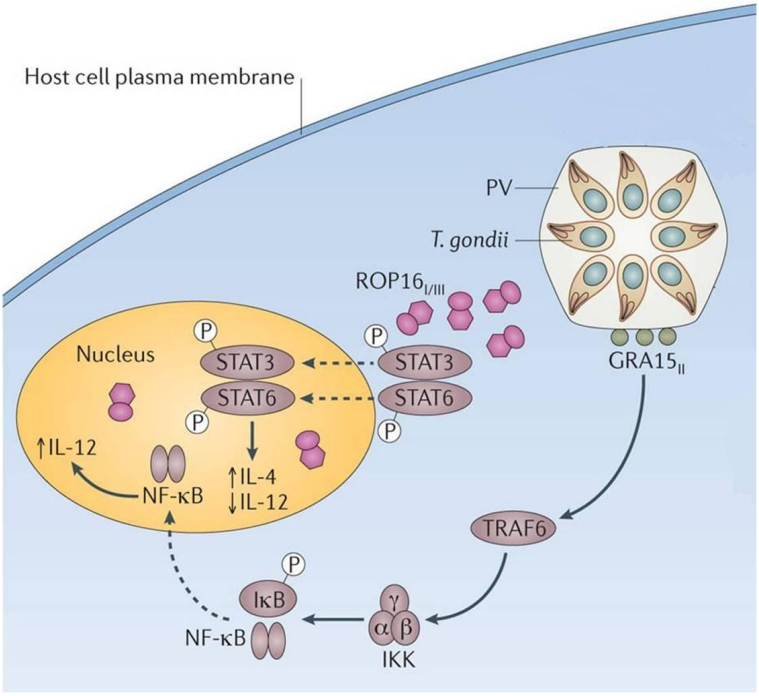

Fig. 6: Strain-dependent interference with the STAT3/6 and NF-κb pathway by *T. gondii*. Sustained STAT3/6 phosphorylation mediated by type I and type III parasite rhoptry kinase ROP16 decrease IL-12 and increase IL-4 transcription promoting the parasite survival. In contrast, a dense-granule protein (GRA15) secreted by type II *T. gondii* mediates the phosphorylation of IκB and subsequent NF-κB activation, which results in increased IL-12 production. Figure is adapted from (91)

Especially the early expression of IL-12 and IFN-γ is critical to limit infection with various intracellular pathogens. For instance, TLR-mediated expression of IL-12 in dendritic cells (DCs) activates an IFN-γ response by natural killer cells (NK) during *T. gondii* infections (Fig. 7). Early expression of IFN-γ activates other cell types and amplifies the immune response to control the infection (92). It was further shown, that TLR11- and TLR12-mediated activation of MyD88 (myeloid differentiation factor 88, an adaptor molecule of TLRs) *via* binding of *T. gondii* profilin on the DC surface triggers this IL-12 production. Profilin is an actin-binding protein, also present in many other apicomplexan parasites (93, 94). In addition, the IL-12 response by DCs is also activated by binding parasite-derived cyclophilin 18 to the chemokine receptor 5 (CCR5) (95). TLR2 and TLR4 are also capable of binding parasitic molecules, notably GPI anchors (96, 97); they are, however not involved in the very early immune response against *T. gondii*. Finally, TLR2 engagement leads to TNF-α production (98), a cytokine which can further potentiate the effects of IL-12 and/or IFN-γ. TLRs are also involved in the induction of a protective immune response during *Cryptosporidium* and *Plasmodium* infections. For instance, TLR4 engagement by *C. parvum* infection and subsequent NF-κB signaling causes NO production in intestinal epithelial cells (99).

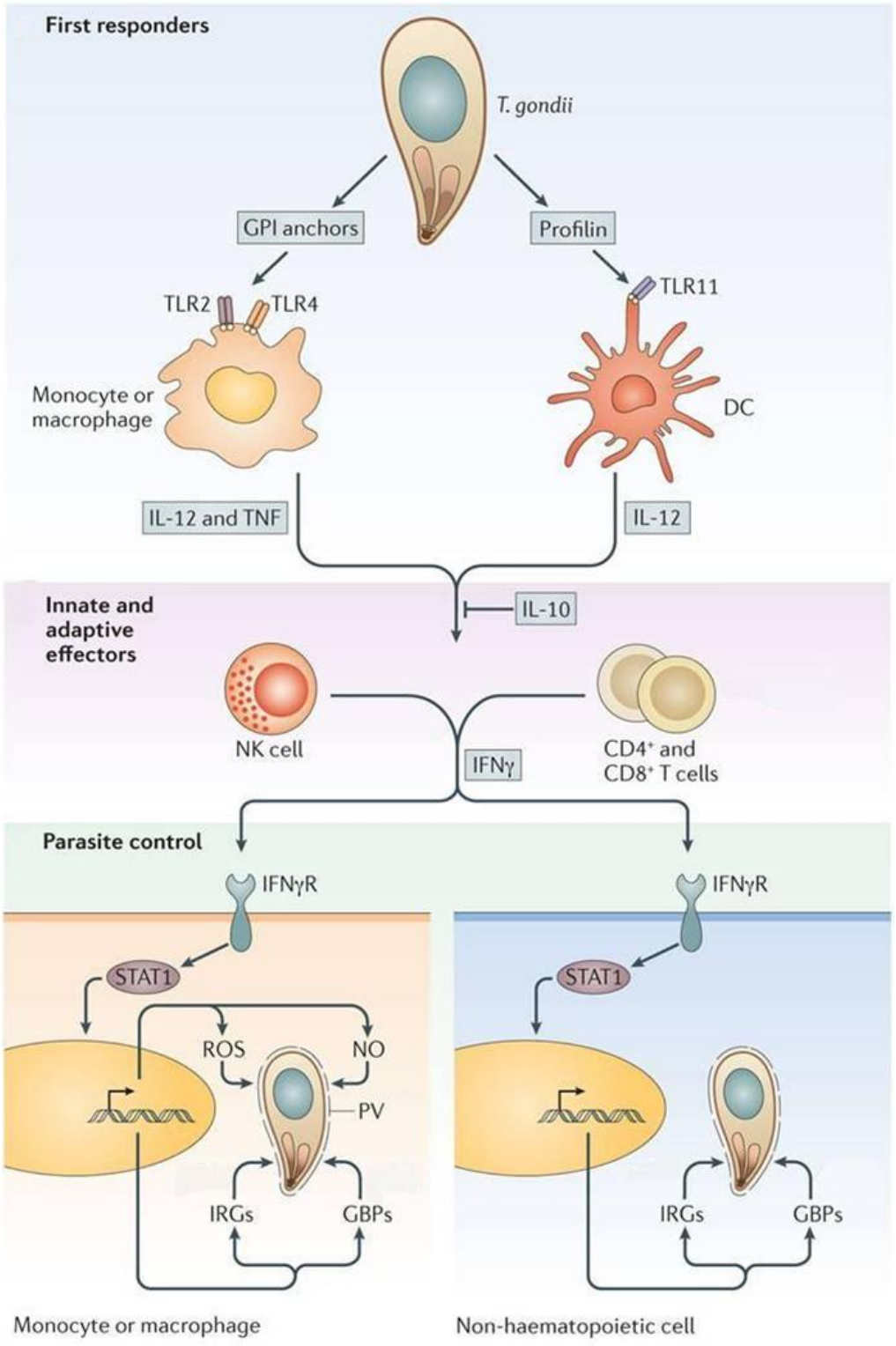

Fig. 7: TLR-mediated immune response to *T. gondii*. TLRs on the surface of innate immune cells (monocytes, macrophages, DC) are activated by parasitic products (GPI, Profilin) resulting in mainly IL-12 production. IL-12 triggers the production of IFN-γ from innate NK cells and later from cells of the adaptive immune response (T cells). IFN-γ is a key cytokine responsible for parasite control. Signalling *via* the IFN-γ receptor (IFNγR) results in STAT1 activation and production of anti-parasitic products including reactive oxygen species (ROS), nitric oxide (NO), immunity-related GTPases (IRG), and guanylate binding proteins (GBP). Figure is adapted from (91)

Moreover, it was shown that *P. falciparum* GPIs are recognized by TLR2 and TLR4 (100). Furthermore, the malaria pigment, haemozoin, and/or the DNA associated with haemozoin as well as protein-DNA complexes of the merozoites activate TLR9 (101-103).

Signaling *via* NLRs or CLRs seems to play a minor role during parasitic infections. Whereas CLRs appeared to be not involved in the immune response, at least the intracellular NLR NOD2 pathway is important for immunity against *T. gondii* (104). Although the *T. gondii* ligand for NOD2 is not known, studies with NOD2-deficient animals showed that the receptor is necessary for an optimal Th1 response and IL-2 production. Similar to DCs, the IFN-γ expression in T cells confers resistance against the acute parasite infection. However, other experiments showed no role for NOD2 in protection against *T. gondii* (105), thus the role of NLRs during *T. gondii* infection is questionable. Accordingly, absence of NOD1 and NOD2 in *P. berghei* infected mice did not influence the mortality or parasitemia (106).

An *Eimeria* infection is accompanied by the production of cytokines including IL-12 and IFN-γ (107). However, little is known about the involvement of PRRs during *Eimeria* infections especially in the chicken. It was shown that an *E. tenella* infection resulted in the increased expression of several TLR transcripts (108) in the chicken. Furthermore, in *Eimeria* spp. a profilin-related protein is present (109), sharing sequence homology with the *T. gondii* profilin, and might therefore be recognized by TLR11 (93) triggering an adequate innate immune response. Interestingly, it was shown that a recombinant *E. tenella* protein, most likely profilin, is capable to induce a pro-inflammatory response leading to production of IL-12, IFN-γ and TNF-α in mice (110). Therefore, TLRs might be very important in initiating the immune response against *Eimeria* spp.

Summing up, sensing of pathogen-associated molecular patterns (PAMPs) by PRRs activates the immune system leading to the production of pro-inflammatory cytokines and chemokines, which coordinate the attraction of immune cells and finally the development of the adaptive and pathogen-specific immune response.

1.2.3 IFN-γ and cell-mediated immune response in parasite infections

Once an infection is established, the fast innate immune response is replaced by the adaptive immunity which is more pathogen-specific. The cytokine and chemokine signaling cause recruitment of immune cells, antigen presentation, and activation and differentiation of T cells. In *T. gondii* infections, early IL-12, TNF-α and INF-γ production by cells of the innate

immune system (Fig. 7), including DCs, macrophages, neutrophils and NK cells, is important to limit tachyzoite replication and to establish the cell-mediated immunity. Whereas the humoral immune response seems to be less important during an established *T. gondii* infection, mainly $CD4^+$ and $CD8^+$ T cells confer resistance (111, 112). Especially the IL-12 secretion by innate cells is necessary for the differentiation of $CD4^+$ T cells into the Th1 subtype, which secrete IFN-γ (113, 114) and subsequently potentiate the immune response. Generally, IFN-γ exerts diverse effects including activation of cells, antigen presentation and suppression of Th2 cytokine expression. It further activates the transcription of various genes by STAT1 signaling, including chemokines, cytokines, reactive oxygen and nitrogen species (115). For instance, macrophage-derived NO plays anti-parasitic and immunosuppressive roles (116, 117). Furthermore, IFN-γ is a potent inducer of tryptophan degradation *via* indoleamine 2,3-dioxygenase 1 (IDO1). The activation of IDO1 in parasitized cells was shown to inhibit the parasite replication *via* limiting tryptophan (118). Another IFN-γ-mediated effect during *T. gondii* infection in mouse is the activation of IRGs (immunity-related GTPase) and GBPs (guanylate binding protein), which localize at the PVM and result in the disruption of vacuole and killing of the parasite (119).

Interestingly, the role of IFN-γ in primary cell-mediated host response against *Eimeria* species is less defined and varies with species (120). Immune response against *E. vermiformis* infecting small intestine involves $CD4^+$ T cells and the production of IL-12 and IFN-γ. Depletion of $CD4^+$ T cells or absence of IL-12 or IFN-γ increased the mouse susceptibility to primary infections (121-124). In contrast, treatment of *E. pragensis*-infected mice, a parasite of the large intestine, with anti-IFN-γ mAb, did not influence the oocyst output (125). Similar results were obtained in experiments of *E. falciformis*-infected IFN-$\gamma^{-/-}$ mice (22). Surprisingly, infection of IFN-$\gamma R^{-/-}$ mice resulted in even less oocyst shedding (126). In *E. falciformis* infection, $CD8^+$ T cells are the main producer of IFN-γ along with minor contribution of $CD4^+$ T cells and NK cells (126, 127). Notable, the absence of IFN-γ or its receptor exacerbated the pathology in *E. pragensis* as well as *E. falciformis* infections. In *E. falciformis* infected IFN-$\gamma R^{-/-}$ mice it was shown, that increased pathology is accompanied by augmented IL-17A and IL-22 production (126). Thus, IFN-γ seems to have important anti-parasitic as well as immune-regulatory roles dependent on the *Eimeria* species.

In infections with *Cryptosporidium* and *Plasmodium* spp. IFN-γ has also a central role. In *Cryptosporidium* spp. infection, IFN-γ production by $CD4^+$ T cells (128, 129) limits the parasite propagation (130, 131). By contrast, $CD8^+$ T cells activated by MHC I-mediated

antigen-presentation by infected hepatocytes, are important producer of IFN-γ during pre-erythrocytic *Plasmodium* infections (132). Cytokine release leads to NO and IL-12 production resulting in amplification of the immune response and protection against *Plasmodium* spp. (133). In the erythrocytic stage, the production of IFN-γ by $CD8^+$ and $CD4^+$ T cells, is also necessary to control the parasite multiplication (134). In addition, the humoral immune response, such as antibodies against surface components of merozoites or infected red blood cells, contributes to protection (135).

A strong cell-mediated immune response however can be detrimental to the host, *e.g.* secretion of pro-inflammatory cytokines contributes to the fatal outcome of cerebral malaria (136). Therefore, the early inflammatory response is controlled by anti-inflammatory cytokines. For example, macrophages activated by *T. gondii* produce IL-10 and TGF-β (137), which counteract the pro-inflammatory response of IL-12 and IFN-γ. Moreover, the Th2 cytokine IL-4 also decreases the IFN-γ and increases the IL-10 (138) concentration. Likewise, an increased NO production diminishes the proliferation of spleen cells (117). Furthermore, infections of $iNOS^{-/-}$ mice with *E. falciformis* impaired the pathology but had no effect on the oocyst yield (22), suggesting a role of NO in controlling the immune response.

In summary, the concurrent occurrence of the pro- as well as anti-inflammatory host response ensures host protection while allowing the parasite development.

1.2.4 Apoptosis and parasite infection

Apoptosis, the programmed cell death, is induced in response to various stress stimuli (*e.g.* chemicals, toxins, irradiation, UV, deprivation of growth factors), signaling *via* death-receptors (Fas), or the release of perforin and granzymes by NK and cytotoxic T cells (Fig. 8). The cystein proteases caspases are the central enzymes of the apoptotic machinery (139, 140). The cleavage of different proteins by caspases results in chromatin condensation, nuclear fragmentation, cytoskeletal restructuring and finally in degradation of the apoptotic cell (140, 141). Apoptosis can also activate the immune response and prevent the dissemination of the pathogen (142, 143). Conversely, pathogens have evolved numerous mechanisms to interfere with the apoptotic machinery of their host cells. Some parasites (*e.g. T. gondii*, *C. parvum*) induce as well as inhibit apoptosis (140). In infections with *T. gondii*, the pro- or anti-apoptotic responses appear to depend on the host cell type and parasite strain (144). For example, an increase in apoptotic cells with a concurrent higher mortality of *T. gondii*-infected mice was observed, when the highly virulent type I strain RH was used (145). This

apoptotic response is mediated by an increase in FAS-/FASL- and TNF-α/TNF-R1-dependent apoptotic events of immune cells, including T and B cells, NK cells, granulocytes and macrophages (145-147). Also during infections with different *Plasmodium* spp., an elevated apoptosis of immune cells, including T and B cells and macrophages, was observed with a concurrent up-regulation of Fas/FasL (148-150). Similar results were obtained in *C. parvum*-infected cells *in vitro*, where the parasite infection resulted in an increased apoptosis of its host cells *via* Fas-FasL receptor (140, 151).

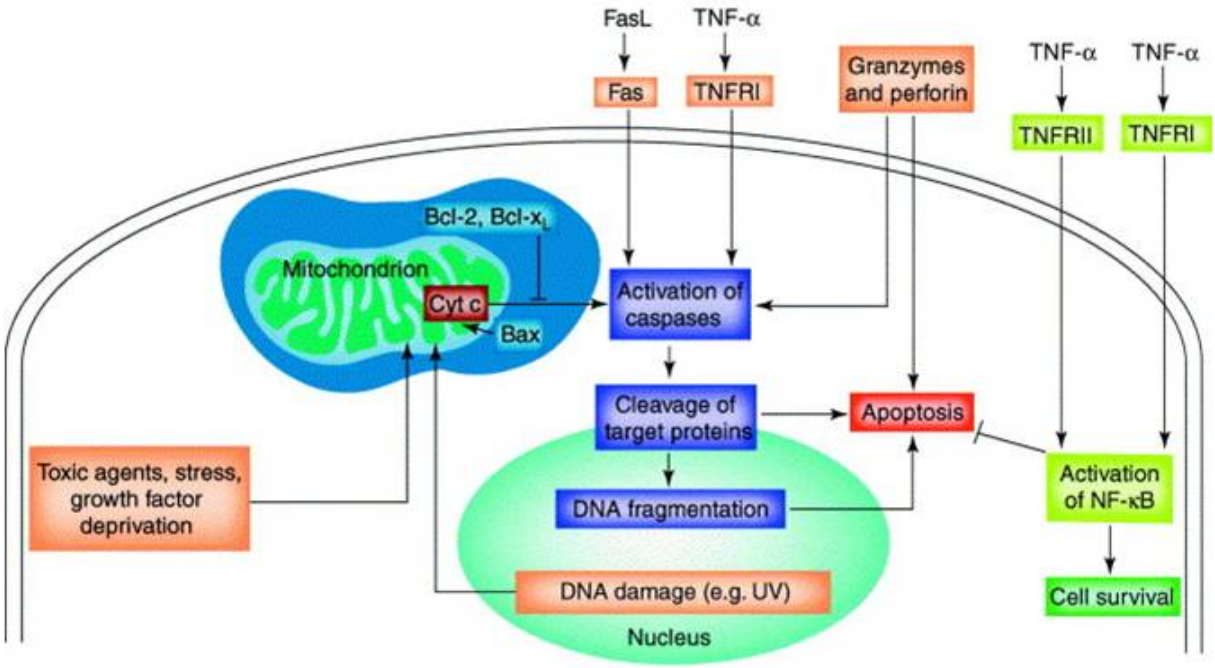

Fig. 8: Simplified model for induction and inhibition of apoptosis. Different stimuli result in activation of caspases and apoptosis. Cellular stress triggers the release of cytochrome c (Cyt c) from the mitochondria resulting in caspase activation. Caspases are also activated *via* the death-receptor pathway (FasL/Fas; TNF-a/TNFRI) or by granzymes and perforin released from activated NK or cytotoxic T cells. Anti-apoptotic pathways include the induction of members of the BCL-2 family as well as NF-κB signalling. Figure is taken from (140)

Notably, *T. gondii* has also evolved many different mechanisms to inhibit apoptosis, which might favor its development. The parasite interferes with the death receptor as well as with the granzyme/perforin pathway of apoptosis (144, 152). Ligation of Fas- and TNF-α to their respective receptors normally leads to activation of caspase 8. In *T. gondii* infection, this pathway was disturbed by a lower activity of the enzyme as well as an increased degradation of the protease (153). In addition, the mitochondrial (stress)-induced pathway of apoptosis (*e.g.* stimulated by damaged DNA) is also inhibited during *T. gondii* infection. Under normal conditions, stress stimuli trigger cytochrome c release into the cytoplasm, resulting in activation of caspase 9, which cleaves and activates caspase 3 and 7 (154). A reduced

cytochrome c release and inhibition of the caspases 9 and 3 was observed during the infection (155, 156) probably mediated *via* NF-κB-induced expression of several anti-apoptotic proteins, including members of the Bcl2 family (61, 155). Consistently, *C. parvum* infection of intestinal epithelial cells also induces anti-apoptotic events *via* NF-κB activation besides apoptosis inducing mechanisms (157).

In brief, apoptotic death of immune cells appears to counteract the overwhelming immune responses, whereas promoting pathogen development. The inhibition of host cell apoptosis diminishes pro-inflammatory responses evoked by apoptotic cells, and thus is beneficial to the pathogen.

1.2.5 Parasite-induced morphological changes in the host cell

Infection of host cells causes re-organization of host organelles and/or cytoskeletal elements. Most apicomplexan parasites reside within a parasitophorous vacuole (PV), which is originally derived from the host cell plasma membrane. The PV is non-fusogenic in nature and protects the parasite from the host's innate defense (4, 158). The PVM also functions as a molecular sieve, which allows diffusion of host metabolites up to 1300-1900 Da (*T. gondii* (159)) or up to 1400 Da (*Plasmodium* spp. (160)). This implies the possibility to gain access to molecules the parasites cannot synthesize itself (*e.g.* tryptophan for *T. gondii* (161)). In *T. gondii* infections, host mitochondria and endoplasmic reticulum re-localize around the PVM (Fig. 9A), which is thought to facilitate the salvage of essential host nutrients (162).

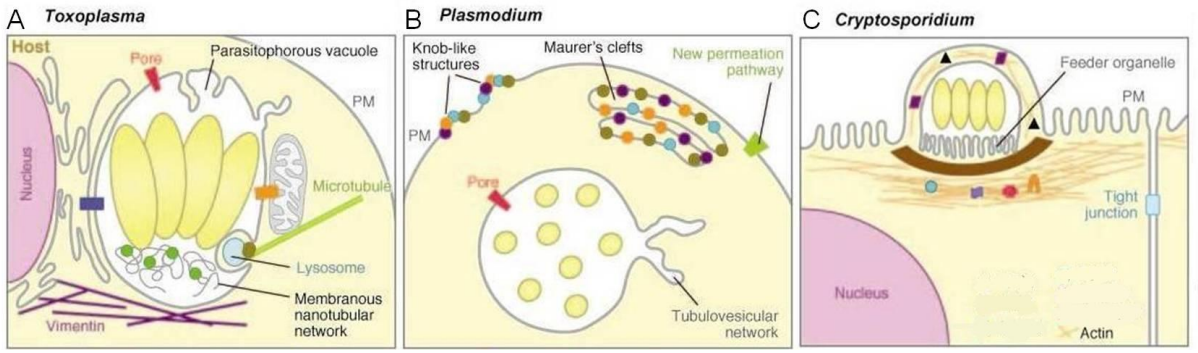

Fig. 9: Schematic representation of host cell infection by apicomplexan parasites. (A) Host organelles, microtubules and vimentin are recruited to the PV of *T. gondii*. **(B)** Infection with *P. falciparum* induces the formation of Maurer's clefts in the cytoplasm and knobs on the surface and a tubulovesicular network in RBCs. **(C)** *C. parvum* infections result in remodelling of host actin. Figure is adapted from (163)

Infection with *P. falciparum* results in the formation of plasma membrane channels in RBCs. These pores (164), are capable to transport purines as well as sugars and ions from the extracellular milieu (165, 166). The formation of a tubulovesicular network, extending from the PVM into the cytosol of the erythrocyte, allows potential uptake of nucleosides and amino acids (167). The Maurer's cleft in the cytosol and the knobs on the surface of *P. falciparum*-infected erythrocytes (163) are of parasite origin (168, 169).

In addition to recruitment of host organelles or remodeling of host cell membranes, also host cytoskeleton is rearranged in the infected cells. Vimentin (filament of the cytoskeleton) and microtubules assemble around the PV of *T. gondii* and are involved in positioning of the vacuole close to the host nucleus and nutrient acquisition respectively (170, 171). Also infections with *Cryptosporidium* results in rearrangement of cytoskeletal elements (Fig. 9C). *Cryptosporidium* resides in a unique compartment, which is considered as intracellular but extra-cytoplasmic, creating an interface of parasite and host consisting of host cell actin (172). The remodeling of host actin just below the PV is considered to be involved in nutrient uptake and anchor the vacuole of *C. parvum* (173). Likewise, the re-localization of host cytoskeleton elements are thought to stabilize the enlarged macromeront of *E. bovis* (174).

In brief, whereas the formation of a PV is a common feature of most apicomplexans, the morphological changes of the respective host cells differ with the parasite species.

1.2.6 Host cell cycle and infection

The cell cycle is divided into four steps, G_1, S, G_2 and M phase. During G_1 phase the cell grows without replicating the DNA content. DNA replication takes place in the S phase followed by G_2 in which the cell increases further in size. Mitosis marks the nuclear division followed by the cytokinesis. Many cells enter the G_0 phase, a resting state after G_1 phase. Such cells are metabolically active, but do not enter the S phase. Of course the eukaryotic cell cycle has to be tightly controlled. Signals from the environment, *e.g.* growth factors, are integrated initiating the proliferative cell cycle. And vice versa, absences of growth factors have to result in conducting the cells into the G_0 phase (175). At each point of the cell cycle, checkpoint controls must occur to ensure the successful completion of one phase. Cyclins and cyclin-dependent kinases (CDKs) control these checkpoints (176).

Some parasites are capable of interfering with the host cell cycle. Prominent examples are *Theileria* spp., which cause uncontrolled proliferation of host lymphocytes by triggering G_1 to

S phase transition. Several signaling pathways, including NF-κB signaling, are modulated, and enhance proliferation and cell survival in *Theileria*-infected cells (177). In contrast, infections of HFFs with *T. gondii* results in the cell cycle arrest at the G_2/M phase. Here, this inhibition of host cell proliferation promotes the parasite replication (178, 179).

1.2.7 Host metabolism and infection

Changes in the host metabolism upon infection might be a consequence of nutrient depletion by the pathogen. Many parasites are auxotroph for key metabolites and thus are dependent on their host cell. *T. gondii* and *Plasmodium* spp. depend on the purine acquisition from their host cells (180, 181). *T. gondii* is also auxotrophic for some amino acids including arginine and tryptophan (182, 183). Microarray analyses of *T. gondii*-infected HFF cells revealed an induced expression of the transferrin receptor, indicating an increased up-take of iron (184). *T. gondii* also scavenges glucose, glutamine, and cholesterol from its host cell (185). Gene expression analyses of *T. gondii*-infected cells illustrated an induced transcription of several glycolytic enzymes within 24 h of infection. In addition, the expression of the lactate dehydrogenase A was up-regulated, which leads to lactate production from pyruvate, whereas TCA cycle enzymes remained unchanged (56, 186). Similar results were obtained by microarray analyses of spleens isolated from *P. berghei*-infected mice (187). In both cases, the glycolysis and the production of lactate is favored over the TCA cycle. Another host pathway affected by *T. gondii* infection is the mevalonate pathway (56), involved in *de novo* synthesis of cholesterol. Although *T. gondii* scavenges cholesterol *via* uptake of low density lipoprotein (188), an induction of the host mevalonate pathway, suggests an infection-mediated increase in cholesterol synthesis to maintain lipid homeostasis (56). Therefore, in response to infection the host cells have to restock nutrients, which might be scavenged by the parasites.

1.3 Aims of this study

Individual *Eimeria* species infect an exclusive tissue and host cell type, and complete their entire life cycle within a single host, which offers a distinct advantage for site-specific parasite-host interactions *in vivo*. This study used *Eimeria falciformis* infecting epithelial cells of the mouse caecum. The use of mouse as a host offers an excellent model to study host responses upon parasite infection. Intracellular parasites reprogram host functions for their survival and reproduction. Conversely, the infected host attempts to defend the microbial insult. The aim of this work was to investigate the host response against an *E. falciformis* infection and identify the determinants of parasite development.

2. Materials and Methods

2.1 Materials

2.1.1 Mouse strains

BALB/c, NMRI and C57BL/6 mice were purchased from the Charles River Laboratories (Sulzfeld, Germany). IDO1 knockout mice (BALB/c strain; Muriel Moser, Institut de Biologie et de Médecine Moléculaires, Université Libre de Bruxelles) and IFN-γR knockout mice (C57BL/6 strain, Uwe Klemm, Max Planck Institute for Infection Biology, Berlin) were used for parasite infections. Animal procedures were performed according to the German Animal Protection Laws as directed and approved by the overseeing authority Landesamt fuer Gesundheit und Soziales (Berlin, Germany).

2.1.2 Parasites

Eimeria falciformis oocysts were originally procured from Bayer Animal Health (Dr. Gisela Greif). *Toxoplasma gondii* tachyzoites (RH strain) were donated by Carsten Lüder, University of Göttingen (USA). *Plasmodium berghei* ANKA strain was propagated in the laboratory of Kai Matuschweski at the Max-Planck-Institute for Infection Biology (Berlin).

2.1.3 Cells

Young adult mouse colonic (YAMC) cells were obtained from Robert Whitehead, Vanderbilt University, USA (189). The murine primary fibroblasts (c-FOS$^{+/+}$ and c-FOS$^{-/-}$) were a kind donation from Marcus Christmann, Department of Toxicology, University of Mainz (190). Human Foreskin Fibroblasts (HFF) were provided by Carsten Lüder, University of Göttingen, Germany.

2.1.4 Reagents

Chemicals	Source
Acrylamide (30%)	Roth, Germany
Ammonium peroxydisulfate (APS)	Sigma-Aldrich, Germany
Bovine serum albumin fraction V	Applichem, Germany
Chloroform	Roth, Germany
Cellulose (DE52)	Whatman, Great Britain

Dulbecco's modified eagle media (DMEM)	Biochrom, Germany
Dithiothreitol (DTT)	Applichem, Germany
Ethanol	Applichem, Germany
Ethylene diamine tetraacetic acid (EDTA)	Applichem, Germany
Ethidiumbromide	Roth, Germany
Fast RED	Dako, Germany
Fetal calf serum	Biochrom, Germany
Fluorescein diacetate	Sigma-Aldrich, Germany
Fluoromount G / DAPI	SouthernBiotech, USA
Glutamine	Biochrom, Germany
Hydrochloric Acid	Applichem, Germany
^{3}H-Thymidin	ICN Biochemicals
Hanks balanced salt solution (HBSS)	Biochrom, Germany
Hydrocortisone	Sigma Aldrich, Germany
Methanol	Roth, Germany
Methyl-DL-tryptophan	Sigma Aldrich, Germany
Na-pyruvate (100 mM)	Biochrom, Germany
Non-essential amino acids (100x)	Biochrom, Germany
Non-fat dried milk powder	Applichem, Germany
Nylon wool	Robbins, USA
Penicillin / Streptomycin	Biochrom, Germany
Pepsin	Sigma-Aldrich, Germany
Paraformaledehyde	Roth, Germany
PBS	Biochrom, Germany
Phenylmethanesulphonylfluoride (PMSF)	Roth, Germany
Potassium dichromate	Merck, Germany
Prestained protein marker	New England Biolabs, Germany
Protease inhibitor cocktail	Sigma-Aldrich, Germany
Recombinant mouse IFN-γ	Peprotech, Germany
Ro61-8048	Tocris Bioscience, Germany
RPMI-1640	PAA, Austria
(S)-(4-Ethylsulfonyl)benzoylalanine hydrochloride	Enzo Life Sciences, Germany
Sodium chloride	Applichem, Germany
Sodium deoxycholate	Calbiochem, Germany

Sodium dodecyl sulfate (SDS)	Applichem, Germany
Sodium hypochlorite (12%)	Roth, Germany
Sodium tauroglycocholate	a gift from M. Kurth, TU Dresden
Streptavidin alkaline phosphatase	Dako, Germany
Tetramethylethylenediamine (TEMED)	Roth, Germany
α-thioglycerol	Applichem, Germany
Tris-HCl	Roth, Germany
Triton X-100	Applichem, Germany
TRIzol reagent	Life Technologies, Germany
Trypan blue	Life Technologies, Germany
Trypsin	Sigma Aldrich, Germany
Xanthurenic acid	Sigma Aldrich, Germany
Xylene	Roth, Germany

2.1.5 Plasticware and other disposables

Product	**Source**
Cryo tubes	Greiner Bio-One, Germany
Cell strainer	BD Biosciences, Belgium
Cover slips	Roth, Germany
Disposable pipettes	Greiner Bio-One, Austria
Eppendorf tubes	Greiner Bio-One, Austria
Falcon tubes	Greiner Bio-One, Austria
Gasket Slides	Agilent, USA
Glass beads ø 0.5 mm	Braun Biotech (Sartorius), Germany
Improved Neubauer counting chamber	Neubauer, Germany
Microarrays (4x44K, mouse)	Agilent, USA
Microscopy slides	Menzel, Germany
Nitrocellulose membrane	Applichem, Germany
Petridishes	Greiner Bio-One, Austria
Pipette Tips	Greiner Bio-One, Germany
RNAse-free barrier tips	Sorenson BioScience, USA
Syringes	BD, Germany
Whatman blotting papers	Schleicher & Schuell, Germany
96 well multiply-PCR plate	Sarstedt, Germany

24 / 48 / 96 well culture cluster	Corning Costar, Germany
T-25 Tissue culture flasks	Greiner Bio-One, Germany

2.1.6 Antibodies

Antibody	**Source**
anti-*E. tenella*	Fiona Tomley, UK
anti-*Tg*Gap45	Plattner et al. (191)
Goat anti-rabbit IgG Alexa Fluor 488 / 594	Life Technologies, Germany
anti-mouse CD45-ef450	eBioscience, Germany
anti-mouse UEA1-FITC	eBioscience, Germany
anti-mouse CD4-ef450	eBioscience, Germany
anti-mouse CD8-Cy5	eBioscience, Germany
anti-mouse CD3	Dako, Germany
anti-mouse B220	eBioscience, Germany
anti-mouse F4/80	eBioscience, Germany
rat anti-mouse IDO1	Biolegend, Germany
biotinylated rabbit anti-rat IgG	Dako, Germany
rabbit anti-mouse IDO1	Genscript, Germany
anti-mouse β-Tubulin	Genscript, Germany
peroxidase-labeled anti-rabbit IgG	GE Healthcare, Germany

2.1.7 Commercial kits

Product	**Company**
BCA Protein Assay Kit	Thermo Scientific, USA
ECL Western Blotting and Analysis System	GE Healthcare, Germany
mouse IFN-γ ELISA Ready-SET-Go	eBioscience, Germany
mouse IL-4 ELISA Ready-SET-Go	eBioscience, Germany
mouse IL-10 OptEIA ELISA Set	BD Biosciences, Germany
Gene Expression Hybridization Kit	Agilent, USA
Immunoblot recycling kit	Alpha Diagnostic
Low RNA input linear amplification kit PLUS (Two-Color)	Agilent, USA
PureLink RNA mini kit	Life Technologies, Germany

RNeasy mini kit	Quiagen, Germany
SuperScript III first-strand synthesis SuperMix for qRT-PCR	Life Technologies, Germany
SuperScript III Platinum SYBR green one-step qRT-PCR kit with ROX	Life Technologies, Germany

2.1.8 Laboratory equipment

Instrument	Company
Bioanalzyer (2100)	Agilent, USA
Casy cell counter (model TT)	Innovatis, Germany
Gel electrophoresis chamber	Amersham Biosciences, USA
Microarray hybridization chamber (SureHyb)	Agilent, USA
Microarray hybridization oven	Agilent, USA
Microarray scanner	Agilent, USA
Microplate reader	Dynatech Laboratories, Germany
Microscope (Apotome Imager Z2)	Zeiss, Germany
Microscope	Leica, Germany
NanoDrop (ND 1000)	Wilmington, USA
PCR cycler	JenaAnalytic, Germany
Photo microscope (Axiophot)	Zeiss, Germany
7300 Real-Time PCR System	Applied Biosystems, Germany
Western blotting chamber	PeqLab, Germany

2.1.9 Software

Programs	Source
Application Suite Software	Leica, Germany
Axio Vision	Zeiss, Germany
Database for Annotation, Visualization and Integrated Discovery (DAVID)	Huang da *et al*. (192)
Endnote	Thomson Reuters, USA
FlowJo Software	Tree Star, USA
GraphPad Prism	GraphPad Software, USA
Ingenuity Pathway Analysis	Ingenuity Systems, USA

Microarray image analysis and feature extraction software	Agilent, USA	

2.1.10 Oligonucleotide primers

Gene	Primer Sequence (5' – 3')	Accession Number
*Mm*IDO1-F	ATTGGTGGAAATCGCAGCTTC	NM_008324.1
*Mm*IDO1-R	ACAAAGTCACGCATCCTCTTAAA	
*Mm*IDO2-F	AAGGCCAACCCCAAAAGGTG	NM_145949
*Mm*IDO2-R	ACCAGGATAGGCGGGAGTC	
*Mm*CxCL9-F	GGAGTTCGAGGAACCCTAGTG	NM_008599
*Mm*CxCL9-R	GGGATTTGTAGTGGATCGTGC	
*Mm*CxCL10-F	CCAAGTGCTGCCGTCATTTTC	NM_021274
*Mm*CxCL10-R	GGCTCGCAGGGATGATTTCAA	
*Mm*CxCL11-F	GGCTTCCTTATGTTCAAACAGGG	NM_019494
*Mm*CxCL11-R	GCCGTTACTCGGGTAAATTACA	
*Mm*IRGM3-F	CTCATCAGCCCGTGGTCTAAA	NM_018738
*Mm*IRGM3-R	CACCGCCTTACCAATATCTTCAA	
*Mm*IRGB6-F	TGGGACCACTAACTTCACACC	NM_011579
*Mm*IRGB6-R	GGCCAGTTGTGCATCATTTTC	
*Mm*GBP2-F	CTGCACTATGTGACGGAGCTA	NM_010260
*Mm*GBP2-R	GAGTCCACACAAAGGTTGGAAA	
*Mm*GBP3-F	GAGGCACCCATTTGTCTGGT	NM_018734
*Mm*GBP3-R	CCGTCCTGCAAGACGATTCA	
*Mm*CD45-F	GTTTTCGCTACATGACTGCACA	NM_001111316
*Mm*CD45-R	AGGTTGTCCAACTGACATCTTTC	
*Mm*EPCAM-F	GCGGCTCAGAGAGACTGTG	NM_008532
*Mm*EPCAM-R	CCAAGCATTTAGACGCCAGTTT	
*Mm*KMO-F	ATTGGCGGTGGTTTGGTTG	NM_133809
*Mm*KMO-R	TCCCTAGCTTCGTACACATCAA	
*Mm*KYNU-F	GCAAACGCCCTTGGATTGTAG	NM_027552
*Mm*KYNU-R	GCCGCTTTGGAGTAGGCTTA	
*Mm*KAT2-F	AGCGGACATACTGAGCAAAGC	NM_011834
*Mm*KAT2-R	TTCCGTTTTCCACAGTGAAGG	
*Mm*GOT2-F	CCTGGGCGAGAACAATGAAGT	NM_010325

*Mm*GOT2-R	ATGGGCGTGTGATTTCCCC	
*Mm*HAAO-F *Mm*HAAO-R	AGACATGATACTACGAGTCCTGG AGCCGCCTTCTCTCAATCAC	NM_025325
*Mm*KAT1-F *Mm*KAT1-R	TGGACCCACTCAAGAATGTGC ATGACCTCGTCTCCTTCATCC	NM_172404
*Mm*KAT3-F *Mm*KAT3-R	TCAACGTCAAATTGATCCAAACG TTCATCCCGTCAGTAGGTTTAGA	NM_173763
*Mm*18S rRNA-F *Mm*18S rRNA-R	TTGACGGAAGGGCACCACCAG GCACCACCACCCACGGAATCG	NR_003278
*Ef*18S rRNA-F *Ef*18S rRNA-R	GAAATGCCTACCCTGGCTTC TCAATCCTTCCCATGTCTGG	AF080614.1
*Ef*ORF470-F *Ef*ORF470-R	AATTTTTAGCGGAGGATCTTTTTG TTGAGCGAAGTCCTCAGATTG	AF311632.1
*Ef*Gam56-F *Ef*Gam56-R	TGGCCGAGCCTAGTACAGTT AAATTTTCGGGGGTCTCAAC	Primers based on ongoing genome-sequencing project (kindly made available by Simone Spork (Humboldt University Berlin) and Christoph Dieterich (Max-Delbrück Center Berlin)
*Ef*Gam82-F *Ef*Gam82-R	ATGATGGGCACTGAGGAGTC GCTTGACAGTCTCAGCAGCA	
*Pb*Ccp3-F *Pb*Ccp3-R	CTGCAGCTATTTATGATGGT TCATCACTTTCATCACCTTT	NW_674653
*Pb*Ccp4-F *Pb*Ccp4-R	GTAGGACAAGCATAGACGAA GAGCATTGAAATCTTCTTGA	NW_674323
*Pb*Fnpa-F *Pb*Fnpa-R	GATTCAAAACATCAAACTGG ATGGCTTCGATATCACACTA	NW_674904
*Pb*Gapdh-F *Pb*Gapdh-R	AATTAAAGA AGCATCTGAGGGTCCAC TTGAATATCCCCATTCATTGTCATACC	XM_670622

2.2 Methods

2.2.1 Propagation of *Eimeria falciformis*

The life cycle of *E. falciformis* was maintained by continuous passage in NMRI mice. In brief, oocysts were stored in potassium dichromate at 4°C up to 3 month. For purification (193), oocysts were washed 3 times in water, sterilized and flotated with NaOCl. Oocyst

numbers were quantified by using a McMaster counting chamber. For the infection experiments, eight-to-twelve-week old animals were orally infected with 100 µl of PBS containing 50 oocysts, unless specified otherwise. Oocyst numbers from individual animals were evaluated by keeping them in separate cages on grids, and collecting the feces on a daily basis. Feces were immersed in water and diluted in saturated NaCl for counting. Animals were weighed every day to monitor the weight loss during infection.

2.2.2 Cell culture

The epithelial cell line (YAMC, Young adult mouse colonic) was cultured in RPMI medium containing 5% FCS, 1 µg/ml insulin, 10 µM α-thioglycerol, 1 µM hydrocortisone and 5 U/ml IFN-γ (33°C and 5% CO_2). Human foreskin fibroblasts (HFF) were maintained in DMEM with 10% FCS, 2 mM glutamine, 1x MEM non-essential amino acids, 100 µg/ml streptomycin and 100 U/ml penicillin in a humidified chamber (37°C, 5% CO_2). The immortalized murine fibroblasts c-FOS$^{+/+}$ 1-98M (wt) and c-FOS$^{-/-}$ 7-98M (knockout) were cultured in DMEM supplemented with 10% FCS, 2 mM glutamine, 100 µg/ml streptomycin and 100 U/ml penicillin (37°C and 5% CO_2).

Confluent cells were harvested by using trypsin-EDTA and seeded into flasks, dishes or plates irrespective of the cell type.

2.2.3 Propagation of *Toxoplasma gondii*

T. gondii tachyzoites (RH strain) were maintained by serial passage in HFF cells. Parasitized cells were cultured in DMEM supplemented with 10% fetal calf serum, 2 mM glutamine, 1x MEM non-essential amino acids, 1 mM sodium pyruvate, 100 µg/ml streptomycin and 100 U/ml penicillin in a humified incubator (37°C, 5% CO_2).

2.2.4 Infection of host cells with parasites

YAMC cells, c-FOS wt and knockout cells were seeded into wells for 24 h, and then infected with *E. falciformis* sporozoites or *T. gondii* tachyzoites at a MOI of 6 and 2, respectively. Tachyzoites were recovered from infected HFF cultures. To obtain *E. falciformis* sporozoites, purified *E. falciformis* oocysts were digested with 0.4% pepsin (pH 3) at 37°C for 1 h followed by 3x washing. The oocyst pellet was mixed with glass beads (ø 0.5 mm) in a 1:1 ratio, and briefly vortexed to release the sporocysts. 0.25% trypsin and 0.75% sodium tauroglycocholate in DMEM containing 20 mM L-glutamine, 100 µg/ml streptomycin and

100 U/ml penicillin was added (37°C for up to 2 h) to sporocyst solution to excyst sporozoites. Sporozoites were column-purified by DE-52 anion exchange chromatography (194) and counted. The parasite-infected cells were washed and either suspended in TRIzol and stored at -80°C for microarray experiments, or the cells were fixed using 4% PFA for immuno-staining.

2.2.5 Indirect immunofluorescence assay

Cells grown on cover slips were fixed in 4% PFA for 10 min at the indicated time points, followed by neutralization with 0.1 M glycine/PBS (5 min, RT). Permeabilization was achieved by 0.2% triton-X100/ PBS for 20 min. Unspecific binding of antibodies was minimized by incubating samples with 2% BSA in 0.2% triton-X100/PBS, prior to incubation with the primary antibody in the blocking solution (anti-*Eimeria tenella*, 1:2000; anti-*Tg*Gap45, 1:3000, 1 h, RT). Samples were washed 3 times with 0.2% triton-X100/ PBS, and the secondary antibody was added (goat-anti rabbit IgG Alexa Fluor 488 or 594, 1:3000, 45min, RT). After washing in PBS, samples were mounted in Fluoromount G and visualized using a fluorescence microscope (Apotome, Carl-Zeiss, Germany) and processed with the AxioVision Documentation software (Carl-Zeiss). Parasite invasion was assessed by counting infected cells per high power field (4 h p. i., 400x magnification, 10 HPFs/sample). To monitor the development of *E. falciformis* at 39 h p. i., the entire cover slip was scanned for trophozoites and schizonts (400x magnification). To quantify *T. gondii* growth, 100 vacuoles were counted and the number of parasites per vacuole determined.

2.2.6 Transmission electron microscopy

Female NMRI were infected with 1500 oocysts, the animals were sacrificed from day 3 to day 8 during infection, and their caeca were removed and washed. Caecal tissues were fixed with 2.5% (v/v) glutaraldehyde and 2.0% (w/v) paraformaldehyde in 100 mM cacodylate buffer (pH 7.4) for 4 h at RT and for additional 12 h at 4 °C. Tissues were rinsed with 100 mM cacodylate buffer (3x, 15 min), and postfixed for 4 h with 2 % (v/v) osmium tetroxide and 3 % (w/v) potassium hexacyanoferrate (II) on ice. Samples were rinsed once with 100 mM cacodylate buffer for 30 min and washed with 5 mM maleate buffer (3x, 15 min). They were stained *en bloc* with 0.5 % (w/v) uranyl acetate, washed again with 5 mM maleate buffer (3x, 15 min), dehydrated in increasing amounts of ethanol and propylene oxide and embedded in Spurr resin. Thin sections were obtained (70-90 nm) with a Reichert Ultra Cut and counterstained with 4% (w/v) uranyl acetate followed by lead citrate. Imaging was done using

transmission electron microscope (Zeiss EM 900) equipped with a wide-angle CCD camera (TRS Systems, Moorenweis, Germany).

2.2.7 Isolation of epithelial cells

Caeca of infected and uninfected animals were isolated, washed in calcium- and magnesium-free Hank's BSS, opened longitudinally and cut into 5 mm sections. Tissues were transferred into tubes and incubated (30 min, 37°C) with Hank's BSS and DTT (1 mM) with a gentle shaking. Supernatants were discarded, and tissues were incubated (30 min, 37°C) in Hank's BSS and EDTA (1 mM), with intensive manual shaking every 10 min. Supernatants, obtain through a 70 µm cell strainer, were transferred into fresh tubes for centrifugation (1500 rpm, 5 min). Pellets were resuspended in 1 ml TRIzol Reagent and stored at -80°C for gene expression analyses or suspended in PBS/ 0.2% BSA/ 5 mM EDTA for flow cytometry.

2.2.8 Flow cytometry

Isolated caecal cells were counted using a Casy counter and adjusted to 10^6 cells/ml. Cells were washed with PBS/ 0.2% BSA/ 5 mM EDTA (1300 rpm, 5 min, 4°C), and treated with anti-mouse FcγR-blocker (20 µg/ml). They were stained with the following fluorescent antibodies for 30 min on ice: CD45-ef450 (1:200) and UEA1-FITC (1:80); CD4-ef450 (1:750) and CD8-Cy5 (1:600) followed by washing (1300 rpm, 5 min, 4°C). Cells were fixed in PBS/ 0.5% PFA and subjected to flow cytometry. Data were analyzed using the FlowJo Software.

2.2.9 Immunohistochemistry

The caeca of infected and uninfected animals were removed, carefully washed and stored in 4% PFA/PBS. Tissues were embedded in paraffin and cut into 2 µm sections. For staining, samples were deparafinized in xylene and rehydrated in a descending sequence of ethanol concentrations and then washed in water. Antigen retrieval was achieved by boiling samples in citric buffer (pH 6.0) in a pressure cooker. Slides were rinsed in water, washed in TBS and the respective primary antibody (rat anti-mouse, mIDO-48, 1:200 Biolegend; CD3, 1:20, Dako; B220, 1:200, eBioscience; F4/80, 1:100, eBioscience) was added (30 min). After washing with TBS, the sections were incubated for 30 min with the secondary antibody (biotinolyted rabbit anti-rat, 1:200, 30 min, Dako). Streptavidin-conjugated alkaline phosphatase (Dako) was applied onto the sections for 30 min, and the reaction was visualized

by Fast RED (Dako). Slides were rinsed in water and counterstained with hematoxylin. Images were obtained using a LEICA DMIL microscope attached with a LEICA DFC 480 camera and processed with LEICA Application Suite (Version 2.8.1). The average number of positively stained cells for at least 10 high power fields per animal was assessed to determine $CD3^+$, $B220^+$ and $F4/80^+$ stained cells.

2.2.10 Western Blot

Immunoblot analysis of the caecal tissue homogenates was performed using the polyclonal rabbit anti-IDO and anti-beta tubulin (Genscript), and horseradish peroxidase-labeled anti-rabbit secondary antibodies (GE Healthcare). The caeca of uninfected or infected female NMRI mice were removed, washed and snap frozen in liquid nitrogen. Total proteins were prepared in a lysis buffer containing 10 mM Tris-HCl (pH 7.2), 150 mM NaCl, 1% Triton X-100, 1% sodium deoxycholate, 1 mM PMSF and protease inhibitor cocktail (Sigma-Aldrich). Tissue samples were homogenized and centrifuged (5 min, 4°C, and 12000 rpm). The protein amount in the supernatant was determined by the bicinchoninic acid assay (Pierce). 30 µg of total protein was separated on a 12% SDS-PAGE and blotted onto a nitrocellulose membrane (Applichem). Unspecific binding was blocked by overnight incubation in 5% skimmed milk powder in TBS containing 0.2 % Tween-20 (TBS-T). The primary antibody (1:1000) was applied in blocking solution for 2 hrs at RT, followed by 3x washes in TBS-T and treatment with the secondary antibody (1:3000, 45 min at RT). Samples were subjected again to 3 washes in TBS-T, and the protein bands were detected by enhanced chemiluminescence (GE Healthcare). The same blots were used to detect anti-beta tubulin (protein loading control) using the immunoblot recycling kit (Alpha Diagnostic). Protein expression was quantified by densitometric method using Adobe Photoshop suite.

2.2.11 Antigen preparation, cell proliferation and cytokine assays

Purified oocysts were digested with 0.4% pepsin (pH 3, 37°C, 1 h; Sigma-Aldrich) and centrifuged (1800 g, 10 min). The oocyst pellet was mixed with 0.5-mm glass beads (Sartorius) in a 1:1 ratio, and briefly vortexed to release free sporocysts. To excyst the sporozoites, DMEM containing 0.25% trypsin, 0.75% sodium tauroglycocholate, glutamine (20 mM), streptomycin (100 µg/ml) and penicillin (100 U/ml) was added and samples were incubated at 37°C up to 2 h. Sporozoites were column-purified by DE-52 anion exchange chromatography (194), and adjusted to $2x10^6$ parasites/ml in DMEM. The parasite antigen was prepared by 3 freeze-thaw cycles in liquid nitrogen and stored at -80°C.

To perform cell proliferation and cytokine assays, spleens and intestinal mesenteric lymph nodes (MLN) were extracted, and single cell suspension was prepared by passaging the tissue through a 70-µm cell strainer. Cell number was adjusted to $3.5x10^6$ cells/ml in RPMI medium supplemented with FCS (10%), glutamine (20 mM), streptomycin (100 µg/ml) and penicillin (100 U/ml). About $3.5x10^5$ cells were incubated with sporozoite antigen (equivalent to $1.17x10^5$ parasites/well) for 48 h at 37°C and 5% CO_2. Supernatants were collected for cytokine detection, and the cells were pulsed with methyl-[^{3}H]-thymidine (1 µCi/well, GE Healthcare) for 20 hrs at 37°C. Incorporation of ^{3}H-thymidine was measured by liquid scintillation counting using a 1450 MicroBeta TriLux Microplate Scintillation and Luminescence Counter (PerekinElmer). The cytokine levels in the supernatants were measured using the mouse ELISA Ready-SET-Go kit (eBioscience).

2.2.12 Pharmacological administration of chemicals in mice

(S)-ESBA ((S)-(4-Ethylsulfonyl)benzoylalanine hydrochloride, Enzo Life Sciences) inhibits kynurenine aminotransferase II (KAT-II) (195), and Ro61-8048 (3,4-dimethoxy-N-[4-(3-nitrophenyl)thiazol-2-yl]-benzenesulfonamide, Tocris Bioscience) is a competitive inhibitor of kynurenine 3-hydroxylase (196). The stock solutions (100 mM) in PBS were prepared for both inhibitors. The animals infected with *E. falciformis* were treated once daily *via* oral tube with 1 mM of Ro 61-8048 or (S)-ESBA diluted in 100 µl PBS. To inhibit indoleamine 2,3-dioxygenase, mice were administered with 1-methyl-DL-tryptophan (5 mg/ml of L- and 2 mg/ml of D-1-MT, Sigma Aldrich) in drinking water supplemented with artificial sweetener (Aspartame), which was changed every two days. Xanthurenic acid (300 mg/kg body weight, Sigma Aldrich) was applied *via* oral tube, or at 200 mg/kg body weight intra-peritoneally. All treatments started two days prior to infection and continued until the end of the experiments.

2.2.13 RNA isolation and transcript analysis

The PureLink RNA mini kit (Life Technologies) was used to extract total RNA following the manufacturer‘s instruction. 100 ng RNA was reverse-transcribed into first-strand cDNA (SuperScript III First-Strand Synthesis SuperMix for qRT-PCR, Life Technologies) for PCR (1.5 mM $MgCl_2$, 0.2 mM dNTP, 1 µM forward and reverse primers, 1.25 U GoTaq DNA Polymerase), or subjected to quantitative real-time PCR (SuperScript III Platinum SYBR Green One-Step qRT-PCR Kit with ROX). Primers used for PCR and qPCR were designed based on the NCBI accession numbers. The gametocyte-specific primer pairs (*Ef*Gam56 and

*Ef*Gam82) were designed based on an ongoing *E. falciformis* sequencing project (courtesy of Dr. Simone Spork and Dr. Christoph Dieterich).

2.2.14 Microarray experiments and data analysis

Total RNA isolated from caeca or from YAMC cell cultures was subjected to the two-color microarray using whole-genome mouse chip (4 x 44K). The microarray chip contains 4 independent 44K arrays on one slide. The samples were tested for integrity using Bioanalyzer (Agilent Technologies) and processed according to manufacturer's instructions. Briefly, extracted RNA was reverse-transcribed into cDNA and then labeled with Cy3 and Cy5 during cRNA synthesis followed by purification and quantification. 825 ng of total cRNA from each sample were mixed with the fragmentation mix and hybridized to the arrays (Agilent Technologies). The chips were scanned at 5 µm resolution using an Agilent scanner (G2565CA high-resolution laser).

The images were extracted for features using G2567AA feature extraction software (Version A 7.1.1.1, Agilent Technologies) using default sections. This program subtracts the background from the features and performs dye normalization to yield refined microarray data. The dye ratios were calculated using the most conservative estimate of error between the universal error model and propagated error. The feature extraction results were entered into a data analysis program (Rosetta Inpharmatics Resolver software, Version 4.0). Significantly modulated genes were identified by anti-correlation of the dye-reversal ratio, which was detected by correlating the ratio between two colors of each sample from the first array and of the same sample in the second array, in which the dye-colors were swapped. Only anti-correlated genes were considered to be differentially regulated. The software also calculates a probability value using a variety of internal controls, including the degree of anti-correlation for each measured ratio. The expression patterns were identified using a 1.5-fold cut-offs and an error-weighted p-value below 0.01.

IPA (Ingenuity Pathway Analysis software, Ingenuity® Systems) and the web-accessible program DAVID (Database for Annotation, Visualization and Integrated Discovery) were used for biological analysis of the gene expression data.

2.2.15 *P. berghei* infection and parasitemia

The mice were infected with 20 x 10^6 *P. berghei* (ANKA) by intraperitoneal injection. A drop of blood from the tail was collected and smeared on a microscopic slide to determine the parasitemia of infected mice. The dried blood smear was fixed in methanol for five minutes followed by Giemsa staining (1:5 diluted in water) for 15 minutes. Slides were rinse with tap water, dried and parasitemia was assessed under the microscope (100x).

2.2.16 Infection of mosquitoes and determination of oocysts

On day 3 of mice infection, a drop of blood from the tail was examined under the microscope to determine the number of exflagellation events. With a sufficient exflagellation number (3/field, 100x), mosquitoes (*Anopheles stephensi*) were fed on the anesthetized mice. The insects were dissected on day 9 post-infection, and the number of fluorescent oocysts in the mosquito mid-gut was quantified under the microscope.

2.2.17 Purification of *P. berghei*

Blood was harvested by heart puncture of isofluoran-anesthetized mice on day 3 p. i. using heparin-treated syringes. Parasites were column-purified using a syringe containing wool, cellulose and glass beads. They were centrifuged (1800 rpm, 8 min), and the pellet was mixed with saponin and centrifuged (1800 rpm, 8 min) again. The pellet was washed with 1 ml PBS (7000 rpm, 2 min) and resuspended in 1 ml TRIzol for quantitative PCR.

2.2.18 Data plotting and statistical analyses

The results were plotted using GraphPad prism suite. All data show the mean ± SEM of two to three independent experiments using 5-6 mice each unless specified otherwise. The two-tailed non-parametric Mann-Whitney test was used to determine the statistical significance, and a p-value below 0.05 was considered as significant.

3. Results

3.1 *Eimeria falciformis* has a stringently regulated life cycle in its natural host

3.1.1 *E. falciformis* completes its entire life cycle in a single host

Transmission electron microscopy was performed (Fig. 10) to investigate *in vivo* stages of *E. falciformis*. The NMRI mice were infected with a dose of 1500 oocysts.

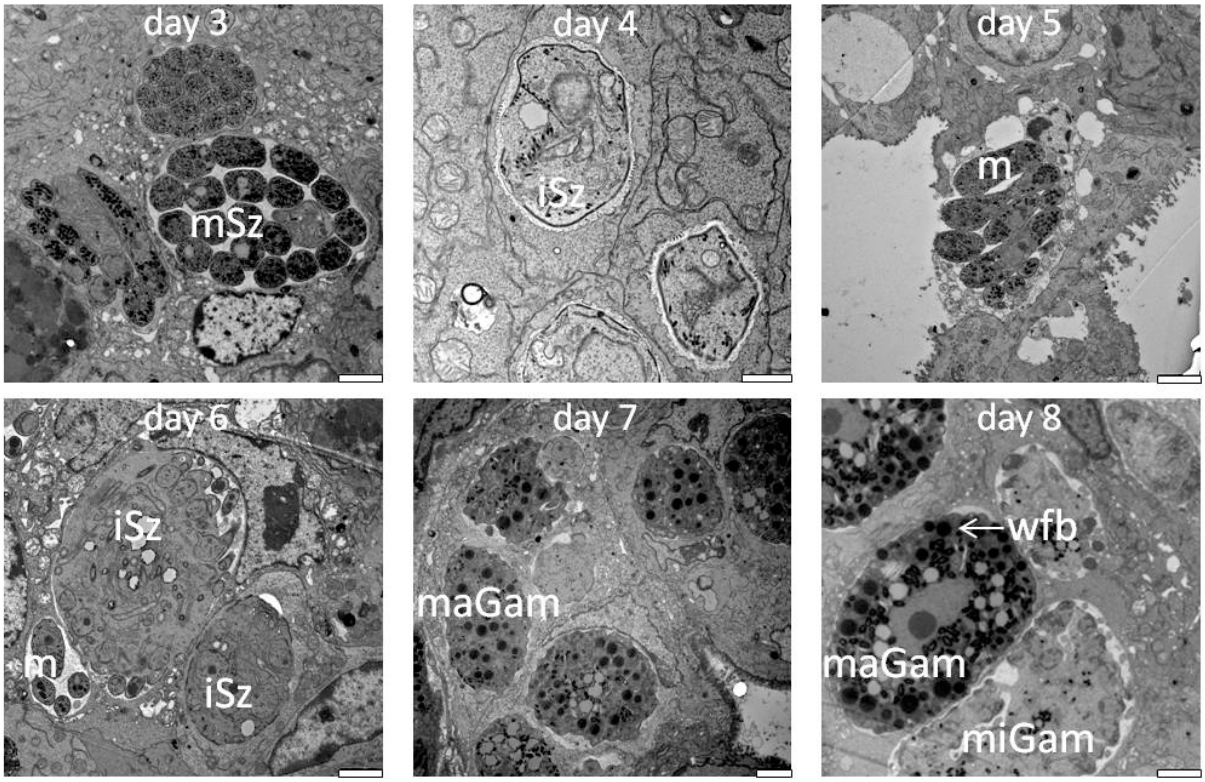

Fig. 10: Life cycle of *E. falciformis* in its natural host, the mouse. NMRI mice infected with 1500 oocysts were dissected from day 3 to day 8 of infection, and parasitized caecal tissue samples were subjected to transmission electron microscopy. Only representative images are shown in the panel. Bars, days 3 and 5-8, 2.5 µm; day 4, 1 µm. mSz, mature schizont; iSz, immature schizont; m, merozoite; maGam, macrogametocyte; miGam, micorgametocyte; wfb, wall-forming body.

Immature and mature schizonts in their vacuoles were visible in the caecum tissue samples from day 3 to day 6, which represent the asexual parasite development (Fig. 10). We detected mature schizonts on day 5 post-infection, which showed a disrupted PV and released merozoites. The schizonts were frequently located just beneath the microvilli of the epithelium. We further observed schizonts in three different developmental stages on day 6. An immature schizont with nuclei at its periphery contained developing merozoites, an immature schizont with budding merozoites, and in the lower left corner a mature schizont

harboring merozoites about to be released following host cell lysis. Imaging of early developmental stages was not feasible on days 1 and 2. However, the parasites could be detected by qPCR (Fig. 11A). The ratio of host to parasite 18S ribosomal RNA or ORF470 (an apicoplast specific gene) increased over 7 days and then declined on day 8, indicating a constant increase in the parasite burden during the infection period.

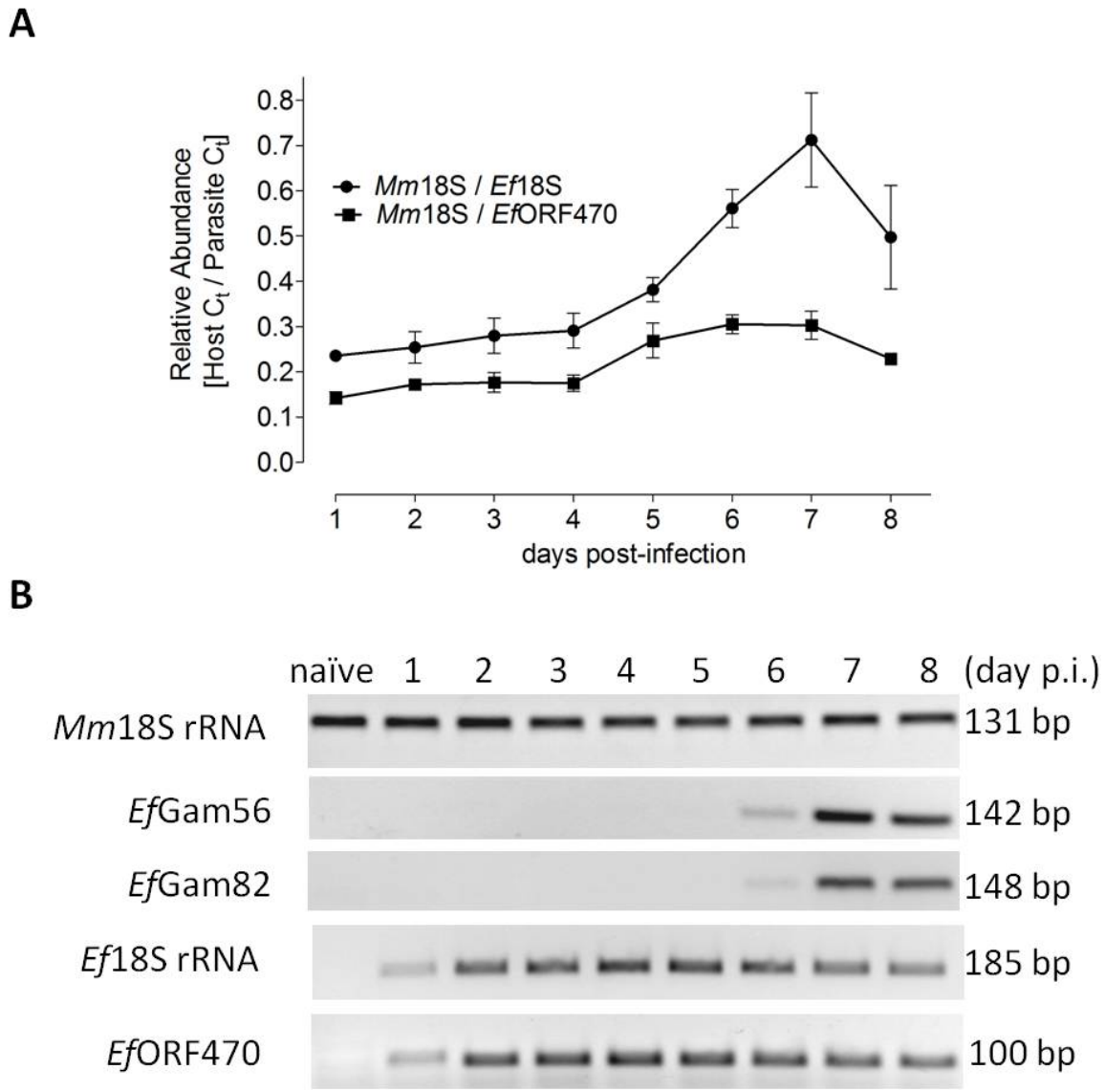

Fig. 11: PCR detection of *Eimeria* growth and transition to sexual development. Total RNA was isolated from the parasitized NMRI animals infected with 50 oocysts and subjected to Real-Time PCR **(A)** or standard PCR **(B)** for indicated transcripts. **(A)** Real-Time PCR of parasite transcript ORF470 and18S rRNA and the mouse 18S rRNA. The host / parasite ratio reflects the increasing amount of parasite transcripts during infection based on the respective C_t values. Bars show the mean ± SEM of three independent experiments. **(B)** The *Ef*ORF470, *Ef*18S and *Mm*18S rRNA was detectable throughout the course of infection. *Ef*Gam56 and *Ef*Gam82 were first detectable on day 6 post-infection.

The onset of sexual development with developing macrogametocytes was first visible on day 7 in infected tissue (Fig. 10). However, the presence of sexual stages from day 6 onwards was confirmed by detection of macrogamont-specific transcripts (*Ef*Gam56 and *Ef*Gam82; Fig. 11B). Figure 10 further depicts a mature macrogamont with a centrally-located nucleus and wall-forming bodies and a mature microgamont in close proximity on day 8 post-infection. The beginning of the sexual development on day 6 is consistent with the oocyst output starting from day 7 onwards.

3.1.2 Dose-dependence of *E. falciformis* infection in the mouse

To elucidate the optimal infectious dose for further experiments, NMRI and BALB/c mice were infected with increasing numbers of *E. falciformis* sporulated oocysts (SOZ; 10, 100, 500, and 1000) and the oocyst output was determined from day 6 to day 14. Irrespective of the inocula, the first batch of oocysts was detectable on day 7, which sustained until day 12 - 13 of infection, indicating a stringently synchronized development of the parasite (Fig. 12). NMRI mice (Fig. 12A, C) infected with 10 oocysts shed in total 1.7×10^6 ($\pm 1.2 \times 10^6$). A 10-fold increase in the applied oocyst dose led to an ~ 3-fold increase in the total numbers ($5.2 \times 10^6 \pm 1.2 \times 10^6$), and administration of 500 oocysts resulted in yet another nonlinear enhancement in the oocyst yield ($7.5 \times 10^6 \pm 2.2 \times 10^6$). Likewise, the highest infectious dose achieved only a slightly enhanced oocyst production ($7.6 \times 10^6 \pm 1.3 \times 10^6$), indicating a saturated infection. In comparison to the outbred NMRI animals, the inbred BALB/c strain infected with 100, 500, and 1000 oocysts shed about 50% less oocysts (Fig. 12B, D), whereas the total numbers of oocysts in the feces of BALB/c mice inoculated with 10 oocysts ($1.4 \times 10^6 \pm 0.6 \times 10^6$) were comparable to the numbers obtained from NMRI mice. Both strains produced the first oocysts on day 7, and the peak days were not influenced by low and high doses, confirming identical prepatent and patent periods regardless of the animal strain or inocula.

In addition to the oocyst counting, the infected animals were weighed every day to assess pathology starting from day 5 p. i. (Fig. 12E, F). The infection resulted in a loss of body weight during day 7 to day 10 p. i. in both strains, which was followed by a recovery from day 11 onwards. Neither in NMRI nor in BALB/c did the infection with 10 oocysts cause a body weight loss above 6%. Even the infection with 500 or 1000 oocysts was well tolerated in the NMRI strain, because the animals did not loose more than 16% of their body weight (Fig. 12E). In contrast, nearly half of the BALB/c mice succumbed to infection with 500 (50%) or

1000 (66.66%) oocysts. However, these data show that both mouse strains have an identical and regulated parasite cycle. Moreover, NMRI mice can be infected even with a very high dose of *E. falciformis* oocysts.

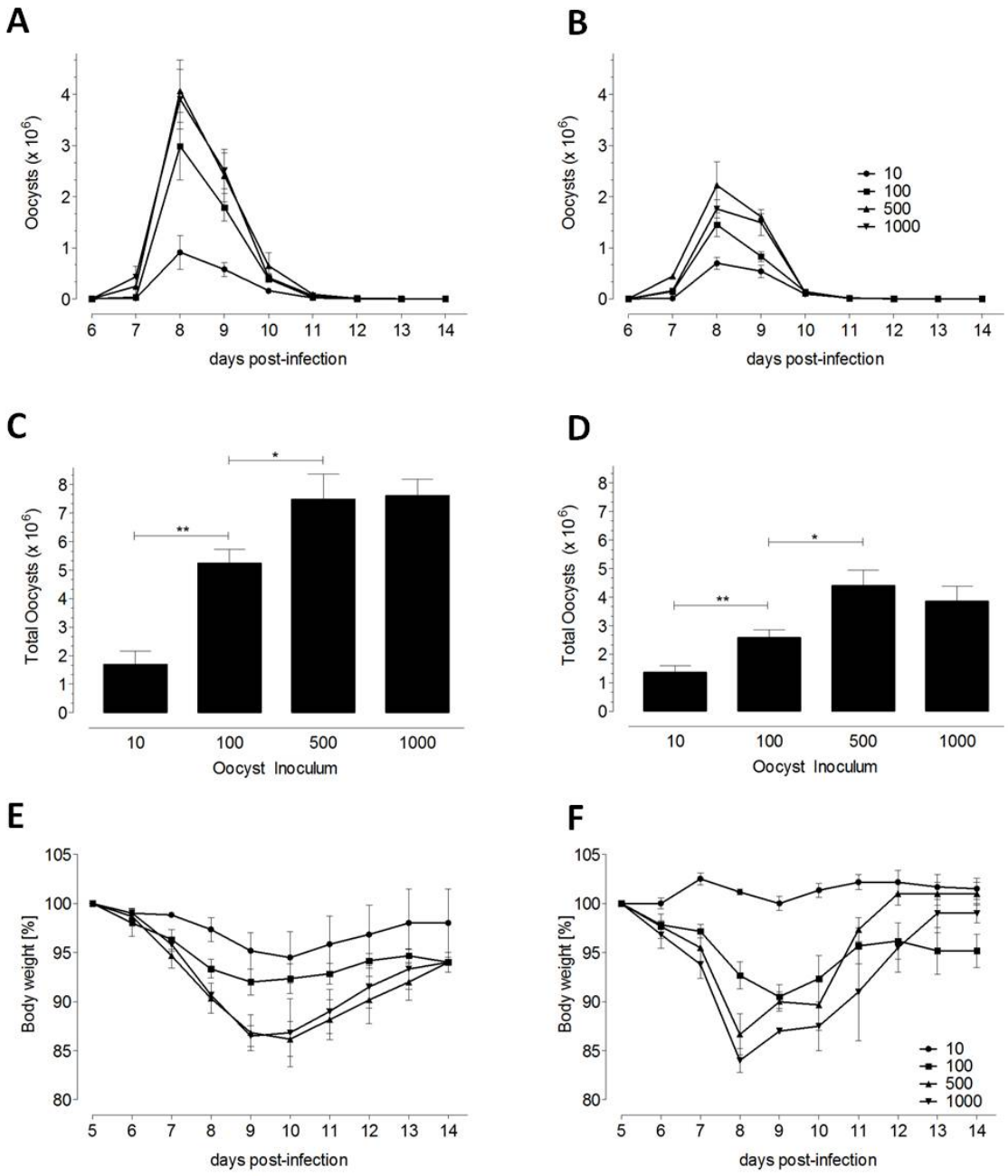

Fig. 12: Dose-dependence of *E. falciformis* infection in mouse and body weight loss. NMRI **(A, C, E)** and BALB/c **(B, D, F)** mice were infected with indicated doses of parasite oocyst and kinetics **(A, B)** and oocyst shedding **(C, D)** in the feces were monitored. The body weights of infected NMRI **(E)** and BALB/c **(F)** were determined to assess pathology and normalized to day 5 post-infection. Graphs show the mean ± SEM of two independent experiments each with 3 animals per group.

3.2 Host response against *E. falciformis* by microarray analyses

3.2.1 *In vitro* microarray analyses

3.2.1.1 *In vitro* microarray using the colonic epithelial cell line YAMC

E. falciformis invades and replicates mainly in the upper half of the colon and caecum (32), therefore a colonic epithelial cell line (YAMC, Young adult mouse colon (189)) was chosen. These cells originate from transgenic mice harboring a temperature-sensitive mutation of the SV40 large tumor antigen, which is under the control of the IFN-γ regulatable MHCII promoter. Cells require IFN-γ and a permissive temperature of 33°C for an optimal growth.

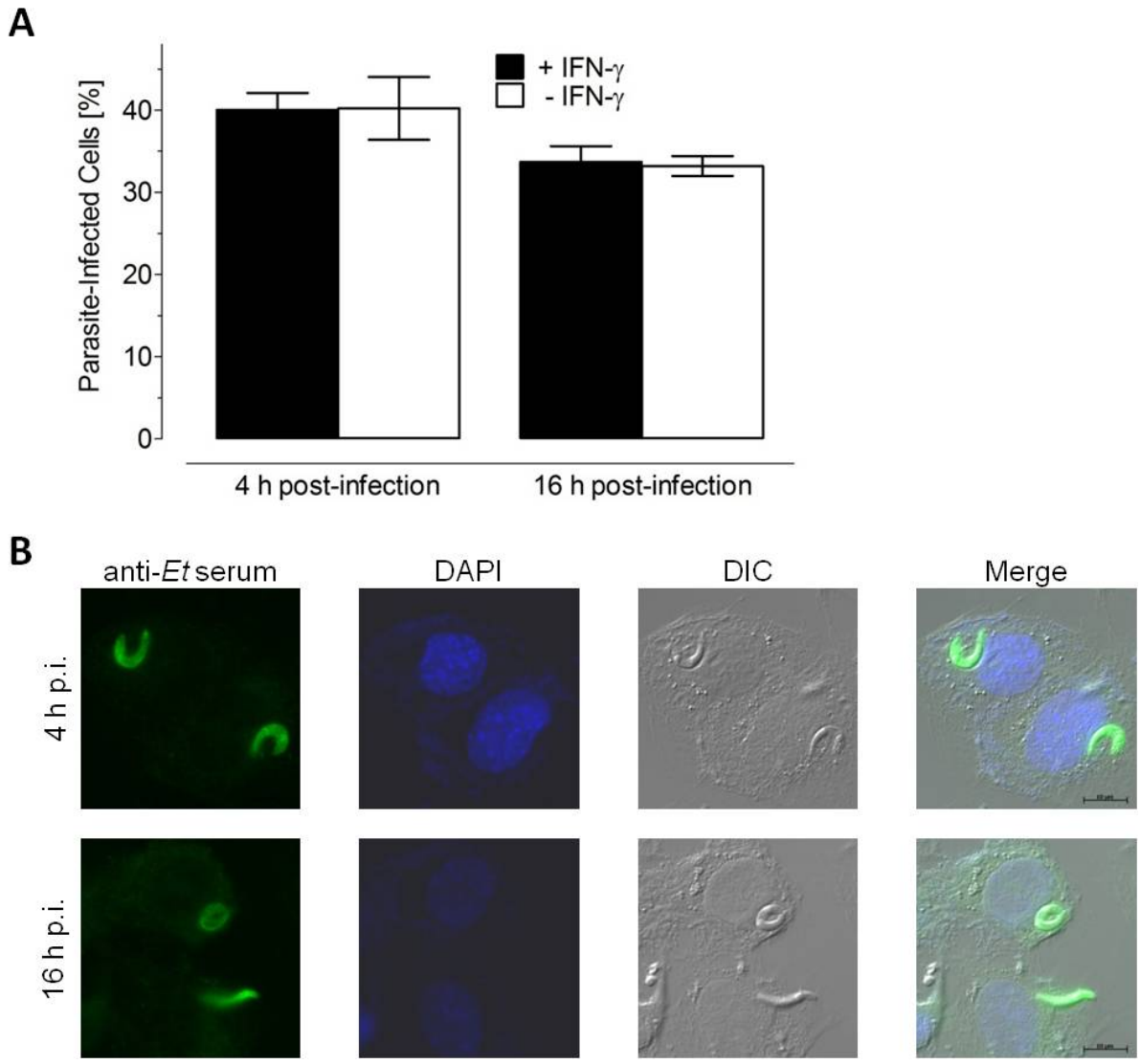

Fig. 13: Invasion and development of *E. falciformis* in YAMC cells. (A) Invasion was determined by counting intracellular sporozoites/HPF. The number of parasitized host cells was comparable in the presence or absence of IFN-γ. Data represent the mean ± SEM of three independent experiments. **(B)** Parasites were immuno-stained using anti-*Eimeria tenella* serum. Bar, 10 µm.

In addition to *E. falciformis* infection of YAMC cells, these cells were also infected with *T. gondii* (RH strain) for comparison. In contrast to the asexual stages of *T. gondii*, no efficient *in vitro* culture for *E. falciformis* exists. Mesfin *et al.* (197) described the presence of trophozoites first visible *in vivo* 18 h post-infection. Although *E. falciformis* can invade host cells *in vitro*, further development into advanced stages is very limited. Therefore, two early time points (4 h and 16 h p. i.) for the microarray were selected. A multiplicity of infection (MOI) of 6 was used to ensure a high percentage of parasitized cells.

About 40% (± 3%) of the cells were infected 4 h p. i. by *E. falciformis* (Fig. 13A). At 16 h p. i. fewer cells were parasitized by *E. falciformis*, when compared to 4 h p. i. (34% ± 3%; Fig. 13A). The intracellular sporozoites rounded up within 4 h (Fig. 13B) and advanced stages of these structures were observed at the 16 h time point. *In vivo* these parasites would develop further into mature trophozoites. However, neither trophozoites nor schizonts were observed in the *E. falciformis*-infected YAMC cells 24 h and 43 h p. i. (data not shown). Infections with *T. gondii* resulted in similar numbers of parasitized cells (44% ± 7%) at 4 h post-infection (Fig. 14A). To further monitor the *T. gondii* development, the parasites per vacuole were quantified (Fig. 14B). About 21% (± 5%) of all vacuoles harbored two parasites 16 h post-infection. Furthermore, the majority of the parasite vacuoles harbored two parasites 24 h p. i., whereas about 15% (± 3%) of them contained 4 parasites. No vacuole with 8 parasites was observed.

As described by Whitehead *et al*. (189), YAMC cells can be cultured without IFN-γ (for a short time). However, the data show that the absence of IFN-γ did not affect the infection or development by *E. falciformis* and *T. gondii* (Fig. 13A, 14A). Therefore, cells for the microarray studies were cultured in the presence of IFN-γ to ensure an adequate growth of the IFN-γ dependent cell line. In addition, the presence of IFN-γ also mimics an environment comparable to the *in vivo* situation. Based on the invasion studies, the two time points, 4 h and 16 h p. i., were suitable for elucidating the *in vitro* host response.

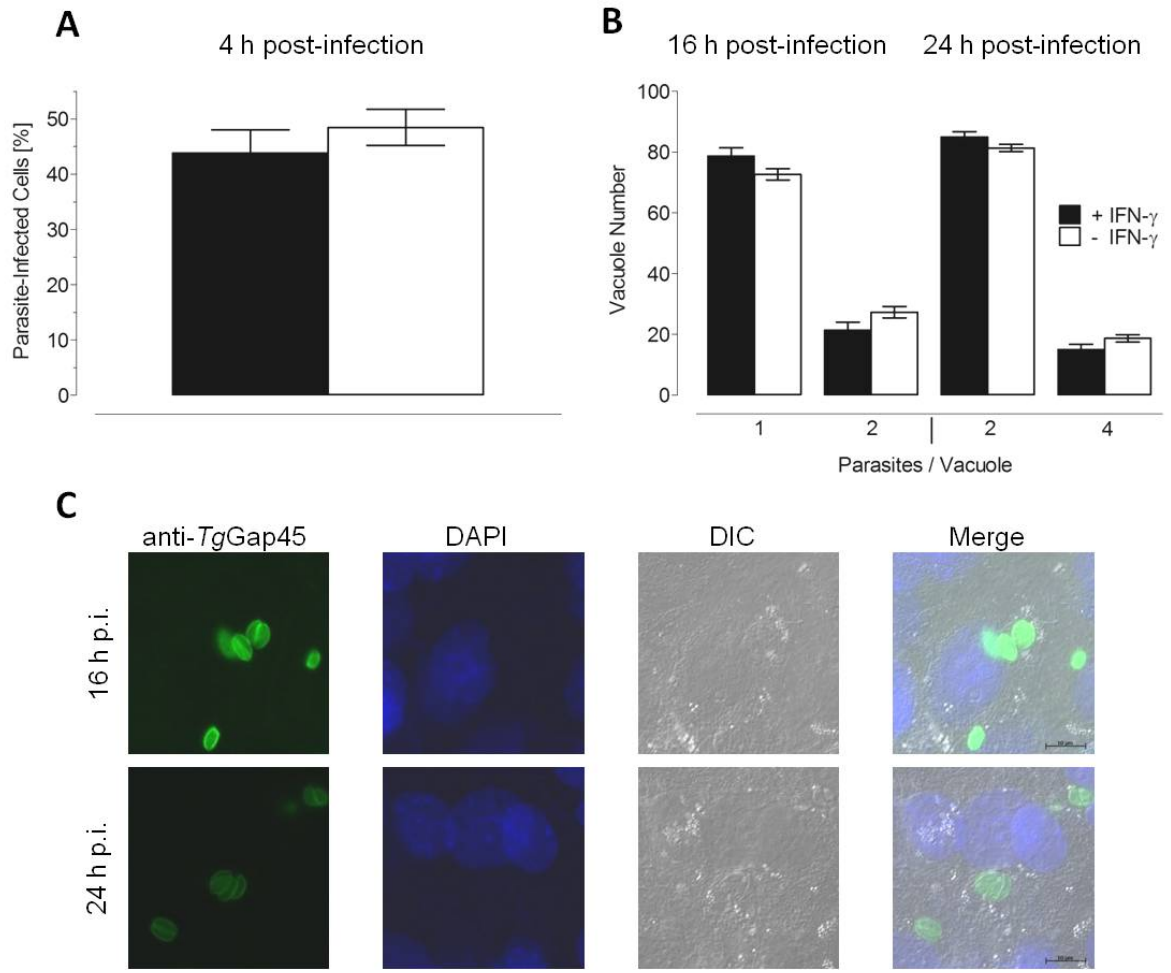

Fig. 14: Invasion and development of *T. gondii* in YAMC cells. (A) Invasion was determined by counting tachyzoites/HPF. Infection was comparable in the presence or absence of IFN-γ. **(B)** The number of parasites per vacuole was assessed at 16 h and 24 h p. i. Data represent the mean ± SEM of three independent experiments. **(C)** Parasites were immuno-stained by using anti-*Tg*GAP45. Bar, 10 µm.

3.2.1.2 *E. falciformis* induces distinct host transcripts in YAMC cells

A two-color dye-swap microarray assay (Agilent 4x44K) was performed using RNA isolated from parasitized cells (4 and 16 h p. i.). The expression patterns were identified using a stringent cut-off of 1.5-fold and an error-weighted p-value of < 0.05. Two independent experiments were performed to increase the reliability of the dataset. Infection caused a substantial modulation of 1239 unique transcripts (1400 probesets). 253 transcripts (43%) were exclusively up-regulated at 4 h p. i., and 335 (57%) genes were down-regulated (Fig. 15A). Nearly half of the induced and 70% of the repressed transcripts exhibited only a moderate alteration in their expression levels ranging from 1.5 to 2-fold (Fig. 15B). 128 (~ 50%) induced and 114 (~ 30%) repressed genes showed a differential expression between 2

and 4-fold. Only a few appeared modulated more than 4-fold, of which 19 were induced and 2 were repressed. None of the genes at 4 h p. i. was changed more than 10-fold.

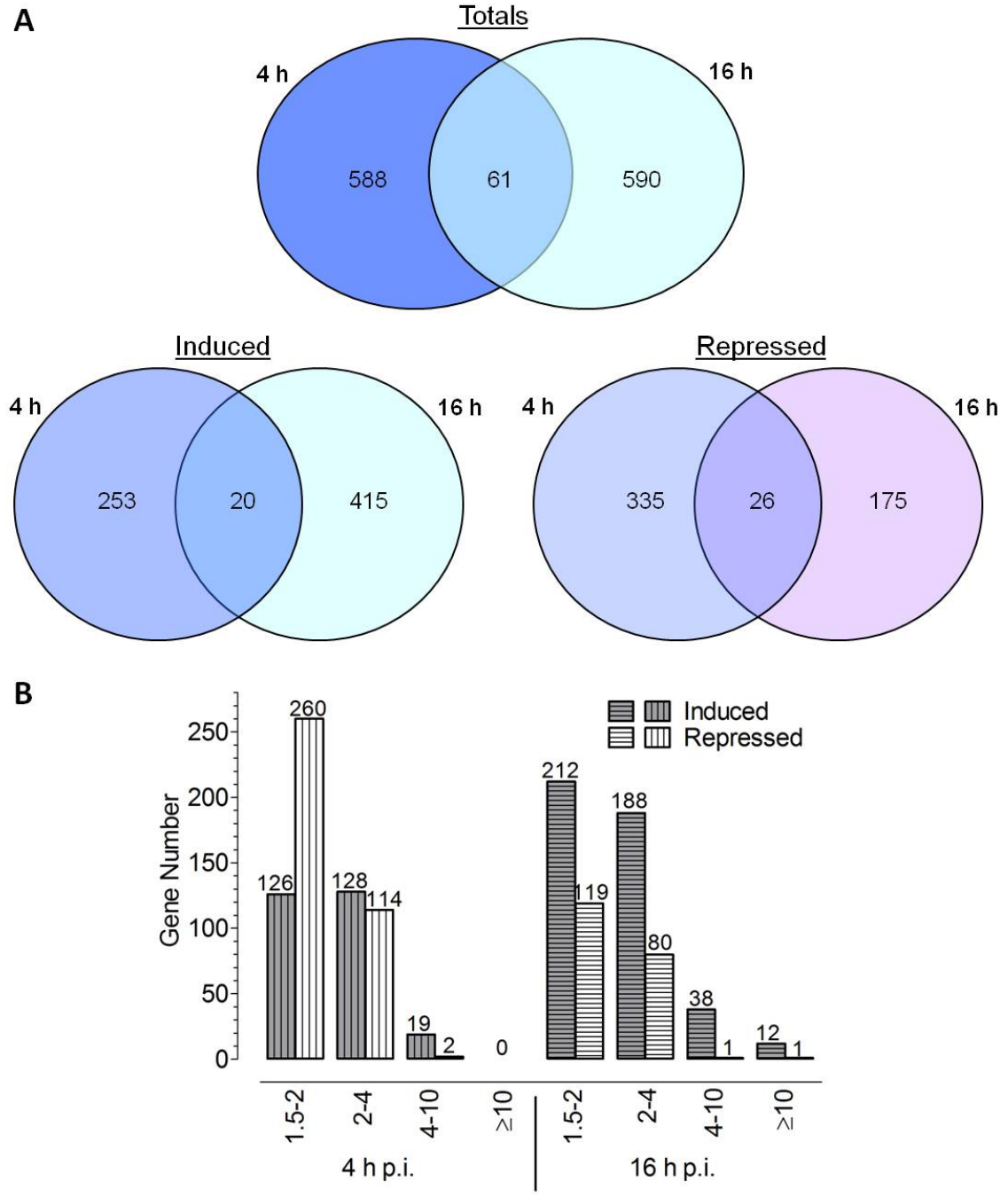

Fig. 15: *E. falciformis*-induced modulation of the mouse transcriptome. (A) Venn diagram of the mouse genes modulated by infection. The diagrams depict the total induced or repressed genes, which appeared regulated based on 1.5-fold cut-off and anti-correlation criteria. The overlapping regions signify commonly modulated genes. **(B)** Fold-change distribution of gene expression during infection.

Among the 590 uniquely modulated transcripts, 415 (70%) were induced and 175 (30%) repressed at 16 h p. i. (Fig. 15A). Thus, nearly twice as much genes appeared up-regulated but only half as much where down-regulated when compared to 4 h infection. About 50% of all

induced genes and 60% of the repressed transcripts at 16 h showed only a moderate fold change of 1.5 to 2-fold (Fig. 15B). For 188 (41%) of the up-regulated and 80 (40%) of the down-regulated genes the fold change varied from 2 to 4-fold. 38 (8%) induced and only 1 (0.5%) repressed transcript showed a 4 to 10-fold change in their expression. 12 (3%) up-regulated and 1 (0.5%) down-regulated transcript showed a fold change greater than 10.

Interestingly, the expression of only 61 genes appeared changed early as well as late during infection (Fig. 15A), 20 of which were induced, and 26 were repressed. In addition, among the 61 genes, 15 genes were reciprocally regulated. These genes were repressed at 4 h but induced at 16 h p. i. (Appendix B).

3.2.1.3 *T. gondii* substantially modulates the mouse transcriptome

YAMC cells were also infected with *T. gondii* tachyzoites, which can invade and replicate leading to a successful parasite development. A total of 1145 host genes (1290 probesets) were modulated in response to infection, most of which appeared only 16 h p. i. (Fig. 16A). Among the 62 genes differentially expressed at 4 h p. i., only 14 genes were uniquely modulated at the early time point (9 induced, 5 repressed). A moderate change of 1.5 to 2-fold was observed for 19 induced and 29 repressed transcripts at 4 h p. i. (Fig. 16B). 6 induced and 3 repressed genes showed a 2 to 4-fold fold-change, and only 5 genes were more than 4-fold up-regulated. Later during infection, 434 (40%) genes were exclusively up-regulated and 649 (60%) were down-regulated (Fig. 16B). Nearly the half of all genes exhibited a 1.5 to 2-fold difference in expression. About 38% (175) of the induced and 41% (280) of the repressed genes showed an altered expression between 2 to 4-fold, and 10 up-regulated and 13 down-regulated genes ranged between 4 to 10-fold. Only 4 transcripts showed a more than 10-fold induction in comparison to uninfected controls.

Although only a few genes were modulated early in response to *T. gondii* infection of YAMC cells, most of them were also present late during infection. In contrast to *E. falciformis*, we did not observe reciprocally regulated genes during early and late infection. Interestingly, a much smaller set of genes (62) was modulated in response to *T. gondii* infection as compared to *E. falciformis* (649) at 4 h post-infection.

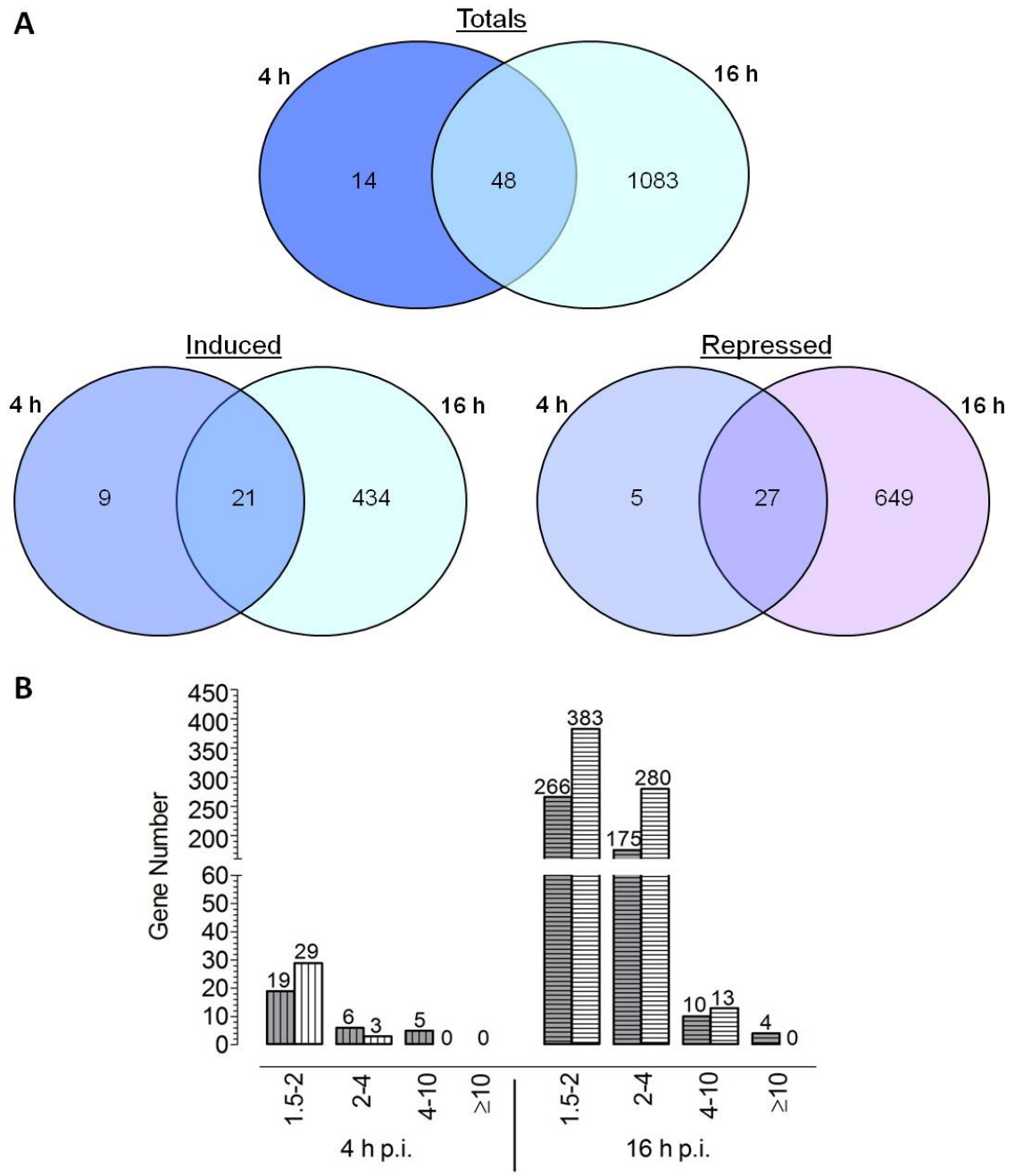

Fig. 16: *T. gondii*-induced modulation of the mouse transcriptome. (A) Venn diagram of mouse genes modulated in response to infection. The diagram depicts the total induced or repressed number of *T. gondii*-infected mouse genes based on 1.5-fold cut-off and anti-correlation criteria. The overlapping regions signify common modulated genes. **(B)** The fold-change distribution of gene expression following infection.

3.2.1.4 Biological categories affected in *E. falciformis* and *T. gondii*-infected cells

To evaluate the functional categories significantly altered (p-value < 0.05) during infection, the data were analyzed by using ingenuity pathway analyses (IPA, Ingenuity® Systems, www.ingenuity.com). Many genes belong to more than one category (for descriptions of the IPA categories see Appendix A), and the number of induced or repressed transcripts within the category does not reflect the direction of a pathway. To resolve such issues, selected transcripts and pathways must be evaluated by literature searches.

The affected categories were grouped into standard cellular processes (Fig. 17), immune response (Fig. 18) and metabolism (Fig. 19). The general cellular functions affected by *E. falciformis* and *T. gondii* infection (Fig. 17) include the cellular development, growth and proliferation, movement, maintenance, assembly and organization, gene expression, cell death, cell-to-cell signaling and interaction, cell cycle, and morphology. Interestingly, the expression of more genes was repressed than induced in each category at 4 h post-*Eimeria* infection, whereas the opposite was observed at 16 h post-infection. In contrast, more genes were up-regulated than down-regulated following 4 h of *T. gondii* infection, and the majority of them were repressed late during infection.

In contrast to genes involved in cellular processes, fewer genes participate in functions associated with the host immune response (Fig. 18) or host metabolism (Fig. 19). Immunity-related categories include inflammation, cell-mediated and humoral immune response as well as immune cell trafficking and antigen presentation. A higher number of immunity-related processes were observed at 16 h post-*Eimeria* infection compared to the early time point. Again, at 4 h post-*Eimeria* infection the expression of more genes was repressed as compared to induced in each category, whereas the opposite was observed at 16 h. The transcription of most immunity-related genes was repressed during *T. gondii* infection.

Significantly altered metabolic processes during *E. falciformis* and *T. gondii* infection include small molecule biochemistry, molecular transport and lipid metabolism. Other categories, including carbohydrate, vitamin and mineral, nucleic acid and amino acid metabolism, did not meet the criteria of statistical significance for all time points.

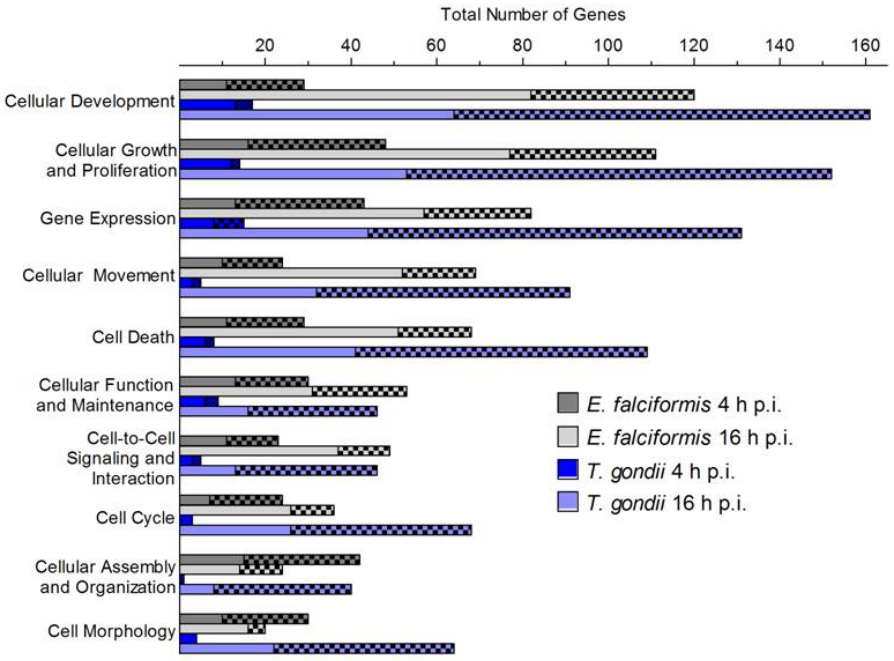

Fig. 17: Cellular phenomena affected in the parasitized YAMC cells. Functional analysis of induced (smooth) and repressed (shaded) genes during *E. falciformis* and *T. gondii* infection of YAMC cells ($p < 0.05$).

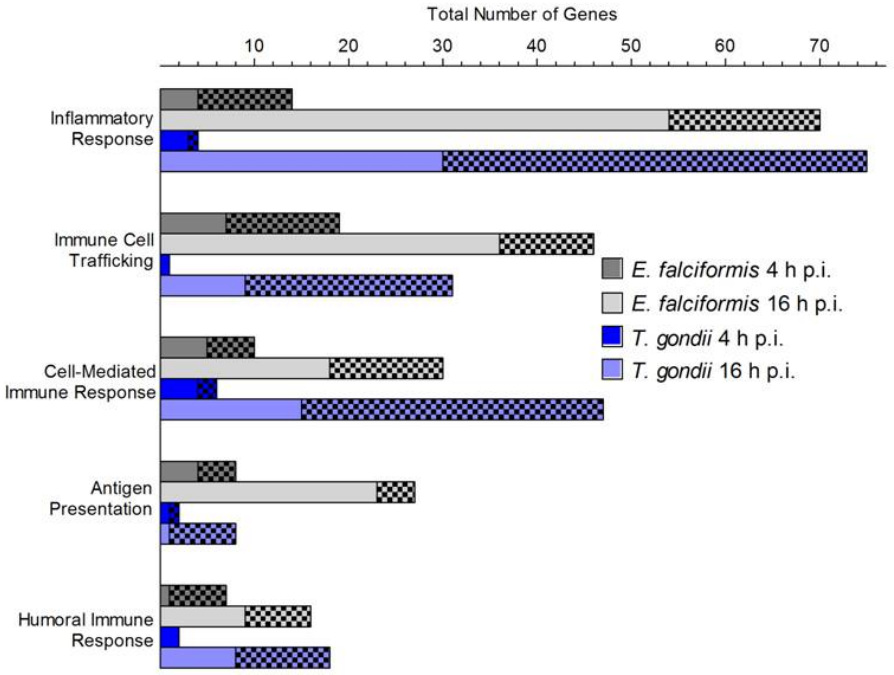

Fig. 18: Immunity-related processes upon infection of YAMC cells with *E. falciformis* and *T. gondii*. Functional analysis of up-regulated (smooth) and down-regulated (shaded) genes following infection ($p < 0.05$).

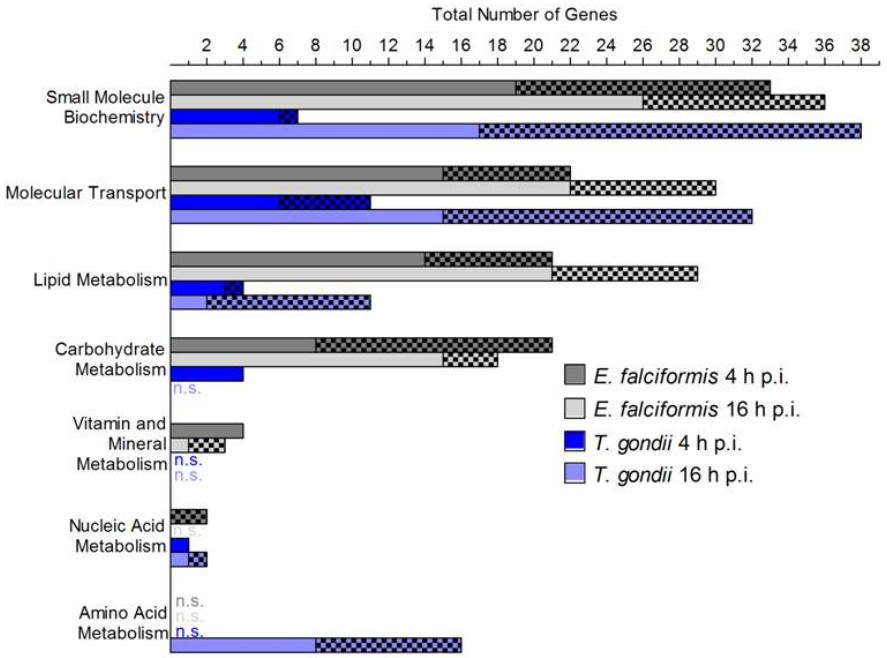

Fig. 19: Metabolic functions changed during infection of YAMC with *E. falciformis* and *T. gondii*. Functional analysis of induced (smooth) and repressed (shaded) genes ($p < 0.05$). n.s., not significant.

3.2.1.5 Pathways modulated during *E. falciformis* and *T. gondii* infection

The web-accessible program DAVID (Database for Annotation, Visualization and Integrated Discovery, (192, 198)) was used to visualize affected pathways. Although about 600 genes were regulated during *Eimeria* infection, less than 10 KEGG (Kyoto Encyclopedia of Genes and Genomes) pathways were affected and only a few genes were involved at the particular time point (Tab. 1). Affected pathways 4 h post-*Eimeria* infection include focal adhesion, MAPK and mTOR signaling, responsible for cell motility, proliferation and survival, and insulin signaling involved in glycogen syntheses, glucose uptake, protein synthesis and MAPK activation. Most of the genes were repressed at 4 h. In contrast, most genes showed an up-regulation at 16 h. The significantly affected pathways also differ at the early and late time points. The only common modulated pathway at the two time points was MAPK signaling. Strikingly, most of the pathways at 16 h p. i. are associated with a protective host response against infections. The pathways include chemokine signaling and cytokine receptor interactions, which are important for recruitment and activation of immune cells. The expression of the Toll-like and NOD-like receptor pathway was also changed, which are pattern recognition receptors leading to an activation of the innate immune response. Also the Jak-STAT signaling pathway was affected, which is a central pathway induced by a variety of

growth factors and cytokines. Its activation regulates growth, proliferation, immune response and cell survival.

Tab. 1: Significantly altered KEGG pathways in *E. falciformis*-infected YAMC cells

4 h post-infection			16 h post-infection		
Pathway	**Number of Genes**		**Pathway**	**Number of Genes**	
	Induced	**Repressed**		**Induced**	**Repressed**
Focal adhesion	1	10	Cytokine-cytokine receptor interaction	15	1
MAPK signaling pathway	4	7	MAPK signaling pathway	12	4
Insulin signaling pathway	1	6	Jak-STAT signaling pathway	11	2
mTOR signaling pathway	1	3	Chemokine signaling pathway	6	4
			Toll-like receptor signaling pathway	5	2
			NOD-like receptor signaling pathway	5	0

Only two pathways were affected 4 h post-*T. gondii* infection whereas more than 10 pathways were modulated late during infection (Tab. 2).

Tab. 2: Significantly altered KEGG pathways in *T. gondii*-infected YAMC cells

4 h post-infection			16 h post-infection		
Pathway	**Number of Genes**		**Pathway**	**Number of Genes**	
	Induced	**Repressed**		**Induced**	**Repressed**
MAPK signaling pathway	3	1	Cytokine-cytokine receptor interaction	14	11
Jak-STAT signaling pathway	3	0	MAPK signaling pathway	8	13
			Regulation of actin cytoskeleton	3	14
			Focal adhesion	6	10
			Jak-STAT signaling pathway	6	9
			Wnt signaling pathway	5	9
			Cell cycle	8	5
			ErbB signaling pathway	5	6
			TGF-beta signaling pathway	0	9
			Toll-like receptor signaling pathway	3	6

The MAP and Janus kinases are responsible for cellular growth and proliferation, which occurred early and late during *T. gondii* infection. Interestingly, in contrast to *E. falciformis* the majority of the pathways late during *T. gondii* infection were repressed. Again, we did observe pathways involved in host defense, including cytokine / receptor interaction and Toll-like receptor signaling. Up- or down-regulated genes were further involved in pathways important for the regulation of the actin cytoskeleton leading to stability, migration and proliferation. The Wnt signaling pathway is important for the regulation of the cell cycle, proliferation, cytoskeletal alterations and calcium homeostasis. The ErbB and TGF-beta signaling pathways regulate proliferation, cell motility, differentiation and apoptosis.

3.2.1.6 Selected genes modulated by *E. falciformis*

Some of the genes appearing changed early or late during infection are either unknown or little is known about their function in the literature (unmapped). IPA analysis of all genes modulated 4 h p. i. revealed 466 mapped and 183 unmapped IDs; therefore about 30% of all genes are not well characterized. Some highly up-regulated and down-regulated genes at 4 h p. i. are summarized in table 3. We found transcripts associated with gene expression, cell death, cellular movement, molecular transport, lipid metabolism, cell cycle, adhesion, morphology and signaling. Their regulation by IFN-γ was deduced by using the interferome database (www.interferome.org).

Tab. 3: Genes highly modulated by *E. falciformis* during early YAMC infection

Symbol	Gene Name	4 h	Biological Classification[$]	IFN-γ Regulation[§]
AOC3	Amine oxidase, copper containing 3	5.42	Cellular movement	--
FOS	FBJ osteosarcoma oncogene	4.09	Gene expression	Yes
SLC3A1	Solute carrier family 3, member 1	3.27	Molecular transport	--
PON1	Paraoxonase 1	3.21	Lipid metabolism	--
HEXIM1	Hexamethylene bis-acetamide inducible 1	3.15	Gene expression	--
TNFRSF25	Tumor necrosis factor receptor superfamily, member 25	3.05	Cell death	Yes
LCAT	Lecithin cholesterol acyltransferase	2.95	Lipid metabolism	--
CLEC7A	C-type lectin domain family 7, member a	2.67	Cell adhesion	--
ICAM2	Intercellular adhesion molecule 2	2.61	Cellular movement	--
STAR	Steroidogenic acute regulatory protein	2.58	Lipid metabolism	--

CSPP1	Centrosome and spindle pole associated protein 1	-3.99	Cell Cycle	--
STRN3	Striatin, calmodulin binding protein 3	-3.27	Cell Cycle	--
ARRDC3	Arrestin domain containing 3	-2.98	Cellular growth and proliferation	--
SOX11	SRY-box containing gene 11	-2.88	Gene expression	--
SOX5	SRY-box containing gene 5	-2.86	Gene expression	--
WNK1	WNK lysine deficient protein kinase 1	-2.71	Cellular growth and proliferation	--
RND3	Rho family GTPase 3	-2.68	Cellular development	--
EXT1	Exostoses 1	-2.62	Cell morphology	--
DUSP6	Dual specificity phosphatase 6	-2.59	Cell signaling	Yes
EIF4E	Eukaryotic translation initiation factor 4E	-2.49	Cellular growth and proliferation	--

[$]Biological classification are based on Ingenuity pathway analyses
[§]Regulation by IFN-γ is based on www.interferome.org
Some genes may correspond to more than one biological category.

IPA analysis of the 16 h sample resulted in 503 mapped and 148 unmapped IDs. Table 4 summarizes some of the induced and repressed genes, which correspond to lipid metabolism, gene expression, transport, cellular function and maintenance, growth and proliferation, morphology, signaling and cell cycle events.

Tab. 4: Highly transcriptional active genes during late *Eimeria* infection of YAMC cells

Symbol	Gene Name	16 h	Biological Classification[$]	IFN-γ Regulation[§]
SAA4	Serum amyloid A 4	19.92	Lipid transport	--
EGR3	Early growth response 3	18.15	Transcription	--
FOS	FBJ osteosarcoma oncogene	17.90	Transcription	Yes
CFI	complement component factor i	15.86	Immune Response	--
SLC8A3	Solute carrier family 8 (sodium/calcium exchanger), member 3	14.59	Calcium ion transport	--
ME3	Malic enzyme 3, NADP(+)-dependent, mitochondrial	13.94	Tricarboxylic acid cycle	--
EGR2	Early growth response 2	7.70	Transcription	Yes
GEM	GTP binding protein	6.78	Signal transduction	--
RERG	RAS-like, estrogen-regulated, growth-inhibitor	6.44	Signal transduction	--
FOSB	FBJ osteosarcoma oncogene B	6.28	Transcription	--
COL11A1	Collagen, type XI, alpha 1	-3.65	Cell adhesion	Yes
WISP2	WNT1 inducible signaling pathway protein 2	-3.27	Cell adhesion	--
ADAMTS5	A disintegrin-like and metallopeptidase with thrombospondin type 1 motif, 5	-3.09	Signal transduction	--

NPAS3	Neuronal PAS domain protein 3	-3.03	Transcription	--
FGF18	Fibroblast growth factor 18	-2.97	Signal transduction	--
CITED4	Cbp/p300-interacting transactivator, with Glu/Asp-rich carboxy-terminal domain, 4	-2.85	Transcription	--
NPY1R	Neuropeptide Y receptor Y1	-2.79	Signal transduction	--
COL10A1	collagen, type X, alpha 1	-2.66	Cell adhesion	--
LRP2	low density lipoprotein receptor-related protein 2	-2.57	Cell proliferation	--
FAT4	FAT tumor suppressor homolog 4 (Drosophila)	-2.57	Cell adhesion	--

[$]Biological classification are based on Ingenuity pathway analyses
[§]Regulation by IFN-γ is based on www.interferome.org
Some genes may correspond to more than one biological category.

3.2.1.7 Selected genes modulated by *T. gondii*

IPA analyses revealed 45 genes as mapped and 17 as unmapped at 4 h p. i., and 847 mapped and 284 unmapped IDs at 16 h post-*T. gondii* infection. Some of the highly induced or repressed transcripts during early and late *T. gondii* infection (Tab. 5 and Tab. 6) are involved in gene expression, signaling, maintenance, growth and proliferation, development, cell morphology, cell cycle, molecular transport and lipid metabolism. Interestingly, 9 genes early during infection and 6 genes late during infection function in gene expression, including the early growth response genes (Egr1, Egr2, Egr3, and Egr4). In addition Egr4 showed the highest fold-change in the microarray analyses.

Tab. 5: Highly transcriptional active genes during early *T. gondii* infection of YAMC cells

Symbol	Gene Name	4 h	Biological Classification[$]	IFN-γ Regulation[§]
EGR2	Early growth response 2	8.22	Gene expression	Yes
EGR4	Early growth response 4	8.2	Gene expression	--
EGR3	Early growth response 3	5.3	Gene expression	--
FOS	FBJ osteosarcoma oncogene	4.91	Gene expression	Yes
CISH	Cytokine inducible SH2-containing protein	4.11	Cell signaling	--
EGR1	Early growth response 1	3.77	Gene expression	Yes
JUNB	Jun-B oncogene	2.69	Gene expression	Yes
IER2	Immediate early response 2	2.63	Cellular function and maintenance	Yes
SOCS2	Suppressor of cytokine signaling 2	1.99	Cellular growth and proliferation	Yes
DUSP2	Dual specificity phosphatase 2	1.96	Cell signaling	--
SIK1	Salt inducible kinase 1	-3.08	Cellular function and maintenance	--

IKZF2	IKAROS family zinc finger 2	-2.47	Gene expression	--
FZD8	Frizzled homolog 8	-2.38	Cellular development	--
COL11A1	collagen, type XI, alpha 1	-1.95	Cell morphology	Yes
ATP2B1	ATPase, Ca++ transporting, plasma membrane 1	-1.78	Molecular transport	--
SOAT1	Sterol O-acyltransferase 1	-1.66	Lipid metabolism	--
CBX3	Chromobox homolog 3	-1.66	Gene expression	Yes
TXNIP	Thioredoxin interacting protein	-1.62	Cellular growth and proliferation	Yes
KIF1B	Kinesin family member 1B	-1.61	Cellular function and maintenance	--
SOX11	SRY-box containing gene 11	-1.60	Gene expression	--

[$]Biological classification are based on Ingenuity pathway analyses
[§]Regulation by IFN-γ is based on www.interferome.org
Some genes may correspond to more than one biological category.

Tab. 6: Highly transcriptionally active genes during late *T. gondii* infection of YAMC cells

Symbol	Gene Name	16 h	Biological Classification[$]	IFN-γ Regulation[§]
EGR4	Early growth response 4	141.95	Gene expression	--
EGR3	Early growth response 3	73.64	Gene expression	--
EGR2	Early growth response 2	56.06	Gene expression	Yes
GEM	GTP binding protein	17.45	Cellular development	--
DUSP2	Dual specificity phosphatase 2	6.05	Cell signaling	--
RGS4	Regulator of G-protein signaling 4	5.39	Cellular growth and proliferation	--
EGR1	Early growth response 1	5.13	Gene expression	Yes
FOS	FBJ osteosarcoma oncogene	4.81	Gene expression	Yes
CISH	Cytokine inducible SH2-containing protein	4.11	Cell signaling	--
IER2	Immediate early response 2	4.07	Cellular function and maintenance	Yes
SIK1	Salt inducible kinase 1	-7.70	Cellular function and maintenance	--
SLC6A19	Solute carrier family 6, member 19	-5.87	Molecular transport	--
ASB15	Ankyrin repeat and SOCS box-containing 15	-5.49	Cellular growth and proliferation	--
IKZF2	IKAROS family zinc finger 2	-5.41	Gene expression	--
KIF11	Kinesin family member 11	-4.47	Cell cycle	Yes
PTX3	Pentraxin related gene	-4.19	Cell-to-cell signaling and interaction	--
IRGA6	Interferon inducible GTPase 1	-4.16	Cell signaling	Yes
CCL20	Chemokine (C-C motif) ligand 20	-4.15	Cellular movement	--
WNK1	WNK lysine deficient protein kinase 1	-4.05	Cellular growth and proliferation	--

DUSP10	Dual specificity phosphatase 10	-3.74	Cell signaling	--

[$]Biological classification are based on Ingenuity pathway analyses
[§]Regulation by IFN-γ is based on www.interferome.org
Some genes may correspond to more than one biological category.

3.2.1.8 Selected genes commonly modulated by *E. falciformis* and *T. gondii*

Although *E. falciformis* and *T. gondii* are both apicomplexan parasites, they regulate only a few genes in the same way (Fig. 20). Interestingly, we did not detect genes, which appeared to be regulated by both parasites at the early time points (4 h *Ef* /4 h *Tg* 0 genes). Only 3 genes were modulated in a similar pattern during early *T. gondii* and early and late *E. falciformis* infection, including the transcription factor FOSB. 4 transcripts were commonly modulated 4 h post-*Eimeria* and during early and late *T. gondii* infection (an unknown gene, an ATPase ATP2B1, the actin-binding protein FLNB, and a protein involved in signaling GPC4). We also found 16 genes which were shared during an *Eimeria* (early and late) and late *T. gondii* infection and 102 transcripts common to an early *E. falciformis* and late *T. gondii* infection (4 h *Ef* /16 h *Tg)*. Some of these genes are involved in transcription, cell cycle and adhesion. Likewise, the majority of the commonly expressed transcripts appeared during late *E. falciformis* and late *T. gondii* infection (151 genes, 16 h *Ef* /16h *Tg*) and participate in transcription, signaling, apoptosis and differentiation processes. We further detected 2 genes expressed late during *E. falciformis* but early in a *T. gondii* infection (an unknown gene, and the signaling molecule SOCS3) and 18 transcripts appearing modulated 16 h post-*Eimeria* and 4 and 16 h post-*T. gondii* infection including the transcription factors EGR1-4, IER2 and JUNB. Apparently, only 2 genes were commonly expressed early and late during an *Eimeria* as well as *T. gondii* infection of YAMC cells, including an unknown gene and the transcription factor c-FOS (see below).

We also found reciprocally regulated transcripts in *E. falciformis*- and *T. gondii*-infected cells (App. C). Five genes were down-regulated in *E. falciformis* infection but up-regulated during *T. gondii* infection. 22 transcripts showed an up-regulation in *E. falciformis* infected YAMC cells, whereas *T. gondii* infection resulted in their down-regulation. Many of these genes however are either unknown or not well described.

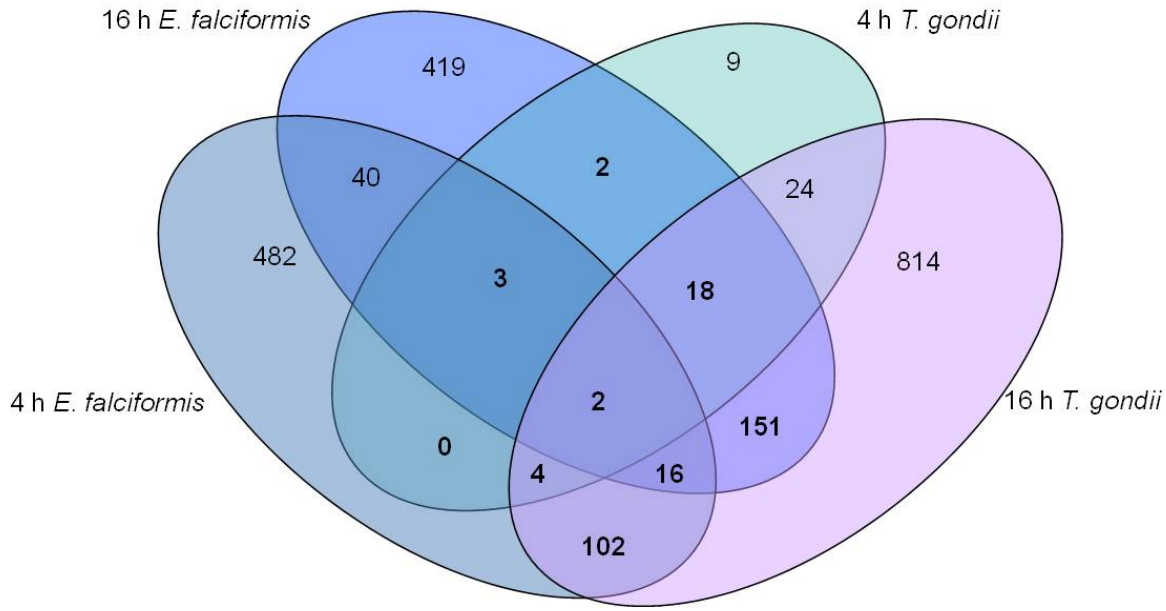

Fig. 20: Temporal expression in *E. falciformis* and *T. gondii*-infected YAMC cells. The overlapping regions demonstrate the distribution of common modulated genes. The dataset includes both exclusion criteria (1.5-fold cut-off, anti-correlation).

3.2.2 *Ex vivo* microarray analyses

3.2.2.1 Analysis of microarray sample

For the *ex vivo* gene expression we chose an early time point (24 h) when infection is established, and a later period (144 h) coinciding with the onset of the sexual development.

The composition of the isolated caecum sample was assessed by flow cytometry and qPCR (Fig. 21). In addition, recruitment of immune cells was visualized by immunohistochemistry (Fig. 22). Most of the purified cells were of epithelial origin (UEA^+, Fig. 21A), however the sample was also composed of immune cells ($CD45^+$), including $CD4^+$ and $CD8^+$ T cells (Fig. 21B). Similar results were obtained with qPCR (Fig. 21C). Transcripts of epithelial origin (EPCAM) appeared about five cycles earlier than the transcript of the immune cell marker (CD45), indicating a 2^5-fold higher amount of EPCAM transcripts than CD45 transcripts.

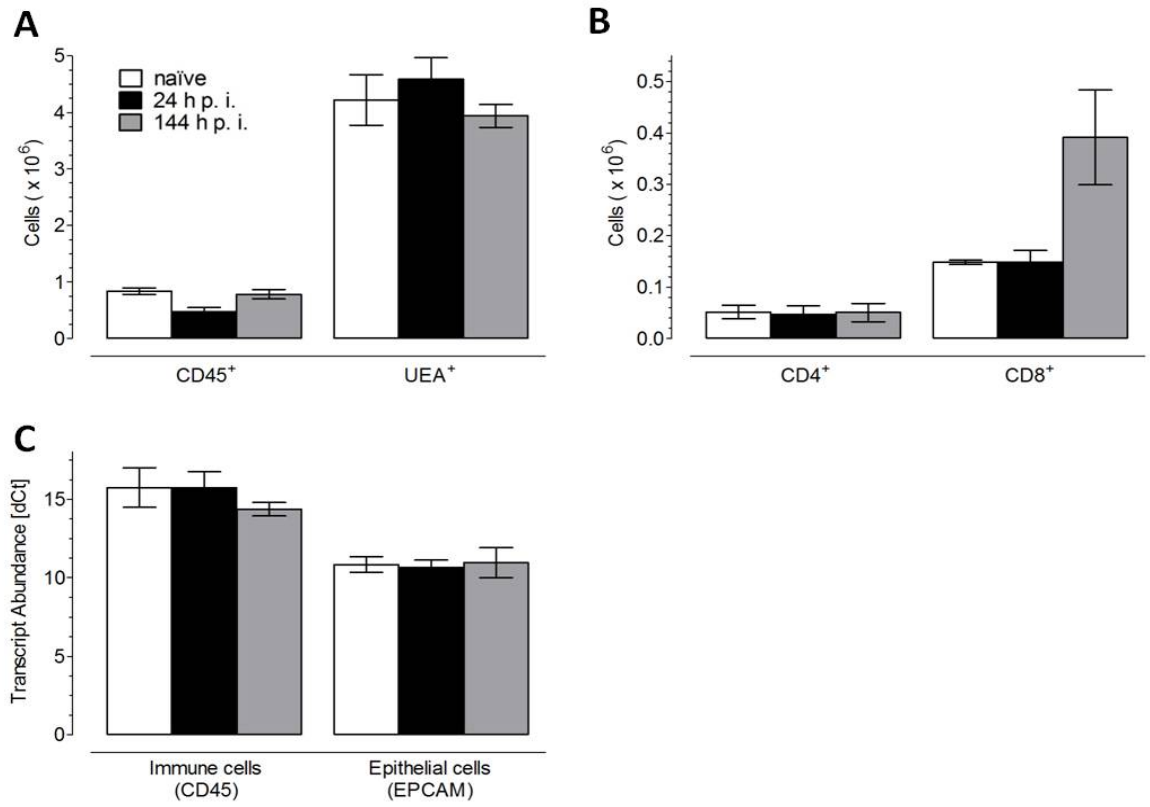

Fig. 21: Quality assessment of the microarray samples. **(A)** Composition of the microarray sample in control and infected animals by flow cytometry. The sample consisted of mainly epithelial cells (UEA^+) along with immune cells ($CD45^+$). **(B)** Detection of $CD4^+$ and $CD8^+$ T cells. **(C)** Transcript abundance of immune (CD45) and epithelial cell (EPCAM) marker in the microarray sample. Bars represent the mean ± SEM of two independent experiments with 3 to 4 animals each.

We also stained uninfected and infected (24 h and 144 h p. i.) caecal tissue to visualize selected immune cells, including $B220^+$ (Fig. 22B), $CD3^+$ (Fig. 22B) and $F4/80^+$ cells (Fig. 22C). As expected, we detected a basal staining for B-cells ($B220^+$), T-cells ($CD3^+$) and macrophages ($F4/80^+$) in naïve animals (Fig 22). Expression of a macrophage-specific marker, but not of B- and T-cell markers was modestly higher 24 hrs post-infection. During the late infection, however, we observed a much greater influx of all cell types to the site of parasite infection. An arbitrary quantification of histological samples confirmed a significant recruitment of the indicated cell types (Fig. 22B-D). Thus, with progression of infection the number of immune cells recruited to the site of infection increased.

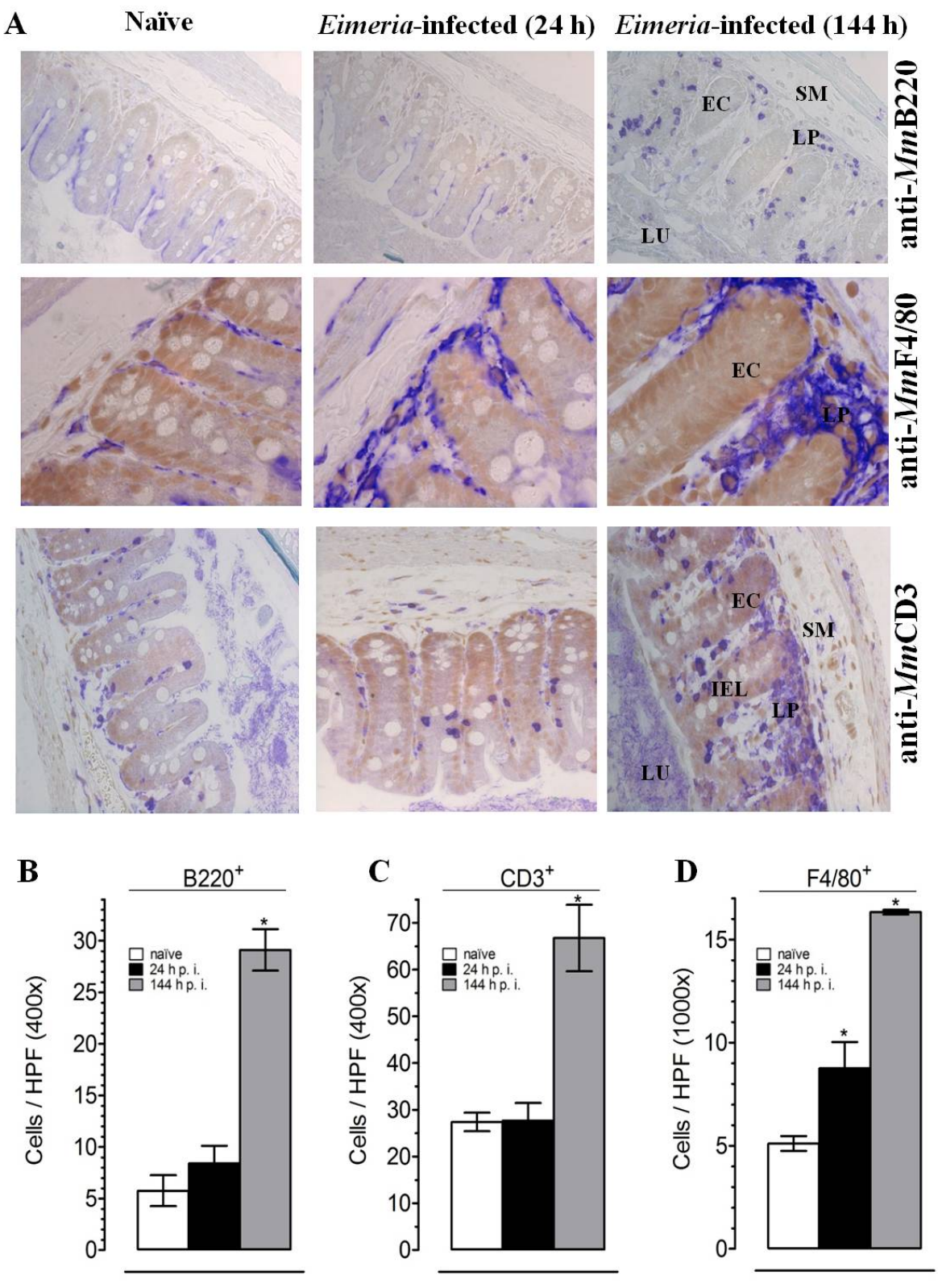

Fig. 22: Recruitment of immune cells in *Eimeria*-infected mice. (A-D) Immunohistochemical staining of B cells (B220+), macrophages (F4/80+) and T cells (CD3+) in the caecum of naïve and infected animals. EC, epithelial cells; HPF, high power field; IEL, intraepithelial lymphocyte; LP, lamina propria; LU, lumen; SM, submucosa. Bar graphs represent the mean ± SEM of two experiments each with 4 animals. (* $p \leq 0.05$)

3.2.2.2 Host response during asexual and sexual development of *Eimeria*

Three independent *ex vivo* microarrays were performed to maximize the consistency of the gene expression results. Only genes which appeared modulated in all three arrays (≥ 1.5 fold change, $p < 0.05$) were considered for further analyses.

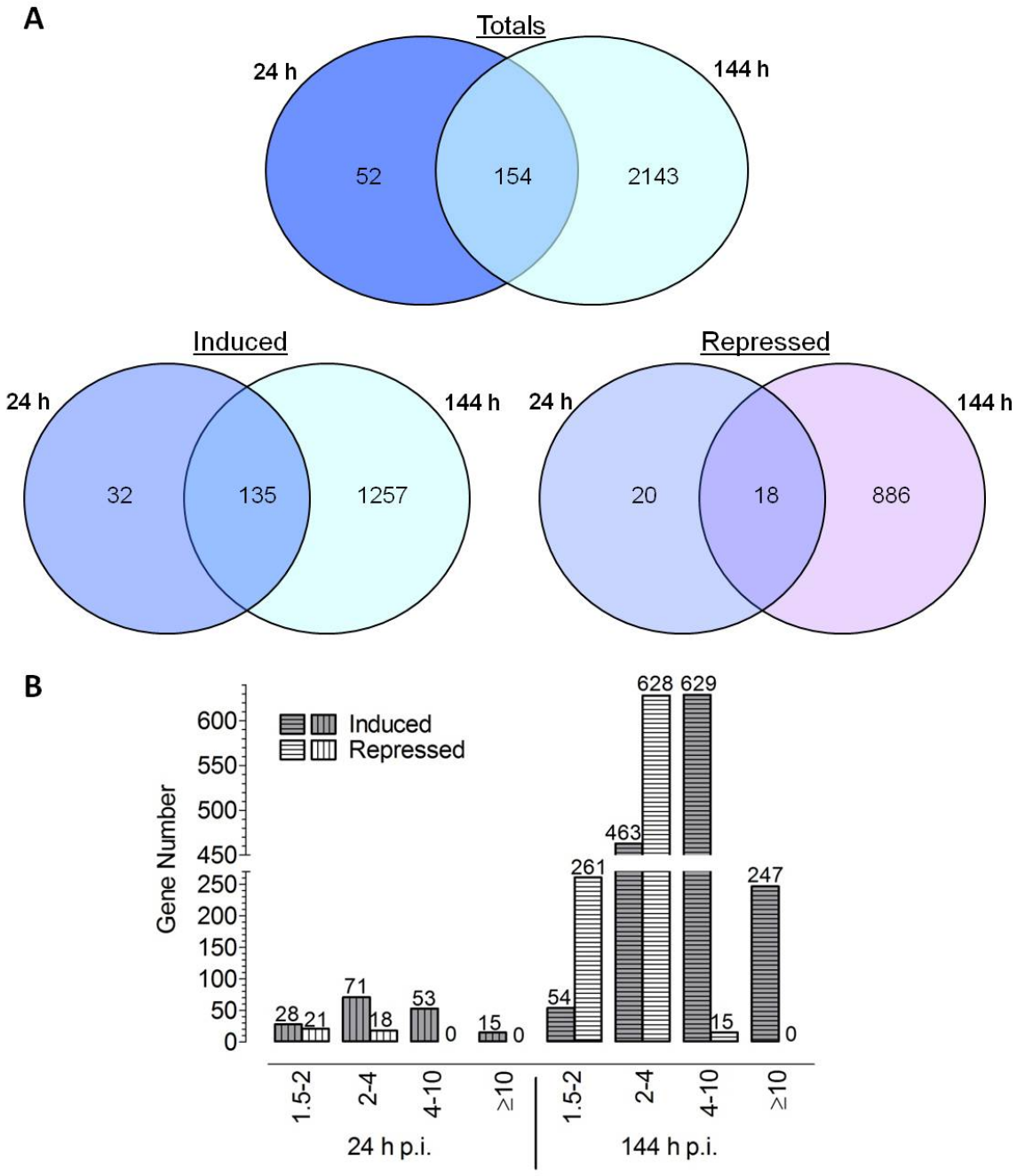

Fig. 23: Modulation of the mouse transcriptome by *E. falciformis*. (A) Venn diagram of differentially regulated mouse genes depicting the total induced or repressed host genes based on 1.5-fold cut-off and anti-correlation criteria. The overlapping regions signify common modulated genes. **(B)** Fold change of gene expression after 24 h and 144 h of infection.

206 genes (236 probes) and 2297 genes (2690 probes) were identified as regulated during early and late of infection (Fig. 23A), respectively. The expression of 32 (61%) genes was exclusively induced and of 20 (39%) genes was down-regulated 24 h post-infection. The host response was more prominent at 144 h p. i. with 1257 induced (59%) and 886 repressed (41%) transcripts. In total, 154 genes were commonly regulated throughout infection (at 24 h and 144 h), of which the majority were up-regulated (135 induced *vs*. 18 repressed). The expression of only one gene, Fer1l3 (myoferlin), was repressed at 24 h but induced at 144 h post-infection. About 17% of the induced (28 genes) and half of the repressed transcripts (21 genes) were only moderately changed in their expression level (1.5 – 2-fold) early during infection (Fig. 23B). About 42% (71 genes) of the induced and 47% (18 genes) of the repressed genes were regulated 2 – 4-fold. The expression of 53 genes (~ 32%) was 4 – 10-fold higher than in uninfected controls, and 15 genes were up-regulated more than 10-fold. Late during infection, 54 induced (~ 4%) and 261 repressed (~ 26%) genes ranged in their fold change between 1.5 and 2-fold. About one third of the induced fraction (463 genes) and 70% of the repressed (628 genes) showed an altered expression of 2 – 4-fold. Interestingly, nearly half of all up-regulated genes were induced by 4 – 10- fold as opposed to only 15 down-regulated genes (~ 2%). Finally nearly 18% (247 genes) were up-regulated more than 10-fold and none of the repressed genes showed such a significant change in expression.

3.2.2.3 Biological classification of *E. falciformis*-modulated mouse genes

The *ex vivo* microarrays were analyzed by IPA to identify functional categories including the general cellular processes (Fig. 24), immune response (Fig. 25) and metabolism (Fig. 26). The expression of most genes was up- than down-regulated in each category early as well as late during infection. This is in contrast with the results obtained from *E. falciformis*-infected YAMC cells, where more genes were repressed than induced early during infection. The top ten processes within the category “general cellular processes” (Fig. 24) were comparable to the *in vitro* situation (Fig. 17) with the exception of the process cellular compromise, which was not significantly altered upon *in vitro* infection.

IPA identified major cellular processes (Fig. 24) significantly altered during the parasite infection, which included cellular development, growth, proliferation, movement, maintenance, morphology, death and signaling. The gene regulation was more prominent 144 h post-infection. The number of modulated transcripts of the category “cell cycle” during late *E. falciformis* infection did not meet the statistical threshold.

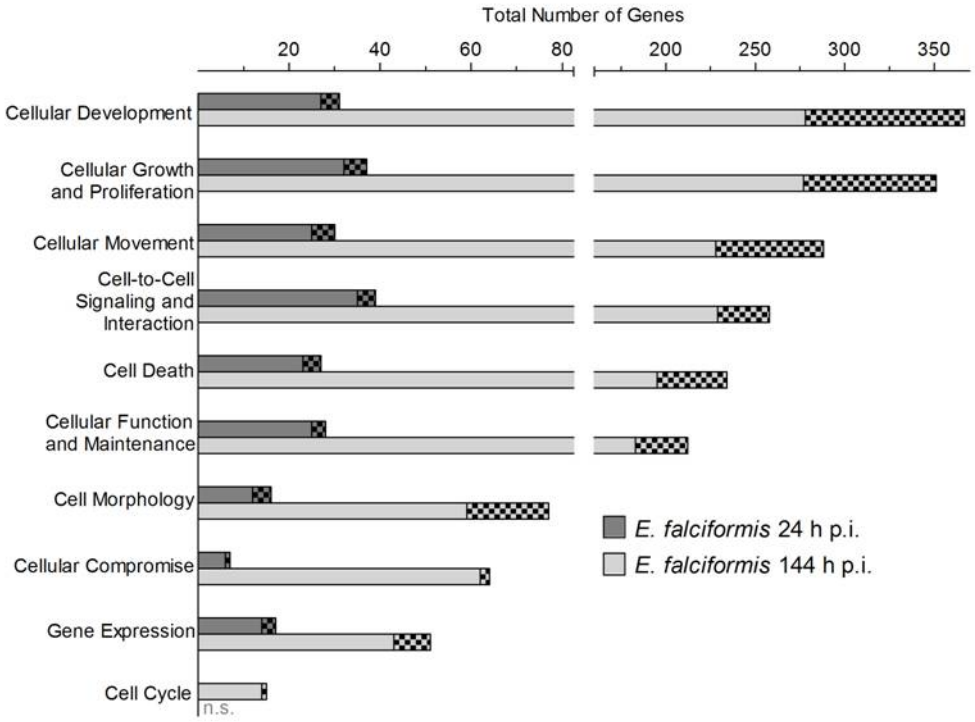

Fig. 24: Cellular phenomena affected during mouse infection by *Eimeria*. Functional analysis of induced (smooth) and repressed (shaded) genes after 24 h and 144 h of infection. n.s., not significant.

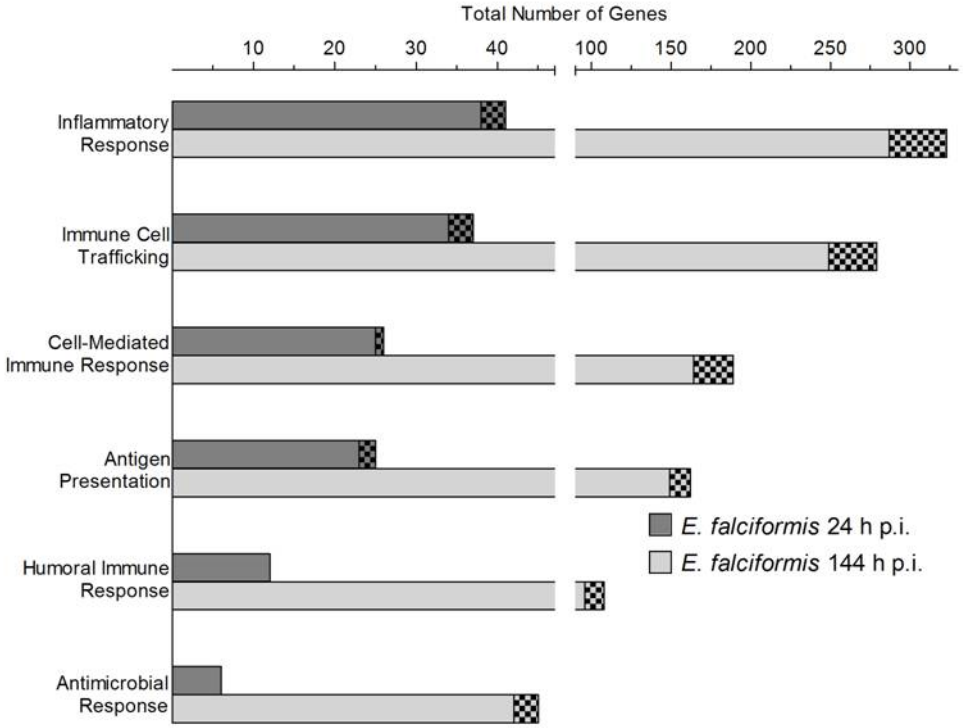

Fig. 25: Immunity-related processes changed upon mouse infection by *E. falciformis*. Functional analysis of up-regulated and down-regulated genes are shown by smooth and shaded columns, respectively.

Likewise, we also noted an appreciably high transcriptional response associated with immunity (Fig. 25) and metabolism (Fig. 26) during advanced infection. The major immune categories significantly enriched during the advanced-stage infection included inflammation, immune cell trafficking, cell-mediated immunity, antigen presentation, and humoral and antimicrobial response.

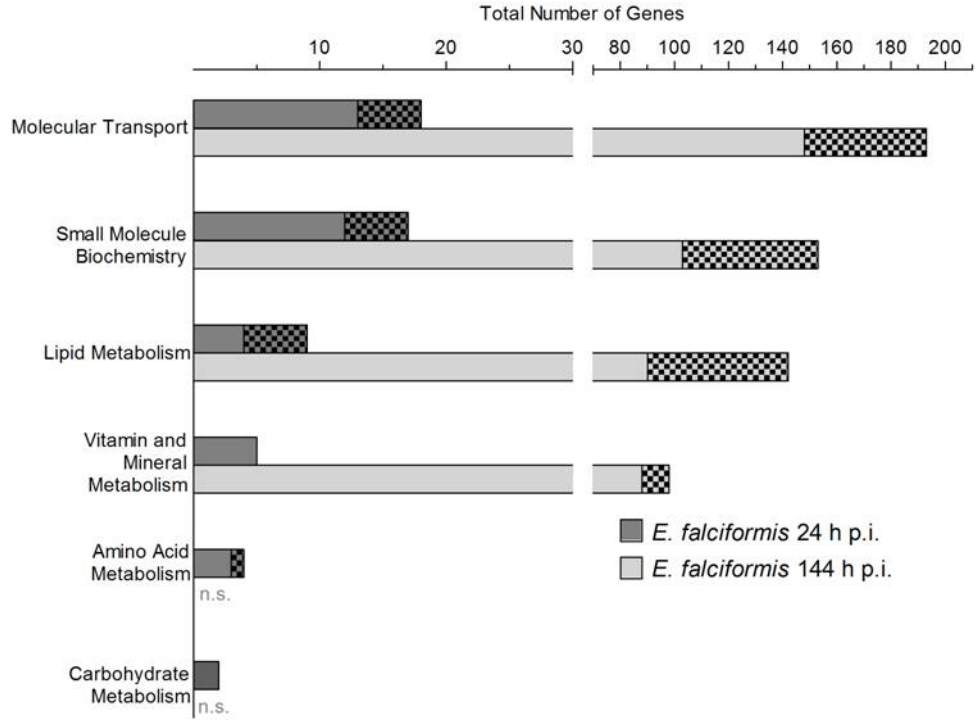

Fig. 26: Metabolic functions affected in animals parasitized with *E. falciformis*. Functional analysis of up-regulated (smooth) and down-regulated (shaded) genes after 24 h and 144 h of infection. n.s., not significant.

The major metabolic processes affected belong to molecular transport, as well as to lipid, amino acid, vitamin and mineral metabolism. The number of modulated transcripts for the categories “amino acid metabolism” and “carbohydrate metabolism” late during *E. falciformis* infection did not meet the statistical threshold.

3.2.2.4 Mouse pathways modulated during *E. falciformis* infection

The genes modulated during an *in vivo* infection were analyzed for enriched pathways using DAVID program (Tab. 7). All pathways affected early during infection were also significantly enriched at the later time point. More genes in the indicated pathways were induced than repressed at 24 h as well as 144 h post-infection. Most of the pathways participate in immune response mechanisms, and some of which were comparable to the late *in vitro* infection

(MAPK, Jak-STAT, cytokine/chemokine signaling and Toll-like receptor signaling). The pathways antigen processing and presentation (MHCI, MHCII), cell adhesion, and NK cell mediated cytotoxicity were exclusive to the *in vivo* infection. The T and B cell receptor signaling pathways were also unique to the *in vivo* infection. The presence of these innate and adaptive immunity-related pathways is consistent with the presence of immune cells in the microarray sample.

Tab. 7: Significantly altered KEGG pathways in *E. falciformis*-infected mouse caecum

24 h post-infection			144 h post-infection		
Pathway	**Number of Genes**		**Pathway**	**Number of Genes**	
	Induced	**Repressed**		**Induced**	**Repressed**
Cytokine-cytokine receptor interaction	13	2	Cytokine-cytokine receptor interaction	68	9
Antigen processing and presentation	12	0	Chemokine signaling pathway	46	10
Cell adhesion molecules	10	1	MAPK signaling pathway	35	15
Jak-STAT signaling pathway	8	0	NK cell mediated cytotoxicity	43	4
Chemokine signaling pathway	7	0	Cell adhesion molecules	40	5
Toll-like receptor signaling pathway	6	0	T cell receptor signaling pathway	31	5
NK cell mediated cytotoxicity	6	0	Jak-STAT signaling pathway	28	7
			B cell receptor signaling pathway	24	4
			Antigen processing and presentation	28	1
			Toll-like receptor signaling pathway	22	3

3.2.2.5 Selected mouse genes modulated by *E. falciformis*

Most of the differentially regulated genes could be mapped by IPA suite. Out of 206 IDs at 24 h post-infection 157 were mapped and 49 unmapped. Among the genes modulated during late infection (2297 IDs), 1816 were mapped and 481 transcripts could not be mapped. The genes highly induced (Tab. 8) or repressed (Tab. 9) participate in cell signaling, growth and proliferation and lipid metabolism. The expression of selected genes was also validated by qPCR (Fig. 27). These included the immunity related GTPases (IRGs), IRGM3 and IRGB6, the guanylate binding proteins, GBP2 and GBP3, and the chemokines CxCL9, CxCL10 and CxCL11.

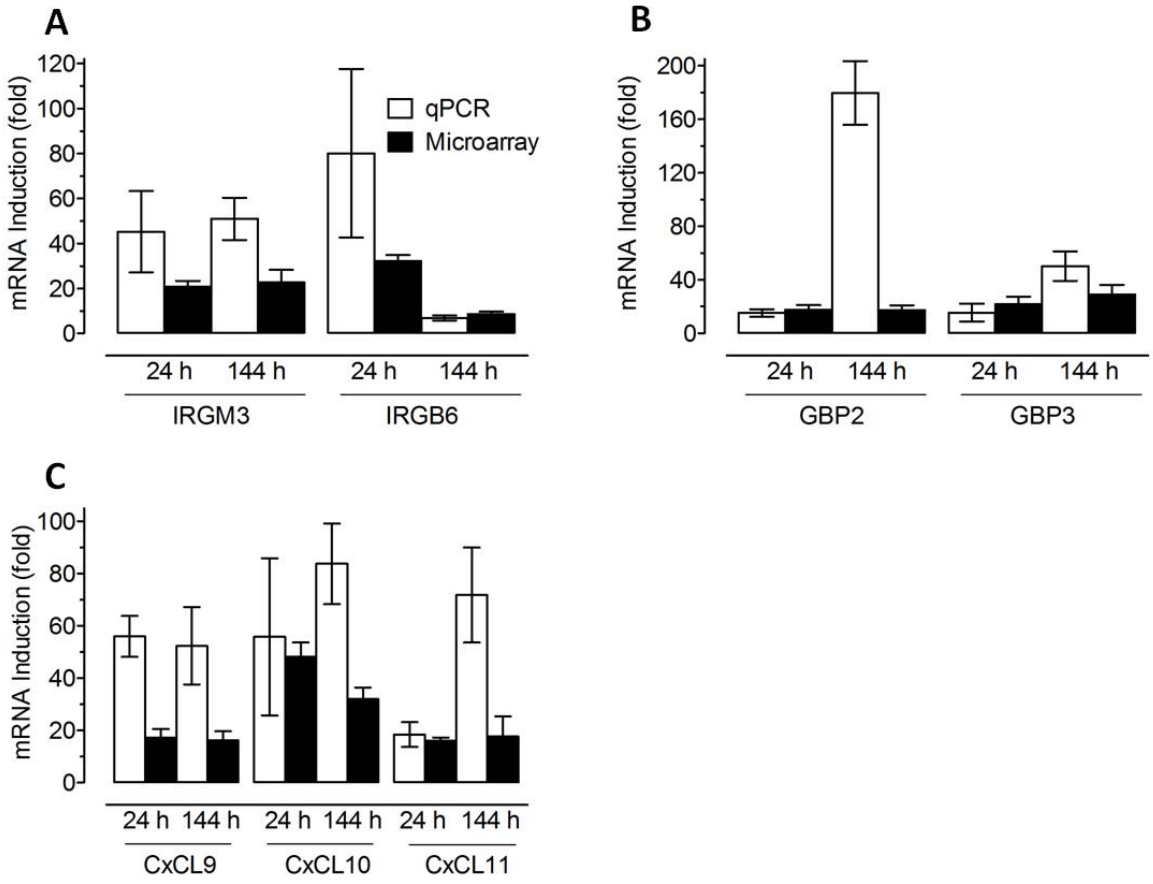

Fig. 27: Validation of microarray results by quantitative PCR. qPCR of the immunity-related GTPases IRGM3 and IRGB6 **(A)**, the guanylate binding proteins GBP2 and GBP3 **(B)** and the chemokines CxCL9, CxCL10 and CxCL11 **(C)**. The fold induction in qPCR studies was normalized to *Mm*18S rRNA. The bars show the means ± SEM of three independent experiments each with 5 animals.

Both GBP2 and GBP3 were induced upon 24 h as well as 144 h post-infection. Likewise, IRGM3 and IRGB6 were substantially upregulated at both time points of infection. We also observed an early upregulation of all tested chemokines, which was sustained until late infection. The transcripts of CxCL9, CxCL10 as well as CxCL11 were induced approximately to the same order of magnitude.

As shown in table 8, a majority of the genes highly induced in response to parasite infection are regulated by IFN-γ as deduced by literature searches and interferome database. Similarly, IPA network analyses revealed the IFN-γ signaling network as the most affected one during early as well as late infections (App. D, E).

Tab. 8: Selected mouse genes induced by *E. falciformis* during early and late infection

Symbol	Gene Name	Fold Change* (±SEM)	Biological Classification[$]	IFN-γ Regulation[§]
24 h post-infection				
IRGA6	Interferon inducible GTPase 1	73.1 ± 35.4	Cell signaling	Yes
CXCL10	Chemokine (CXC motif) ligand 10	48.1 ± 5.6	Cell-to-cell signaling and interaction	Yes
IDO1	Indoleamine 2,3-dioxygenase 1	34.8 ± 5.5	Inflammatory response	Yes
IRGB6	T cell specific GTPase 1	32.1 ± 2.7	Cell signaling	Yes
IRGM3	Interferon gamma induced GTPase	20.8 ± 2.5	Cell signaling	Yes
GBP2	Guanylate-binding protein 2	17.7 ± 3.5	Cell-to-cell signaling and interaction	Yes
CXCL9	Chemokine (CXC motif) ligand 9	17.3 ± 3.3	Cell-to-cell signaling and interaction	Yes
GBP3	Guanylate-binding protein 3	21.9 ± 5.5	Cell signaling	Yes
MPA2L	Guanylate-binding protein 6	19.5 ± 4.1	Cell signaling	Yes
CXCL11	Chemokine (CXC motif) ligand 11	16.0 ± 1.3	Cell-to-cell signaling and interaction	Yes
SOCS1	Suppressor of cytokine signaling 1	15.8 ± 1.2	Cellular growth and proliferation	Yes
C2TA	Class II transactivator	12.1 ± 1.2	Gene expression	Yes
IRGM2	Interferon inducible GTPase 2	10.0 ± 0.6	Cell signaling	Yes
IFNG	Interferon gamma	9.3 ± 1.9	Inflammatory response	Yes
GBP5	Guanylate-binding protein 5	8.2 ± 1.7	Inflammatory response	Yes
STAT1	Signal transducer and activator of transcription 1	8.2 ± 0.8	Gene expression	Yes
IRGD	Interferon gamma inducible protein 47	7.3 ± 0.7	Inflammatory response	Yes
IL18BP	Interleukin 18 binding protein	7.2 ± 0.6	Inflammatory response	--
PSMB9	Proteasomal subunit, beta type 9 (large multifunctional peptidase 2)	6.8 ± 0.5	Cell-to-cell signaling and interaction	--
CD274	CD 274 antigen	6.6 ± 0.4	Inflammatory response	--
144 h post-infection				
IFI202B	Interferon activated gene 202B	147.4 ± 60.0	Cellular growth and proliferation	Yes
CLEC7A	C-type lectin domain family 7, member A	83.5 ± 3.1	Cell signaling	--
CXCL10	Chemokine (CXC motif) ligand 10	70.0 ± 37.5	Cell-to-cell signaling and interaction	Yes
CCL4	Chemokine (CC motif) ligand 4	61.3 ± 18.5	Cellular movement	Yes
SPP1	Secreted phosphoprotein 1	59.8 ± 23.6	Inflammatory response	Yes
IRGA6	Interferon inducible GTPase 1	59.5 ± 30.3	Cell signaling	Yes
GBP8	Guanylate-binding protein 8	38.5 ± 4.7	Cell signaling	Yes
IDO1	Indoleamine 2,3-dioxygenase	37.1 ± 11.4	Inflammatory response	Yes

	1			
GBP3	Guanylate-binding protein 3	29.0 ± 7.1	Cell signaling	Yes
MS6A6B	Membrane-spanning 4-domains, subfamily A, member 6B	29.1 ± 8.7	Inflammatory response	--
CCL8	Chemokine (CC motif) ligand 8	27.9 ± 7.7	Cellular movement	Yes
IFNG	Interferon gamma	25.5 ± 10.3	Inflammatory response	Yes
VIM	Vimentin	25.4 ± 4.9	Cell-to-cell signaling and interaction	--
EGR2	Early growth response 2	24.6 ± 6.8	Cellular growth and proliferation	Yes
IFI204	Interferon activated gene 204	23.4 ± 3.1	Cellular growth and proliferation	Yes
IRGB6	T cell specific GTPase 1	23.3 ± 4.7	Cell signaling	Yes
IRGM3	Interferon gamma induced GTPase	22.8 ± 5.5	Cell signaling	Yes
IL1B	Interleukin 1 beta	22.1 ± 3.6	Inflammatory response	Yes
CCL24	Chemokine (CC motif) ligand 24	21.8 ± 4.7	Cell-to-cell signaling and interaction	--
FCGR2B	Fc receptor, IgG, low affinity IIb	21.6 ± 2.3	Inflammatory response	--

*Fold change is adjusted to the nearest decimal point.

[$]Biological classifications are based on Ingenuity pathway analyses.

[§]Regulation by IFN-γ is based on www.interferome.org and literature searches.

IFN-γ signaling was apparent within 24 h of infection, and nearly all genes in the network showed an induction (App. D). The cytokine-regulated network was more notably induced during late infection, and a few genes also exhibited a downregulation (App. E). Table 8 summarizes the most upregulated genes after 24 and 144 h of infection. Interestingly, 17 of the 20 most upregulated genes early during infection are regulated by IFN-γ. The number is equally impressive at the later time point (15 of the 20 genes). Some of these genes are immunity-related GTPases (IRGA6, B6, D, M2, M3), guanylate-binding proteins (GBP2, 3, 5, 6, 8), chemokines (CxCL9, 10, CCL4) and IDO1. In contrast, only 1 IFN-γ-regulated gene (FHL1) was downregulated (Tab. 9). Interestingly, lipid metabolism and molecular transport categories were particularly enriched among the most repressed genes. In brief, these data suggested a key role of IFN-γ-mediated signaling in *Eimeria*-infected animals.

Tab. 9: Selected mouse genes repressed by *Eimeria falciformis* during early and late infection

Symbol	Gene Name	Fold Change* (±SEM)	Biological Classification[$]	IFN-γ Regulation[§]
24 h post-infection				
CLDN8	Claudin 8	-3.4 ± 0.8	Cell morphology	--
GPAM	Glycerol-3-phosphate acyltransferase, mitochondrial	-2.7 ± 0.9	Lipid metabolism	--
ACSL1	Acyl-CoA synthetase long-chain family member 1	-2.8 ± 0.7	Lipid metabolism	--
ANGPT2	Angiopoietin 2	-2.6 ± 0.1	Cellular growth and proliferation	--
IL1R1	Interleukin 1 receptor, type 1	-2.4 ± 0.4	Cell signaling	--
EGF	Epidermal growth factor	-2.3 ± 0.2	Cell signaling	--
ACSM3	Acyl-CoA synthetase medium-chain family member 3	-2.2 ± 0.3	Lipid metabolism	--
FHL1	Four and a half LIM domains 1	-2.2 ± 0.3	Cellular growth and proliferation	Yes
KCNE3	Potassium voltage-gated channel, Isk-related subfamily, gene 3	-2.0 ± 0.2	Molecular transport	--
FER1L3	Myoferlin	-1.8 ± 0.1	Cellular growth and proliferation	--
144 h post-infection				
SLC8A1	Solute carrier family 8, member 1	-6.4 ± 1.7	Molecular transport	--
PTK2	Pprotein tyrosine kinase 2	-5.1 ± 1.0	Cellular growth and proliferation	--
PRLR	Prolactin receptor	-4.6 ± 0.7	Cell signaling	--
IL1R1	Interleukin 1 receptor, type 1	-4.6 ± 1.3	Cell signaling	--
TRIM2	Tripartite motif protein 2	-4.2 ± 1.1	Cellular growth and proliferation	--
KITL	Kit ligand	-4.1 ± 1.1	Cellular movement	--
GHR	Growth hormone receptor	-3.8 ± 0.2	Cell signaling	--
CFTR	Cystic fibrosis transmembrane conductance regulator	-3.8 ± 0.9	Molecular transport	--
HOXB5	Homeo box B5	-3.4 ± 0.7	Cellular development	--
VLDLR	Very low density lipoprotein receptor	-3.4 ± 0.7	Lipid metabolism	--

*Fold change is adjusted to the nearest decimal point.

[$]Biological classifications are based on Ingenuity pathway analyses.

[§]Regulation by IFN-γ is based on www.interferome.org and literature searches.

.

3.2.3 Genes commonly modulated during *in vitro* and *in vivo* infection by *Eimeria*

E. falciformis successfully invades and replicates within the intestinal epithelial cells of the caecum, whereas the *in vitro* development is extremely limited. The results of the arrays were compared to find similarities or differences between the host gene expression *in vitro* and *in vivo* (Fig. 28).

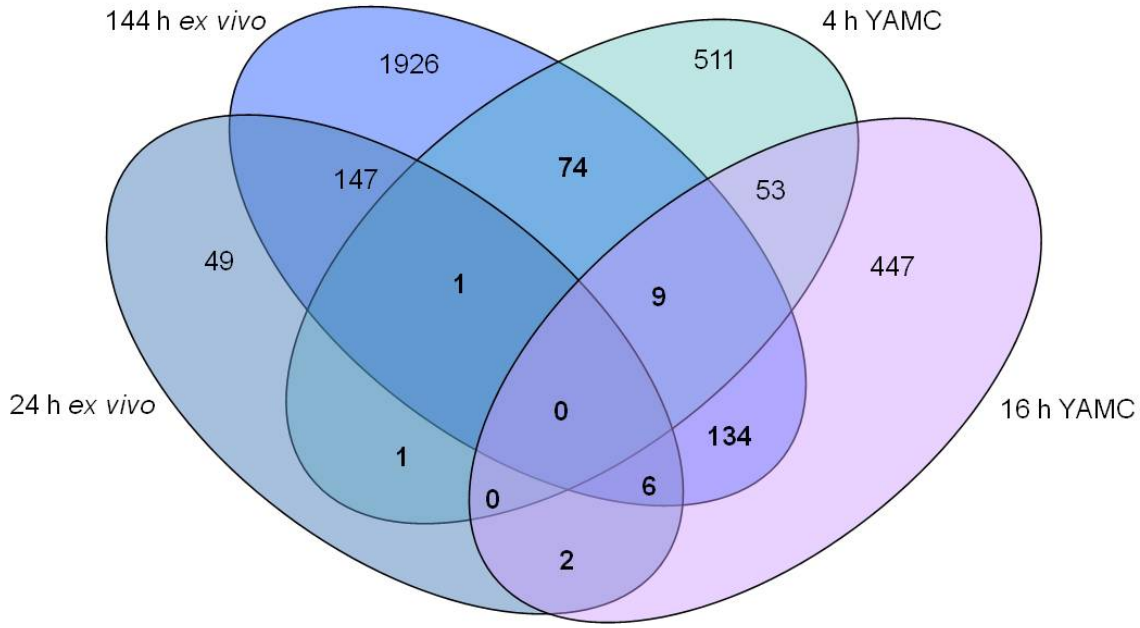

Fig. 28: Gene expression in response to *E. falciformis* infection of mouse or YAMC cells. The overlapping regions demonstrate common modulated genes. The dataset includes both exclusion criteria (1.5-fold cut-off, anti-correlation).

Only a few genes showed common expression patterns between the *in vitro* and *in vivo* conditions. 85 genes modulated during early *in vitro* infection were also expressed at one of the time points *in vivo*. These genes participate in biological categories including transcription (*e.g.* ARID5A, MXD1, ZBTB32) and immune response (CLEC7A, LAT2, LAG3). Only one gene is expressed early and late *in vivo* and early *in vitro* (THPO, a humoral growth factor), whereas 9 are commonly expressed early and late *in vitro* and late *in vivo* (*e.g.* DUSP4, 6, and 10). The majority of genes (134 transcripts) at 16 h p. i. *in vitro* was shared with the late *in vivo* time point, and included genes participating in transcription, immune response and death. Only 2 genes were commonly regulated early *in vivo* and late *in vitro* (transporter SLC35A1, and an unknown gene). Additionally, 6 genes were present early and late *in vivo* as well as late *in vitro* (*e.g.* the protein kinase PRKG2 and the transcription factor STAT1).

Interestingly, nearly half of all genes (40 out of 85) modulated at 4 h and one of the time points *in vivo* (4 h / 144 h; 4 h / 16 h / 144 h; 4 h / 24 h / 144 h; 4 h / 24 h) and nearly one

third of genes (57 out of 151) shared between 16 h and *in vivo* time points (16 h / 4 h / 144 h; 16 h / 144 h; 16 h / 24 h; 16 h / 24 h / 144 h) were reciprocally regulated (App. F). 47 genes with a reduced expression *in vitro* were induced *in vivo*, and 45 genes up-regulated *in vitro* were down-regulated *in vivo*. These genes function in processes including proliferation and cell cycle (*e.g.* GPC1, MAGI2, GNE, MS4A4B) and apoptosis (DIDO1, BMP4, NEU3, TRP53INP1). In addition, three genes also reciprocally regulated *in vitro* and *in vivo* were dual-specificity phosphatases (DUSP 6, 10, and 4), which are negative regulators of MAP kinases involved in proliferation, apoptosis and differentiation.

3.3 C-FOS is required for an optimal *in vitro* growth of *E. falciformis* and *T. gondii*

The expression of only one annotated gene, c-FOS (FBJ osteosarcoma oncogene), was up-regulated in YAMC cells infected with *E. falciformis* and *T. gondii* at both time points. IPA analyses identified c-FOS as a central transcription factor associated with several other cellular proteins (App. G-J). FOS signaling was apparent as early as 4 h post-*Eimeria* infection, when many genes in the network showed a downregulation (App. G). The FOS-regulated network was more notably induced during late infection, and only a few genes in this network exhibited a downregulation (App. H). IPA network analyses also identified FOS as a significantly modulated gene during *T. gondii* infection (App. I-J).

Next, we investigated the importance of c-FOS for *E. falciformis* and *T. gondii* infection using murine fibroblasts. Wild-type ($FOS^{+/+}$) or c-FOS knockout cells ($FOS^{-/-}$) were infected (MOI 2), incubated for 4 h and 43 h, fixed and immunostained to examine infection and development of *E. falciformis* (Fig. 29 A). The absence of FOS did not influence the invasion (Fig. 29B), however the parasite development was quite diminished (Fig. 29C). We detected 70% fewer trophozoites and schizonts in the $FOS^{-/-}$ cell line when compared to the parental control. Similarly, the knockout cells infected with *T. gondii* (26 h p. i.) harbored a higher percentage of smaller vacuoles with 2 and 4, and a lower proportion of bigger vacuoles with 8 parasites in comparison to wild type host cells (Fig. 29E). In summary, FOS expression is required for an optimal *in vitro* development of *E. falciformis* and *T. gondii*.

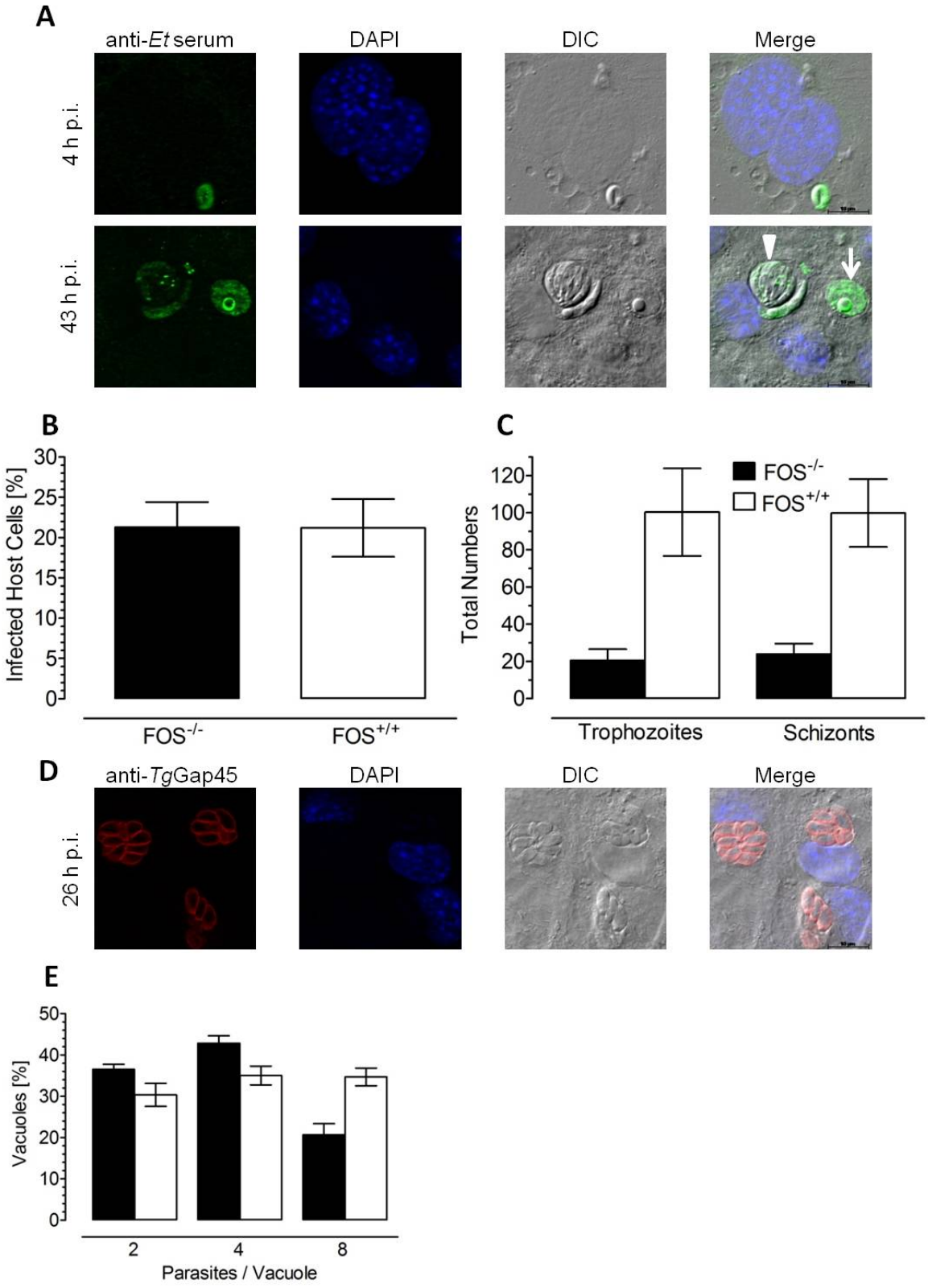

Fig. 29: Mouse c-FOS is required for *E. falciformis* and *T. gondii.* **(A)** Parasites were immunostained by using anti-*E. tenella* serum. Infection was determined 4 h p. i. by counting intracellular sporozoites/HPF (upper panel). Development was assessed 43 h p. i. by scanning the cover slip for trophozoites (arrow) and schizonts (arrow head). **(B)** Infection of $FOS^{+/+}$ and $FOS^{-/-}$ cells by *E. falciformis*. **(C)** Development of *E. falciformis* into trophozoites and schizonts. **(D)** Replication of *T. gondii* was assessed using anti-*Tg*Gap45. **(E)** The number of *T. gondii* per vacuole in $FOS^{+/+}$ and $FOS^{-/-}$ cells. Bar, 10 µm. Data represent the mean ± SEM of two independent experiments.

3.4 *E. falciformis* co-opts the mouse tryptophan catabolism for its development

E. falciformis-infected mice showed an induced expression of the indoleamine-2,3 dioxygenase 1 (IDO1), which is the initial and rate-limiting enzyme of the kynurenine pathway in mammals (Fig. 30). IDO1 expression results in the degradation of the essential amino acid tryptophan and concurrent accumulation of downstream products, summarized as kynurenines. The biological function of IDO1 is quite diverse and controversial including an immune-suppressive to an antimicrobial role (199-202). We investigated the role of IDO1 during *E. falciformis* infection of the mouse.

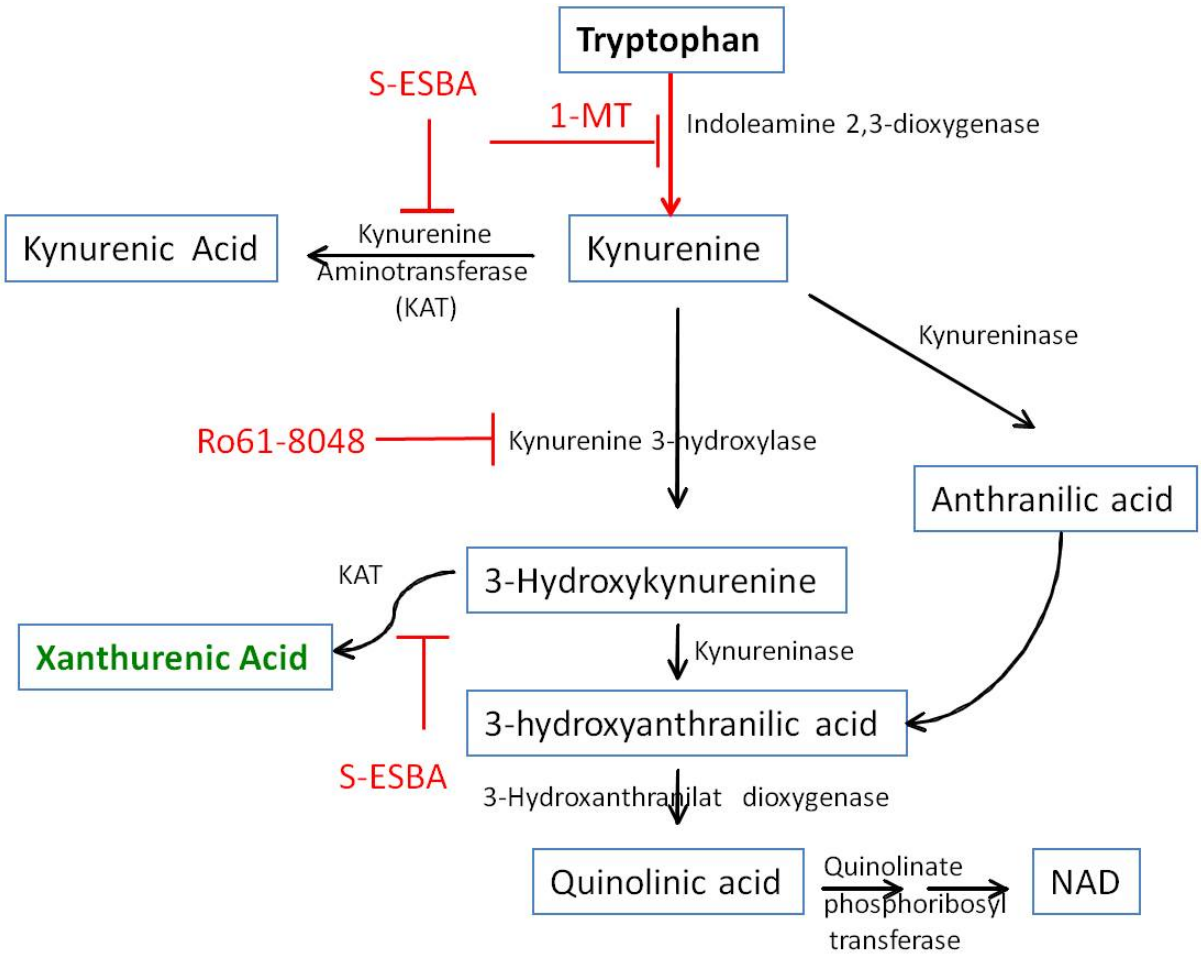

Fig. 30: Tryptophan catabolism in mouse. The kynurenine pathway depicting degradation of tryptophan into different metabolites and associated enzymes. Inhibitors used in this study of indicated enzymes are shown in red colour. Production of xanthurenic acid resonates with induction of IDO in mice, most of which is excreted in the urine as the end metabolite of tryptophan catabolism.

3.4.1 *E. falciformis* induced the expression of IDO1 in mouse caecum epithelia

To examine the expression of IDO1 during the life cycle of *E. falciformis*, the naïve control and parasite-infected mice were sacrificed at different time points, and samples were isolated for quantitative PCR and Western Blot.

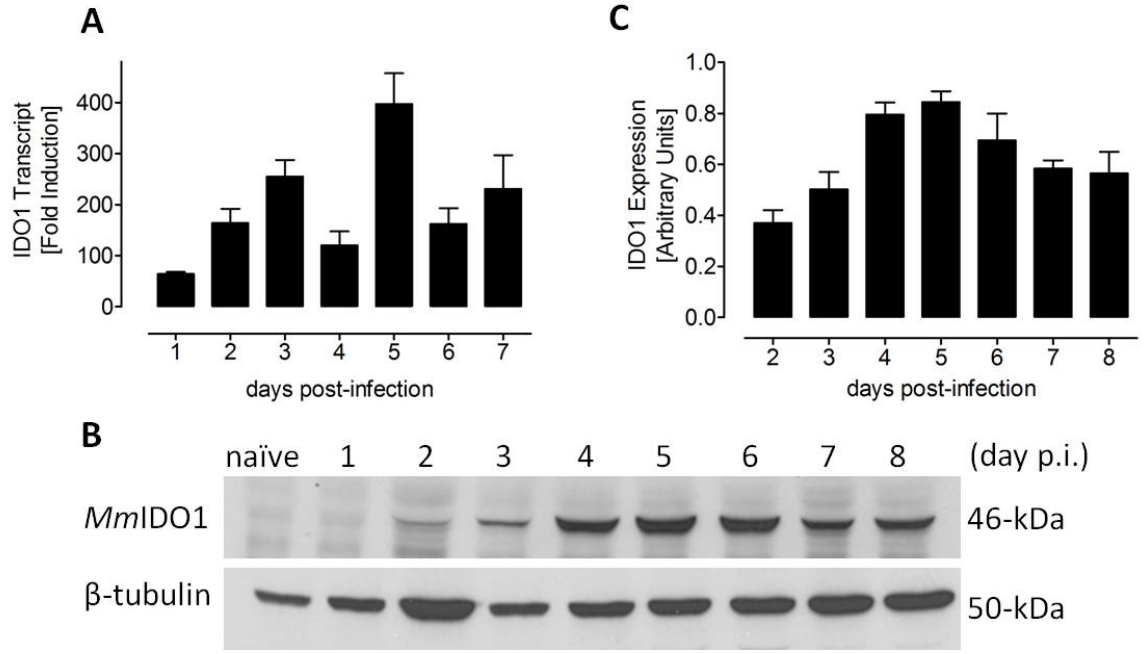

Fig. 31: *E. falciformis* induced IDO1 in the mouse caecum epithelium. (A) Quantitative PCR of IDO1 transcript in parasitized and enriched epithelial cells. The fold induction was normalized to the *Mm*18S rRNA. The bars show the means ± SEM of three independent experiments. **(B)** Immunoblot of the caecum tissue collected on various days of infection. *Mm*IDO1 was detected as a single band of 46-kDa, and β-tubulin (50-kDa) was included as a loading control. **(C)** Expression of IDO1 was calculated by densitometric means and normalized to β-tubulin. Three independent blots were used, and the means ± SEM are shown.

As shown in figure 31, qPCR data validated the microarray results. The IDO1 transcript was present throughout the parasite infection. Compared with the uninfected control, the IDO1 expression was up-regulated by 64-fold (± 7) on the first day of infection and increased further on day 2 (164 ± 39) and day 3 (255 ± 56) to a maximum on day 5 (397 ± 104). IDO1 expression was lower on day 4 (120 ± 47) and day 6 (162 ± 53) and then increased to a moderate 231-fold (± 114) on day 7. IDO1 expression was further validated at protein levels (Fig. 31B). In accord with qPCR data, immunoblot analyses of uninfected and infected caeca revealed a similar outcome. Interestingly, IDO1 protein as a 46 kDA band was first detectable on day 2 of infection, which then persisted throughout the parasite life cycle until day 8 (Fig. 31B). The observed lag in protein expression suggests a post-transcriptional regulation of IDO1. Again, IDO1 expression reached its maximum on day 5 and then declined until day 7,

as evaluated by densitometry analyses of Western Blots from three independent *in vivo* infections (Fig. 31C). In brief, we show that *E. falciformis* infection of mouse results in induced expression of host IDO1 in the parasitized caecum.

To investigate the site of IDO1 expression within the infected host tissue, the caeca of control and infected animals were subjected to immunohistochemical (IHC) staining (Fig. 32).

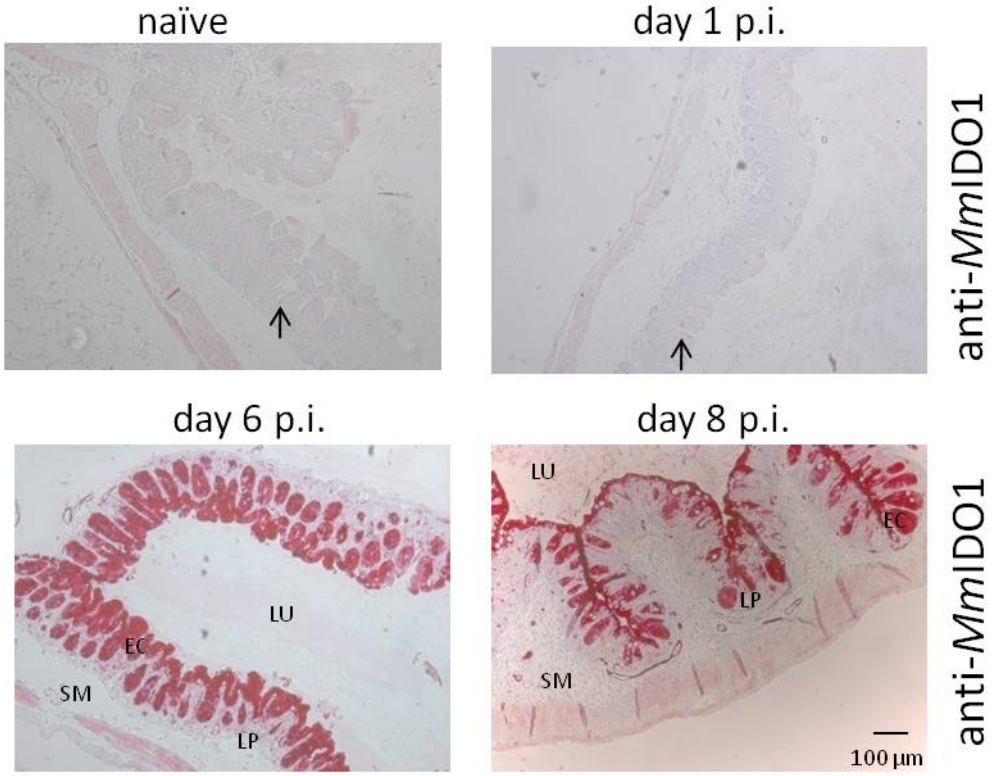

Fig. 32: IDO1 is expressed in the host cells of *E. falciformis*. Immunohistochemical staining of IDO1 in the caecum of naïve and infected (day 1, day 6, and day 8) BALB/c mice. EC, epithelial cell; LU, lumen, LP, lamina propria; SM, submucosa; p.i., post-infection; arrow, IDO1-stained cells; bar 100 µm.

Similar to the immunoblots, no IDO1 staining in the tissue of naïve animals was observed. Neither epithelial nor cells of the lamina propria appeared obviously stained for IDO1 protein until 24 h post-infection. Only a few single cells located within the epithelia (Fig. 32, arrow), and some lamina propria cells, appeared weakly stained for IDO1 in naïve and in infected mice (day 1 p. i.). In contrast, on day 6 as well as on day 8 nearly all cells of the lamina propria showed IDO1 expression in response to infection. However, the staining was most prominent in the caecal epithelial cells on days 6 and 8 of infection, which corresponds to Western Blot analysis (Fig. 31C). A decline on day 8 is presumably due to disruption of the epithelial cells as a consequence of parasite egress. In summary, IDO1 is induced in the

parasitized host tissue and its expression is mostly restricted to the epithelial cells of the caecum, which concurrently represent the parasite host cells. Collectively, we demonstrate a strong and selective induction of IDO1 in the epithelial cells of mouse caecum in response to infection with *E. falciformis*.

3.4.2 The tryptophan catabolism is induced in parasitized mice

The expression of the other enzymes of the kynurenine pathway was also examined (Fig. 33). We isolated parasitized samples throughout the course of infection (day 1 – day 7), and quantified the transcript expression of all major enzyme isoforms.

In brief, the expression of IDO2, catalyzing the same reaction like IDO1, kynurenine 3-hydroxylase (KMO), responsible for converting kynurenine into 3-hydroxykynurenine, and kynureninase (KYNU), utilizing 3-hydroxykynurenine to form 3-hydroxyantrhanilic acid, were detectable and increased during the parasite infection. The production of kynurenic acid from kynurenine and of xanthurenic acid from 3-hydroxykynurenine, is catalyzed by enzymes called kynurenine amino-transferases (KAT 1 – 4). Interestingly, mRNA levels of KAT2 and KAT4 (GOT2) were highly up-regulated and detectable throughout the parasite life cycle, whereas the transcript expression of KAT1 and KAT3 was either undetectable and/or down-regulated. The enzyme catalyzing one of the last reactions of the pathway producing quinolinic acid (3-hydroxyanthranilat dioxygenase, HAAO) showed an increased transcript abundance on day 1 and 5 to 7. Its mRNA was undetectable on day 2 to 4 p. i., however. Some of these enzymes (IDO2, KMO, KYNU, and GOT2) were also induced in microarray studies. In conclusion, these results are indicative of an enhanced tryptophan catabolism in the parasitized animals.

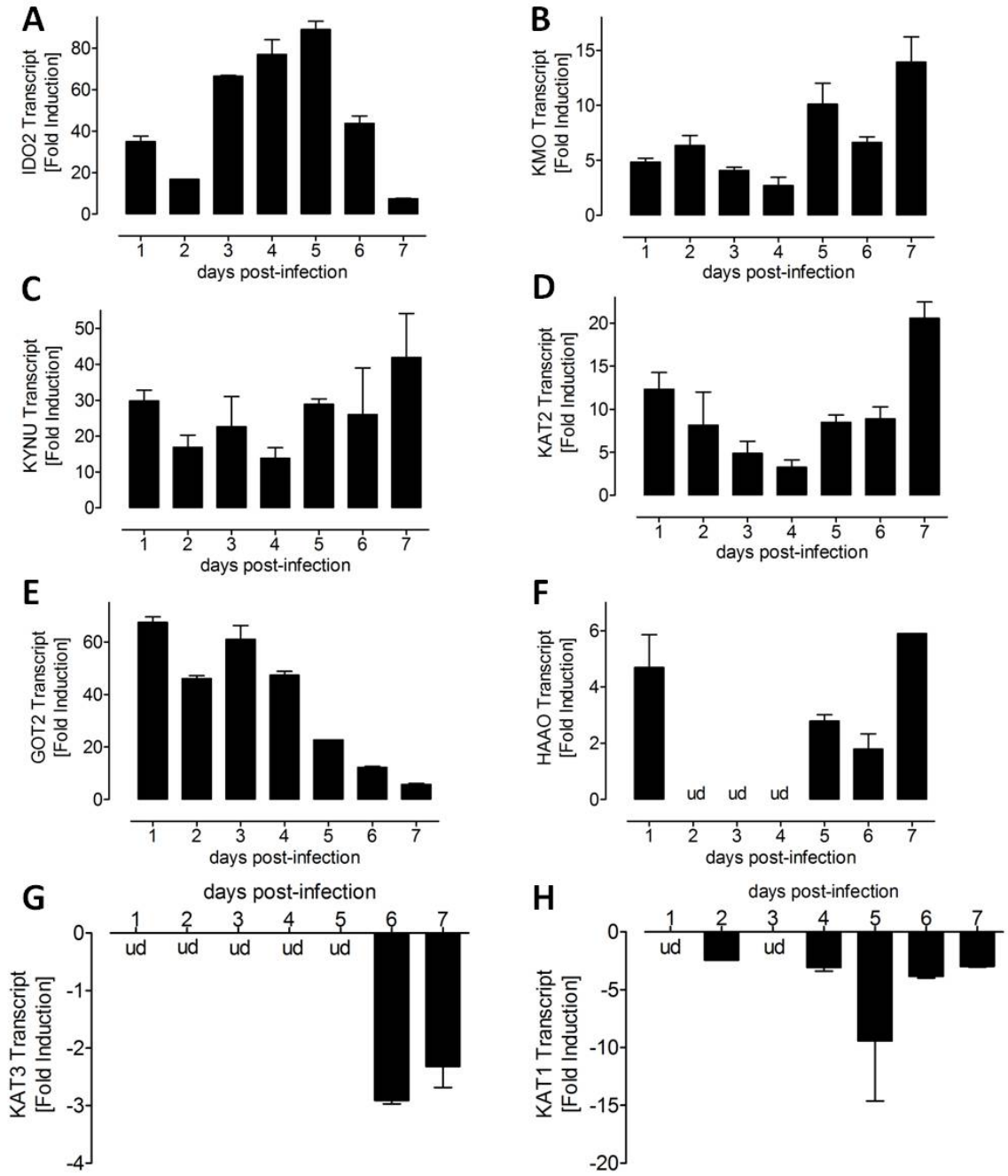

Fig. 33: The kynurenine pathway is induced during *E. falciformis* infection. Quantitative PCR of **(A)** indoleamine-2,3-dioxygenase 2 (IDO2), **(B)** kynurenine 3-hydroxylase (KMO), **(C)** kynureninase (KYNU), **(D)** kynurenine aminotransferase 2 (KAT2), **(E)** kynurenine aminotransferase 4 (GOT2), **(F)** 3-hydroxyanthranilat dioxygenase (HAAO), **(G)** kynurenine aminotransferase 3 (KAT3), and **(H)** kynurenine aminotransferase 1 (KAT1). The fold induction was normalized to the *Mm*18S rRNA. The bars show the means ± SEM of two independent experiments. ud, undetectable.

3.4.3 IDO1 is expressed in the parasitized caecum in an IFN-γ-dependent manner

Because IFN-γ is a key cytokine during primary infections with murine *Eimeria spp*. (124, 125) and is also the most potent inducer of IDO1 (203, 204), we determined the IFN-γ dependency of IDO1 expression during *E. falciformis* infection. IFN-γR$^{-/-}$ and wild type animals were infected, sacrificed on day 6 p. i. and stained for IDO1 protein (Fig. 34). Wild type animals showed an intense IDO1 staining in the epithelial cells of the caecum, and nearly all epithelial cells on day 6 expressed IDO1 in response to infection. Some cells of the lamina propria also expressed the protein. In IFN-γR$^{-/-}$ animals, however, IDO1 staining was virtually absent. Only a few intraepithelial lymphocytes showed a positive IDO1 staining. No IDO1 expression was observed in the cells of the lamina propria confirming an IFN-γ-dependent expression of IDO1 in *E. falciformis*-infected animals.

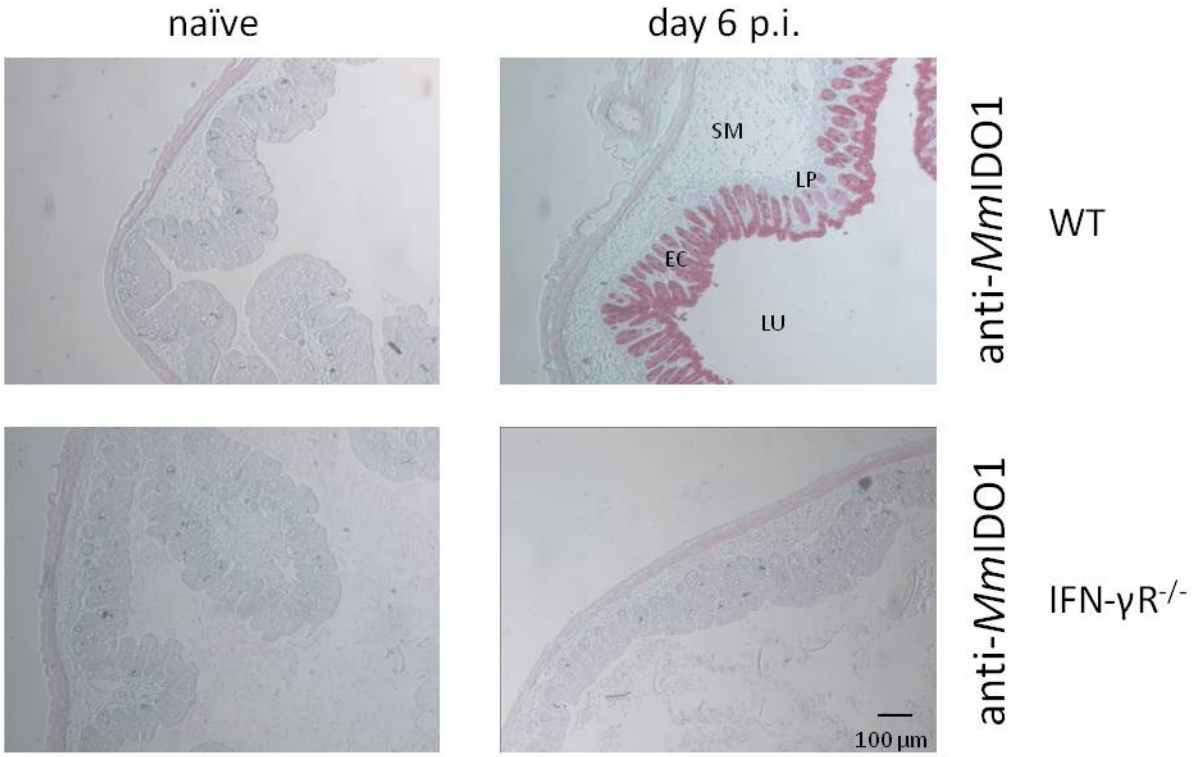

Fig. 34: IDO1 expression is IFN-γ dependent during *E. falciformis* infection of the mouse. Immunohistochemical staining of IDO1 in the caecum of naïve and infected (day 6) wild type (WT) and IFN-γR$^{-/-}$ mice. EC, epithelial cell; LU, lumen, LP, lamina propria; SM, submucosa; p.i., post-infection; bar 100 µm.

3.4.4 Host IDO1 is required for parasite optimal development

As shown at the transcriptional and protein level (Fig. 31), the host enzyme was highly induced during the life cycle of *E. falciformis* in the parasitized tissue. Induced expression of IDO1 exerts an antimicrobial effect on susceptible pathogens, likely by depleting the subcellular tryptophan (199). *E. falciformis* is most likely a tryptophan auxotroph as described for its close relative *T. gondii*. To examine the significance of IDO1 for the *in vivo* development of *E. falciformis*, knockout and inhibition studies were performed.

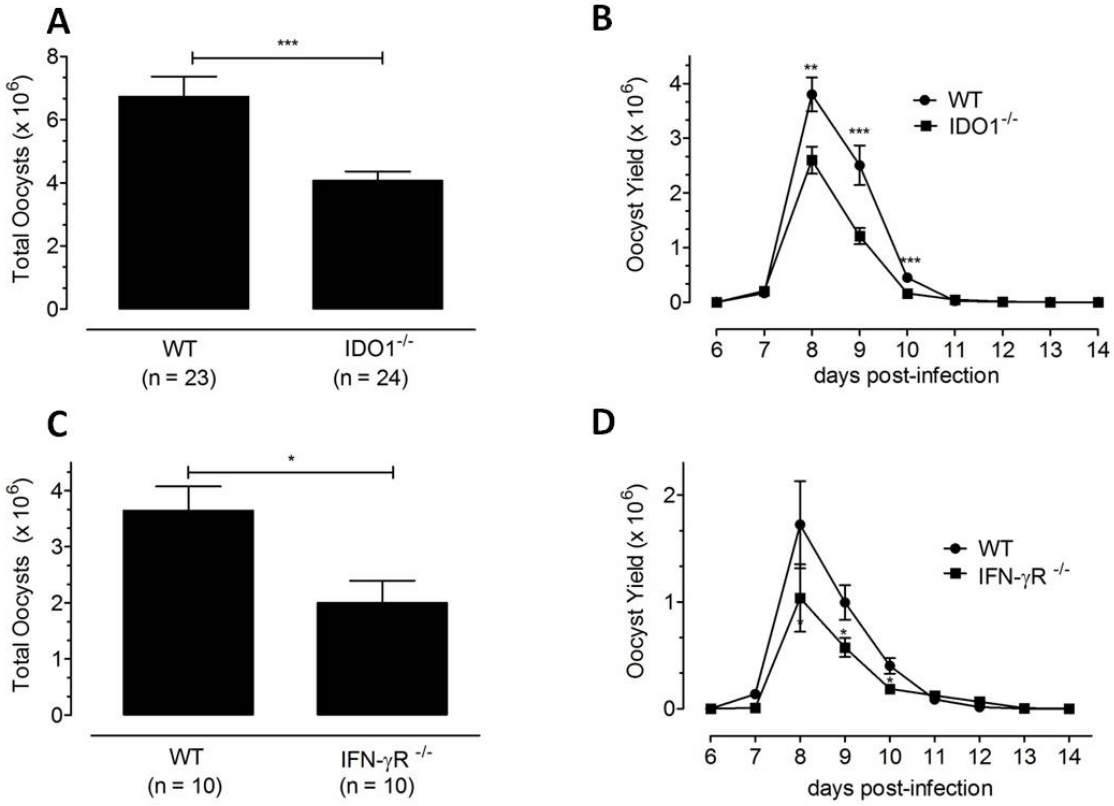

Fig. 35: The oocyst yield is reduced in *E. falciformis*-infected IDO1$^{-/-}$ and IFN-γR$^{-/-}$ mice. (A) WT BALB/c and IDO1$^{-/-}$ mice were infected with 50 oocysts, and the parasite development was quantified by counting the number of oocysts shed in feces. **(B)** Kinetics of oocyst release from day 6-14 post-infection. **(C)** Total oocyst yield and **(D)** kinetics in IFN-γR$^{-/-}$ mice and their C57Bl/6 controls. The bars show the means ± SEM of two-four independent experiments with five to six animals/group. * p≤ 0.05, ** p≤ 0.005, *** p≤ 0.0005.

BALB/c IDO1$^{-/-}$ (Fig. 35) and 1-Methyltryptophan- (1-MT) treated mice (Fig. 36) were infected and the oocyst output as well as the body weight loss was monitored and compared to infected wild type and untreated control animals. Surprisingly, IDO1 deficiency remarkably reduced the total oocyst numbers (Fig. 35A; $p < 0.0001$). Compared to wild type (WT) BALB/c mice ($6.7 \times 10^6 \pm 3.1 \times 10^6$), the IDO1$^{-/-}$ mice shed about 40% less oocysts (4.1×10^6

± 1.4 x 10^6). This observed reduction is due to the decreased oocyst output during the peak days of the infection. The IDO1-deficient animals shed significantly less oocysts than the wild type controls on all peak days (day 8, $p < 0.001$; day 9 and 10, $p < 0.0001$) (Fig. 35B). The kinetics of oocyst shedding however remained unaltered in the IDO1$^{-/-}$ group (Fig. 35B).

Due to the IFN-γ-dependent expression of IDO1 during *Eimeria* infection, we also tested the oocyst output in IFN-γR$^{-/-}$animals. The oocyst numbers in IFN-γR$^{-/-}$ animals was also reduced by 40% when compared to wild type animals (Fig. 35C). Similarly to IDO1$^{-/-}$-infected animals, the prepatent or patent period was not altered during infection as the peak days of oocyst shedding remained unchanged (Fig. 35D).

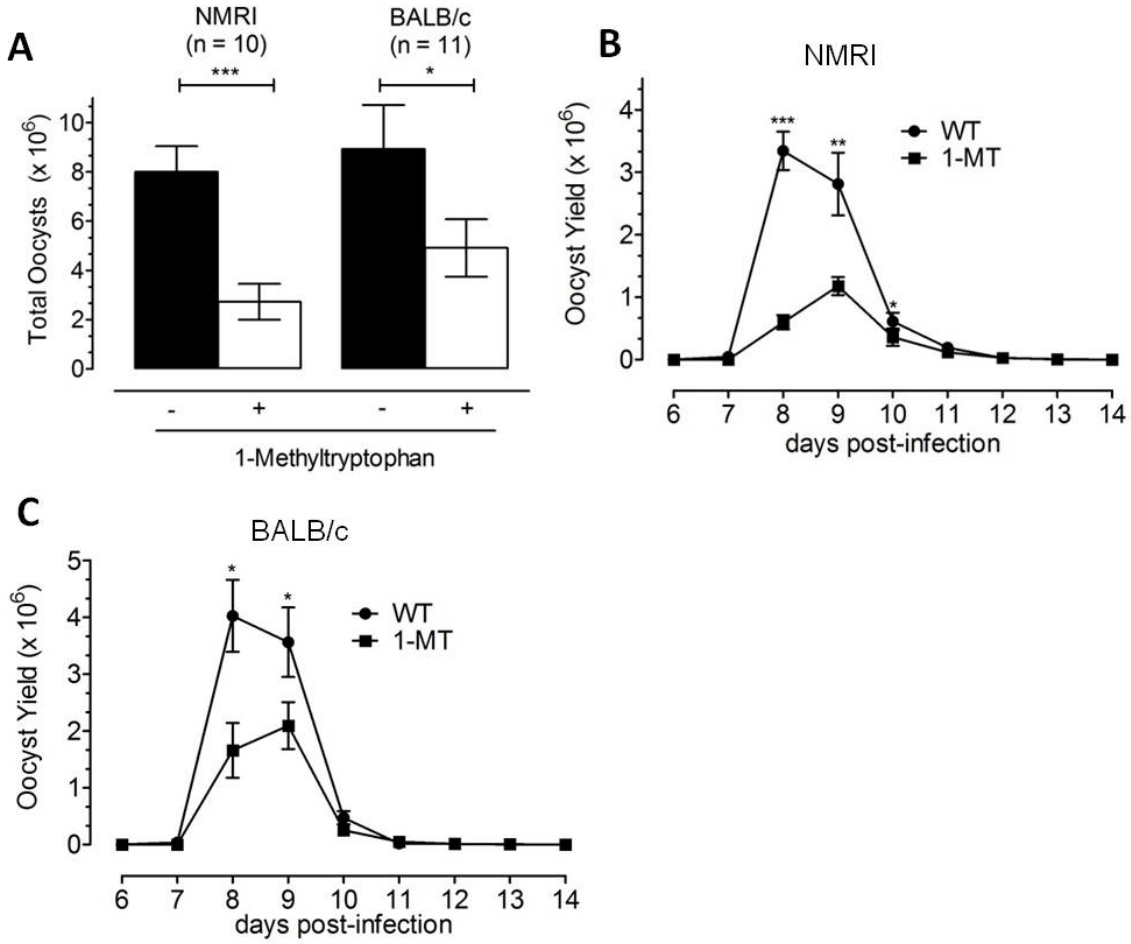

Fig. 36: Effect of 1-MT treatment on the *in vivo* development of *E. falciformis*. (A) Outbred NMRI or inbred BALB/c animals were infected with 50 oocysts and the number of oocysts shed in feces was determined. **(B)** Kinetics of oocyst output in 1-MT-treated NMRI and **(C)** BALB/c. Graphs show mean ± SEM of two independent experiments each with 5-6 animals per group. * $p \leq 0.05$, ** $p \leq 0.005$, *** $p \leq 0.0005$.

The growth of *E. falciformis* was not completely abolished in the absence of IDO1, which might be attributed to the presence of IDO2 (Fig. 33). This prompted us to inhibit the total

IDO activity using a specific and competitive inhibitor (1-MT) (Fig. 36). The biochemical inhibition of IDO with 1-MT, which was applied via the drinking water during the whole infection period, yielded similar results. 1-MT treated NMRI shed about 65% ($p < 0.0001$) and BALB/c 45% ($p < 0.001$) fewer oocysts compared to their untreated control animals (Fig. 36A). These differences were most prominent during the peak period of oocyst shedding from day 8 to 10 (Fig. 36B, C). Collectively, the absence or inhibition of the rate-limiting enzyme of the kynurenine pathway is detrimental to the parasite development.

Furthermore, neither the absence of IDO1 nor the biochemical inhibition of the host enzyme by 1-MT did negatively affect the morbidity. Infection of IDO1$^{-/-}$ (Fig. 37A) as well as 1-MT treated animals (Fig. 37B, C) led to a body weight loss during day 7 to 9 and 10, respectively, which was comparable to the untreated wild type mice. In contrast, IFN-γR$^{-/-}$ showed a higher body weight loss (Fig. 37D) than their controls, which may be due to an increased pathology as described previously (22).

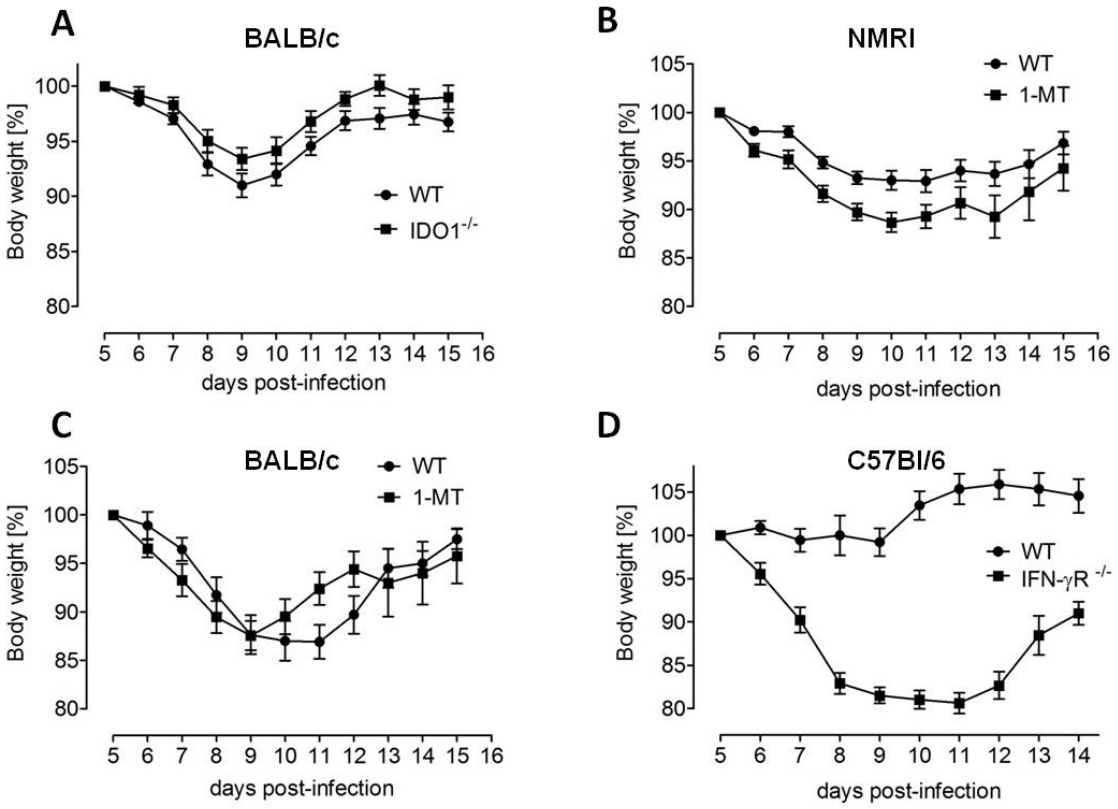

Fig. 37: Body weight loss in *E. falciformis*-infected animals. (A) Body weight loss in WT BALB/c and IDO1$^{-/-}$ mice, **(B)** in untreated or 1-MT treated NMRI and **(C)** BALB/c. **(D)** Body weight loss in WT C57Bl/6 and IFN-γR$^{-/-}$ animals. Graphs show mean ± SEM of two-four independent experiments each with 5-6 animals per group.

3.4.5 IDO1$^{-/-}$ and 1-MT-treated animals showed a normal immune response

Induction of IDO1 activity is known to exert immuno-regulatory effects (205, 206). To test this during an *E. falciformis* infection *in vivo*, IDO1$^{-/-}$, 1-MT treated and wild type animals were infected and sacrificed on day 1, 6 and 8. Cells of the caecum draining lymph nodes (MLN) and the spleen were isolated, purified and stimulated with sporozoite antigen for 48 hrs. To monitor the antigen-specific T-cell response their proliferation was measured by ^{3}H-thymidine incorporation. The 1-MT-treatment (Fig. 38A, B) did not result in apparent differences and also the proliferative response of IDO1$^{-/-}$ mice (Fig. 38C, D) did not show remarkable differences neither in cells of the MLN nor in spleen cells. Thus, inhibition or absence of IDO1 revealed a comparable parasite-specific proliferation compared with the wild type control.

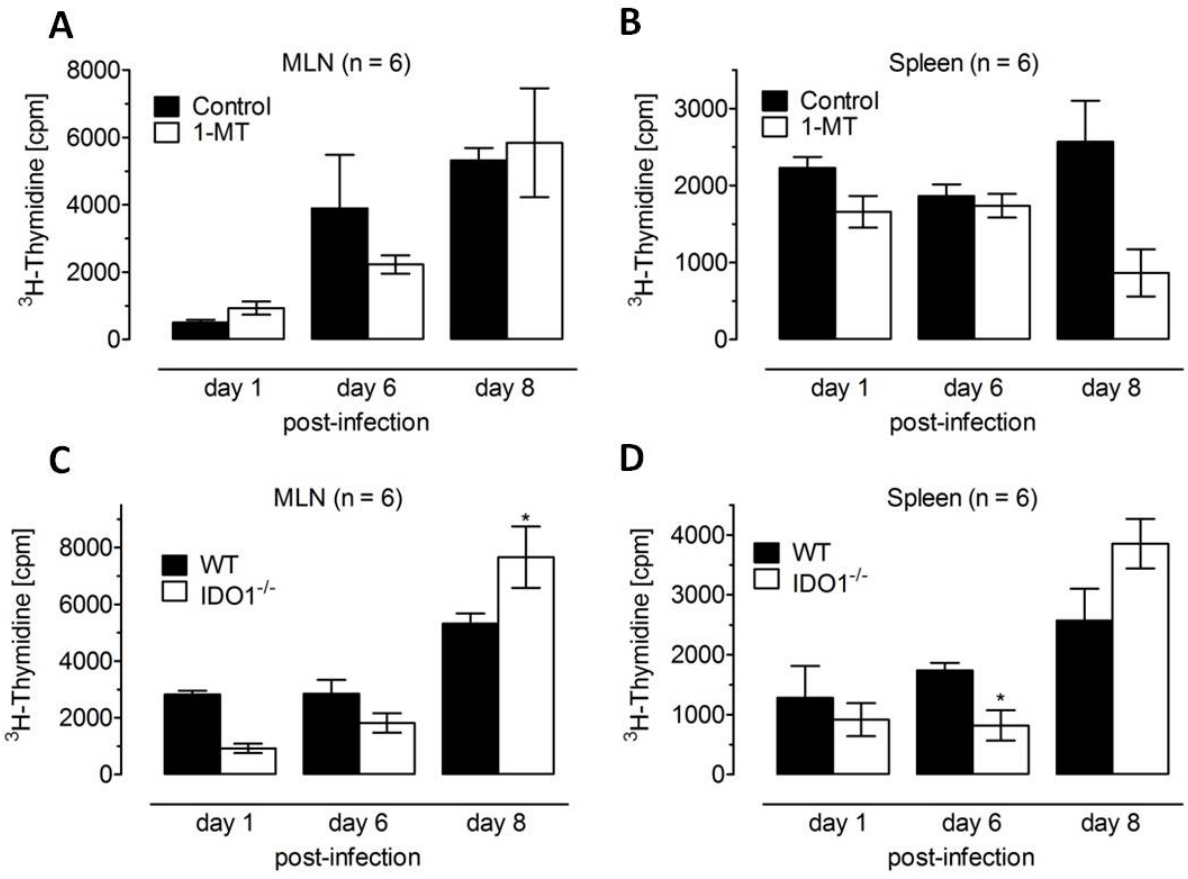

Fig. 38: Inhibition or absence of IDO1 in *Eimeria*-infected mice does not impair their parasite-specific T-cell response. All mice were infected with 50 oocysts. Cell proliferation in **(A, B)** 1-MT-treated or **(C, D)** IDO1$^{-/-}$ and respective control mice on d1, d6 and d8 of infection. The incorporation of ^{3}H-thymidine into immune cells isolated from the mesenteric lymph nodes (MLN) and spleen after 48 hrs of stimulation with the sporozoite antigen was determined. Graphs depict mean ± SEM of two experiments, each with transgenic and 1-MT-treated mice and 6 animals per group. * $p \leq 0.05$.

Furthermore, the supernatants of the cells stimulated with the parasite antigen were used for cytokine ELISAs. We first analyzed the key cytokine of an *E. falciformis* infection (IFN-γ) to monitor potential differences in untreated wild types, 1-MT-treated and IDO1$^{-/-}$ mice (Fig. 39A, B). No notable differences with the control groups in the IFN-γ levels were detectable following an *E. falciformis* infection. Therefore, a decline in parasite growth in the IDO1-deficient mice is not likely due to an amplified immune response. In addition, the concentration of two anti-inflammatory cytokines was also measured in treated and control animals on day 12 of infection (Fig. 39C, D). However, neither differences in IL-4 (Fig. 39C) nor IL-10 (Fig. 39D) measurements were statistically significant due to high variations, although the IL-10 concentration was modestly lower in inhibitor-treated mice. Other tested cytokines, TNF-α and IL-17, were undetectable during infection in control as well as 1-MT treated animals (data not shown).

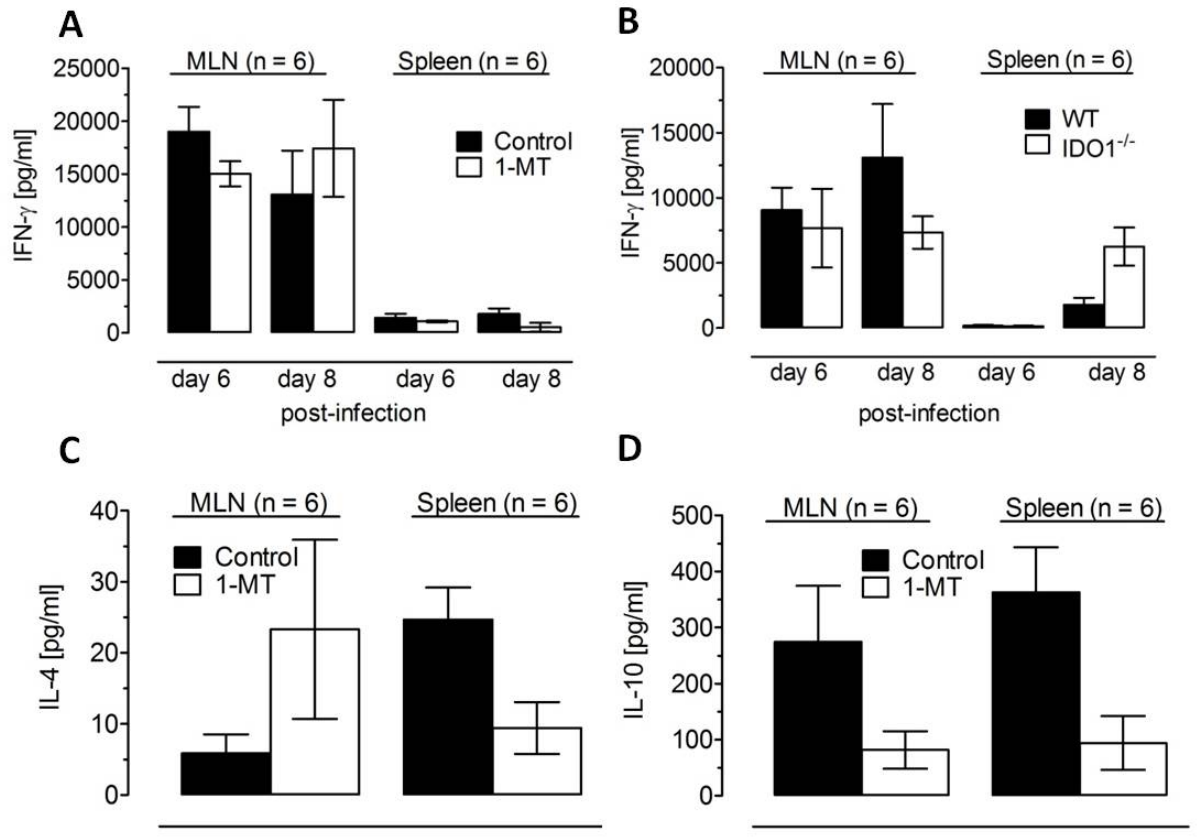

Fig. 39: Inhibition or absence of IDO1 in *Eimeria*-infected mice does not impair their parasite-specific cytokine response. Supernatants of the antigen-stimulated cells from the figure 38 were quantified for IFN-γ levels in 1-MT-treated **(A)** or IDO1$^{-/-}$ **(B)** and control mice on d6 and d8 of infection. IL-4 **(C)** and IL-10 **(D)** concentration in 1-MT-treated mice and control animals on d12 of infection. Graphs depict mean ± SD of one representative experiment with 6 animals per group.

3.4.6 Inhibition of kynurenine pathway interferes with the parasite oocyst production

As shown before, inhibition or absence of the key enzyme in tryptophan catabolism significantly reduced the oocyst numbers. To further evaluate the importance of the kynurenine pathway during an *Eimeria* infection, two more enzymes of this pathway were inhibited (Fig. 40).

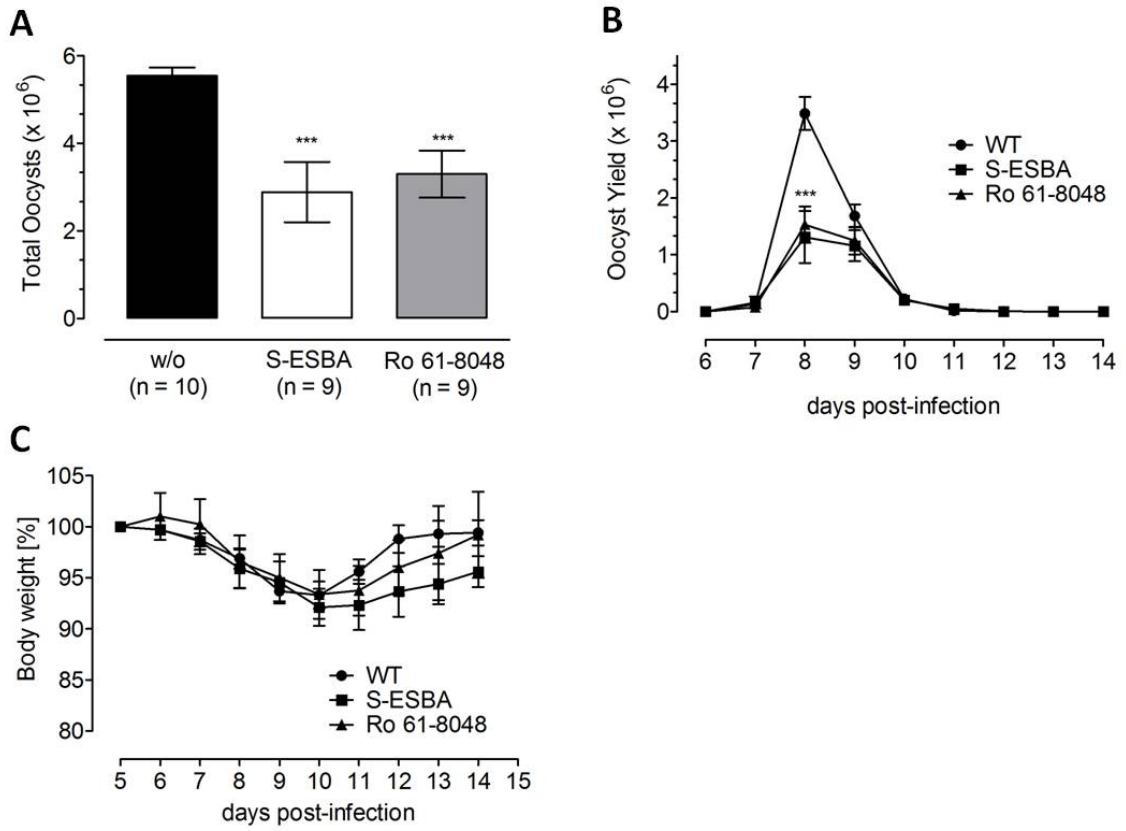

Fig. 40: Inhibition of kynurenine aminotransferase and 3-kynurenine hydroxylase impaired the life cycle of *E. falciformis*. BALB/c mice infected with 50 oocysts were treated with (S)-4-(ethylsulfonyl)benzoylalanine.hydrochloride (S-ESBA) or Ro61-8048. **(A)** Total oocyst yield and **(B)** output kinetics were quantified in treated and control animals. **(C)** Body weight of animals was monitored to deduce any signs of morbidity in the treated groups. The graphs show the means ± SEM of two independent experiments each with five mice per group. ***, $p \leq 0.0005$.

The kynurenine aminotransferase (KAT), catalyzing the production of kynurenic acid as well as xanthurenic acid, was inhibited by (S)-4-(ethylsulfonyl) benzoylalanine.hydrochloride (S-ESBA.HCl) (195). The kynurenine 3-hydroxylase (KMO), responsible for the conversion of kynurenine into 3-hydroxykynurenine, was blocked by 3,4-Dimethoxy-N-[4-(3-nitrophenyl)-2-thiazolyl]benzenesulfonamide (Ro 61-8048) (196). The mouse can tolerate relatively high doses of S-ESBA (5 mM) (207) and Ro61-8048 (200 mg/kg body weight) (208) *via* different application routes without apparent signs of mortality and morbidity. We applied both

inhibitors by oral gavage and their oocyst output was compared to control carrier-treated BALB/c animals (Fig. 40).

Strikingly, the administration of both competitive inhibitors considerably diminished the total amount of oocysts found in the feces (Fig. 40A). Inhibition of KAT by S-ESBA caused a reduction of 48% ($2.9 \times 10^6 \pm 1.1 \times 10^6$, $p < 0.001$). The inhibition of KMO by Ro 61-8048 reduced the total oocyst numbers by 41% ($3.3 \times 10^6 \pm 1.5 \times 10^6$, $p < 0.01$) when compared to untreated BALB/c mice ($5.5 \times 10^6 \pm 0.6 \times 10^6$). The application of the inhibitors yielded a normal kinetics of oocyst shedding (Fig. 40B), indicating no apparent influence on the prepatent or patent period. In addition, exposure to the drugs had no effect on morbidity as scored by the loss in body weight of the experimental animals compared with respective control groups (Fig. 40C). Consistent with the above findings, we show that perturbation of three distinct enzyme activities along the kynurenine pathway exerts a similar phenotype, strongly suggesting the requirement of a downstream metabolite for an efficient parasite development.

3.4.7 Xanthurenic acid can restore the oocyst yield in IDO1-deficient mice

Xanthurenic acid (XA) is an end metabolite of the kynurenine pathway. The enzyme kynurenine aminotransferase catalyzes the transamination reaction of 3-hydroxykynurenine into xanthurenic acid (Fig. 30). In the mouse, the urinary amount of XA is increased 3-fold in response to induction of IDO (209). All enzymes of the kynurenine pathway biochemically inhibited in this study are located upstream of the XA production. Furthermore, XA is known to be a gametocyte-activating factor for another apicomplexan species, *Plasmodium spp*. and is present in the mosquito head as well as in the insect's mid-gut (49). To evaluate a putative role of XA during an *E. falciformis* infection of mice, the metabolite was orally applied to $IDO1^{-/-}$ animals.

As expected, the absence of IDO1 reduced the amount of oocysts ($3.2 \times 10^6 \pm 1 \times 10^6$) to nearly half when compared with the wild type control (Fig. 41A). Interestingly, the XA-treatment rescued the reduced oocyst numbers in $IDO1^{-/-}$ animals. In comparison to the IDO1-deficient mice XA-treated $IDO1^{-/-}$ shed 55% more oocysts ($6.9 \times 10^6 \pm 2.3 \times 10^6$, $p < 0.0001$). The oocyst yield of XA-treated $IDO1^{-/-}$ mice was comparable with the oocyst output of the untreated wild types ($5.3 \times 10^6 \pm 1.3 \times 10^6$). The slight increase in total oocyst number in the XA-treated animals in comparison to wild types was not significant. Furthermore, treatment of wild type mice with XA did also not result in any considerable differences (data not

shown). The course of infection was not affected (Fig. 41B) and the treatment did not negatively influence the infection-associated loss in body weight (Fig. 41C).

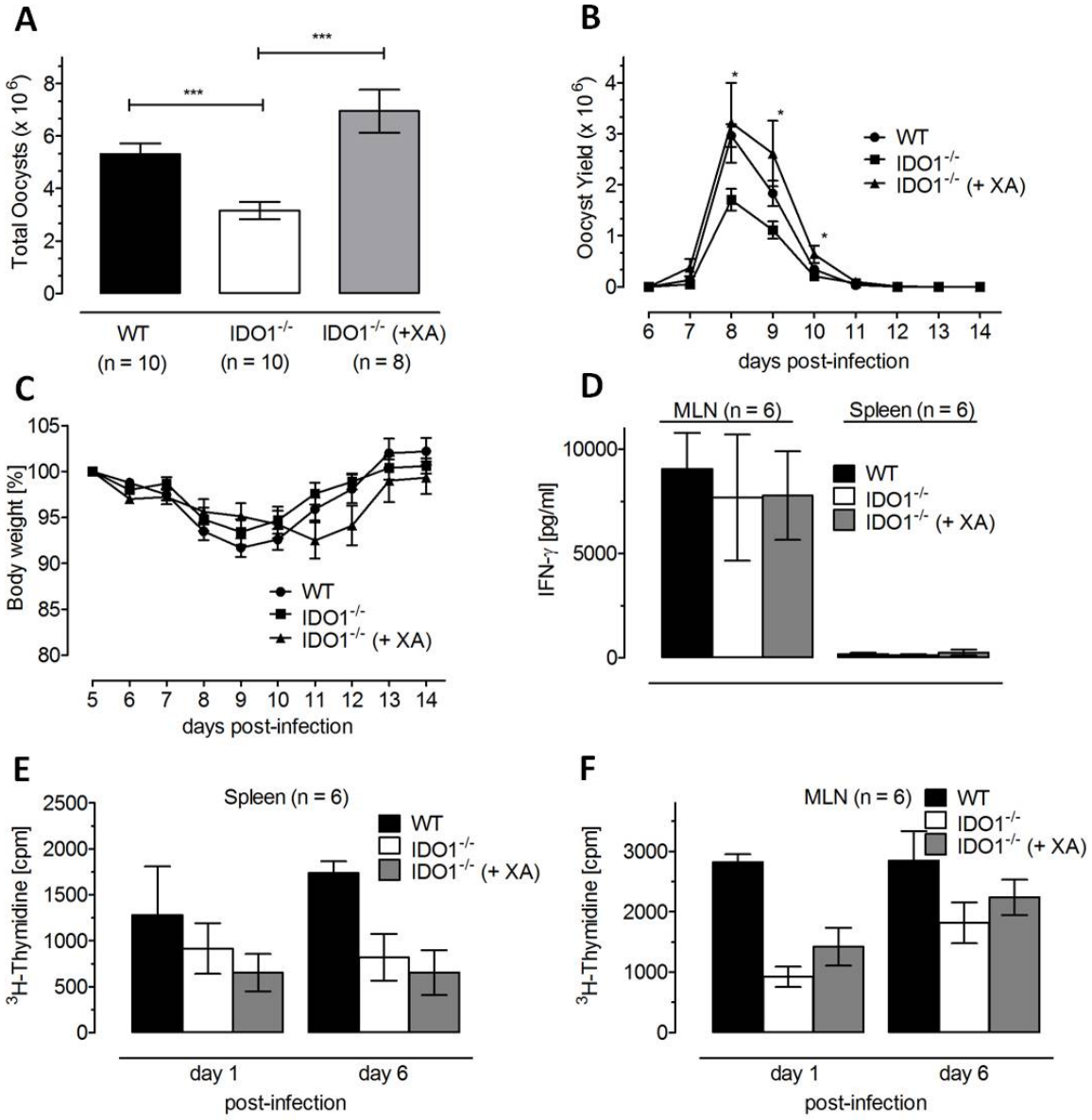

Fig. 41: Xanthurenic acid can completely restore the oocyst output in IDO1$^{-/-}$ mice. (A) Total parasite yield, as well as the **(B)** kinetics of oocyst shedding was measured in the indicted groups. **(C)** Body weight of animals was monitored to deduce any signs of morbidity in the groups. **(D)** IFN-γ levels in supernatants of antigen-stimulated cells from day 6. **(E, F)** Cell proliferation in IDO1$^{-/-}$, IDO1$^{-/-}$ (+ XA) and control mice on d1 and d6 of infection. The incorporation of ^{3}H-thymidine into immune cells isolated from the mesenteric lymph nodes (MLN) and spleen after 48 hrs of stimulation with the sporozoite antigen was determined. The bars show the means ± SEM of two independent experiments with five animals per group. *, $p \leq 0.05$; ***, $p \leq 0.0005$.

The T cell proliferation (Fig. 41E, F) and IFN-γ levels (day 6, Fig. 41D) in response to parasite antigen were also measured to assess the involvement of the immune response. Again, we did detect a comparable ^{3}H-thymidine incorporation and IFN-γ concentrations in

wild types, IDO1$^{-/-}$ and XA-treated IDO1$^{-/-}$. Therefore, a rescue of the parasite growth in the XA-treated IDO-deficient mice is not likely associated with changes in the immune response.

As shown before, infection of IFN-γR$^{-/-}$ mice resulted in a decreased oocyst output (Fig. 35). To test whether this reduction is a consequence of a missing IDO1 induced XA production in IFN-γR$^{-/-}$ mice, the metabolite was administered to parasitized IFN-γR$^{-/-}$ animals (Fig. 42).

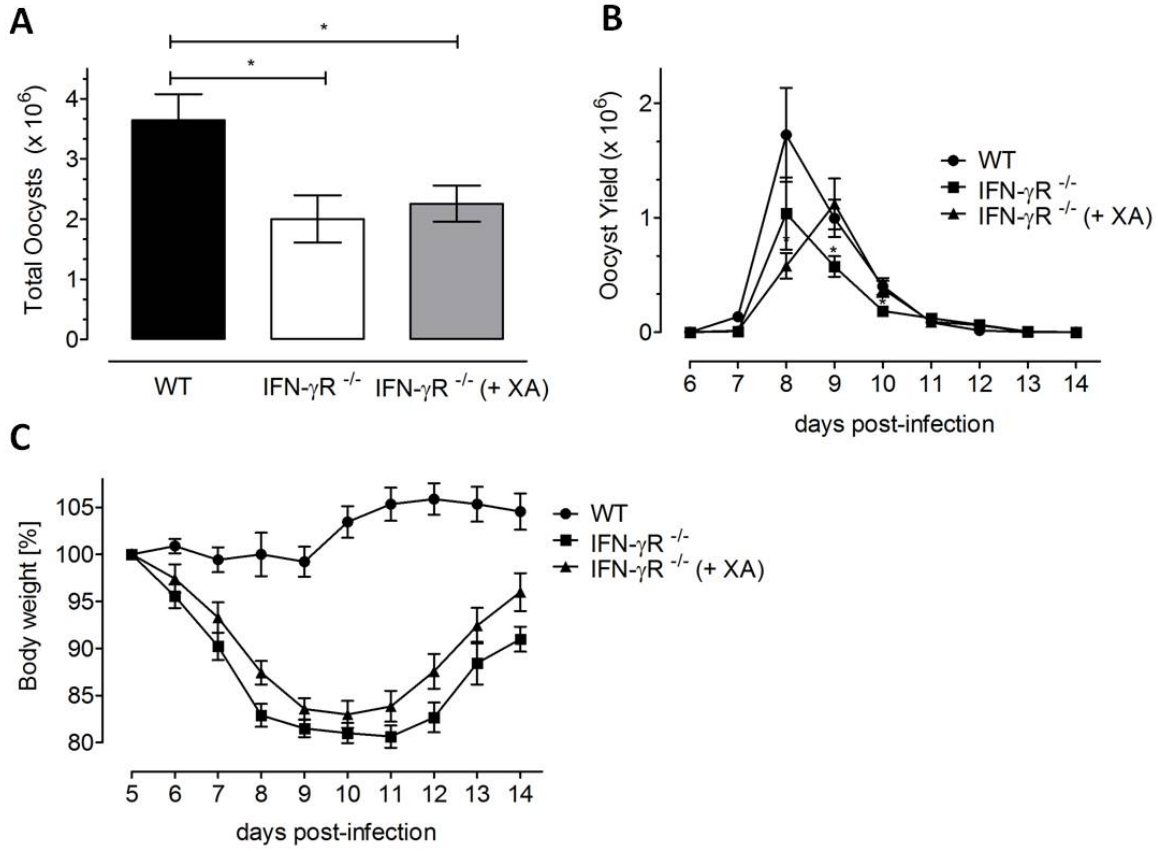

Fig. 42: Xanthurenic acid did not restore the impaired parasite development in IFN-γR$^{-/-}$ mice. **(A)** Total parasite yield, as well as the **(B)** kinetics of oocyst shedding was measured in the indicated groups. **(C)** Body weight of animals was monitored to deduce any signs of morbidity in the groups. The bars show the means ± SEM of two independent experiments with five mice per group.*,$p \leq 0.05$.

XA-treated animals also shed less oocysts (~ 33%) when compared to their wild type controls. These numbers however were comparable to the amount of shed oocysts in untreated infected IFN-γR$^{-/-}$ animals (Fig. 42A). Neither in the IFN-γR$^{-/-}$ nor in the XA-treated transgenic mice the prepatent or patent period was altered during infection, the peak days of oocyst shedding remained the same (Fig. 42B). Similar to IFN-γR$^{-/-}$ mice, the XA-treated animals showed a higher body weight loss (Fig. 42C) than their controls, which may be due to an increased pathology as described previously (22, 126). In brief, the application of XA to IFN-γR$^{-/-}$

animals, however, did not rescue the parasite development, which might be a consequence of an increased Th17 response associated with an exaggerated intestinal pathology (126).

3.4.8 The effect of xanthurenic acid is likely confined to the microgamete maturation in the definitive host

The above experiments however indicated an important role of host IDO and the resulting XA production for the development of *E. falciformis* in its murine host. To address whether the asexual and/or sexual stages are affected by the absence of IDO1 and XA, we infected IDO1$^{-/-}$ (+/- XA) and parental animals, and performed quantitative PCR of caecum-derived RNA samples (Fig. 43). *Ef*18S rRNA was used to quantify differences in the asexual development (day 3 to 5). The presence of *Ef*Gam82 and *Ef*Gam56 (day 6 to 8) indicated the macrogametocyte, and thus the sexual development (Fig. 43). Specific amplification of individual expressed sequence tags and their expected sizes were confirmed by gel electrophoresis (Fig. 43A). We compared the abundance of each transcript among the three parasitized mice samples. No apparent and significant change was observed in relative abundance of *Ef*18S rRNA (Fig. 43B), *Ef*Gam82 (Fig. 43C), and *Ef*Gam56 (Fig. 43D) expression in the IDO1$^{-/-}$-derived caeca samples and also irrespective of the XA treatment, when compared with the parental samples. These results show that the aforementioned effect of host IDO1 and XA on the parasite life cycle is not mediated *via* their action on asexual or macrogametocyte development.

In addition, we also tested the importance of IDO1 and XA-treatment in *P. berghei*-infected mice, a parasite known to depend on XA for its microgamete maturation in the mosquito host (49). The mice were infected with the parasite and the parasitemia and transcript abundance of gametocyte and gamete-specific genes (*Pb*Ccp3, *Pb*Ccp4, *Pb*FNPA, (210)) was determined in IDO1$^{-/-}$ (+/- XA) and wild type mice. Furthermore, mosquitoes were fed on infected animals, and dissected to evaluate the yield of *P. berghei* oocysts. As expected, we detected no significant differences in the parasitemia (Fig. 44A, B) or the transcript abundance of gametocyte-specific genes (Fig. 44C-E). The oocyst yield was also comparable to their wild type controls (Fig. 44F). These data indicate an apparently insignificant role of mouse tryptophan metabolism for the blood stages of *P. berghei*. Nevertheless, exploitation of tryptophan catabolism by both apicomplexan parasites in their definitive host, however, appears to be evolutionarily conserved, despite a switch of two- to/from one-host life cycles.

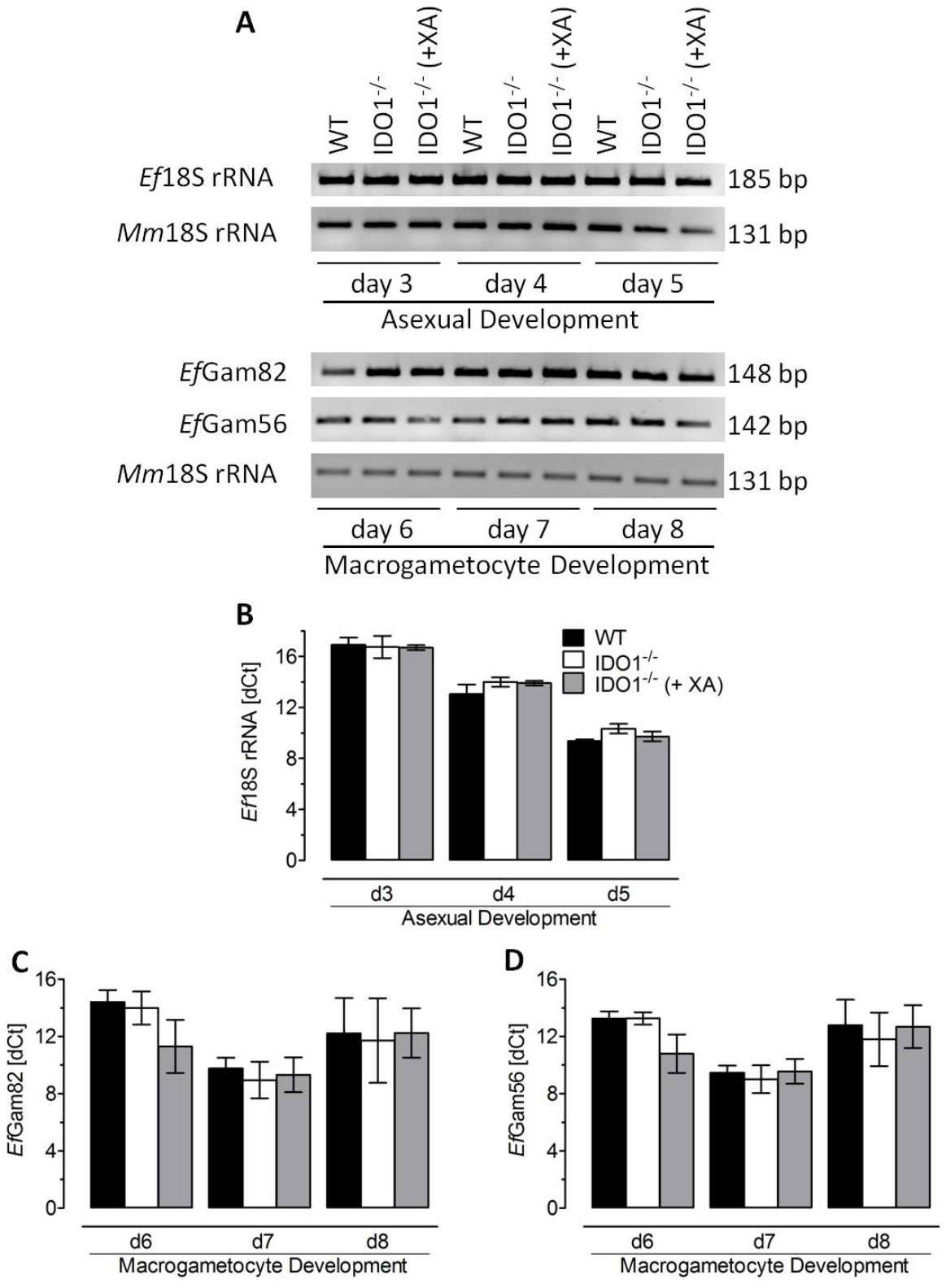

Fig. 43: *E. falciformis* shows a normal asexual and macrogametocyte development in the absence of IDO1. The animals were infected with 1500 oocysts and treated with XA, as indicated. Total RNA derived from the parasitized caeca was subjected to quantitative PCR. **(A)** Specific detection of the indicated parasite (*Ef*18S rRNA, *Ef*Gam82, and *Ef*Gam56) and host (*Mm*18S rRNA) expressed sequence tags by quantitative PCR followed by gel electrophoresis. **(B)-(D)** To evaluate the abundance (dCt) of individual transcripts, **(B)** *Ef*18S rRNA, **(C)** *Ef*Gam82, and **(D)** *Ef*Gam56 in each animal group, their Ct values were normalized to respective host samples (*Mm*18S rRNA). The error bars represent the means ± SEM of two independent experiments.

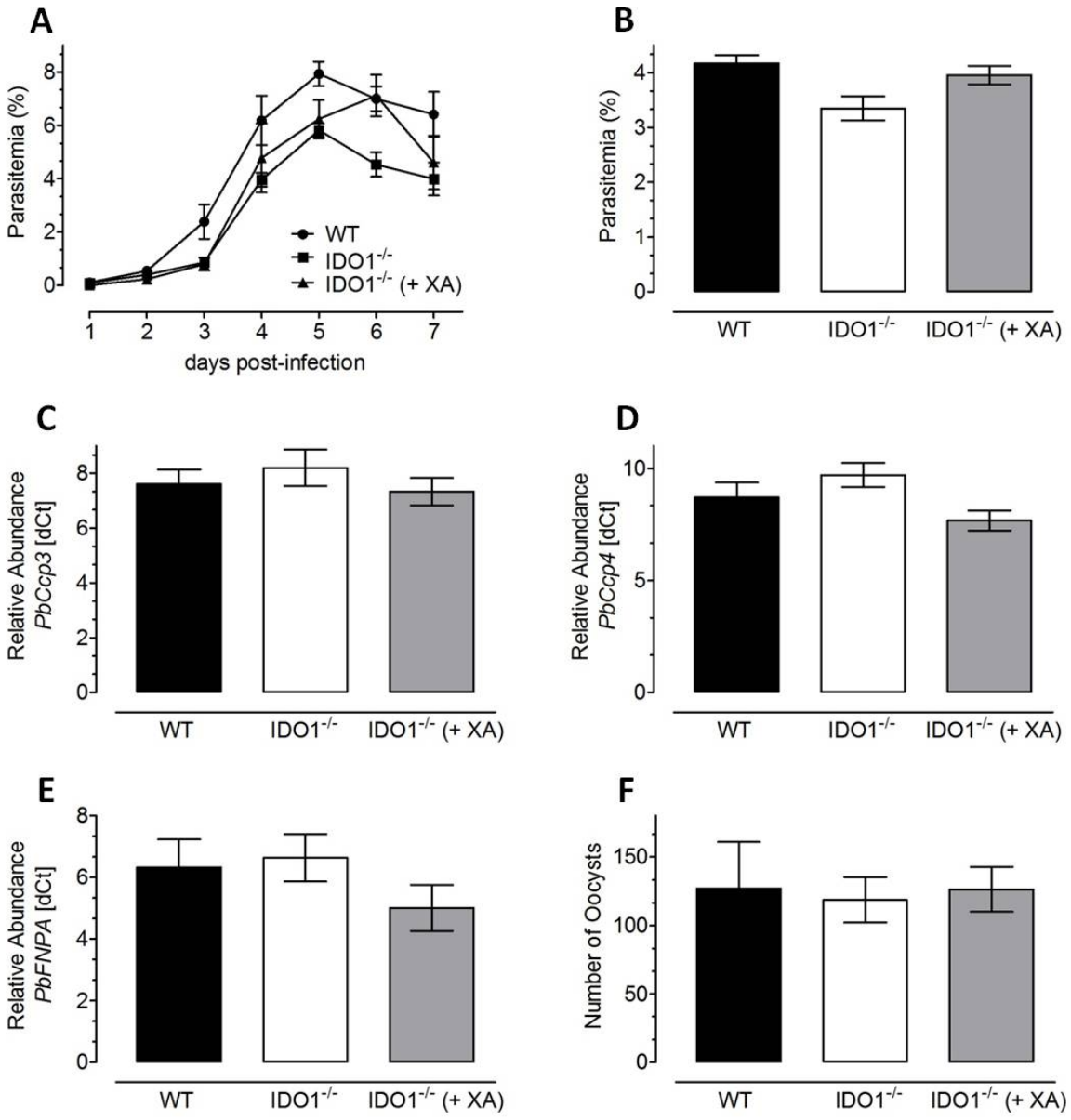

Fig. 44: IDO1-deficient animals do not show an impaired *P. berghei* development. (A) The parasitemia kinetics were deduced by Giemsa-stained blood smears over a period of 7 days. Bars represent the means ± SD of one experiment with 3 mice per group. **(B)** Parasitemia on day 3 p. i. in WT, IDO-/- and XA-treated transgenic mice. The animals were infected with *P. ber*ghei and treated with XA, as indicated. **(C-E)** Relative abundance of the indicated parasite transcripts (*Pb*Ccp3, *Pb*Ccp4, *Pb*FNPA) normalized to *Pb*Gapdh on day 3 p.i. **(F)** Mosquitoes were fed on *P. berghei*-infected mice and total oocysts were counted following dissection of the mosquitoes on day 9. The error bars represent the means ± SEM of two independent experiments.

4. Discussion

4.1 Microarray experiments

The objective of the gene expression experiments was to identify host-parasite interactions in response to an *E. falciformis* infection of mouse host cells. The study also compared the host responses induced by two apicomplexan parasites and the *in vivo* and *in vitro* infection with *E. falciformis*.

4.1.1 *In vitro* gene expression analyses

For the *in vitro* assays a colonic epithelial cell line (YAMC, Young Adult Mouse Colon (189)) was selected, which is similar to the natural host cells to *E. falciformis*, a parasite mainly replicating in the caecum and the upper half of the colon (31). The use of IFN-γ in the cell culture systems additionally mimics the natural environment of an *in vivo* infection. The two selected time points (4 h and 16 h p. i.) coincide with the completion of invasion and the beginning of trophozoite formation. The decreased number of parasitized cells 16 h p. i. might be due to parasite egress, as shown for *E. bovis* sporozoites (211), or just a consequence of an aborted development. However, no further development was observed in *E. falciformis*-infected YAMC cells. The success of an *in vitro* development of *E. falciformis* may therefore be determined during the early development. We further did not observe differences in the growth of *T. gondii* irrespective of IFN-γ (5 U/ml), which were reasonably below the reported inhibitory concentration of ~16 U/ml in *T. gondii*-infected HFF cells (199). Importantly, *T. gondii* infection was persistent in YAMC cells for 43 h, whereas no development was observed in *E. falciformis*-infected cells. Therefore, gene expression analyses using *T. gondii*-infected YAMC cells provided a required comparative control in this study.

4.1.1.1 *Eimeria* induces a strong host response soon after invasion

Microarray experiments revealed a strong host cell response shortly after *E. falciformis* infection. The numbers of modulated transcripts early and late during *E. falciformis* YAMC infection were comparable. Interestingly, the expression of only a few genes appeared commonly changed during both time points, suggesting a discrete response to the early and late infection. The strong early response is in contrast to data reported from *E. bovis*-infected bovine endothelial cells. These infection experiments resulted in only 12 modulated genes 4 h p. i. (212). However, in the *E. bovis* approach only 45 genes appeared regulated 4 days post-

infection. The differences might be attributed to a different *Eimeria* species as well as host-cell type. Similar to *E. bovis*-infected cells, *T. gondii*-infected YAMC cells lacked a distinct early response. This was the most apparent difference between *T. gondii*- and *E. falciformis*-infected YAMC cells. Nevertheless, contrasting results have been reported for *T. gondii*-infected porcine or human cells (56, 213). The infection of a porcine kidney epithelial cell line (PK13) and of HFFs resulted in a considerably modulated host response shortly after parasite infection. These reports, however, differ in the host cell type (mouse – pig – human) and *T. gondii* strain. Our microarray experiments were performed with the RH type I strain, whereas the PK13 cells were infected with a temperature-sensitive mutant of the RH strain, and HFFs were exposed to the PDS strain, a slow-growing (ME49) type II strain. Therefore, host response to *T. gondii* is most likely dependent on the host cell and/or parasite strain. In comparison to *E. falciformis*, the *T. gondii* infection was persistent; suggesting that a lack of an early host response might favor the parasite survival and/or development in YAMC cells.

4.1.1.2 *In vitro* model of *E. falciformis*-infected YAMC cells

Microarray analyses of *E. falciformis*-infected YAMC cells resulted in a massive modulation of the mouse transcriptome. The KEGG pathways which appeared modulated upon *Eimeria* infection are summarized in a proposed model (Fig. 45).

Upon infection of YAMC cells, the expression of transcription factors including members of the AP-1 and EGR family was induced. These transcription factors initiate the expression of genes, which are involved in a variety of biological processes including immune response, apoptosis, growth and differentiation. Moreover, initial parasite-induced signaling leads to transcriptional induction of NOD-like, TLR and MAPK signaling pathways. Although no TLR family member was induced *in vitro*, several DUSPs, which negatively regulate the TLR-mediated MAPK-signaling, appeared modulated upon early and late infection. Furthermore, cytokines or chemokines produced in response to infection might exert their function on neighboring host cells. In addition, cytokines in the medium (IFN-γ) initiate the Jak-STAT signaling cascade, and potentiate the host immune response. Moreover, cytokine-cytokine receptor interactions or the signaling of growth factors *via* integrins can affect the adhesion properties of the host cells. Other pathways modulated by *E. falciformis* infection include the insulin and mTOR signaling, which regulate protein synthesis, sugar and lipid metabolism and which are induced in response to growth factors and hormones. Many of the listed host proteins can potentially regulate the parasite development. A variety of knockout

cells and mice are available (red, green, Fig. 45), which can be used to examine the effect of indicated host determinants on the parasite development.

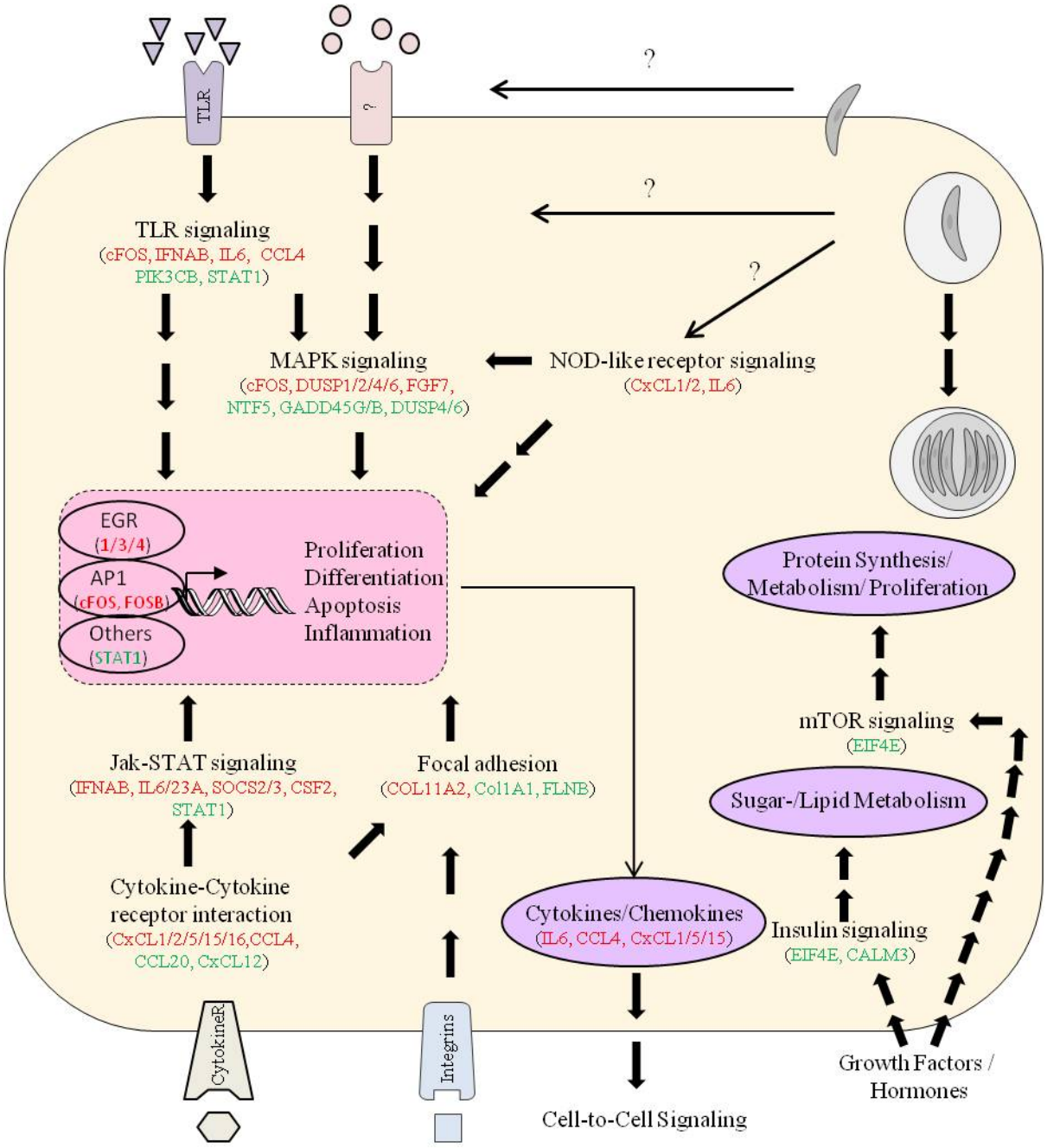

Fig. 45: *In vitro* model of host response upon *E. falciformis* infection of YAMC cells. The model is based on gene expression analyses, literature searches and proposed hypotheses. Only selected host pathways (KEGG) are indicated. Question marks signify potential parasite-induced signaling. The colour-coded (red or green) proteins, induced or repressed in our analyses, signify the available biological resources such as knockout lines and transgenic mice.

4.1.1.3 A set of host genes are reciprocally modulated by *E. falciformis* and *T. gondii*

Interesting candidates determining the *in vitro* growth of *E. falciformis* might be genes, which were reciprocally regulated in comparison to *T. gondii* (Tab. 10). Many of these genes are either unknown or not well described, however. The genes repressed early during *Eimeria*, but induced during *Toxoplasma* infection are involved in pre-mRNA splicing (TRA2A) (214), ribosome synthesis (NOL5A), mitosis (centrosomal protein, CNTLN) (215), maintenance and reorganization (RAI14) (216) as well as in restructuring of the actin cytoskeleton (FLNB) (217). One can speculate that it would be rather detrimental for the host cell to repress central cellular processes of transcription, translation and cell division already early upon invasion. In addition, maintenance of the integrity of the cytoskeleton is an important feature of cell survival.

In contrast, genes up-regulated 4 h post-*Eimeria* infection but down-regulated following an infection with *T. gondii* are described to regulate T-cell development (ZBTB1) (218), osmotic stress (TSC22D2) (219), or protein transport (MITD1). All genes inversely regulated during late *Eimeria* and *Toxoplasma* infection were induced by *E. falciformis* but repressed by *T. gondii* infection. These genes participate in proliferation of the crypt cells in the small and large intestine (220) and support the development of goblet cells (DLL4) (221), or are produced by these cell types (MUC13) promoting anti-apoptotic and proliferative effects (222). Many of the reciprocally-regulated transcripts also participate in cell death events, such as a member of the protein kinase C family with anti-apoptotic properties (PRKCE) (223), a peroxisomal protein whose over-expression induces apoptosis (PXT1) (224), and a stress response protein with pro-apoptotic and anti-proliferative functions (TRP53INP1) (225). Other proteins, e.g. CFLAR (226, 227) and DUSP1 (228, 229) have been described as anti- as well as pro-apoptotic. Especially the modulation of pro- and anti-apoptotic genes upon infection may represent the complexity of the apoptosis pathway indicating that the infected cells can either initiate the death program if the infection progresses or prevent if the infection resolves (230, 231).

Other inversely regulated genes mediate immune responses. DUSP1 (232) and DUSP10 (233), two key regulators of MAPK activity, participate in the negative regulation of acute inflammatory responses. The major type I IFN (IFNAB) (234), RSAD2, an interferon stimulated gene with importance in the innate immunity against viruses (235), and BCL6, a transcription factor involved in B and T cell maturation (236), regulate the immune responses

against various external stimuli. Many other genes induced by *Eimeria* but repressed by *T. gondii*, participate in maintaining the structure of the cytoskeleton, such as gap junction formation (GJD4) (237), organization and interaction with actin (ENC1) (238) and production of hyaluronic acid (HAS2) (239), which is a structural component of the extracellular matrix. Induced expression of genes involved in maintenance of the cytoskeleton might hint towards a more distinct disruption of the host cells, which could be detrimental for the *E. falciformis* development. Other inversely regulated genes included a transcription factor with protective roles against oxidative DNA damage (NCOA7) (240), a protein ortholog to the bacterial methylcitrate dehydrogenase with a possible metabolic function in the oxidative conversion of propionyl-CoA into pyruvate (IRG1) (241), and genes of unknown or less described function (19-32, TMEM140, GM8995).

Tab. 10: Table of reciprocally regulated mouse genes during YAMC infection. The table depicts selected transcripts showing a reciprocal regulation during *E. falciformis* and *T. gondii* infection of YAMC cells.

		E. falciformis		***T. gondii***	
Symbol	**Gene**	**4 h**	**16 h**	**4 h**	**16 h**
Morphology					
RAI14	Retinoic acid induced 14	-3.34	-	-	1.93
FLNB	Filamin, beta	-1.68		1.57	1.54
GJD4	Gap junction protein, delta 4	-	3.42	-	-1.86
ENC1	Ectodermal-neural cortex 1	-	1.52	-	-1.97
HAS2	Hyaluronan synthase 2	-1.61	2.14	-	-1.80
Immune response					
ZBTB1	Zinc finger and BTB domain containing 1	2.06	-	-	-2.06
DUSP1	Dual specificity phosphatase 1	-	2.02	-	-2.31
DUSP10	Dual specificity phosphatase 10	-2.12	2.15	-	-3.74
IFNAB	Interferon alpha B	-	2.98	-	-1.81
BCL6	B cell leukemia/lymphoma 6	-	2.15	-	-1.74
RSAD2	Radical S-adenosyl methionine domain containing 2	-	2.26	-	-3.33
Proliferation					
CNTLN	Centlein, centrosomal protein	-2.20	-	-	1.68
DLL4	Delta-like 4	-	4.05	-	-1.62
MUC13	Mucin 13, epithelial transmembrane	-	3.96	-	-2.60
Apoptosis					
TRP53INP 1	Transformation related protein 53 inducible nuclear protein 1	-	2.59	-	-2.77

PXT1	Peroxisomal, testis specific 1	-	2.54	-	-1.89
CFLAR	CASP8 and FADD-like apoptosis regulator	-	1.76	-	-1.74
PRKCE	Protein kinase C, epsilon	-	2.77	-	-1.74
Transcription					
TRA2A	Transformer 2 alpha homolog	-3.17	-	-	2.62
NCOA7	Nuclear receptor coactivator 7	-	1.86	-	-1.55
Protein metabolism					
NOL5A	Ribonucleoprotein homolog	-2.04	-	-	1.69
MITD1	MIT, microtubule interacting and transport, domain containing 1	2.24	-	-	-1.78
Others					
TSC22D2	TSC22 domain family, member 2	2.24	-	-	-1.67
IRG1	Immunoresponsive gene 1	-	2.20	-	-2.37
TMEM140	Transmembrane protein 140	-	1.94	-	-2.02
19-32	Mus musculus similar to monoclonal antibody kappa light chain	-	4.21	-	-1.71
GM8995	Predicted gene 8995	-	1.71	-	-2.91

However, whether any of these genes determine *E. falciformis* growth in cell culture remains to be determined. Furthermore, it might even be of more interest to investigate the function of genes present in *T. gondii* but absent in *E. falciformis*-infected cells and vice versa. One such group, the immunity-related GTPase family, will be discussed below.

Nevertheless, the most apparent differences between *T. gondii*- and *E. falciformis*-infected YAMC cells include the lack of an early response in *T. gondii*-infected cells and the higher number of repressed transcripts at 16 h post-infection. These differences might be in part a consequence of the presence of several rhoptry kinases in *T. gondii* (44 in *T. gondii* (242) *vs.* 10 in *E. falciformis* (unpublished data)). These proteins are released during the invasion process and some are known to be potent virulence factors (*e.g.* Rop16, Rop18) by manipulating the host cell signaling pathways and transcription (243, 244).

4.1.2 *Ex vivo* gene expression analysis

Determination of the infectious dosage was critical for the *ex vivo* microarray experiments. The oocyst yield remained constant with increasing inoculums from 500 to 1000 oocysts suggesting a crowding effect. This means that the fertility of the parasite decreased with an increased infectious dose as described for different avian *Eimeria* species (245). We infected the mice with a quite high oocyst number, which was still well tolerated by the animals. Most

pathological changes occurred on the peak days of oocyst shedding, and the animals did not show any sign of pathology on the selected time points of 24 and 144 h post-infection. Importantly, these time points coincide with interesting steps within the *Eimeria* life cycle. Mesfin *et al.* (197) described the presence of trophozoites within the tissue 18 h p. i. and first mature schizonts were visible 48 h post-infection. Accordingly, the first time point (24 h) coincides with the beginning of the asexual schizogony. To mark the onset of sexual development (144 h), we used Gam82 and Gam56, which are the markers of sexual development in three avian *Eimeria* species, *E. maxima*, *E. tenella* and *E. acervulina.* These 82- and 56-kDa gametocyte-specific antigens were first described in wall forming bodies of macrogametocytes of *Eimeria maxima* (246, 247). We show here that homologues of these macrogametocyte-specific genes (*Ef*Gam82, *Ef*Gam56) are also expressed in *E. falciformis*, and mark the onset of sexual development.

4.1.2.1 The murine response correlates with the severity of infection

The number of induced or repressed transcripts was increased from 24 h to 144 h post-*E. falciformis* infection. Similar results have been obtained from microarray studies of *E. maxima*, *E. acervulina* and *E. tenella*-infected chickens. The reported number of up- or down-regulated transcripts in intraepithelial lymphocytes isolated from infected chicken intestines increased with the progression of infection (248, 249). The infection of mice with *E. falciformis* leads to an infection of the intestinal epithelial cells of the caecum. Following 24 h of infection, the parasites completed invasion and trophozoite formation. Mesfin *et. al.* (197) observed the first mature schizont 48 h p. i. Therefore, upon trophozoite formation the asexual replication, the first schizogony takes place. With progression of infection, the number of parasitized host cells as well as of parasites increases as shown by ribosomal RNA analyses and corresponds to a more substantial modulation of the host transcriptome. In addition, the infection also recruited and activated immune cells. Therefore, the early response to *E. falciformis* infection involved only a few genes, whereas the progression of infection coincided with an accelerated host response.

4.1.2.2 *In vivo* model of *Eimeria*-mouse interactions

Many of the *Eimeria*-modulated mouse genes constitute basal signaling and immunological pathways (KEGG). Some of these are summarized in figure 46 and discussed below in the context of our proposed *in vivo* model.

The transcription factors of the EGR and STAT family were highly induced upon infection of mouse caecum. These transcription factors regulate the expression of immunity-related genes as well as of other genes involved in apoptosis, growth and differentiation. The expression of some TLRs (TLR4, 7) was also induced. Similar to *T. gondii* infections, GPI-anchored surface proteins might be sensed via TLR4 (97) and initiate the signaling cascade. Several DUSPs, which counter-regulate a TLR-mediated signaling via MAPK, were induced. Chemokines are secreted to recruit lymphocytes, which potentiate the immune response by secreting several cytokines. Especially IFN-γ and IL-12, secreted *e.g.* by dendritic cells, induce Th_1 cell differentiation. Furthermore, attracted immune cells might directly target parasitized cells by *e.g.* mediating NK cell-mediated cytotoxicity. Cytokines can also lead to Jak-STAT pathway activation and induction of genes involved in immunity and inflammation. For example, IFN-γ secreted by several immune cells is sensed by the IFN-γ receptor and induces the induction of genes of the IRG and GBP family *via* Jak-STAT signaling. Members of this family attack several pathogens, including parasites (119, 250). However, *T. gondii* type I strain evolved mechanisms to interfere with their PVM disrupting nature (251). Therefore, it might also be possible for *E. falciformis* to interfere with the host IRGs and GBPs to prevent a disruption of the PV. Furthermore, IFN-γ also induces the expression of IDO1, the rate-limiting enzyme of the tryptophan catabolism, whose expression is required for an optimal parasite development (252).

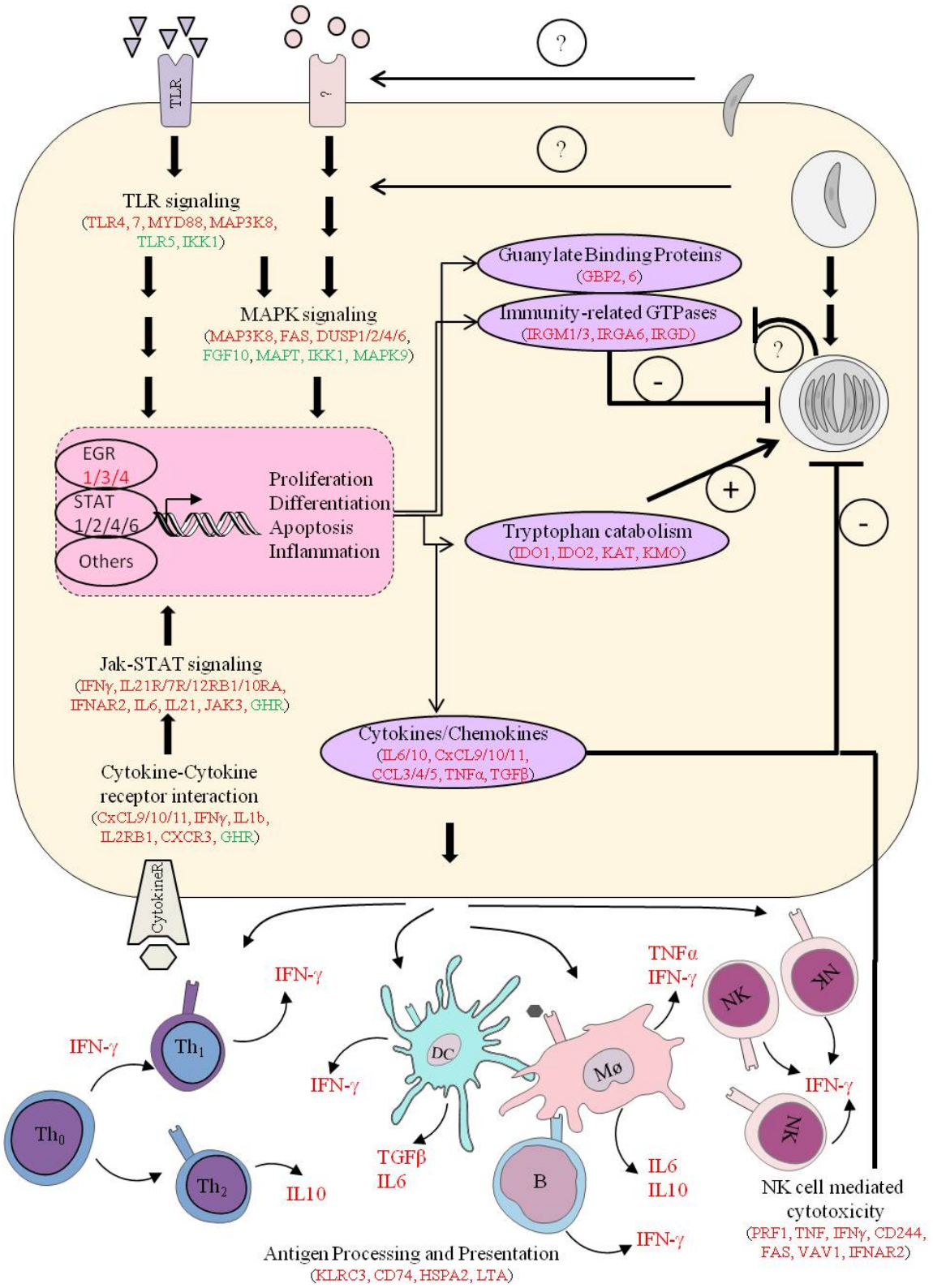

Fig. 46: Proposed *in vivo* model of *Eimeria*-mouse interactions. The model is based on gene expression analyses, experimental support for indicated host proteins and proposed hypotheses. Only selected host pathways potentially influencing the parasite development are indicated. The colour-coded (red or green) proteins, induced or repressed in our analyses and for which transgenic animals are available, are shown. The plus (+) and minus (-) signs in circles denote a positive or negative impact of a given pathway on the parasite's *in vivo* life cycle. Question marks signify potential parasite-induced signaling.

4.1.3 Differentially regulated genes during *in vitro* and *in vivo* infection by *Eimeria*

We compared the productive *in vivo* development of *E. falciformis* with the abortive growth *in vitro* to identify potential candidates limiting the parasite development in cell culture. Due to the high number of differentially regulated genes, only a few are discussed below (Tab. 11, for a complete list of reciprocally-regulated genes see App. F).

Many of the genes reciprocally regulated in the *in vitro* and *in vivo* studies were not annotated in the gene ontology database. Others participate in different biological functions including proliferation, apoptosis and immune response. Some of the genes repressed early during the *in vitro* development, but induced *in vivo* play a role in the regulation of cellular growth, including the proteins promoting (GPC1) (253) and inhibiting (MAGI2) (254) cell proliferation. Also the *in vivo* induced genes, RASSF2 (255) and GADD45G (256) negatively influence the cell growth and induce apoptosis. Some genes induced early *in vitro*, but repressed *in vivo* have pro-apoptotic (DIDO1) (257) or anti-proliferative (GNE) (258) functions. Similarly, genes reciprocally-regulated between late *in vitro* infection and *in vivo* studies regulate apoptosis and/or proliferation. Some genes repressed 16 h p. i. but induced *in vivo* promote either cell cycle arrest (MS4A4B) (259) or progression (TACSTD2, (260), CKS1B (261)). Interestingly, we detected a number of genes repressed late *in vitro* but induced *in vivo* with opposing effects, such as pro-apoptotic (BMP4) (262) or anti-apoptotic proteins (NEU3) (263), as well as genes with more than one role including proliferative and anti-apoptotic (ID2) (264) and anti-proliferative and pro-apoptotic (GADD45B) (265, 266) capacities. Likewise, genes induced late *in vitro* but repressed *in vivo* play a role in increasing proliferation (FER1L3) (267) or promoting cell cycle arrest and apoptosis (TRP53INP1) (225). However, a down-regulation of pro-apoptotic genes *in vitro* should favor the survival of host cells and thus the parasite development. By contrast, a down-regulation of anti-apoptotic or up-regulation of pro-apoptotic genes should obstruct *in vitro* parasite growth.

Interestingly, only two genes in our assays were induced *in vitro* during *Eimeria* infection but appeared repressed *in vivo* as well as in *T. gondii*-infected YAMC cells (TRP53INP1, DLL4). TRP53INP1 plays an anti-proliferative and pro-apoptotic role (225), whereas DLL4 is involved in maintaining intestinal stem cell homeostasis (220) and T-cell development (268).

Tab. 11: Table of selected reciprocal regulated genes during YAMC and mouse infection. Displayed are the selected commonly modulated transcripts and their functions during *in vivo* and *in vitro E. falciformis* infection, which showed a contrary expression profile.

		in vitro		*ex vivo*	
Symbol	**Gene**	**4 h**	**16 h**	**24 h**	**144 h**
Proliferation					
GPC1	Glypican 1	-1.61			3.9
MAGI2	Membrane associated guanylate kinase, WW and PDZ domain containing 2	-1.63			5.91
GNE	Glucosamine (UDP-N-acetyl)-2-epimerase/N-acetylmannosamine kinase	2.05			-2.18
MS4A4B	Membrane-spanning 4-domains, subfamily A, member 4B		-2.33		10.15
TACSTD2	Tumor-associated calcium signal transducer 2		-2.14		3.03
CKS1B	CDC28 protein kinase 1b		-1.51		1.61
FER1L3	Myoferlin		2.04	-1.84	3.95
Apoptosis					
DIDO1	Death inducer-obliterator 1	1.95			-1.96
BMP4	Bone morphogenetic protein 4		-2.24		2.08
NEU3	Neuraminidase 3		-1.63		8.42
Proliferation and Apoptosis					
GADD45G	Growth arrest and DNA-damage-inducible 45 gamma	-1.61	-2.07		3.36
RASSF2	Ras association (RalGDS/AF-6) domain family member 2	-1.60			10.63
ID2	Inhibitor of DNA binding 2		-1.91		3.91
GADD45B	Growth arrest and DNA-damage-inducible 45 beta		-1.75		3.78
TRP53INP1	Transformation related protein 53 inducible nuclear protein 1		2.59		-3.37
Immune response					
DUSP6	Dual specificity phosphatase 6	-2.59	2.60		3.20
DUSP10	Dual specificity phosphatase 10	-2.12	2.15		10.23
DUSP4	Dual specificity phosphatase 4	-2.01	3.39		6.73
DUSP16	Dual specificity phosphatase 16		1.62		-1.99
DLL4	Delta-like 4 (Drosophila)		4.05		-2.03

Another group of genes down-regulated early during *in vitro* infection but induced late in the caecal epithelium of infected mice belong to the family of dual-specificity phosphatases (DUSP). As the negative regulators of MAP kinases, these proteins are of central importance

during proliferation, apoptosis or differentiation processes. In general, many DUSPs appeared modulated during the *in vivo* (DUSP1, 2, 4, 6, 10, 11, 16) or *in vitro* (DUSP1, 2, 4, 6, 10, 16, 18) growth of *Eimeria*, whereas only the expression of DUSP1, 2 and 10 was changed in *T. gondii*-infected YAMC cells. Interestingly, the three DUSPs (DUSP6, 10 and 4) repressed early *in vitro* were induced 16 h *in vitro* as well as 144 h *in vivo*. The down-regulation of these phosphatases early during infection of YAMC cells may counteract their important regulatory role and thus might determine the fate of the *Eimeria* development or the invaded cells.

4.1.4 Biological functions affected by the parasite infection

This section discusses the function and possible role of some of the highly-regulated transcripts in the context of various biological categories.

4.1.4.1 Regulation of gene expression

The infection of mice as well as of YAMC cells with *T. gondii* and *E. falciformis*, respectively, resulted in changes in the transcriptional activity of key transcription factors of the AP-1, EGR, STAT or NF-κB family (Fig. 47).

Signaling events initiated by PRR (see below) engagement cause post-translational activation of AP-1, followed by expression of pro-inflammatory genes among many others. Active AP-1 is a dimeric complex consisting mainly of members of the JUN (c-JUN, JUNB, JUND) and FOS (cFOS, FOSB, FRA1, FRA2) family, which is implicated in a variety of biological processes. CFOS is among the most differentially-regulated genes during *in vitro* infection of YAMC cells with *E. falciformis* and *T. gondii*. It is also one of the two genes modulated upon infection with both apicomplexan species at both time points and is discussed in more detail below. Besides cFOS, also the AP-1 members FOSB (*E. falciformis* 4 h and 16 h, *T. gondii* 4 h) and JUNB (*E. falciformis* 16 h; *T. gondii* 4 h and 16 h) were induced upon infection, albeit modestly. JUNB and FOSB regulate the expression of immunity-related genes, including CCL5, IFN-γ and MMP-1, -3, and -9 (269-271). Hence, induced expression of members of the AP-1 complex is involved in setting up the immune response in parasitized YAMC cells. JUNB, however, is also involved in growth inhibitory (272, 273) as well as cell cycle promoting events (274). In *H. pylori* infections of mice, increased JUNB levels correlated with a decreased cell proliferation (275, 276). Furthermore, proteins of the JUN family heterodimerize with members of the FOS family to exert their functions. It was shown that the dimerization is also responsible to keep cFOS in the nucleus and stabilize its expression levels

by reducing proteasomal degradation (277). Therefore, induction of JUNB upon infection might stabilize the cFOS protein and thus supporting its beneficial effect on the parasite growth (see below).

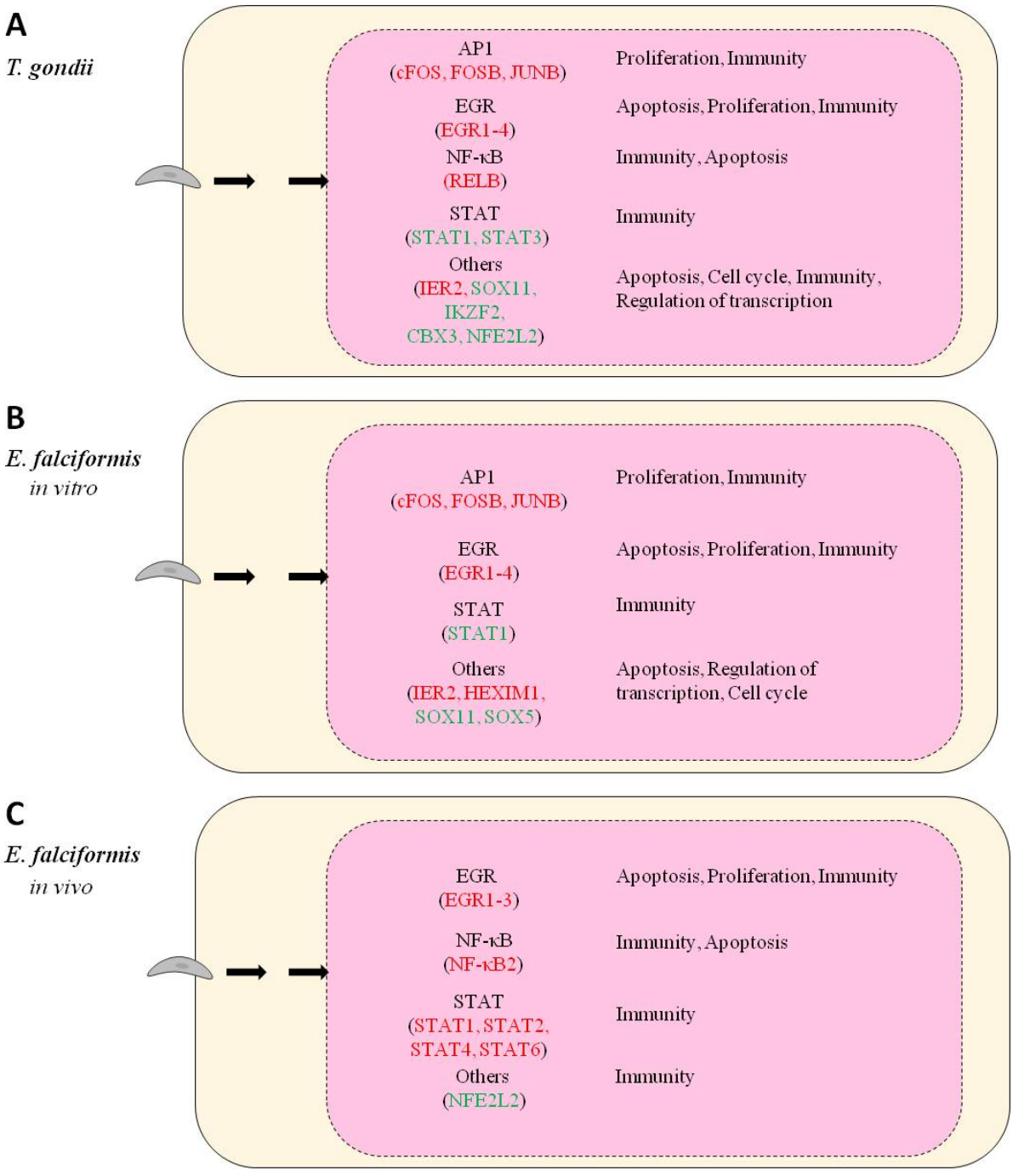

Fig. 47: Overview of selected transcription factors modulated upon YAMC and mouse infection. Induced (red) and repressed (green) genes and their primary functions are shown.

The induced expression of the transcription factors of the early growth response (EGR1 to 4) family was quite prominent during infection. Members of the EGR family were induced during late *in vivo* and *in vitro Eimeria* as well as during *T. gondii* infection. Interestingly,

although only a few genes were regulated early during *T. gondii* infection, all four EGR members were induced in contrast to an early *Eimeria* infection. Conspicuously, members of the EGR family were highly induced during late *T. gondii* infection (> 50-fold).

This family of zinc-finger transcription factors is induced in response to a variety of different stimuli and regulates cell growth, differentiation and apoptosis. EGR3 (highest induced EGR upon *E. falciformis* infection) and EGR2 have been shown to induce apoptosis by up-regulation of the FasL expression in hepatitis B virus (HBV)-infected liver cells (278). Interestingly, during HBV infection, a virus protein (HBx, regulatory X protein) interacts with the EGRs to ameliorate the DNA-binding (278), therefore enhancing FasL expression and inducing apoptosis of T cells expressing the Fas receptor (279). It was also shown that RNA interference of EGR3 resulted in a decreased proliferation of growth factor stimulated endothelial cells (280). Furthermore, EGR2 (72) as well as EGR1 (281) were shown to be induced in *T. gondii*-infected cells. For EGR2 induction it was hypothesized that it is induced by the parasite *via* rhoptry secretion (72). Together with EGR1 and p38 MAPK signaling it is required to induce SOCS1 (suppressor of cytokine signaling 1) expression in *T. gondii*-infected macrophages (281) to counteract the parasiticidal IFN-γ signaling. However, SOCS1 up-regulation was not detected, neither in *E. falciformis* nor in *T. gondii*-infected YAMC cells. It is conceivable that EGR2 in *Eimeria*-infected YAMC cells is also induced by rhoptry secretion. Whether the induction of a transcription factor by the parasite secretome might favor parasite development or might rather trigger host protection mechanisms remains to be examined. The function of EGR4, however, which was more than 100-fold induced late during *T. gondii* infection, is not well described yet. Its expression seems to be important in the spermatogenesis as EGR4 knockout male mice were infertile (282). EGR4 is also capable of forming complexes with the NF-kb proteins p50 and p65 and induces the expression of several inflammatory genes in human T cells (283).

Not many members of the NF-κB family appeared modulated in our gene expression studies, however. Exceptions are RELB, induced late during *T. gondii* growth, and NF-κB2 (p52) induced 144 h post *in vivo* development of *E. falciformis*. Both of these NF-κB family members control *T. gondii* infection. RELB is involved in regulating NK cell activity as well as IFN-γ secretion by T cells, and thus regulates the innate and adaptive immunity (59). In contrast, NF-κB2 participates in inducing apoptosis in T cells, which might favor the parasite development *in vivo* (60).

Similar to the aforementioned transcription regulators, the STAT family also mediates a variety of biological functions *via* influencing the expression of a number of target genes. Cytokine signaling (*e.g.* IFN-γ, IFN-α) activates the Janus kinase, which phosphorylates STAT proteins, resulting in their dimerization and nuclear translocation (73). STAT1 was induced 24 and 144 h p. i. *in vivo*, whereas its expression was down-regulated during late *E. falciformis* and *T. gondii* growth *in vitro*. Dimerization of STAT1 with STAT2 or STAT3 enhances transcription of interferon-stimulated genes, including the IRGs (immunity-related GTPases) (see below). Infection of STAT1-deficient mice with *T. gondii* (74) or *C. parvum* (76) increased the susceptibility to infection. Similar, infection of STAT1-deficient cells with *E. falciformis* resulted in increased schizont numbers (21). Therefore, the observed induction of STAT1 *in vivo* appears to control the parasite development. The expression of STAT1 is down-regulated *in vitro*, which might facilitate the growth of the cultured pathogens. Strikingly, STAT3 was also repressed during late *T. gondii* growth. Its dimerization and translocation into the nucleus results in the expression of IFN-γ activated sequences (GAS) (284). As a consequence, many IRGs were repressed during *T. gondii* development. Therefore, a decreased expression of STAT1 and STAT3 might be a parasite strategy to counteract host immune responses. On the other hand, sustained activity of STAT3 as well as of STAT6 promote replication of *T. gondii* (285). The rhoptry protein (Rop16) secreted by the highly virulent type I strain can activate STAT3 leading to a decreased IL-12 production (78). A down-regulation at the transcriptional level, however, does not mean that the proteins are not expressed.

Other STAT proteins significantly altered include STAT2 (induced 24 h p. i.), STAT6 and STAT4 (induced 144 h p. i.). STAT2 is activated in response to IFN-α/β signaling and builds a complex with STAT1 and IRF9 (IFN-regulatory factor 9) (284). This complex then activates several immunity-related genes, including genes involved in anti-viral defense and antigen-presentation (286, 287). STAT4 and STAT6 can also be activated in response to IL-12 and IL-4, respectively. Deficiency of STAT4 is comparable to a deficiency of IL-12, both of which lead to a reduced IFN-γ secretion and a lower NK cell-mediated cytotoxicity (288). Whereas STAT4 mediates pro-inflammatory responses, STAT6 is involved in Th2 cell differentiation (289, 290). Induction of a transcription factor that is crucial for differentiation of T cells towards the less inflammatory Th2 response might be a host mechanism to counteract an overwhelming immune response.

Among the highest up- or down-regulated transcripts, we also detected transcription factors, which are not members of the aforementioned families. IER2 (immediate early response 2), an immediate early gene with a supposed pro-apoptotic activity (291), was induced during *T. gondii* as well as *E. falciformis* infection of YAMC cells. Among the most exclusive genes at 4 h post-*Eimeria* infection, we observed the transcription regulator HEXIM1 (Hexamethylene bis-acetamide inducible 1). It forms a complex with a small nuclear RNA (7SK RNA) and the transcription regulator P-TEFb (positive transcription elongation factor b). P-TEFb activates RNA polymerase II resulting in an efficient transcription of candidate genes (292). The complex of P-TEFb with HEXIM1 and 7SK RNA is inactive, but can be rapidly converted into an active state by dissociation of the inhibitory factors (HEXIM1, 7SK RNA) (293). Thus, HEXIM1 contributes to maintain the equilibrium between induction and repression of transcription. The early up-regulation of HEXIM1 in *E. falciformis*-infected YAMC cells might therefore reflect a host cell response to counteract the massive induction of the host transcriptome. In contrast, *T. gondii* infection did not result in an early response, which might explain the absence of an induction of the transcriptional regulator HEXIM1.

We also observed transcription factors with a down-regulated expression profile, which regulate the cell cycle, transcription and immune response. SOX11 (SRY-box containing gene 11) was repressed during early and late *E. falciformis in vitro* development and 4 h post-*T. gondii* infection. SOX5 (SRY-box containing gene 5) was exclusively down-regulated 4 h post-*Eimeria* infection. They belong to the SOX gene family, which regulate the cell cycle by binding to the minor groove of DNA for activation or repression of their target genes. SOX5 was shown to inhibit cell cycle progression in neural progenitors (294), whereas SOX11 expression promotes cell survival (295) and growth (296). CBX3 (Chromobox homolog 3) is another down-regulated gene during *T. gondii* infection. CBX3 is a member of the heterochromatin protein 1 family (HP1), which is involved in gene regulation. Its association with a transcriptional repressor (PAX3) resulted in an increased expression of target genes in HEK293 cells (297). Down-regulation of CBX3 therefore may favor gene silencing during parasite infection. Among the repressed transcription factors in *T. gondii*-infected cells was also IKZF2 (IKAROS family zinc finger 2), which is a marker for T cell activation and proliferation (298) and is also involved in NK cell activity (299). The transcription factor NFE2L2 (nuclear factor, erythroid derived 2), which occurred among the most down-regulated transcripts during *in vivo* infection, was also repressed in *T. gondii*-infected YAMC cells (16 h p. i.). NFE2L2 is a transcription factor for antioxidant genes. NFE2L2-deficiency resulted in an increased mortality of mice by LPS-induced sepsis due to an elevated

inflammatory response (300). Additionally, mice lacking NFE2L2 were more susceptible to DSS-induced colitis due to decreased levels of detoxifying enzymes like heme oxygenase-1 and glutathione S transferase as well as due to increased expression of pro-inflammatory cytokines (301).

In summary, infection of mice or cells by *E. falciformis* and *T. gondii* modulates various transcriptional regulators, whose action can regulate the expression of a variety of other genes.

4.1.4.2 Immune response affected by infection

An infection directly leads to an immune response against the pathogen, which is in part reflected at the transcriptional level. Many of the genes modulated in response to *E. falciformis* or *T. gondii* infection participate in innate and acquired immune processes. Several of these immunity-related genes were also among the highest regulated transcripts in the microarray approaches.

4.1.4.2.1 Immune signaling in response to infection

Initiation of the immune response, *e.g.* chemokine expression, is induced by innate immune signaling pathways *via* the PRR (TLRs, NLRs, and CLRs)-mediated activation of transcription factors including NF-κB or AP-1. We did not, however, observe a changed expression of TLRs during the early *in vivo* and early and late *in vitro* time points (Tab. 12). Infection of YAMC cells with *T. gondii* resulted in repressed expression of endosomal TLRs (TLR3, TLR7) at the late time point. In contrast, during late infection of mice with *E. falciformis*, the expression of TLR4 and TLR7 appeared induced, whereas TLR5 was repressed. In addition, MYD88, an important TLR adapter molecule, was up-regulated early as well as late during mouse infection, suggesting a role of TLR signaling in initiating the immune response against *Eimeria*. This is consistent with microarray studies of *E. tenella*-infected chicken (108), in which immune cells show an up-regulated expression of several TLRs, including TLR4 and TLR7 within 12 h of infection. It should be noted that TLRs are mainly described in the context of bacterial or viral infections. The TLRs in the plasma membrane (TLR5, TLR4) are activated in response to bacterial flagellin (302) and LPS (303), respectively. Nevertheless, TLR4 is also known to recognize parasitic glycosylphosphatidyl-inositol (GPI)-anchored proteins (GPIs) of *T. cruzi*, *T. gondii* and *P. falciparum*, and is involved in the immune response against these pathogens (98, 100, 304). The endosomal

TLR3 and TLR7, which recognize microbial nucleic acids (305, 306), are also involved in the immune response against *T. gondii* (307). The individual absence of TLR3 or TLR7 did not influence *T. gondii* infection, whereas mice lacking a common component (UNC93B1) of TLR3, 7 and 9 signaling showed an increased susceptibility to infection due to an altered cytokine production (307). Interestingly, the repression of TLR3 and TLR7 in *T. gondii*-infected YAMC cells might favor the parasite development.

Tab. 12: Selected genes involved in initiation of immune response. Induced (+), repressed (-) or absent (/) genes in response to *E. falciformis* and *T. gondii* infection.

Gene	*E. falciformis*		*T. gondii*	Primary function
	in vivo	*in vitro*	*in vitro*	
TLRs				Recognition of microbial structures, *e.g.* TLR4 recognizes GPI-anchored proteins
TLR3	/	/	-	
TLR4	+	/	-	
TLR5	-	/	/	
TLR7	+	/	/	
CLRs				Recognition of microbial structures, induction of immunity
CLEC7A	+	+	/	
CLEC1B	/	+	/	
CLEC5A	+	/	/	
CLEC4E	+	/	/	
CLEC4D	+	/	/	
CLEC4N	+	/	/	
CLEC4B1	+	/	/	
CLECA2	+	/	/	
DUSPs				Negative regulation of MAPK signaling, involved in cytokine production
DUSP1	+	+	-	
DUSP2	+	+	+	
DUSP4	+	-/+	/	
DUSP6	+	-/+	/	
DUSP10	+	-/+	-	
Others				
MYD88	+	/	/	Adapter for TLR signaling
PTX3	/	-	-	Binding of complement, apoptotic cells, microorganisms, induction of immunity

Other PRRs modulated in our microarray studies belonged to the C-type lectin receptors (CLRs). Although not much is known about CLRs during parasite infections, several C-type lectins appeared up-regulated late during *in vivo* development. These receptors are mainly expressed in cells of the immune system, including dendritic cells and macrophages. Among them is CLEC7A (C-type lectin domain family 7, member a), one of the highest induced transcripts during *Eimeria* infection. So far, CLEC7A is described in sensing fungal, plant or bacterial molecules. It recognizes carbohydrate structures and induces protective immunity against fungi (308). CLEC7A is also important for the recognition of *Mycobacterium*

tuberculosis (309). Other C-type lectins, which were induced upon *Eimeria* infection of mice, include CLEC5A, CLEC4E, CLEC4D, CLEC4N, CLEC4B1 and CLEC4A2. These PRRs have been described to be involved in the immune response against mycobacterial, viral or fungal infections by involving neutrophils, macrophages and dendritic cells (310-313). That CLRs are also induced in *E. falciformis* infected caecum suggests their participation in recognizing parasite molecules.

In addition, the expression of PTX3 (pentraxin related gene), a secreted pattern recognition receptor, was reduced late during *T. gondii* as well as during *E. falciformis* infection of YAMC cells. PTX3, produced and released in response to pro-inflammatory stimuli, binds to complement components, apoptotic cells and microorganisms including bacteria, fungi and viruses (314). The absence of PTX3 increased the susceptibility of mice to a fungal pathogen (315), and macrophages derived from PTX3 over-expressing mice show an enhanced production of NO in response to IFN-γ (316). Therefore, reducing the expression of a gene involved in innate immunity may be advantageous for the parasite.

Finally, TLR engagement results in the activation of NF-κB and/or MAPK-mediated activation of the AP-1 complex *via* phosphorylation events. The MAPK signaling is further negatively controlled by a group of phosphatases called dual-specificity phosphatases (DUSP). Members of the DUSP family regulate the activity of MAPK by dephosphorylating the threonine and tyrosine residues (317). Many DUSPs were induced (DUSP1, 2, 4, 6, 10, 11) during late *in vitro* and *in vivo Eimeria* development. Notably, DUSP4, 6 and 10 were repressed during the early *in vitro* development but induced at the late time point. DUSP1, 4 and 10 negatively regulate the production of pro-inflammatory cytokines including IL-6, -12 and TNF-α (318-320). However, absence of DUSP1 is also reported to increase the production of the anti-inflammatory cytokine IL-10 (318). DUSP4-deficient macrophages produced less NO, thus leading to increased replication of *Leishmania mexicana* (319). Correspondingly, over-expression of DUSP6 decreased the replication of *L. major* (321). DUSP2 was among the highest induced mRNAs late during *T. gondii* infection. DUSP2 is induced by growth and stress signals in activated T and B cells, macrophages and mast cells (322, 323). In contrast to DUSP1 and 10, TLR engagement of DUSP2-deficient macrophages resulted in a decreased production of pro-inflammatory mediators (324). Interestingly, DUSP2 transcription is also inducible by p53 in response to oxidative stress, suggesting a role of this phosphatase in p53-mediated apoptosis (325). Noticeably, DUSP2 is the only dual-specificity phosphatase which was induced in *E. falciformis* as well as *T. gondii*-infected YAMC cells.

Other dual-specificity phosphatases (DUSP4, 6, 7, 16, 18) were either completely absent in *T. gondii*-infected cells, or appeared reciprocally-regulated (DUSP1 and DUSP10, induced in *E. falciformis* but repressed in *T. gondii* infection). Finally, the presence of several DUSPs upon infection highlights their importance in maintaining a balance between inflammatory responses directed against the parasites and the potential damaging event of overwhelming immune responses.

In summary, infection of mice or cells by *E. falciformis* and *T. gondii* affects the transcription of some PRRs, whose engagement results in the initiation of immune responses.

4.1.4.2.2 Modulation of chemokines, cytokines and other immunity-related genes

Especially during the infection of mice with *E. falciformis*, the expression of many chemokines was induced (Tab. 13). Chemokines are secreted in response to infection and recruit innate (NK, DCs, macrophages, eosinophils) and adaptive (T cells, B cells) immune cells to the site of inflammation. Therefore, increased chemokine expression coincides with the detected significant increase in the numbers of lymphocytes and macrophages in the *Eimeria*-infected caeca. Some chemokines also have homeostatic, wound healing or angiogenic functions. CxCL9, CxCL10 and CxCL11 were highly induced early as well as late during mouse infection with *E. falciformis*. The progression of infection resulted in the induction of additional members of the CxC (CxCL13, CxCL14, CxCL19) as well as CC (CCL1, CCL2, CCL7) subfamily and their receptors (CxCR3, CxCR4, CCR7). The IFN-γ inducible chemokines (CxCL9-11) signal *via* the CxCR3 receptor (present on *e.g.* T and NK cells (326, 327)), which was also induced. CxCL10 expression was required to control mouse infection with *T. gondii* (328). Furthermore, treatment of *T. cruzi*-infected mice with neutralizing antibodies against CxCL9 and CxCL10 resulted in higher parasite burden (329). Likewise, inhibition of the CXCR3 receptor by a known inhibitor (AMG487) in *E. falciformis*-infected animals resulted in a notably higher oocyst shedding in the drug-treated animals (330). These data suggest an important function of epithelial chemokines in the inception of the adaptive immune response and control of parasite infection.

Interestingly, the infection of YAMC cells with *T. gondii* resulted in a repression of CxCL10, which might favor the parasite development. Consistent with the *ex vivo* results, the infection of YAMC cells with *Eimeria* or *T. gondii* resulted in the modulation of selected chemokines. The expression of CxCL1, CxCL5, CxCL12, CxCL15 and CxCL16 was exclusively induced during *E. falciformis* infection (*in vitro* and *in vivo*). Others (CxCL2, CCL4) were also

induced following *T. gondii* infection. The chemokines CxCL1 and CxCL2 were among the highest up-regulated transcripts in *E. falciformis*-infected YAMC cells. Together with CxCL5, these cytokines mediate neutrophil migration into the inflamed tissue (331). Although *in vitro* induction of these chemokines does not lead to recruitment of leukocytes, it does reflect that the cell system used mimics a natural environment. Nevertheless, these chemokines may also have other functions *in vitro*. For example, CxCL2 has a wound healing function (332) and increases proliferation of colorectal cancer cells (333). Likewise, CxCL1 positively influenced the growth of ovarian epithelial cancer cells (334). Nevertheless, we also observed a down-regulation of a single cytokine *in vitro* (CCL20, 4 h /16 h post-*Eimeria*, 16 h post-*T. gondii*). CCL20 is an inflammatory cytokine, which signals *via* CCR6, and is involved in the recruitment of immune cells including neutrophils, immature DCs and Th17 cells. It is also reported that an increased production of this cytokine promoted the growth of colorectal cancer in mice *via* recruitment of regulatory T cells (335). Moreover, CCR6-mediated activation of T cells *via* DCs was shown to be essential to combat oral infections with *S. typhimurium* (336). Therefore, the down-regulation of CCL20 expression may be beneficial to the growth of the parasites, or it could just reflect a mechanism to counteract the pro-inflammatory response.

The interleukins were also altered in response to infection, although to a lesser extent. IL-7, IL-15 and IL-18 were the only interleukins repressed upon mouse infection. They participate in inducing the proliferation and activation of immune cells. Especially innate NK cells stimulated by the action of IL-15 and IL-18 (337, 338) proliferate and secrete IFN-γ, which might determine the course of infection. Other cytokines appeared induced upon mouse infection. The increased expression of IL-10 and IL-4 mRNA at 144 h could contribute to counteract a hyperactive immune response. Both cytokines are capable of down-regulating Th1 cytokines (IFN-γ, IL-2, TNF-α, IL-12) and promote an less inflammatory Th2 cell subtype (339-341). On the other hand, pro-inflammatory cytokines were also induced upon infection. The expression of IL-16, a chemokine attracting several immune cells including T cells, eosinophils, monocytes and DCs (342), as well as of IL-1α and -1β, involved in regulation and coordination of pro-inflammatory signals (343, 344), were induced during late mouse infection. Interestingly, IL-1R1 was among the highest repressed transcripts early as well as late during infection. The absence of IL-1R1 was shown to exacerbate DSS-induced colitis (345) as well as intestinal damage by *Citrobacter rodentium* (346). Therefore, down-regulation of the IL-1R1 receptor may contribute to the pathology during an *Eimeria* infection or may represent a mechanism to counteract an overwhelming immune response. Noticeably,

IL-1α was the only interleukin which appeared modulated (repressed) during late *T. gondii* infection of YAMC cells. Interestingly, the treatment of *T. gondii*-infected human astrocytoma-derived cells with this cytokine resulted in increased tachyzoite numbers (347). A repression of IL-1α in YAMC-infected cells might therefore contribute to the host immune response.

Tab. 13: Selected cytokines and chemokines. The table depicts genes, which were induced (+), repressed (-) or absent (/) upon infection with *E. falciformis* and *T. gondii*.

Gene	*E. falciformis*		*T. gondii*	Primary function
	in vivo	*in vitro*	*in vitro*	
CXCL				Recruitment of immune cells, wound healing, proliferation
1/5/12/15/16	+	+	/	
2	+	+	+	
10	+	/	-	
9/11/13/14/19	+	/	/	
CCL				
1/2/7	+	/	/	
4	+	+	+	
20	/	-	-	
CXCR				
3/4/7	+	/	/	
ILs				Regulation and coordination of immune response, attraction and proliferation of immune cells
6	+	+	/	
1α	+	/	-	
1β/4/10/16/21/22	+	/	/	
23	/	+	/	
7/15/18	-	/	/	

Strikingly, the expression of IL-21 and IL-22 (144 h) as well as of IL-6 (144 h and 16 h) and IL-23 (16 h) cytokines, which are involved in Th17 responses, were induced upon *Eimeria* infection. The Th1 cytokine IL-6 is responsible for driving pro-inflammatory responses, whereas IL-21 is rather an anti-inflammatory cytokine by inhibiting IFN-γ production from Th1 cells. However, these cytokines together with TGF-β, which was also induced late during mouse infection, also mediate Th17 differentiation (348-350). In addition, IL-23 is involved in stimulating the accumulation and function of this specialized subtype of T helper cells (348). It was shown that an increased pathology upon *E. falciformis* infection of IFN-γR$^{-/-}$ mice correlates with an elevated secretion of the Th17 cytokines (IL-17A, IL-22). Furthermore, IL-22 may exert a direct anti-parasite effect during infection (126). Consistently, the increased expression of different cytokines involved in regulating Th17 responses

underlines the importance of this specialized T cell subset during infections with *E. falciformis*. The presence of these cytokines in our *in vivo* model might contribute to the mild pathology observed on the peak days of oocyst shedding as well as to the defense against the parasite. However, IFN-γ which is present upon mouse infection with *E. falciformis* counteracts a Th17 expansion (351) and thus prevents an exaggerated pathology as observed in the IFN-γ ablated animals (126). Thus our *in vivo* results reflect a balance between the roles of IFN-γ in contributing to the host defense concomitant with the prevention of an overacting pathology.

Some members of the SOCS family were also modulated upon infection of mice or YAMC cells (Tab. 14). The SOCS1 (suppressor of cytokine signaling) (352) expression, induced during mouse infection, is important to protect the host from overshooting pro-inflammatory responses. SOCS1 can directly bind to JAK kinases and inhibit their catalytic activity. It has also been shown that SOCS1 expression in *T. gondii*-infected macrophages decreases IFN-γ-mediated NO production, which is beneficial for the parasite (353). SOCS1 expression therefore may benefit the host cell and the parasite. Although SOCS1 was not induced *in vitro*, three other members of the SOCS family were highly up-regulated especially during *T. gondii* infection (CISH (Cytokine inducible SH2-containing protein), SOCS2, and SOCS3). Increased mRNA expression of CISH was also observed in *T. gondii*-infected murine macrophages leading together with SOCS1 to a reduction in the IFN-γ-mediated NO secretion (353). Similar to SOCS1, CISH can interact with the JAK-STAT signaling pathway by binding to the cytokine receptor and therefore competes with the STATs (354). SOCS3 expression was up-regulated during *Eimeria* and *T. gondii* infection. Interestingly, SOCS3 is involved in IL-23-mediated differentiation of T cells into Th17 cells. The absence of SOCS3 enhances Th17 cell number (355). Therefore, an up-regulation of SOCS3 may reduce a Th17 response to benefit the host as well as the parasite by reducing Th17 accompanied pathology (126). However, no role of SOCS2 in IFN-γ signaling has been reported so far, it is likely that it is involved in anti-inflammatory activities (356) to counter-regulate the immune response.

Other highly induced (SPP1, AOC3, ICAM2 and SAA4) and repressed (KITL, PRLR, GHR) transcripts during mouse or YAMC infections with *E. falciformis* also exert important immunological functions (Tab. 14). Interestingly, SPP1 (secreted phosphoprotein 1, 24 h/144 h) is required to mount an efficient innate and acquired immune response. The absence of SPP1, involved in chemotaxis of several immune cells, resulted in decreased NK cell recruitment during infection with influenza A virus, and subsequent decrease in survival

(357). Furthermore, SPP1-deficiency diminishes IFN-γ and IL-12 production, which results in an increased burden of *Listeria monocytogens* in mice (358).

Tab. 14: Selected genes with immunological functions. The table depicts genes, which were induced (+), repressed (-) or absent (/) upon infection with *E. falciformis* and *T. gondii*.

Gene	*E. falciformis*		*T. gondii*	Primary function
	in vivo	*in vitro*	*in vitro*	
SOCS				Regulation of immune response
1	+	/	/	
2	-	+	+	
3	+	+	+	
CISH	/	/	+	
MMPs				Tissue remodeling, activation of cytokines/growth factors/antimicrobial peptides by proteolytic activities
3/7	+	/	/	
10/13	+	+	/	
Others				
SPP1	+	/	/	Chemotaxis of immune cells
KITL	-	/	/	Migration/maturation/proliferation of mast cells and eosinophiles
PRLR	-	/	/	Regulation of immunity, proliferation
GHR	-	/	/	Regulation of immunity
AOC3	/	+	/	Leukocyte recruitment, oxidative enzyme
ICAM2	/	+	/	Lymphocyte recirculation
SAA4	/	+	/	Acute phase protein

A down-regulated molecule late during mouse infection, KITL (kit ligand) is involved in immune-regulatory processes including maturation, proliferation, survival and migration of mast cells (359) *via* binding to its receptor c-KIT. Mast cells are capable of secreting several chemokines and cytokines including IFN-γ and TNF-α. KITL is also crucial for the activation and infiltration of eosinophils during inflammatory processes. The absence of the KITL/c-KIT pathway diminishes mast cell and eosinophil infiltration (360). Thus, a decreased expression of KITL/c-KIT may also be involved in controlling an overshooting immune response. We also observed a repressed transcription of two receptors (GHR, PRLR) during mouse infection, which are involved in growth, development, electrolyte transport and immune-regulation. Especially for prolactin an anti-parasitic capacity has been shown. In this regard, presence of prolactin restricts the growth of *T. gondii* in peripheral blood mononuclear cells (361). It also reduces the blood parasitemia during a *Trypanosoma cruzi* infection with a concurrent increase in proliferation of T lymphocytes and enhanced NO production by macrophages (362). Likewise, treatment of *T. cruzi*-infected animals with growth hormone (the substrate of the GHR), resulted in increased TNF-α, IFN-γ and NO concentration and a decreased parasite burden (363). Thus, a down-regulation of molecules involved in pro-

inflammatory processes may be a mechanism counteracting an overwhelming immune response but also could be coincidental beneficial for the parasite growth.

AOC3 (Amine oxidase, copper containing 3, 4 h p. i.) and ICAM2 (intercellular adhesion molecule 2, 4 h p. i.) are involved in cellular movement, including chemotaxis, rearrangement and transmigration of cells. AOC3, also known as vascular adhesion protein 1 (VAP1) contributes to leukocyte recruitment *in vivo* (364). It is an ectoenzyme catalyzing the oxidative deamination of amines into aldehydes resulting in the release of ammonium and hydrogen peroxide (365). Its function in leukocyte recruitment *in vitro* is unlikely. However, its oxidative enzyme activity might be important for the host defense (366). ICAM2 is a ligand for LFA1 (lymphocyte function-associated antigen-1). In contrast to ICAM1, which is strongly up-regulated in response to inflammation and supports lymphocytes migration into inflamed tissue, ICAM2 is responsible for normal recirculation of lymphocytes on resting epithelium (367).

SAA4 (serum amyloid A 4), an apolioprotein constituent of the HDL particle (368), was the highest induced transcript 16 h post-*Eimeria* infection. SAA4 belongs to the serum amyloid a family, proteins which function in a variety of biological processes. These acute phase proteins are induced by inflammatory stimuli, which cause infiltration of immune cells (369) and expression of chemokines and cytokines (370). Furthermore, SAA4 is also capable of activating matrix metalloproteinases (MMPs) (371). Some MMPs appeared up-regulated during *Eimeria* infection (Tab. 14), including MMP3 and 7 during *in vivo* infection and MMP10 and 13 during late *in vivo* and *in vitro* development. Members of this family are secreted from a variety of cell types including neutrophils, T cells and macrophages (372) and degrade the components of the extracellular matrix and are therefore involved in tissue remodeling (373). For example, the capacity of MMP13 to cleave extracellular matrix molecules is involved in destruction of lung matrix during tuberculosis (374). MMPs also process different cytokines, growth factors and antimicrobial peptides (375). For instance, MMP7 proteolytically activates the antimicrobial peptide α-defensin, which is present in the paneth cells of the small intestine and important for mucosal immunity (376). MMP7-deficiency increases the susceptibility to infections with *Salmonella typhimurium* (377). Likewise, MMP3 also function in defense against bacteria at the mucosal interface, as MMP3-knockout mice show an increased burden of *Citrobacter rodentium* (378). The elevated susceptibility to infection in MMP3 knockout animals was associated with a decrease in $CD4^+$ lymphocytes in the lamina propria. These data suggest that a MMP3-deficiency

disturbs the homing of immune cells to the site of inflammation (378). The observed up-regulation of different MMPs during *Eimeria* infection, therefore may contribute to the tissue damage and/or activation of an efficient immune response.

In summary, infections with *E. falciformis* and *T. gondii* resulted in a considerable modulation of immunity-related genes. The induction or repression of these molecules is likely to determine the progression of the immune response against the parasites. Pro-inflammatory responses, which potentiate inflammatory processes simultaneously, activate anti-inflammatory or counter-regulatory mechanisms, thus illustrating the complex interaction between the host and the parasite.

4.1.4.2.3 IFN-γ signaling is prominently induced during *Eimeria* infection of mouse

The expression of many genes is regulated by IFN-γ, which signals *via* the JAK-STAT pathway. This cytokine overarches innate and adaptive immune responses. A variety of cells including DCs, NK cells, macrophages and T cells are capable of secreting this cytokine, which exerts numerous functions. IFN-γ (and TNF-α) activate macrophages to produce NO (117). Furthermore, IFN-γ is involved in Th1 cell differentiation and also increases the production of Th1 cytokines (IL-6 and TNF-α). Moreover, IFN-γ also induces IRGs (immunity-related GTPases) in *T. gondii*-infected mice, which leads to disruption of the PVM and kills the parasite (119) (see below). Last but not least, IFN-γ is the most potent inducer of IDO1 and tryptophan catabolism in infected cells.

A majority of the genes highly induced in response to the parasite infection *in vivo* are regulated by IFN-γ as confirmed by IPA suite. IFN-γ signaling was apparent within 24 h of infection, and nearly all genes in the network showed an induction (App. D). The cytokine-regulated network was more notably induced during late infection, and a few genes also exhibited a downregulation (App. E). Interestingly, 17 of the 20 most upregulated genes early during infection are regulated by IFN-γ (Tab. 8). The number is equally impressive at the later time point (15 of the 20 genes). Some of these selected genes include immunity-related GTPases (IRGA6, B6, D, M2, M3), guanylate-binding proteins (GBP2, 3, 5, 6, 8), chemokines (CxCL9, 10, CCL4) and IDO1. In contrast, only 1 gene (FHL1) regulated by IFN-γ was downregulated (Tab. 9). Furthermore, *in vitro* analyses of highly induced or repressed IFN-γ-regulated transcripts also revealed only a few ones (3 out of 20) (Tab. 3, 4).

In brief, the above data indicate a host response correlating with the severity of infection, and suggested a key role of IFN-γ-mediated signaling in *Eimeria*-infected animals.

Interestingly, the expression of several members of the IRG family, including IRGM1, IRGM2, IRGM3, IRGA6, IRGB6 and IRGD were highly repressed during *T. gondii* infection (Tab. 15). In contrast, the expression of these proteins was not changed during *in vitro E. falciformis* development, but most of them were highly induced during early and late mouse infection.

Tab. 15: IRG and GBP proteins modulated in response to *E. falciformis* and *T. gondii* infection.

Gene	*E. falciformis*		*T. gondii*	Function
	in vivo	*in vitro*	*in vitro*	
IRGs				Resistance to microorganisms in a pathogen-specific manner
IRGA6	+	/	-	
IRGB6	+	/	-	
IRGD	+	/	-	
IRGM1	+	/	-	
IRGM2	+	/	-	
IRGM3	+	/	-	
GBPs				Antimicrobial effect
GBP1	+	/	-	
GBP2	+	/	-	
GBP4	+	/	-	
GBP3	+	/	/	
GBP5	+	/	/	
GBP6	+	/	/	
GBP8	+	/	/	

Members of this family confer resistance to a variety of microorganisms in a pathogen-specific manner. For example, IRGM1- (immunity-related GTPase family, M) deficiency causes an increased susceptibility to protozoans (*T. gondii* (379), *L. major* (380) and *T. cruzi* (381)) as well as to bacterial infections (*Listeria monocytogenes* (382) and *Mycobacterium tuberculosis* (383)). Similarly, IRGM3 (interferon gamma induced GTPase) knockout mice were more susceptible to *T. gondii* (384) and *L. major* (380) but no differences in *T. cruzi* (385) and *L. monocytogenes* (382) infection were observed. However, resistance to the non-virulent *T. gondii* strain is associated with the expression of some of these interferon-inducible GTPases. It was shown, that many IRGs, including IRGA6, IRGM2, IRGB6 and IRGM3 are recruited onto the parasite vacuole, which causes vacuole disruption and killing of the parasite (119). In contrast, as shown by Liesenfeld *et al.* (386), none of these IRG proteins associated with the PVM of *P. berghei*-infected cells, and thus are not involved in resistance mechanisms

against this apicomplexan parasite. Interestingly, the virulent *T. gondii* type I strain can phosphorylate IRGA6 *via* its Rop18 kinase and aborts its accumulation on the vacuole (251). Therefore, similar to virulent type I strain *T. gondii*, *Plasmodium* may harbor virulence factors, which also inactivate IRG proteins (251, 386). Hence, many IRGs (IRGM1, IRGM3, IRGD, IRGM2 and IRGB6) were repressed by type I strain of *T. gondii* used in this study, which may also favor parasite replication.

YAMC infection with *T. gondii* also resulted in a decreased expression of three guanylate binding proteins, GBP1, GBP2 and GBP4. Similar to the IRGs, the expression of these proteins is IFN-γ inducible. GBP members are also known for their antimicrobial effect on bacteria as well as on parasites (250, 387, 388). For example, GBP1$^{-/-}$ mice infected with *L. monocytogenes*, *M. bovis* or *T. gondii* show an increased microbial burden (388, 389) and the animals harboring a collective deletion of GBP1-3, 5 and 7 on chromosome 3 succumb to parasite infection (390). Furthermore, several GBPs including those highly induced during *Eimeria* infection (GBPs 2, 3, 6, 8), were also induced upon *Listeria monocytogenes* and *T. gondii* infection. Similar to the IRGs, they accumulate around the PV of the avirulent *T. gondii* strain ME49 (250). Interestingly, especially the presence of GBP1 and GBP2 was substantially decreased around the PV of the virulent *T. gondii* strain. These two GBPs were also repressed in our gene expression studies of *T. gondii*-infected YAMC cells. Their biological function remains largely unknown, however.

In summary, several IRG and GBP family members were highly induced during mouse infection, thus suggesting their involvement in the host response against *Eimeria* infection. The expression of these IRGs (and GBPs) might also contribute to the self-limiting nature of an *E. falciformis* infection. Nevertheless, due to the pathogen-specific action of these GTPases, the involvement of these proteins in resistance mechanism against *E. falciformis* remains to be elusive.

4.1.4.3 Apoptosis

Apoptosis, the programmed cell death, is a mechanism during normal developmental and homeostatic processes. Nevertheless, apoptosis is also an important part of the immune response. Apoptosis allows the host cell to avoid dissemination of intracellular pathogens to neighboring cells. The apoptotic cell also activates and amplifies the immune response. In contrast, it is in the interest of the pathogen to prevent apoptosis of the parasitized cell and

promote apoptosis of surrounding immune cells to counteract an anti-parasitic response. However, apoptosis of the host cell might also help the intracellular pathogen to disseminate and infect new neighboring cells. The balancing action of pro- and anti-apoptotic mechanisms therefore, might be beneficial for the host and/or the parasite. Microarray experiments of infected caecal tissue or YAMC cells revealed several genes involved in cell death and survival. Some of these genes were also among the highest modulated transcripts throughout infection (Fig. 48).

The pro-apoptotic protein BIM (BCL2-LIKE 11) is induced during late mouse infection, which counteracts several anti-apoptotic proteins of the BCL-2 family. Pro-apoptotic proteins, such as BIM or BMF (BCL2 modifying factor) induced during YAMC infection with *E. falciformis*, trigger the release of mitochondrial cytochrome c in the stress induced pathway of apoptosis and lead to activation of caspase 9 (391). The granzyme B/perforin pathway of apoptosis induction was also affected during late mouse infection. Perforin 1 (induced in mouse) is produced by NK cells and cytotoxic T cells. It can integrate in the membrane of the target cell, resulting in pore formation, which enables the entry of granzyme B and subsequent activation of caspase 3 (392, 393). In addition genes functioning in the death receptor pathway of apoptosis were also induced, which included FAS/FASL (144 h) and TRAIL/APO2L (24 and 144 h) activating caspase 8 (394). Caspase 8 as well as 9, process the effector caspase 3 and 7.

The expression of caspase 7 was repressed *in vitro* upon early *Eimeria* and late *T. gondii* infection. In *T. gondii*-infected mice, IFN-γ mediated up-regulation of FAS on T cells mediated apoptosis of these cells (146). Up-regulation of FAS/FASL-mediated apoptosis was also observed during infections with *C. parvum* and *Plasmodium* spp. (150, 151). Notably, a reduction in the number of anti-parasitic immune cells is advantageous for the parasite.

Other molecules highly induced by our studies included pro-apoptotic genes, such as TNFRSF25 (Tumor necrosis factor receptor superfamily, member 25; 4 h *Eimeria*, 16 h *T. gondii*), and LAG3 (lymphocyte-activation gene 3; 4 h and 144 h *Eimeria*). It was shown that binding of the ligand (TNFSF15) to TNFRSF25 results in the induction of the cell death program as well as in NF-κb-mediated activation of an inflammatory response (395). Induction of TNFRSF25 during *in vitro* infection therefore might be rather harmful than beneficial for the parasite development. LAG3, which is structurally similar to the CD4 molecule, can interact with MHC II molecules (396, 397), and is known as a positive

regulator of NK cell-mediated cytotoxicity and a negative regulator of T cell activation and IL-12 biosynthesis. Interestingly, simultaneous blockage of LAG3 and another inhibitory receptor (PD-1) during *Plasmodium yoelii* infection of mice resulted in more parasite specific $CD4^+$ and $CD8^+$ T cells and increased the parasite clearance (398).

A few other pro-apoptotic molecules were repressed (DUSP6, GAS1) during *Eimeria* infection. The DUSP6-mediated dephosphorylation of the MAP kinases ERK1/2 was shown to increase apoptotic events in endothelial cells (399). GAS1 (growth arrest specific 1) is a gene with anti-proliferative but also pro-apoptotic properties. An over-expression of GAS1 resulted in a cell cycle arrest in HIH3T3 cells (400) and supported apoptosis in a glioma cell line *via* caspase-3 activation (401). Therefore, down-regulation of DUSP6 and GAS1 should protect the infected cells from apoptosis. The highest down-regulated gene early and late during *T. gondii* infection (SIK1, salt-inducible kinase 1) has a regulatory role in the active sodium transport (402) as well as in apoptosis (403). SIK1 is involved in anoikis (403); this special form of apoptosis is induced by loss of adhesion from the extracellular matrix. Interestingly, the inactivation of SIK1 decreased p53-mediated anoikis and increased survival of human mammary epithelial cells (403). Similarly, a down-regulation of SIK1 could favor survival of *T. gondii*.

However, also anti-apoptotic genes were modulated. The expression of IAP2 (baculoviral IAP repeat-containing 3), a member of the IAP family of apoptotic regulators, was induced late during *E. falciformis* infection of mouse. Members of this family can bind to caspases and inhibit their activity or interfere with the receptor-induced signaling pathway (404, 405). Likewise, another inhibitory protein, c-FLIP (CASP8 and FADD-like apoptosis regulator) (406) was induced late during *in vivo* and *in vitro Eimeria* infection but repressed in response to late *T. gondii* infection. C-FLIP expression is known to inhibit the FAS-receptor mediated apoptosis in *T. cruzi* as well as *T. parva* infection (407, 408). Other anti-apoptotic transcripts highly modulated by *E. falciformis*, included EGF (Epidermal growth factor) and FHL1 (Four and a half LIM domains 1), exclusively repressed *in vivo*, and EIF4E (Eukaryotic translation initiation factor 4E) and EXT1 (Exostoses 1), exclusively repressed early *in vitro*. The EGF signaling regulates growth and differentiation of intestinal epithelial cells and is involved in normal gut development. Inhibition of the EGF receptor decreased the proliferation rate and increased the cell death (409). Also for an FHL1 splice isoform, which is mainly expressed in muscle cells, an anti-apoptotic function has been shown (410). EIF4E promotes translational initiation, cell survival and proliferation, and reduce apoptotic events (411).

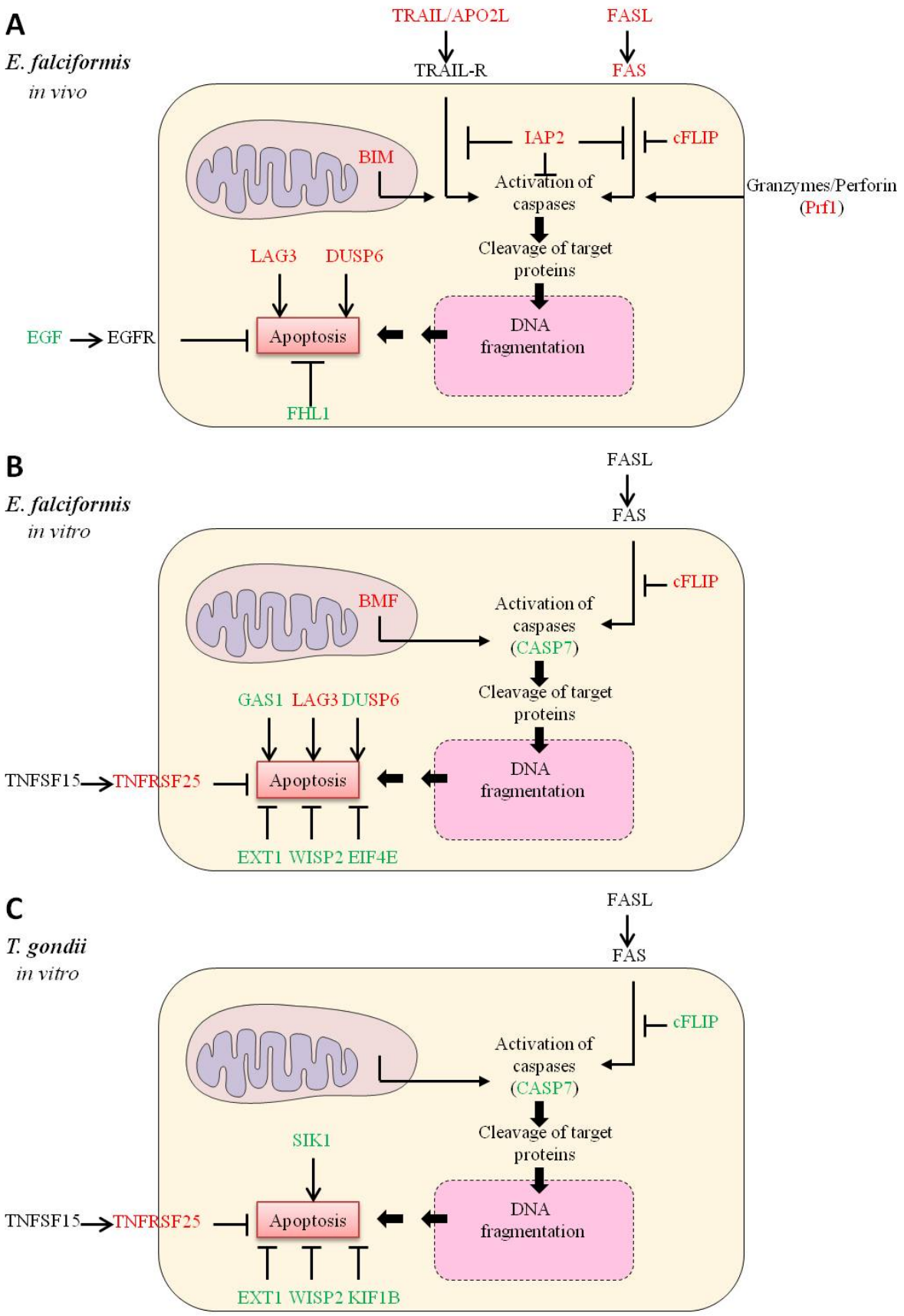

Fig. 48: Schematic overview of selected apoptosis genes modulated upon mouse and YAMC infection. Induced (red) or repressed (green) proteins upon **(A)** mouse or YAMC infection by **(B)** *E. falciformis* and **(C)** *T. gondii*.

EXT1 contributes to the elongation and maturation of heparan sulfate proteoglycans, and protein interactions, thereby regulating cellular growth and behavior (412). A knockdown of EXT1 reduces the cellular growth and increases apoptosis in myeloma cells (413). Hence, repression of anti-apoptotic genes may favor apoptosis of the host cells and/or neighboring immune cells. Furthermore, the transcription of another anti-apoptotic gene (WISP2, WNT1 inducible signaling pathway protein 2), was highly repressed *in vitro* (16 h post *Eimeria* and *T. gondii* infection). A mouse neuroblastoma cell line (Neuro2a) over-expressing WISP2 was shown to be resistant to H_2O_2-induced apoptosis (414), and repression of WISP2 expression using antisense oligos decreases the proliferation of human breast carcinoma cells (415). In accord, the absence of KIF1B (kinesin family member 1B), a gene exclusively and highly down-regulated during *T. gondii* development, has been shown to reduce the survival of neurons (416). Therefore, down-regulation of WISP2 as well as KIF1B should exert an apoptotic and anti-proliferative effect during *T. gondii* infection.

In brief, dependent on the cell type (immune cell *vs*. host cell) the action of pro- or anti-apoptotic mechanisms might support the host or the parasite. Both of these events are expected to be tightly controlled to ensure host as well as parasite survival.

4.1.4.4 Morphology

The most pronounced morphological changes occur most often at the end of each infection, resulting in the disruption of the host cell. During mouse infection, these changes coincide with cellular infiltrates, edema and loss of the crypt architecture (34). The morphological changes in an infected host cell include cellular enlargement, or restructuring of host cell organelles and cytoskeleton. A number of genes with morphological functions were highly induced or repressed during infection (Tab. 16). SAA4 (serum amyloid A 4), an apolipoprotein and part of the HDL particle (368), was the highest induced transcript 16 h post-*Eimeria* infection. SAA4 is an acute phase protein involved in inflammatory processes (369, 370). These proteins are also capable of activating matrix metalloproteinases (MMPs) (371) and the conversion of plasminogen into its active form plasmin (417). Both, plasmin and MMPs can degrade components of the extracellular matrix. For example, MMP13 (induced late *in vitro* and *in vivo Eimeria* development) is involved in destruction of the lung matrix during tuberculosis (374). Furthermore, an increased expression of SAA1 and SAA4 was also observed in tumor tissue. The authors concluded that this might lead to an enhanced plasminogen activation resulting in matrix degradation and tumor dissemination (417).

Moreover, we also observed an elevated expression of MMP10, MMP13, and of PLAUR (plasminogen activator, urokinase receptor) upon *Eimeria* infection. It is known from *Plasmodium* spp., that they co-opt host plasminogen present in the ingested blood meal to facilitate ookinete invasion in the mosquito midgut (418). However, whether activation of genes involved in degradation of the extracellular matrix is a host defense mechanism or facilitates parasite invasion/evasion and development remains to be studied.

Tab. 16: Selected genes with morphological function modulated upon infection. Genes, which are induced (+), repressed (-) or absent (/) during *E. falciformis* and *T. gondii* infection are shown.

Gene	*E. falciformis*		*T. gondii*	Primary function
	in vivo	*in vitro*	*in vitro*	
COL				Cell migration, adhesion, proliferation
11A1/1A1 /12A1	/	-	-	
10A1	/	-	/	
9A3/11A2	/	+	/	
15A1	/	/	+	
MMPs				Matrix degradation
3/7	+	/	/	
10/13	+	+	/	
ITGs				Cell attachment and signaling
A1/A7/A9 /AM/AE/ AX/AL	+	/	/	
B2/B7	+	/	/	
Others				
SAA4	/	+	/	Matrix degradation
PLAUR	+	+	/	
CLDN1	/	-	-	Transport, cell adhesion
PTKS2	-	/	/	Migration, adhesion
FERMT1	-	/	/	Cell adhesion

Several genes, encoding for the components of the extracellular matrix were also regulated, including highly repressed collagen transcripts. Collagens control cell migration, adhesion and proliferation. COL11A1 (collagen, type XI, alpha 1), also repressed during *T. gondii* infection, and COL10A1 (collagen, type X, alpha 1) appeared more than 2-fold down-regulated during *E. falciformis* infection. The type X and XI collagen are generally described to be expressed in the cartilage matrix. COL10A1 and COL11A1 have however been detected in human breast cancer cells (419) and colorectal cancers (420), respectively. The authors concluded that COL10A1 and COL11A1 expression might be important for invasion and metastasis of cancer cells. Other members repressed during *Eimeria* and *T. gondii* infection of

YAMC cells included COL1A1 and COL12A1. The expression of other collagens however, such as COL9A3, COL11A2 and COL15A1, was induced.

The expression of another structural molecule, CLDN1 (claudin 1), was also highly repressed 16 h post-*Eimeria* and *T. gondii* infection. Claudins belong to tight junctions, which ensure transport between epithelial cells and regulate cell adhesion (421). Interestingly, it was shown that CLDN1 together with other host cell molecules is essential for the successful invasion of the hepatitis C virus (422) and that the transmembrane protein is down-regulated in infected cells, which may protect the host cells from a super-infection with other pathogens (423). However, the importance of collagen and claudin proteins during an *in vitro E. falciformis* infection remains to be determined.

During mouse infection, we also observed highly repressed transcripts with function in cell morphology. The PTK2 gene (protein tyrosine kinase 2) is involved in cell migration and adhesion (424). It is a scaffold protein as well as a kinase, which coordinates formation of focal adhesions (425). Furthermore, the absence of PTK2 in epithelial cells of the intestine increases the severity of DSS-induced colitis by enhancing apoptosis and reducing epithelial cell repair. Thus, PTK2 is also an important anti-apoptotic factor necessary after mucosal damage (426). Similar to the aforementioned gene, severe colitis was also observed in mice deficient for FERMT1 (fermitin family homolog 1, repressed *in vivo*), a protein causing cell adhesion by regulating the function of integrins (427). The development of colitis was induced by the loss of the intestinal epithelial barrier function due to a reduced activation of integrins. Therefore, down-regulation of factors, which antagonize epithelial damage and enhance the epithelial barrier function might be a cause or consequence of the gut pathology observed during an advanced *Eimeria* infection. In addition, several integrin signaling proteins (*e.g.* ITGA1, 7, 9) were induced during mouse infection. Integrins are transmembrane receptors involved in cell attachment and signaling, which cause actin reorganization and activation of signaling cascades involving MAPK or others. Their increased expression may contribute to increase the cellular stability during infection.

In summary, many genes in our studies are involved in morphological processes of the cell or the surrounding tissue. Stabilizing the host cell by for instance integrin expression might be beneficial for the host as well as for the parasite. Similar, inducing molecules which destabilize the cell can also favor the host or the parasite development.

4.1.4.5 Cell Cycle

Several apicomplexan parasites are capable of interfering with the host cell cycle for their own benefits. While *Theileria* spp. induces the proliferation of their host cells to ensure their dissemination, *T. gondii* rather inhibits host cell cycle to gain a better environment for replication (177-179). In our studies, several genes involved in proliferative and cell cycle processes were highly regulated during *E. falciformis* as well as *T. gondii* infection (Fig. 49).

Several genes, which promote the cell cycle, were repressed during infection. STRN3 (striatin, calmodulin binding protein 3), a nuclear DNA binding protein with high expression during mid S phase and G2 phase (428), and WNK1 (WNK lysine deficient protein kinase 1), a protein involved in cellular growth and proliferation, were repressed following *E. falciformis* and *T. gondii* infection. WNK1 is a serine/threonine protein kinases (429), which also localizes to the mitotic spindle during cell division (430). A decrease in its mRNA levels reduced growth and differentiation of neuronal progenitor cells (431), and a knockdown of the protein reduced the survival of HeLa cells due to cell division defects (430). Likewise, ASB15 (ankyrin repeat and SOCS box-containing 15), involved in tissue development and cell growth (432), was repressed *in vitro*. Over-expression of ASB15 in muscle cells increased protein synthesis and muscle growth (433). FZD8 (fizzled homolog 8), a receptor involved in the Wnt signaling pathway and important for cell proliferation and apoptosis, was also repressed upon YAMC infection. Its knockdown in lung cancer cells inhibited their proliferation (434). In addition, KIF11 (Kinesin family member 11) expression was repressed in *T. gondii* infection, and CSPP1 (centrosome and spindle pole associated protein 1), a protein concentrated at the spindle pole and central spindle during mitosis and cytokinesis (435), was repressed *in vivo*. KIF11 inhibition causes a mitotic arrest in HeLa cells (436). Similarly, depletion of CSPP1 is associated with cell cycle arrest (437). Hence, increased expression of proliferative genes should support cell growth, whereas their repression may exert the opposite effect.

Only a single cell cycle promoting gene (FER1L3 (myoferlin)) however was highly induced during infection of mice with *E. falciformis*. It is involved in membrane repair mechanisms after damage. Silencing of FER1L3 has been shown to reduce the proliferation in endothelial cells (438). Interestingly, FER1L3 was induced late during *E. falciformis* infection of mice and YAMC cells but repressed early during mouse infection. It was the only reciprocally regulated gene in *E. falciformis* infected mice. Its expression profile might hint towards its

importance during progression of infection. If this may have any biological relevance however during an *Eimeria* infection remains unknown.

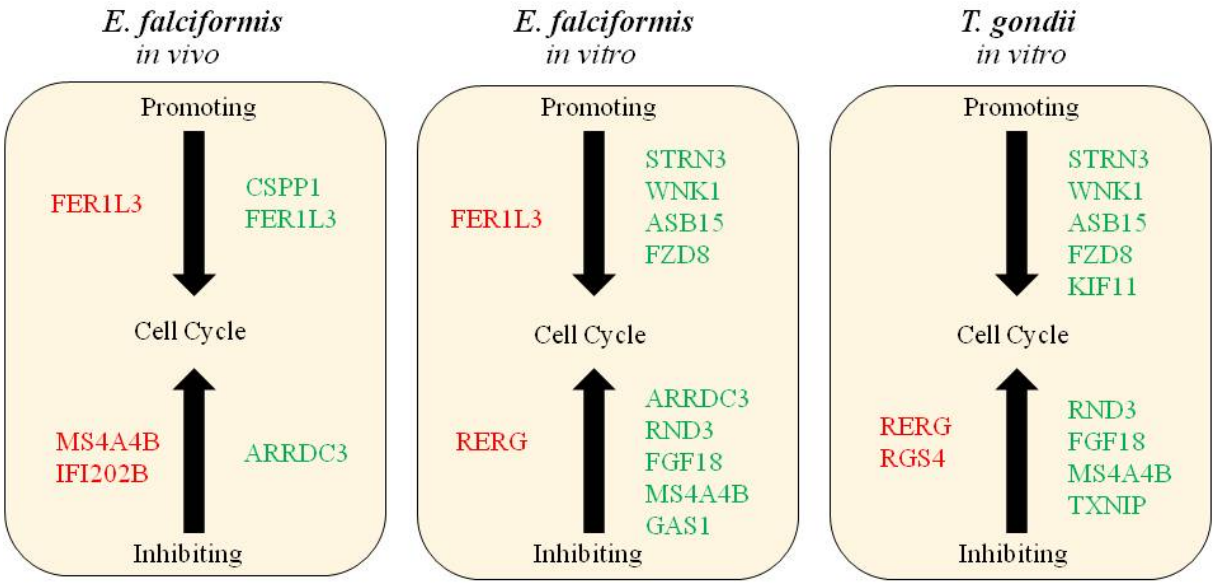

Fig. 49: Genes promoting or inhibiting the cell cycle modulated by *E. falciformis* and *T. gondii*. Induced (red) or repressed (green) genes during *E. falciformis* and *T. gondii* infection are shown.

We also observed the repression of genes with anti-proliferative function. An over-expression of ARRDC3 (arrestin domain containing 3), repressed *in vitro* and *in vivo* by *E. falciformis*, decreases tumor proliferation, whereas its knockdown exerted the opposite effect (439). Also, RND3 expression (Rho family GTPase 3), down-regulated by *E. falciformis* and *T. gondii*, was shown to reduce proliferation and transformation (440). Therefore, down-regulation of ARRDC3 and RND3 should support cellular growth. Furthermore, FGF18 (fibroblast growth factor 18), a ligand for FGFR3, repressed *in vitro*, reduces proliferation in intestinal crypt cells in mice (441). Similarly, MS4A4B (membrane-spanning 4-domains, subfamily A, member 4B) negatively regulated proliferation of murine T cells by S-G2/M phase arrest (259), and over-expression of GAS1 (growth arrest specific 1) decreased the proliferation of HIH3T3 cells (400). In addition, TXNIP (Thioredoxin interacting protein) was repressed in *T. gondii*-infected YAMC cells. Its over-expression induced cell-cycle arrest in different cancer cell lines (442), and mice lacking TXNIP show an increased epithelial cell proliferation in the intestine (443). Therefore, down-regulation of FGF18, GAS1, MS4A4B, and TXNIP can potentially support proliferation. However, these genes might also function in other categories. For example, TXNIP is also an endogenous inhibitor of thioredoxin (444), a protein involved in transcription, protein-folding and proteolysis. A down-regulation of TXNIP expression can therefore also have other effects, such as inhibition of thioredoxin.

Induced genes associated with inhibition of cellular growth and proliferation, included RERG (RAS-like, estrogen-regulated, growth-inhibitor) and RGS4 (regulator of G-protein signaling 4), which were up-regulated *in vitro*. RERG is a small GTPase and a member of the RAS superfamily, which mediates proliferation and differentiation (445). RERG expression was shown to be induced by estrogen in breast cancer cells, which inhibits their cell growth (446). Likewise, RGS4 inhibits the cell proliferation *via* reduction of a G protein-mediated p38 MAPK activation (447). In addition, IFI202B (Interferon activated gene 202B), which was the highest induced transcript late during *in vivo* infection, has anti-apoptotic (448) and anti-proliferating properties (449). Notably, induction of anti-proliferative genes may negatively regulate the cell growth.

In summary, many genes which appeared modulated during infection participate in the regulation of proliferation and the host cell cycle. However, we did observe the modulation of genes with proliferative as well as anti-proliferative capacities. Therefore, a distinct conclusion if the infection results in an overall proliferative or anti-proliferative response remains to be elusive.

4.1.4.6 Metabolism

Among the highly modulated genes, we observed genes, which participate in transport activities across the membrane or lipid and sugar metabolism. Some of these genes will be discussed in more detail below.

4.1.4.6.1 Transporters

Strikingly, many transporters of different ions including sodium, calcium and chloride were highly induced or repressed during infection (Tab. 17). SLC8A3 (solute carrier family 8, member 3), induced 16 h post-*Eimeria*, and SLC8A1 (solute carrier family 8, member 1), repressed 144 h p. i., are major sodium/calcium exchangers, important to maintain calcium homeostasis (450, 451). Similarly, the expression of the ATPase ATP2B1 (ATPase, Ca^{2+} transporting, plasma membrane 1), highly reduced during *T. gondii* and *Eimeria* infection, regulates the active efflux of Ca^{2+} to maintain Ca^{2+} homeostasis across the plasma membrane. In addition, the over-expression of ATP2B1 was shown to reduce the proliferation of vascular smooth muscle cells (452). Another protein, GEM (GTP binding protein), induced during *Eimeria* and *T. gondii* infection, interacts with the beta-subunit of voltage-dependent Ca^{2+} channels, which mediate Ca^{2+} influx (453). The beta-subunits are responsible for the

successful trafficking of the pore-forming alpha-subunits to the plasma membrane (454), and GEM can inhibit the channel activity (453).

Tab. 17: Selected transporters and their function upon infection. The table depicts selected genes induced (+), repressed (-) or absent (/) during *E. falciformis* and *T. gondii* infection. The table is based on gene expression analyses and literature searches.

Gene	*E. falciformis*		*T. gondii*	Function	
	in vivo	*in vitro*	*in vitro*		
Ca^{2+}					Ca^{2+} homeostasis
SLC8A3	/	+	/	Na^+/ Ca^{2+} exchanger	
SLC8A1	-	/	/	Na^+/ Ca^{2+} exchanger	
ATP2B1	-	-	-	Ca^{2+} efflux	
GEM	+	+	+	Inhibitor of Ca^{2+} channel	
Na^+				Activation of Na^+/K^+ ATPase, Na^+ export	
SIK1	/	-	-		
Cl^-					
CLDN8	-	/	/	Cl^- absorption	
KCNE3	-	/	/	Cl^- secretion	
CFTR	-	-	/	Cl^- secretion	
Others					
LRP2	/	-	/	Vitamins, lipoproteins, hormones, enzymes	
SLC3A1	+	+	/	Cystine, dibasic amino acids	
SLC6A19	/	/	-	neutral amino acids	

The most down-regulated gene during early and late *T. gondii* infection (SIK1; salt-inducible kinase 1) regulates the active sodium transport *via* activation of a Na^+,K^+-ATPase (402) as well as apoptosis (403) (Section 4.1.4.4). A stringent regulation of the Na^+,K^+-ATPase, which actively controls the sodium and potassium transport across the cell membrane, is essential to maintain several important cellular functions including the cell volume. Increases in the intracellular sodium concentration lead to SIK1 activation followed by an increased Na^+,K^+-ATPase activity and subsequent sodium export (402).

Some of the transporters strongly repressed during *Eimeria* infection regulate the chloride concentration across the membrane. Of these, CLDN8 (claudin 8) is a component of tight junctions and regulates paracellular permeability. Depletion of CLDN8 led to the loss of the paracellular chloride conductance in the collecting duct, suggesting its role in the re-absorption of chloride ions (455). KCNE3 (potassium voltage-gated channel, Isk-related subfamily, gene 3), repressed during mouse infection, is required for chloride secretion across the intestinal epithelium (456). Another gene, CFTR, highly repressed during late *in vitro* and *in vivo Eimeria* development, is involved in chloride ion secretion and in regulation of the epithelial fluid balance (457). Down-regulation of CFTR by *E. falciformis* could therefore counteract the diarrhea, which is observed during the peak days of oocyst shedding.

Other highly modulated molecules associated with transport activities included LRP2 (low density lipoprotein receptor-related protein 2), repressed 16 h post-*Eimeria* infection, SLC3A1 (solute carrier family 3, member 1), induced 4 h and 144 h post-*Eimeria* infection, and SLC6A19 (solute carrier family 6, member 19), exclusively repressed during *T. gondii* infection. LRP2 is a transmembrane glycoprotein (458) mediating the uptake of vitamins, lipoproteins, hormones and enzymes (459). SLC3A1 is a transporter for the import of cystine and dibasic amino acids (460). Cystine following its reduction to cysteine, is a precursor for gluthatione, an important antioxidant, which can prevent damage caused by reactive oxygen species (461). Its up-regulation may alleviate the effect of reactive oxygen species produced in response to infection. SLC6A19 facilitates the absorption of neutral amino acids in the intestine including tryptophan (462). Its decreased expression might obstruct parasite growth.

In summary, regulation of transporter or transport-associated molecules demonstrates the importance of nutrient uptake and ion homeostasis during parasite infection.

4.1.4.6.2 Lipid metabolism

Early during *Eimeria* infection of YAMC cells, several genes associated with lipid metabolism were induced (Tab. 18). Among them was PON1 (Paraoxonase 1), which counteracts lipoprotein oxidation (463) and thus has antioxidant properties. Interestingly, it was shown that the absence of PON1 in mice infected with *Trypanosoma congolense* reduced host survival, suggesting a protective role of this enzyme (464). Another enzyme highly induced during *Eimeria* infection (4 h p. i.) was LCAT (Lecithin cholesterol acyltransferase). It is normally associated with HDL for esterfication of cholesterol into cholesteryl esters (465). Similarly, SAA4 was one of the highest induced transcripts 16 h post-*Eimeria* infections, which is also a constituent of the HDL particle. Moreover, overexpression of STAR (steroidogenic acute regulatory protein; induced early during *Eimeria*-infection) in murine macrophages represses cholesterol biosynthesis. Besides that, STAR also increases the cholesterol efflux (466). FDPS (farnesyl diphosphate synthase), a downstream target of STAR, was also repressed late during *Eimeria* infection. For *T. gondii*, a cholesterol-auxotroph parasite, it was described that the parasite accesses its main sterol from the host cell (467). This might be also true for the close relative, *E. falciformis*. *De novo* synthesis of cholesterol however is dependent on the host mevalonate pathway, which does not exist in the parasites. Interestingly, an up-regulation of several host pathway enzymes was observed in *T. gondii*-infected HFFs (56). In contrast, we did not observe an induction of the host

mevalonate pathway neither upon *E. falciformis* or *T. gondii* infection of YAMC cells and mice. Furthermore, we rather observed a decreased expression of a mevalonate pathway enzyme (FDPS) and an increase in an enzyme associated with cholesterol efflux in *E. falciformis*-infected cells, which might therefore reduce the availability of cholesterol for the intracellular parasite.

Tab. 18: Modulated genes of the lipid metabolism upon infection. Selected genes, which were induced (+), repressed (-) or not altered (/) in *E. falciformis* and *T. gon*dii infections.

Gene	*E. falciformis*		*T. gondii*	Function
	in vivo	*in vitro*	*in vitro*	
Cholesterol biology				
LCAT	/	+	/	Esterfication
STAR	/	+	/	Repression of biosynthesis, increase of efflux
FDPS	/	-	/	Biosynthesis
SOAT1	/	/	-	Esterfication
Lipid catabolism				
ACSL1	-	/	/	Beta-oxidation pathway
ACSM3	-	/	/	Beta-oxidation pathway
ACOT12	-	/	/	Acetyl-CoA hydrolysis
Transport				
SAA4	/	+	/	Constituent of HDL
VLDLR	-	+	/	Uptake of Lipids
Others				
PON1	/	+	/	Lipoprotein oxidation
GPAM	-	/	/	Triaglycerol and glycerophospholipid synthesis

Interestingly, SOAT1 (sterol O-acyltransferase 1) was among the strongest down-regulated transcripts early and late during *T. gondii* infection. This enzyme is important for the formation of cholesteryl ester. The proliferation of the cholesterol auxotroph *T. gondii* was reduced by 60% in cells deficient of SOAT1. Moreover, SOAT1 inhibition resulted in a reduced parasite proliferation in a dose-dependent manner (468). Therefore, the observed reduced mRNA levels of SOAT1 could be detrimental to the parasite development. However, cells express other enzymes for cholesterol esterification (*e.g.* LCAT (465)), which may compensate a repression of SOAT1. Furthermore, it was shown that *T. gondii* expresses two SOAT1 homologues, which form cholesteryl esters using host lipids (469). As mentioned before, microarray data on *T. gondii*-infected HFF cells revealed an induction of several mevalonate pathway enzymes (56), a phenomenon we did not observe in parasite-infected

YAMC cells. These differences might be attributed to a different host cell type (mouse *vs.* human) and time point (4 h and 16 h *vs*. 24 h p. i.) in these studies.

Infections of mice with *E. falciformis* also resulted in an altered lipid metabolism. Some highly repressed transcripts included ACSL1 (acyl-CoA synthetase long-chain family member 1) and ACSM3 (acyl-CoA synthetase medium-chain family member 3), which catalyze the degradation of fatty acids by the beta-oxidation pathway. In contrast, GPAM (glycerol-3-phosphate acyltransferase) initiates the synthesis of triacylglycerol and glycerophospholipids, which contributes to the phospholipid composition of the cell. Moreover, GPAM expression is important in immunological processes. The infection of GPAM-deficient mice with coxsackievirus B3 increased the mortality due to elevated virus titer concomitant with increased concentrations of pro-inflammatory cytokines and decreased T cell response (470). Absence of GPAM also resulted in an increased production of reactive oxygen species in the liver mitochondria and an enhanced cell death (471).

Late during mouse infection, we also observed genes involved in lipid metabolism, including ACOT12 (acyl-CoA thioesterase 12) and VLDLR (very low density lipoprotein receptor). ACOT12 is involved in cleaving the thioester bond between the acyl group and the CoA to release the acid and CoA. Many of these thioesterases, including ACOT12, are located in peroxisomes, organelles involved in lipid catabolism (472). VLDLR belongs to the low density lipoprotein (LDL) receptor family and regulates the uptake of exogenous lipids (473).

Taken together, some genes of the host lipid metabolism were highly altered during parasite infection. Nevertheless, there are not enough genes of a given pathway which allow a distinct conclusion that parasite infection modulates host lipid metabolism for its own benefits. Furthermore, down-regulation or absence of genes involved in the cholesterol biology might be rather detrimental for the parasite development.

4.1.4.6.3 Carbohydrate metabolism

Interestingly, in contrast to *T. gondii*-infected HFF cells (56) hexokinase 2 (HK2) and lactate dehydrogenase (LDHA) were the only two glycolytic enzymes induced during *T. gondii* infection of YAMC cells (Fig. 50). HK2 catalyzes the reaction of glucose into glucose-6-phosphate, and was also induced during *E. falciformis* infection of YAMC cells. Additionally, enolase 2 (ENO2), converting 2-phosphoglycerate into phosphoenol-pyruvate, was induced 16 h after *Eimeria* infection. Furthermore, hexokinase 3 (HK3 induced) and

phosphofructokinases (PFKP induced, PFKM repressed), were the only glycolytic enzymes modulated *in vivo* by *E. falciformis*.

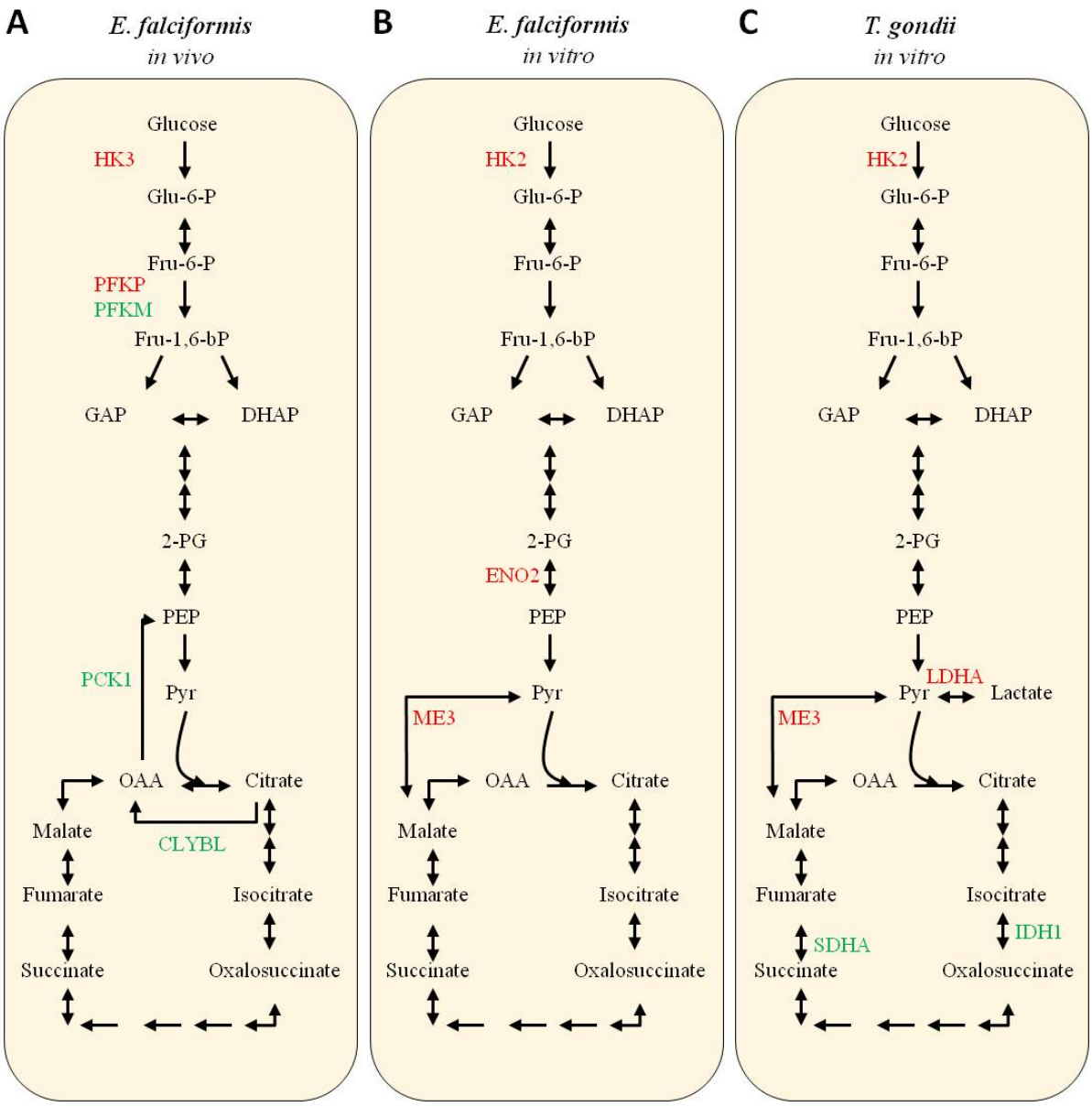

Fig. 50: Glycolytic and TCA cycle enzymes modulated in response to infection. Schematic figure of selected mouse genes, which were induced (red) or repressed (green) upon **(A)** mouse or **(B)** *E. falciformis* and **(C)** *T. gondii* infection of YAMC cells.

Other enzymes modulated upon infection participate in the TCA cycle. Unlike parasitized HFF cells, we observed the repression of IDH1 (isocitrate dehydrogenase 1) and SDHA (succinate dehydrogenase complex, subunit A) in *T. gondii*-infected YAMC cells. Another enzyme, ME3 (malic enzyme 3), converting malate into pyruvate, was induced during *T. gondii* and *E. falciformis* infection. In addition, CLYBL (citrate lyase) and PCK1

(phosphoenolpyruvate carboxykinase), were repressed *in vivo* (144 h p. i), and convert citrate into oxalacetate and oxalacetate into phosphoenolpyruvate, respectively.

Glycolysis and the TCA cycle are central metabolic pathways in cells providing energy and important precursors for several other biosynthetic pathways. Induced expression of pathway enzymes might be beneficial to restock the energy requirements of the parasitized host cells or to provide carbon sources for the parasite. *T. gondii* uses host glucose as a carbon source which might be also true for *E. falciformis*. Import of host glucose into the parasites might result in an increased glucose influx which in turn might increase the activity of glycolytic enzymes.

However, based on our studies it can be concluded that glycolysis and TCA cycle were influenced by the apicomplexan infection, albeit the extent of modulation in YAMC cells was much lower than reported, previously.

4.2 C-FOS supports the *in vitro* growth of *E. falciformis* and *T. gondii*

FBJ osteosarcoma oncogene (c-FOS) is part of the activator protein 1 (AP-1) complex. It is an important transcription factor involved in several biological processes including pro-inflammatory responses, cell proliferation, differentiation, apoptosis and transformation (474). Under normal conditions, c-FOS expression is very low (475) but the expression can be rapidly induced by external stimuli including LPS and IFN-γ (476). Therefore, c-FOS belongs to the immediate early gene family of transcription factors. Microarray analyses of infected YAMC cells identified c-FOS as the only annotated gene, which appeared induced during early and late infection of *E. falciformis* as well as *T. gondii*. Interestingly, no apparent induction was observed *in vivo*. However, c-FOS is an immediate early gene which may explain the absence of induction in *E. falciformis*-infected mice at 24 h and 144 h post-infection. Furthermore, the absence of a transcriptional response on the distinct time points does not mean that the protein is not expressed and thus present.

We observed a significant reduction in the development of *E. falciformis* in $FOS^{-/-}$ cells. *T. gondii* infection of $FOS^{-/-}$ cells also resulted in a slow growth phenotype. In contrast, infection of $FOS^{-/-}$ mice with *Salmonella enterica serovar typhimurium* was shown to result in an increased bacterial proliferation although a higher production of pro-inflammatory cytokines (TNF-α and IL-12) was observed (476). The increased pro-inflammatory phenotype in the $FOS^{-/-}$ mice was accompanied by an increase in apoptotic events. It was suggested that the

induction of apoptosis in macrophages and other immune cells may enhance proliferation of *Salmonella* in the $FOS^{-/-}$ mice. Therefore, the authors concluded that c-FOS has a role in the protective immunity against *Salmonella* (476). Furthermore, infection with different *Leishmania* spp. resulted in degradation or down-regulation of several AP-1 family members including c-JUN and c-FOS, which was mediated by a parasite protease (GP63) (477). Along with STAT and NF-κB, AP-1 is responsible for iNOS transcription in macrophages and production of TNF-α, IL-1β and IL-12 (478). These molecules are required to efficiently control *Leishmania* parasites. Therefore, the active interference of the parasite with a host factor accounts for a protective role of c-FOS also during a *Leishmania* infection. Nevertheless, similar to our results, in Hepatitis C virus (HCV)-infected cells the expression of c-FOS was up-regulated. Consistently, RNA interference of c-FOS expression reduces HCV propagation, whereas its over-expression increases the virus replication (479). These results resemble ours, where we also observed a reduced development of *E. falciformis* and *T. gondii* in the parasitized $FOS^{-/-}$ cells in comparison to the wild type controls. In contrast to the *Salmonella* infection, c-FOS supports the development of the parasites as well as of a virus (HCV) *in vitro*. However, viruses largely depend on their host cell for replication. Therefore, the mechanistic background of the positive effect of c-FOS expression during *Eimeria* infection remains to be determined. These differences between our observed results and the above described effects on a *Salmonella* or *Leishmania* infection might be also contributed to the differences of an *in vitro* and an *in vivo* situation. Therefore, c-FOS expression might be more important for the *in vitro* development of *E. falciformis* whereas *in vivo* the transcription factor might be part of the defense response.

4.3 The role of IDO induction during *E. falciformis* infection of the mouse

Microarray analyses of *E. falciformis*-infected caecal cells revealed an induced expression of indoleamine 2,3-dioxygenase 1 (IDO1) during mouse infection. IDO1 is the first and the rate-limiting enzyme of tryptophan degradation *via* the kynurenine pathway (Fig. 30) in mammals. Whereas mammals and some microorganisms depend on exogenous tryptophan supply, plants, fungi and some bacteria can synthesize this amino acid *de novo*. These organisms use the shikimate pathway for the production of chorismate, a precursor for the synthesis of aromatic amino acids, folate and ubiquinone (480). There is genetical and/or biochemical evidence that some apicomplexan parasites (*T. gondii*, *P. falciparum* and *C. parvum*) can synthesize chorismate (481-483), but they lack the enzymes for tryptophan synthesis. It is also likely that *Eimeria* spp. are auxotroph for tryptophan. Besides protein biosynthesis,

tryptophan is also needed to make biologically active metabolites, such as serotonin and kynurenines. Serotonin is a neurotransmitter present in the gut, platelets and the central nervous system. It is derived from tryptophan by tryptophan hydroxylase (TPHA) and aromatic acid decarboxylase (AADC) and mediates intestinal movements, cardiovascular activities, mood, sleep and appetite. Serotonin is also a precursor for the hormone melatonin, which is responsible for the circadian rhythm. Only 1–2 % of ingested tryptophan is converted into serotonin (484), and ~95 % is metabolized along the kynurenine pathway (485, 486).

The initial and rate-limiting reaction of the kynurenine pathway, the conversion of tryptophan into formylkynurenine, is catalyzed by three different enzymes: Tryptophan 2,3-dioxygenase (TDO), indoleamine 2,3-dioxygenase 1 (IDO1) and indoleamine 2,3-dioxygenase 2 (IDO2). These enzymes differ in their structure, localization, function, substrate specificity and the mechanism of induction. Once N-formylkynurenine is produced, it is rapidly hydrolyzed to kynurenine by formamidase (AFMID). Kynurenine can be further processed to anthranilic acid by kynureninase (KYNU), or to kynurenic acid (KYNA) by kynurenine aminotransferase (KAT), or to 3-hydroxykynurenine (3-HK) by the kynurenine 3-hydroxylase (KMO). The latter is converted to either xanthurenic acid by kynurenine aminotransferase, or into 3-hydroxyanthranilic acid (3-HANA) by kynureninase. 3-HANA is the substrate for 3-hydroxyanthranilate dioxygenase (3-HAO) producing quinolinic acid (QUIN). Quinolinic acid can produce nicotinamide adenine dinucleotide (NAD^+) by the action of quinolinate phosphoribosyl transferase (QPRTase). Therefore, this pathway produces NAD^+, several biological active metabolites, and regulates tryptophan concentration in the plasma.

This study shows that *E. falciformis* induces IDO1 expression at the site of infection. Many other enzymes of the kynurenine pathway, including IDO2, KMO, KYNU, KAT and HAAO are also induced during the parasite life cycle. Moreover, we have shown that IDO1 and two downstream enzymes are required for an efficient *E. falciformis* development in the mouse as discussed below.

4.3.1 The kynurenine pathway is induced in parasite-infected mice

IDO1 is constitutively expressed in various tissues (*e.g.* lung, placenta) and inducible in several cell types, including dendritic cells, macrophages, monocytes, epithelial cells and fibroblasts (204). This study shows IDO up-regulation in the caecal epithelial cells infected by *E. falciformis*. Parasite infection resulted in the induction of IDO1 in the intestinal epithelial

cells of the caecum, which are host cells for *E. falciformis*. Although, transcript was induced within day 1 p. i., protein (46-kDa) was first detectable on day 2 of infection, which then persisted throughout the parasite life cycle. The observed lag in protein expression suggests a post-transcriptional regulation of IDO1. In addition, the observed fluctuation in IDO1 gene expression indicates a transcriptional feedback mechanism. Generally, IDO1 is expressed in response to pro-inflammatory cytokines (IL-1, TNF- α) (487, 488), LPS (489) and anti-inflammatory stimuli including CTLA4 engagement (490) on antigen-presenting cells. The most potent inducer of IDO1 expression however is IFN-γ, which is also important to control *Eimeria* infections (491-493). In line, as shown by IHC, IDO1 was undetectable in the caeca of IFN-γR$^{-/-}$ mice parasitized with *E. falciformis*.

Other members of the kynurenine pathway including IDO2 were also induced during *E. falciformis* infection. IDO2 is constitutively expressed mainly in kidney, epididymis, testis and liver (494). Unlike IDO1, IDO2 is not inducible by IFN-γ and expressed despite the absence of the cytokine in IFN-γ-knockout mice (494). Its function during infection is therefore rather questionable. The expression of two KAT isoforms (KAT2 and GOT2) was also up-regulated. KAT1 and KAT2 are the major enzymes in mammals, which convert kynurenine into kynurenic acid, and 3-hydroxykynurenine into xanthurenic acid (495-497). Other parasite-induced enzymes included KMO, KYNU and HAAO. Taken together, our results indicate an overall induction of the mouse kynurenine pathway by *E. falciformis*.

4.3.2 IDO1 is required for the parasite development

IDO1 induction during infections is a widely occurring phenomenon across the field of various pathogens. It has been postulated that IDO induction is one of the early host defense mechanisms (498). Induction of IDO1 initiates tryptophan degradation, an essential amino acid for many pathogens. IFN-γ-mediated induction of IDO1 has been reported to exert detrimental effects on the growth of different viruses, such as genital herpes simplex virus type 2 (201) and cytomegalovirus (499) *in vitro*. The growth of bacteria, like *Chlamydia* (200) and group B streptococci (500) was also negatively affected. Moreover, the development of *T. gondii* was inhibited by IDO1 expression in IFN-γ-treated HFF cells (182). Interestingly, the growth inhibition of *T. gondii* and *Chlamydia psittaci* could be reversed by exogenous tryptophan (501). Together, these reports postulated that IDO1 contributes to the host defense by depleting the subcellular levels of tryptophan available to susceptible microbes. This is, however, in contrast to our results, in which inhibition or absence of IDO1 did not promote

the parasite development. Instead, it inhibited *E. falciformis* growth *in vivo*. Tryptophan starvation is therefore questionable as a host defense mechanism in *E. falciformis* infection of mouse, although this parasite might be a tryptophan auxotroph pathogen like *T. gondii*. The *in vivo* role of IDO1, however, is still quite controversial. For example, *in vivo* blocking of IDO increases the burden of parasites, such as *T. gondii* (502) and *Trypanosoma cruzi* (503) and of fungi (*Candida albicans*, (504)) in mice, which appears consistent with its *in vitro* antimicrobial role. In contrast, inhibition or deficiency of enzyme during other parasitic (*Leishmania donavoni*, (502); *Trichuris muris*, (505)) and bacterial (*Citrobacter rodentium*, (506)) infections reduced the pathogen burden in animals. Moreover, 1-methyltryptophan (1-MT), a competitive inhibitor of IDO, had none (herpes simplex virus 1) to a negative (murine leukemia virus) influence on the virus replication in mice (502, 507), which occasionally differs with *in vitro* findings (508). Likewise, IDO1 as a positive determinant of *Eimeria* growth does not coincide with its canonical antimicrobial function, albeit a potential depletion of tryptophan in the infected host cell. It must be noted that a fair comparison of different models is not feasible even within a parasite phylum (*i.e.* Apicomplexans) due to dissimilar setups, let alone with other pathogens as mentioned elsewhere (502). Together, it can be concluded that the *in vivo* function of IDO1 during infection with intracellular pathogens appears to be rather pathogen- and/or stage-specific.

4.3.3 *Eimeria*-infected IDO1$^{-/-}$ mice develop an apparently normal immune response

IDO1 is also believed to be an important immuno-regulatory enzyme. Inhibition of IDO by 1-methyl tryptophan in pregnant mice led to fetal rejection (202), suggesting IDO activity is important for fetal tolerance mechanism. The immune-regulatory function of IDO might be mediated *via* suppression of T cell proliferation (509, 510) as a consequence of tryptophan starvation leading to a cell cycle arrest (203) and/or an increased apoptosis caused by kynurenine metabolites (511-513). Blocking of IDO in a toxoplasmosis model resulted in increased parasite burden but exerted no apparent effect on the mouse immune response. In contrast, inhibition of IDO by 1-MT in *Leishmania*-infected mice reduced the parasite burden with a concurrent increase in IFN-γ and reduced IL-10 levels (502). These data from different models of infection do not allow to decide whether IDO contributes to the host resistance *via* depletion of tryptophan and/or due to its anti-proliferative and immune-regulatory effects. However in our infection model, the *Eimeria*-infected IDO1 knock-out mice displayed a normal Th1 and IFN-γ response, precluding an influence of immune modulation on the parasite growth in these animals.

4.3.4 Xanthurenic acid is needed by the parasite

The inhibition of three distinct enzymes of the tryptophan catabolism did result in decreased oocyst numbers. The reduced oocyst yield of IDO1 knockout animals could not be explained by an enhanced immune response against the parasite. Notably, all three enzymes catalyze reactions up-stream of xanthurenic acid (XA) production. XA is an end metabolite of the tryptophan degradation and the urinary amount of XA is increased 3-fold in response to induction of IDO1 in mouse (204). It is presumed that XA is produced as part of the detoxification process, because its precursor, 3-hydroxykyurenine, mediates generation of free radicals and apoptosis (514, 515). Increased XA concentrations in the urine were also used as a diagnostic tool for vitamin B_6 deficiency, because another kynurenine pathway enzyme located downstream of 3-hydroxykynurenine (kynureninase) depends on vitamin B_6 (516).

Importantly, however, XA promotes the sexual development of *Plasmodium* spp. in the mosquito mid-gut (49). In insects, the products of the kynurenine pathway are generally required for the eye development, metamorphosis and behavior (517, 518). The tryptophan catabolism in the mosquito initiates with tryptophan degradation (catalyzed by tryptophan 2,3-dioxygenase) and terminates in the production of kynurenic acid (produced by kynurenine aminotransferase) and xanthurenic acid (product of 3-hydroxykynureninase transaminase), due to the absence of the enzyme kynureninase (519). Finally, ingestion of *Plasmodium* gametocytes by the mosquito induces gametocyte maturation. In general, a lower temperature, a higher pH and/or a mosquito-derived gametocyte activating factor (520-522), identified as XA (49), facilitate sexual development of *Plasmodium*. Interestingly, at a non-permissive pH of 7.3 (pH of mouse blood) a decreased temperature and the presence of XA are sufficient to induce gametogenesis *in vitro* (522, 523). XA, in particular, promotes exflagellation of the male gametes in the mid-gut of the mosquito. It was shown, that XA triggers an increase in cytosolic calcium, which is essential for the differentiation into mature gametes. The identity of an XA-receptor and the exact signaling events are not known, however (524, 525). Similar to *Plasmodium*, XA appears to be required for *E. falciformis* development. We show that administration of XA to IDO knockout animals restored the parasite growth. The attempt to restore the reduced oocyst output in IFN-$\gamma R^{-/-}$ animals by XA administration, however, were not successful. We have shown that IDO1 expression is absent in infected IFN-$\gamma R^{-/-}$ animals, demonstrating the IFN-γ-mediated IDO1 expression during *E. falciformis* infection. However, as recently described by Stange *et al*., the reduced oocyst yield in IFN- $\gamma R^{-/-}$ mice is due to elevated Th17 responses in line with dramatically increased intestinal pathology (22). Most

likely, the pathological and immunological implementations in this infection model superimposed any beneficial effect of XA.

We further did not observe differences in the Th1 or IFN-γ response in WT, IDO1$^{-/-}$ or XA-treated transgenic animals. Therefore we speculate that XA may enhance the sexual development of *E. falciformis*. However, our *E. falciformis* data also do not show that the asexual growth and macrogametocyte development of *E. falciformis* are influenced by IDO1 and XA. Therefore, we suggest that the effect of XA on *E. falciformis* development in mouse is similar to *Plasmodium* in mosquito host, *i.e.,* on the maturation of male gametes. Furthermore, the beneficial effect of XA appears to be confirmed to the definite host, because neither the absence of IDO1 nor the treatment with XA altered the parasitemia in *P. berghei*-infected mice. In this model we did also not observe differences in the abundance of gametocytes in mice and oocysts produced after mosquito feeding on infected WT, IDO1$^{-/-}$ or XA-treated transgenic animals. These results support the previous findings that at least two triggers of gametogenesis for *Plasmodium* spp. are needed, a drop in temperature and XA (or an increased pH). Therefore, mosquito-derived XA might be also more important than a mouse-derived metabolite for *Plasmodium* spp.

Importantly, we have shown that XA, a by-product of tryptophan degradation is required for an optimal progression of *E. falciformis* in the mouse. Exploitation of tryptophan catabolism by both apicomplexan parasites in their respective definite host therefore appears to be evolutionarily conserved. Whether *Plasmodium* species also induce the only counterpart of mammalian IDO (i.e. tryptophan 2,3-dioxygenase) in mosquito to co-opt the tryptophan catabolism remains to be determined.

4.4 Outlook

This study identified a number of mouse genes with potential roles during parasite infection. A detailed comparative analysis of *E. falciformis* and *T. gondii*-infected cells can be used to identify host proteins, which determine the parasite development. Comparison of the *in vitro* and mouse response with microarray analyses of other pathogens could result in characterizing specific host responses against *E. falciformis*. Furthermore, the YAMC cells used in our microarray approach did not allow a development of *E. falciformis* upon invasion; although as cells derived from the colon they resemble the natural environment. Therefore, it will be worth to study the transcriptional response in other cell lines. Similar to the YAMC cells, they should resemble the natural environment. Candidate cell lines might be the

intestinal epithelial cell lines m-ICc12 or CMT-93. The first mentioned cell line is characterized by maintaining a crypt phenotype (526) and crypt epithelial cells serve as host cells of *E. falciformis*. Furthermore, in contrast to YAMC cells, CMT-93 cells, derived from murine rectum carcinoma, show an improved schizont development (22). In addition, YAMC cells have to be cultured in the presence of IFN-γ. This cytokine is also present during mouse infection, thus its presence during *in vitro* studies again resemble the natural environment. Nevertheless, IFN-γ is present already prior to infection alerting the cells which might contribute to a reduced replication efficiency of the parasites in YAMC cells. Therefore, further experiments in other cell lines should include responses in the absence or presence of IFN-γ.

C-FOS expression appears to support the *in vitro* development of *E. falciformis* and *T. gondii*. Interestingly, over-expression of c-FOS in HCV-infected cells by genetic and biochemical means (phorbol 12-myristate 13-acetate treatment), increased the virus replication (479). It will be interesting to evaluate whether a similar over-expression of c-FOS in *E. falciformis*-infected cells can further promote the parasite development. In addition, microarrays of *E. falciformis* and *T. gondii*-infected c-FOS wild type and knockout cell lines might dissect the importance of the transcription factor for their *in vitro* development. Whether c-FOS has a role during mouse infection is another interesting question. C-FOS expression was induced *in vivo* albeit modestly with no statistical significance. The use of c-FOS$^{-/-}$ mice should allow such a testing.

It is absolutely essential to improve the *in vitro* culture of *E. falciformis*. Further assays should aim at defining the significance of other highly-modulated mouse genes for parasite infection (Tab. 19). Infection of knockout mice or cell lines with *E. falciformis* should be the first step to elucidate their roles. Table 19 shows candidate genes according to the availability of knockout animals and cells.

The transcription factors of the early growth response family (EGR1 to 4) were all induced upon early and late *T. gondii* infection. EGR2 is the best described member of this family and its expression is induced upon rhoptry secretion during *T. gondii* infection (72). In contrast to *T. gondii*-infected YAMC cells, EGR expression was absent during early *E. falciformis* infection *in vitro*. Thus, inducing its expression early during infection may alter the *Eimeria* development *in vitro*. Likewise noticeable in the microarray experiments was the regulation of many DUSPs during *Eimeria* infection. DUSPs regulate the activity of MAP kinases by

dephosphorylating threonine and tyrosine residues (317). Moreover, in *T. gondii* infections of YAMC cells the expression of only three DUSPs was modulated (DUSP2, 1, 10). Interestingly, DUSP1 and DUSP10 expression was induced by *Eimeria* but repressed by *T. gondii* 16 h post-infection. Infection of cells deficient in DUSP expression may elucidate their function during parasite infection.

Tab. 19: Parasite-modulated host factors and pertinent biological resources available.

Host gene	**Biological resource**
EGR 1-4	knockout mouse of EGR1 (527), EGR3 (528), EGR4 (529), double knockout of EGR1/EGR4 (530) EGR2/3 overexpressing cells (531)
c-FOS	knockout mouse (532)
TLR family	several knockout mice (http://myv.ne.jp/obs/index.files/tlr_eng.htm#3rd)
DUSPs	knockout mouse of DUSP1 (533), DUSP2 (534), DUSP4 (319), DUSP6 (535) Inhibitor for DUSP1/DUSP6 (536)
C-type Lectins	knockout mouse of CLEC7A (308), CLEC4E (311), CLEC4N (312), CLEC4A2 (313)
Chemokines	knockout mouse of CXCR3 (537), CCR5 (538), neutralizing antibodies against CXCL9/10/11 (329, 539)
SPP1	knockout mouse (540)
MMPs	knockout mouse of MMP3 (378), MMP7 (377), MMP10 (541), MMP13 (542)
IRGs	Visualization of IRGA6, IRGM3, IRGB6, IRGM1 and IRGD by antibodies (119); IRGA6-deficent cell (119); knockout mice of IRGM1 and IRGD (382), IRGM3 (384), IRGA6 (386)
GBPs	Visualization of GBP1, GBP2, GBP3, GBP4, GBP5, GBP7 by antibodies (250); knockout mice of GBP2 (https://www.komp.org/), GBP1, GBP6, GBP7 and GBP10 (387)
Kynurenine-Pathway	knockout mouse of KAT2 (543), KMO (www.komp.org/geneinfo.php?project=CSD40845), IDO2 (www.komp.org/geneinfo.php?geneid=31197)

Unlike *in vitro E. falciformis* infection, several IRGs (immunity-related GTPases) and some GBPs (guanylate-binding proteins) were highly repressed during *T. gondii* infection of YAMC cells. In contrast, IRGs and GBPs were highly induced during mouse infection with *E. falciformis*. The use of mice lacking one or more IRG or GBP proteins can reveal their possible functions during *E. falciformis* infection.

This study identified IDO1 and XA as host determinants of *E. falciformis* growth. Further experiments using mice lacking the key-enzymes of XA production (kynurenine

aminotransferase or kynurenine 3-hydroxylase) can further consolidate the role of tryptophan catabolism in the parasite cycle. Furthermore, under normal conditions, the XA-concentration in the serum of mammals is ~0.7 µM (544, 545), a level which is clearly not sufficient to induce exflagellation in *P. berghei in vitro* (546). In this regard, another interesting question will be to determine the local XA concentration in the caecum of the infected animals (*e.g.* HPLC).

To elucidate the mechanism of XA action on the parasite life cycle, detection of microgametocytes would be necessary (qPCR, microscopy). Ongoing sequencing projects on *E. falciformis* should identify stage-specific proteins to improve immunostaining techniques (IHC, IFA). In addition, CCP proteins, which were used in this study to determine the transcript abundance of *P. berghei* gametocytes, is a family of proteins containing a special domain with conserved C-terminal part (LCCL domain) with proposed function in gametocyte development and oocyst maturation (210). In *Plasmodium*, these proteins are transcribed mainly in the gametocyte stage (210). CCPs are present across the apicomplexan phylum, including *T. gondii* and *Eimeria* (547). Characterization of CCP homologs in *Eimeri*a can provide markers of the gametocyte development in this parasite.

List of Figures

List of Tables

Appendix A

App. A: List of definitions of the IPA high-level functional categories.

Amino Acid Metabolism

Describes functions associated with the metabolism of amino acids, for example the generation of serine and the degradation of tryptophan.

Antigen Presentation

This category contains all annotations of antigen presenting cells and the antigen presenting process. Objects are restricted to antigen presenting cells and their subclasses unless noted as an exception.

Antimicrobial Responses

This category contains all host immunologic responses to pathogens (viruses, bacteria, fungi) as well as mechanisms that indicate directly (clearance, neutralization) or imply immune responses to them (delay in removal, replication, or viremia; elimination, inactivation, inhibition, removal, repression).

Carbohydrate Metabolism

Describes functions associated with the metabolism of carbohydrates, for example the activation of glycogen and consumption of carbohydrate.

Cell Cycle

Describes the functions and stages of the cell cycle including cell division. Functions associated with mitosis and meiosis are included in this category. Some examples of functions in this category are assembly of telomeres, cell cycle progression and G0 phase of cells.

Cell Death

Describes functions associated with cellular death and survival. Some examples of functions included in this category are cytolysis, necrosis, survival, and recovery of cells.

Cell Mediated Immune Response

Objects in this category are restricted to T lymphocytes and their subclasses and natural killer cells and their subclasses unless noted as an exception. All lymphoid cells known to naturally express a TCR and the additional cell type of natural killer cell are included in this category; the category is restricted to more differentiated forms of these cells and the processes that such cells would perform.

Cell Morphology

Describes functions associated with the morphology of cells. Some examples include enlargement, fluidity, size and transformation of cells. This category also includes some cellular components that are involved in determining cell morphology such as projection of axons and remodeling of cytoskeleton.

Cell Signaling

Describes functions that are involved in intracellular signaling pathways. Specifically it describes functions associated with signaling molecules such as cyclic AMP, nitric oxide, and calcium, signaling functions such as tyrosine phosphorylation and guanine nucleotide exchange, as well as receptor-mediated signaling interactions.

Cell-to-Cell Signaling and Interaction

Describes functions that are involved in intercellular interactions such as binding, detachment, communication, pheromone response, and stimulation. This category also includes functions associated with specific cellular

components that are involved in signaling and interaction such as, intercellular junction and cell substratum contact.

Cellular Assembly and Organization

Describes functions associated with subcellular components that are involved in cellular organization and assembly of cellular substructures. Examples of functions in this category include alignment of actin filaments and aggregation of liposomes.

Cellular Compromise

Describes functions associated with the damage or degeneration of cells or any process that might compromise the function of the cell. Examples of functions included in this category are atrophy, damage, disruption, and swelling of cells.

Cellular Development

Describes functions associated with the development and differentiation of cells. This includes cellular functions that are involved in specific kinds of differentiation such as myogenesis and hematopoesis of cells, as well as developmental functions such as maturation and senescence of cells.

Cellular Function and Maintenance

Describes functions associated with the normal cellular functions that maintain cellular homeostasis. This includes functions such as engulfment, phagocytosis, regulation, and statsis of cells.

Cellular Growth and Proliferation

Describes functions associated with the growth and proliferation of cells. Some examples of these functions include colony formation, proliferation, and outgrowth of cells.

Cellular Movement

Describes functions associated with movement and localization of cells. Some examples of these functions include chemotaxis, infiltration, rearrangement, and transmigration of cells.

Gene Expression

Describes functions associated with gene expression. Some examples include acetylation of chromatin, transcription of gene and elongation of mRNA.

Humoral Immune Response

Only B lymphocytes and their subclasses, their products and tissue structures are contained in this category as it is restricted to antibody production and the effector of antibody production, the B lymphocyte unless noted as an exception (Example: binding to helper inducer T lymphocytes).

Immune Cell Trafficking

This category contains all the movement associated functions for all the cell types. It contains these specific processes regardless of object: accumulation, activation, adhesion, arrest in cell movement, cell-cell adhesion, cell movement, chemoattraction, chemokinesis, chemorepulsion, chemotaxis, circulation, delay in accumulation, delay in cell movement, delay in infiltration, delay in migration, delay in recruitment, diapedesis, dissemination, distribution, egression, emigration, homing, infiltration, influx, invasion, localization, locomotion, margination (excludes chromatin), migration, mobility, mobilization, onset of cell movement, onset of migration, recruitment, redistribution, relocalization, rolling, sequestration, trafficking, transdifferentiation, transmigration.

Inflammatory Response

This category is restricted to the mature cell types known to be effectors in inflammatory responses, specifically myeloid cells of the dendritic and monocyte lineage and the neutrophils as well as soluble factors such as complement and acute phase proteins and processes such as fever, degranulation, phagocytosis, respiratory burst, and swelling.

Lipid Metabolism

Describes functions associated with the metabolism of lipids, for example absorption of cholesterol and adiposis.

Molecular Transport

Describes functions associated with the intra- and extracellular movement of molecules, including small molecules, ions, DNA, RNA, protein, lipids and carbohydrates. Examples include efflux of glutamate and depletion of DNA.

Small Molecule Biochemistry

Describes functions associated with small molecules, for example the generation of nitric oxide and metabolism of indole. Functions associated with DNA, RNA, protein, lipids and carbohydrates are described by more specific categories and therefore are not included in this category.

Vitamin and Mineral Metabolism

Describes functions associated with the metabolism of vitamins and minerals. Examples include the accumulation of calcium and inactivation of retinoic acid.

Appendix B

App. B: Reciprocally regulated mouse genes during *E. falciformis* infection of YAMC cells.

Symbol	Gene	4 h	16 h	Biological Process
Dusp6	Dual specificity phosphatase 6	-2.59	2.60	Signal transduction
2610203C20Rik	RIKEN cDNA 2610203C20 gene	-2.52	3.09	-
Fn1	Fibronectin 1	-2.43	1.93	Cell adhesion
Zfhx1b	Zinc finger E-box binding homeobox 2	-2.16	1.94	Transcription
Zcchc7	Zinc finger, CCHC domain containing 7	-2.13	1.51	-
Dusp10	Dual specificity phosphatase 10	-2.12	2.15	Signal transduction
Chka	Choline kinase alpha	-2.06	1.64	Lipid metabolism
Pctk2	PCTAIRE-motif protein kinase 2	-2.01	1.83	Signal transduction
Dusp4	Dual specificity phosphatase 4	-2.01	3.09	Signal transduction
Mier1	Mesoderm induction early response 1 homolog	-1.90	1.59	Transcription
Atad2	ATPase family, AAA domain containing 2	-1.66	1.50	Transcription
Akap2	A kinase (PRKA) anchor protein 2	-1.64	1.71	Signal transduction
Has2	Hyaluronan synthase 2	-1.61	2.14	Carbohydrate metabolism
Tet2	Tet oncogene family member 2	-1.59	2.43	Cell cycle
Malat1	Metastasis associated lung adenocarcinoma transcript 1	-1.55	2.02	-

Appendix C

App. C: Table of reciprocally regulated genes during YAMC infection. Mouse transcripts, which showed a reciprocal regulation during *E. falciformis* and *T. gondii* infection of YAMC cells.

		E. falciformis		***T. gondii***	
Symbol	**Gene**	**4 h**	**16 h**	**4 h**	**16 h**
TRA2A	Transformer 2 alpha homolog	-3.17	-	-	2.62
RAI14	Retinoic acid induced 14	-3.34	-	-	1.93
NOL5A	Ribonucleoprotein homolog	-2.04	-	-	1.69
CNTLN	Centlein, centrosomal protein	-2.20	-	-	1.68
TSC22D2	TSC22 domain family, member 2	2.24	-	-	-1.67
MITD1	MIT, microtubule interacting and transport, domain containing 1	2.24	-	-	-1.78
ZBTB1	Zinc finger and BTB domain containing 1	2.06	-	-	-2.06
19-32	Mus musculus similar to monoclonal antibody kappa light chain	-	4.21	-	-1.71
DLL4	Delta-like 4	-	4.05	-	-1.62
MUC13	Mucin 13, epithelial transmembrane	-	3.96	-	-2.60
GJD4	Gap junction protein, delta 4	-	3.42	-	-1.86
IFNAB	Interferon alpha B	-	2.98	-	-1.81
PRKCE	Protein kinase C, epsilon	-	2.77	-	-1.74
TRP53INP1	Transformation related protein 53 inducible nuclear protein 1	-	2.59	-	-2.77
PXT1	Peroxisomal, testis specific 1	-	2.54	-	-1.89
RSAD2	Radical S-adenosyl methionine domain containing 2	-	2.26	-	-3.33
IRG1	Immunoresponsive gene 1	-	2.20	-	-2.37
BCL6	B cell leukemia/lymphoma 6	-	2.15	-	-1.74
DUSP1	Dual specificity phosphatase 1	-	2.02	-	-2.31
TMEM140	Transmembrane protein 140	-	1.94	-	-2.02
NCOA7	Nuclear receptor coactivator 7	-	1.86	-	-1.55
CFLAR	CASP8 and FADD-like apoptosis regulator	-	1.76	-	-1.74
GM8995	Predicted gene 8995	-	1.71	-	-2.91
ENC1	Ectodermal-neural cortex 1	-	1.52	-	-1.97
DUSP10	Dual specificity phosphatase 10	-2.12	2.15	-	-3.74
HAS2	Hyaluronan synthase 2	-1.61	2.14	-	-1.80
FLNB	Filamin, beta	-1.68		1.57	1.54

Appendix D

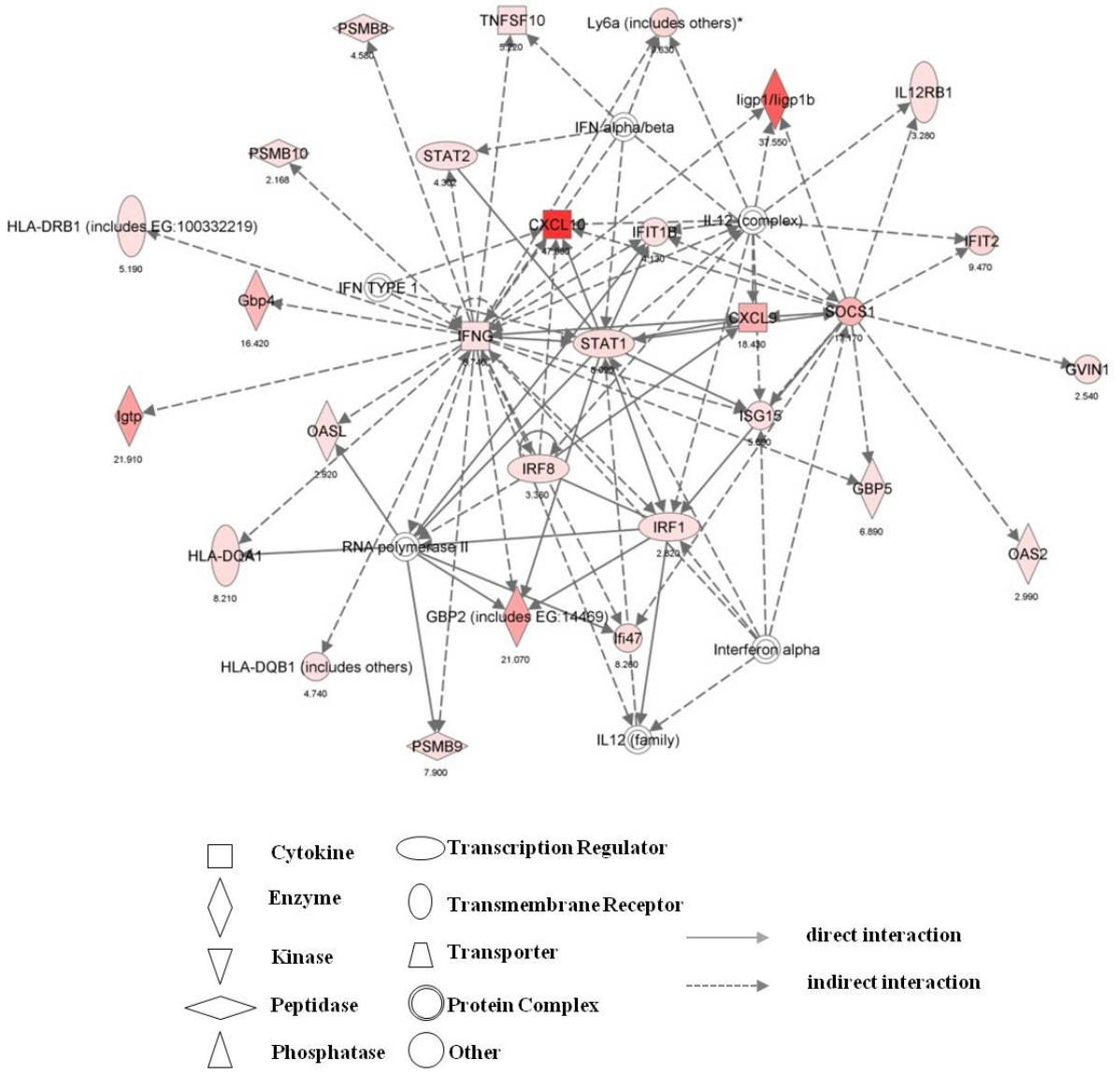

App. D: *Eimeria* infection of the mouse perturbs host IFN-γ-signaling. The IFN-γ-regulated protein network modulated in the parasitized mouse caecum epithelial cells at 24 h post-infection. Ingenuity Pathway Analysis was used to generate a network of IFN-γ-regulated mouse genes induced (red) or repressed (green; absent at 24 h) in the parasitized samples. The numbers indicate fold-changes in the expression levels.

Appendix E

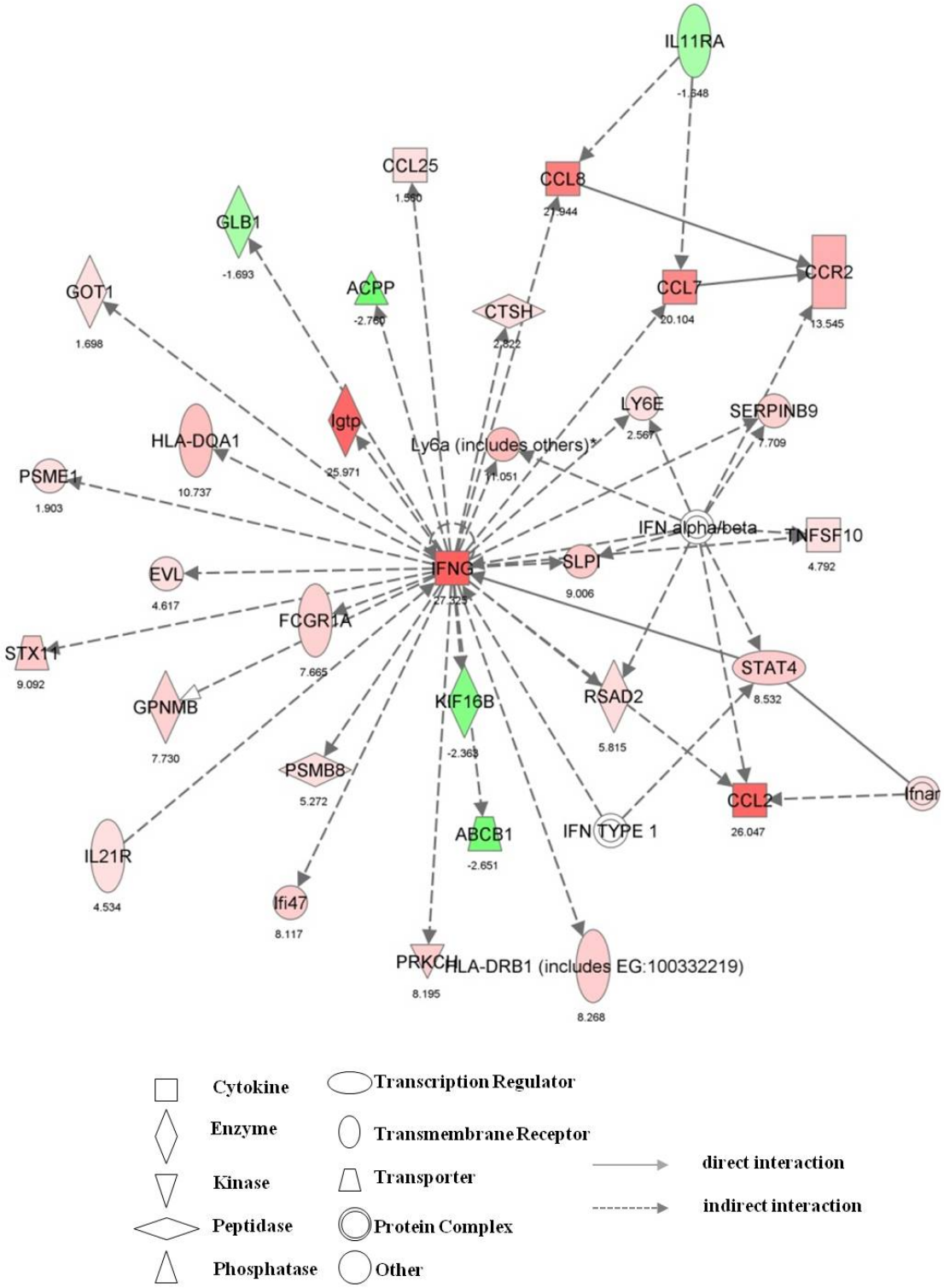

App. E: *Eimeria* modulates IFN-γ-signalling in the mouse. The IFN-γ-regulated network in the parasitized mouse caecum cells during late (144 h) infection. Ingenuity Pathway Analysis was used to generate IFN-γ-regulated network. The proteins induced or repressed upon infection are shown in red and green colours, respectively. The numbers below the shapes indicate fold-changes in the expression levels.

Appendix F

App. F: Transcripts showing a contrary expression profile during *E. falciformis* infection of YAMC cells and mouse.

		in vitro		*ex vivo*	
Symbol	**Gene**	**4 h**	**16 h**	**24 h**	**144 h**
DUSP6	Dual specificity phosphatase 6	-2.59	2.60		3.20
PPP2R5E	Protein phosphatase 2, regulatory subunit B (B56), epsilon isoform	-2.47			2.26
SLC16A6	Solute carrier family 16, member 6	-2.22			2.36
ZFHX1B	Zinc finger E-box binding homeobox 2	-2.16	1.94		13.4
DUSP10	Dual specificity phosphatase 10	-2.12	2.15		10.23
THPO	Thrombopoietin	-2.06		2.09	3.14
DUSP4	Dual specificity phosphatase 4	-2.01	3.39		6.73
GYK	Glycerol kinase	-2.00			2.31
QK	Quaking	-1.97			18.22
RCBTB1	Regulator of chromosome condensation (RCC1) and BTB (POZ) domain containing protein 1	-1.88			1.82
MTMR4	Myotubularin related protein 4	-1.84		2.09	
KLHL25	Kelch-like 25 (Drosophila)	-1.79			2.11
4831426I19RIK	RIKEN cDNA 4831426I19 gene	-1.67			4.04
RUNX2	Runt related transcription factor 2	-1.66			17.44
SNAG1	Sorting nexin 18	-1.66			3.55
BC025446	cDNA sequence BC025446	-1.64			2.19
MAGI2	Membrane associated guanylate kinase, WW and PDZ domain containing 2	-1.63			5.91
GPC1	Glypican 1	-1.61			3.9
TRPS1	Trichorhinophalangeal syndrome I	-1.61			6.22
GADD45G	Growth arrest and DNA-damage-inducible 45 gamma	-1.61	-2.07		3.36
RASSF2	Ras association (RalGDS/AF-6) domain family member 2	-1.60			10.63
CUGBP2	CUGBP, Elav-like family member 2	-1.52			6.82
SPON2	Spondin 2, extracellular matrix protein	1.66			-2.37
WHRN	Whirlin	1.70			-3.03
VLDLR	Very low density lipoprotein receptor	1.73			-3.66
4632404H12RIK	RIKEN cDNA 4632404H12 gene	1.91			-2.56
AW70209	AW702099	1.92			-1.88

9				
WWC2	WW, C2 and coiled-coil domain containing 2	1.92		-2.85
AV242843	AV242843	1.94		-2.26
DIDO1	Death inducer-obliterator 1	1.95		-1.96
GNE	Glucosamine (UDP-N-acetyl)-2-epimerase/N-acetylmannosamine kinase	2.05		-2.18
KRBA1	KRAB-A domain containing 1	2.12		-1.82
INADL	InaD-like (Drosophila)	2.17		-1.79
ZKSCAN 1	Zinc finger with KRAB and SCAN domains 1	2.2		-2.29
1600014C 10RIK	RIKEN cDNA 1600014C10 gene	2.32		-1.96
VWCE	Von Willebrand factor C and EGF domains	2.43		-3.21
SCML4	Sex comb on midleg-like 4 (Drosophila)	2.7		-1.88
CLPB	ClpB caseinolytic peptidase B homolog (E. coli)	3.15		-2.06
CDADC1	Cytidine and dCMP deaminase domain containing 1	4.14		-2.03
9930013L 23RIK	RIKEN cDNA 9930013L23 gene		-3.07	8.81
A430107P 09RIK	RIKEN cDNA A430107P09 gene		-2.37	9.25
MS4A4B	Membrane-spanning 4-domains, subfamily A, member 4B		-2.33	10.15
ADRB2	Adrenergic receptor, beta 2		-2.28	4.29
BMP4	Bone morphogenetic protein 4		-2.24	2.08
TACSTD2	Tumor-associated calcium signal transducer 2		-2.14	3.03
ST8SIA4	ST8 alpha-N-acetyl-neuraminide alpha-2,8-sialyltransferase 4		-2.10	7.93
PIF1	PIF1 5'-to-3' DNA helicase homolog (S. cerevisiae)		-2.03	8.94
PRMT3	Protein arginine N-methyltransferase 3		-2.03	1.96
ID2	Inhibitor of DNA binding 2		-1.91	3.91
LY6H	Lymphocyte antigen 6 complex, locus H		-1.91	7.01
TTYH1	Tweety homolog 1 (Drosophila)		-1.91	2.82
XLR4B	X-linked lymphocyte-regulated 4B		-1.83	2.84
B230218O 03	hypothetical protein B230218O03		-1.82	6.92
STAT1	Signal transducer and activator of transcription 1		-1.82	5.85 6.76
AY512922	Gm10165 predicted gene 10165		-1.79	4.76

GADD45 B	Growth arrest and DNA-damage-inducible 45 beta	-1.75		3.78
SATB1	Special AT-rich sequence binding protein 1	-1.74		11.44
CHST12	Carbohydrate sulfotransferase 12	-1.7		8.19
4930431B 09RIK	Family with sequence similarity 46, member C	-1.66		5.53
ZDHHC2	Zinc finger, DHHC domain containing 2	-1.66		4.96
NEU3	Neuraminidase 3	-1.63		8.42
EPB4.1L4 A	Erythrocyte protein band 4.1-like 4a	-1.59		1.97
TGFB1I1	Transforming growth factor beta 1 induced transcript 1	-1.63		4.08
CKS1B	CDC28 protein kinase 1b	-1.51		1.61
KCNQ1	Potassium voltage-gated channel, subfamily Q, member 1	1.57		-1.82
EEA1	Early endosome antigen 1	1.61		-2.01
DUSP16	Dual specificity phosphatase 16	1.62		-1.99
MATN2	Matrilin 2	1.63		-2.95
SLC17A5	Solute carrier family 17 (anion/sugar transporter), member 5	1.64		-1.99
LRFN3	Leucine rich repeat and fibronectin type III domain containing 3	1.72		-2.20
FOXA2	Forkhead box A2	1.83		-3.6
SETD7	SET domain containing (lysine methyltransferase) 7	1.83		-2.76
A630007B 06RIK	RIKEN cDNA A630007B06 gene	1.89		-1.93
SLC35A1	Solute carrier family 35 (CMP-sialic acid transporter), member 1	1.90	-1.80	
CYP2D22	Cytochrome P450, family 2, subfamily d, polypeptide 22	1.96		-2.88
FER1L3	Myoferlin	2.04	-1.84	3.95
PRKG2	Protein kinase, cGMP-dependent, type II	2.06	-1.90	-2.36
SOCS2	Suppressor of cytokine signaling 2	2.14		-2.25
2900041A 09RIK	Tubulin polymerization promoting protein	2.26		-2.92
TMPRSS2	Transmembrane protease, serine 2	2.27		-1.96
NAP1234 09-1	NAP123409-1	2.44		-2.19
SYPL	Synaptophysin-like protein	2.49		-1.89
LMCD1	LIM and cysteine-rich domains 1	2.52		-2.63
TRP53IN P1	Transformation related protein 53 inducible nuclear protein 1	2.59		-3.37
HMGA2	High mobility group AT-hook 2	3.15		-2.39
BRUNOL	CUGBP, Elav-like family member 6	3.20		-1.91

6			
METTL7A	Methyltransferase like 7A1	3.25	-2.52
SATB2	Special AT-rich sequence binding protein 2	3.96	-2.43
DLL4	Delta-like 4 (Drosophila)	4.05	-2.03
AUTS2	Autism susceptibility candidate 2	17.49	-2.88

Appendix G

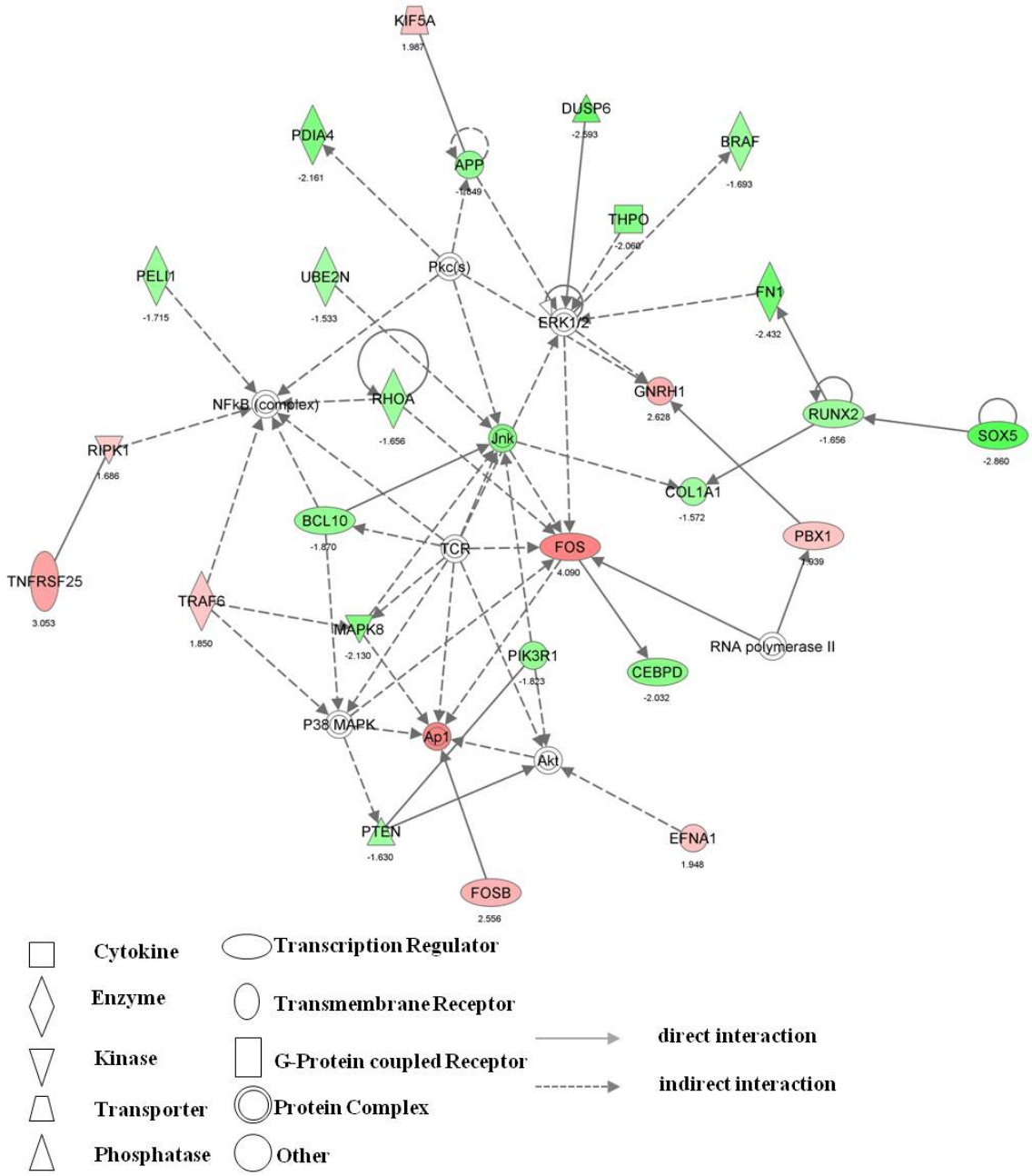

App. G: *Eimeria* infection of YAMC cells identifies FOS as a central molecule. The protein network modulated in the parasitized YAMC cells at 4 h post-infection. Ingenuity Pathway Analysis was used to generate a network of mouse genes induced (red) or repressed (green) in the parasitized samples. The numbers indicate fold-changes in the expression levels.

Appendix H

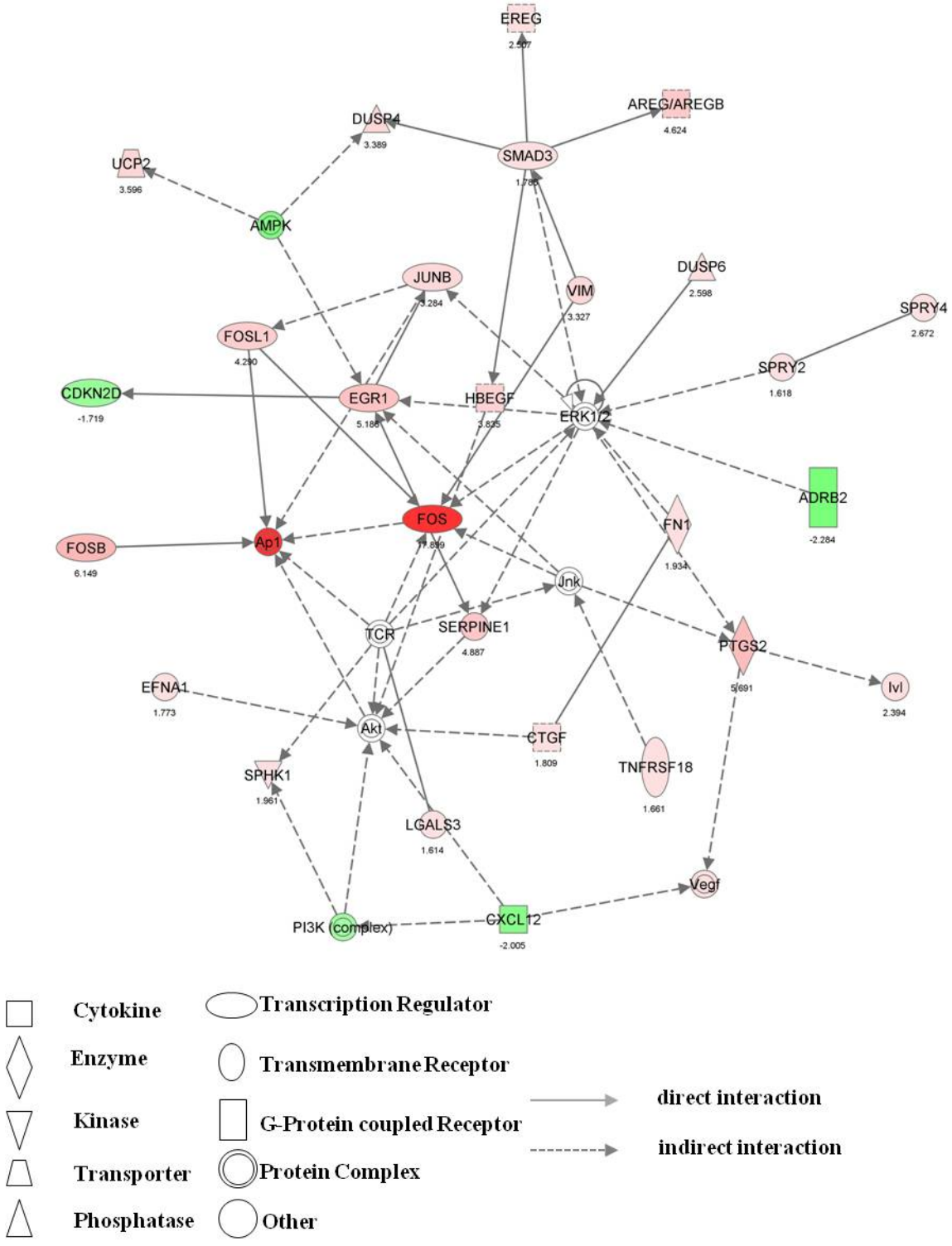

App. H: FOS expression is pivotal during late YAMC infection by *Eimeria*. The protein network modulated in the parasitized YAMC cells at 16 h post-infection. Ingenuity Pathway Analysis was used to generate a network of mouse genes induced (red) or repressed (green) in the parasitized samples. The numbers indicate fold-changes in the expression levels.

Appendix I

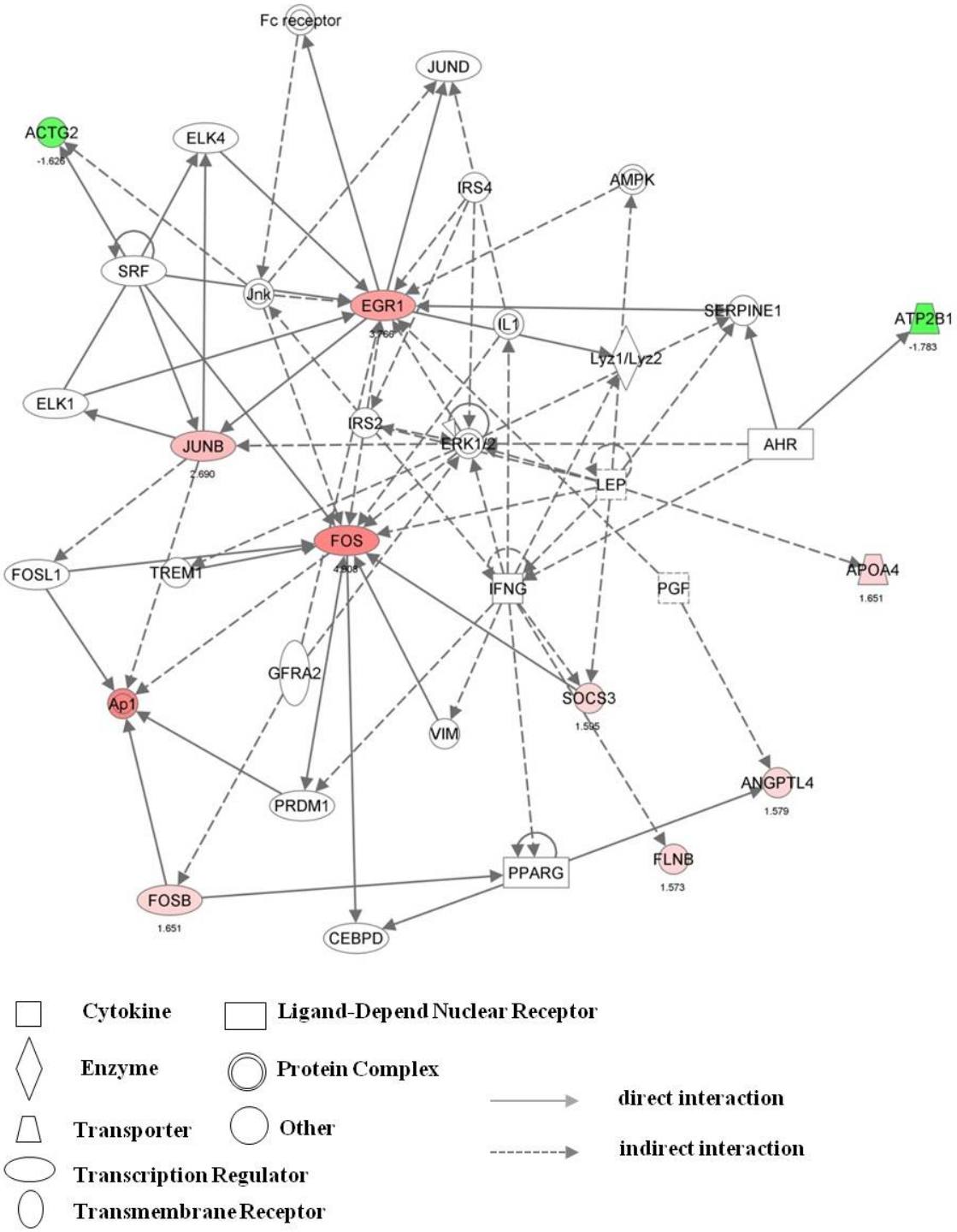

App. I: The FOS-regulated network early during *T. gondii* infection. The protein network modulated in the parasitized YAMC cells at 4 h post-infection. Ingenuity Pathway Analysis was used to generate a network of mouse genes induced (red) or repressed (green) in the parasitized samples. The numbers indicate fold-changes in the expression levels.

Appendix J

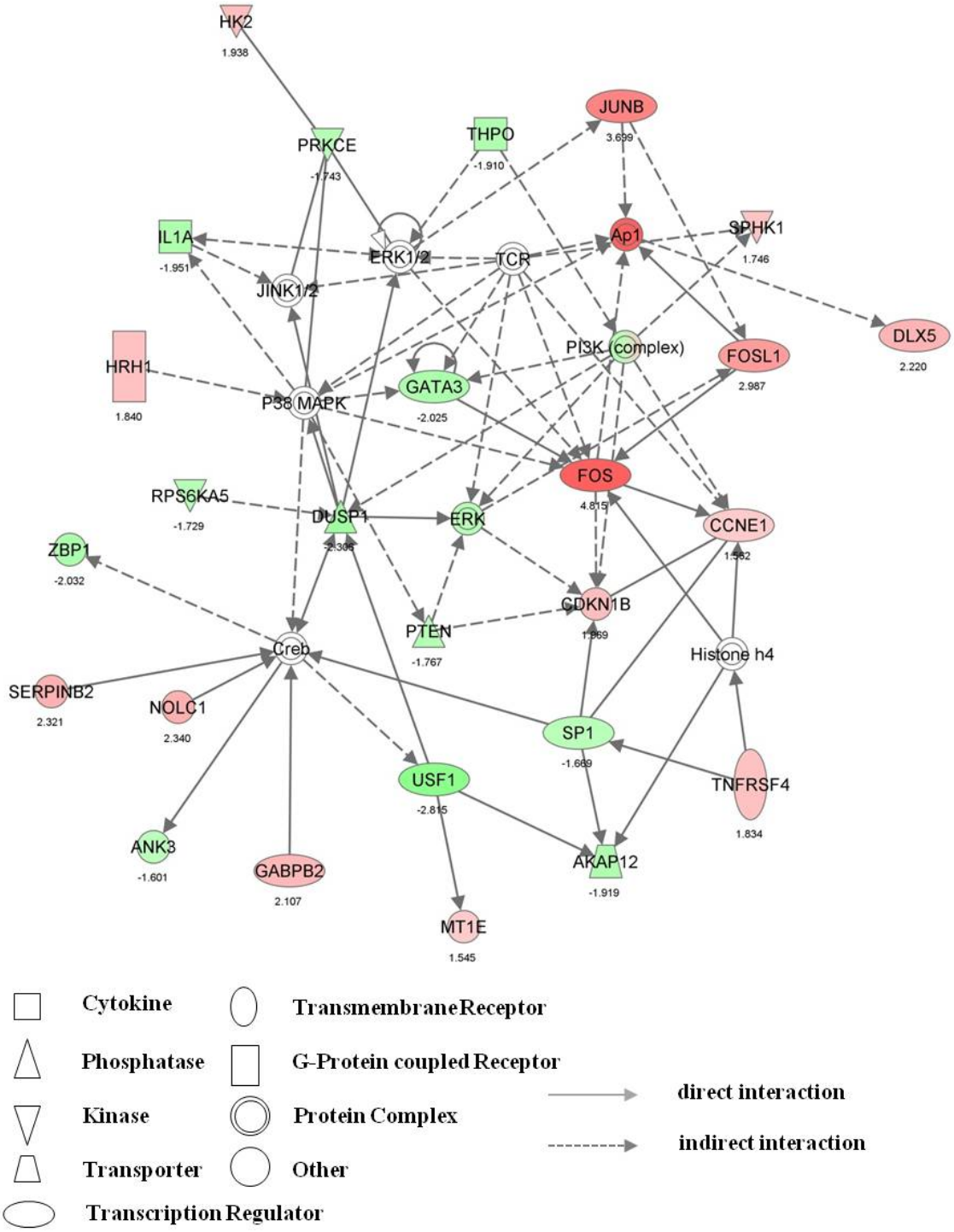

App. J: The FOS-regulated network is more pronounced during late *T. gondii* infection. The protein network modulated in the parasitized YAMC cells at 16 h post-infection. Ingenuity Pathway Analysis was used to generate a network of mouse genes induced (red) or repressed (green) in the parasitized samples. The numbers indicate fold-changes in the expression levels.

References

1. Levine ND (1987) The number of species of rodent coccidia and of other protozoa. *The Journal of protozoology* 34(4):362-363.

2. Ajioka JW, Fitzpatrick JM, & Reitter CP (2001) Toxoplasma gondii genomics: shedding light on pathogenesis and chemotherapy. *Expert reviews in molecular medicine* 2001:1-19.

3. Carruthers VB & Sibley LD (1997) Sequential protein secretion from three distinct organelles of Toxoplasma gondii accompanies invasion of human fibroblasts. *European journal of cell biology* 73(2):114-123.

4. Mordue DG, Desai N, Dustin M, & Sibley LD (1999) Invasion by Toxoplasma gondii establishes a moving junction that selectively excludes host cell plasma membrane proteins on the basis of their membrane anchoring. *The Journal of experimental medicine* 190(12):1783-1792.

5. Nichols BA & Chiappino ML (1987) Cytoskeleton of Toxoplasma gondii. *The Journal of protozoology* 34(2):217-226.

6. Morrissette NS & Sibley LD (2002) Cytoskeleton of apicomplexan parasites. *Microbiology and molecular biology reviews : MMBR* 66(1):21-38; table of contents.

7. Nichols BA & O'Connor GR (1981) Penetration of mouse peritoneal macrophages by the protozoon Toxoplasma gondii. New evidence for active invasion and phagocytosis. *Laboratory investigation; a journal of technical methods and pathology* 44(4):324-335.

8. Melo MB, Jensen KD, & Saeij JP (2011) Toxoplasma gondii effectors are master regulators of the inflammatory response. *Trends in parasitology* 27(11):487-495.

9. Zhu G, Marchewka MJ, & Keithly JS (2000) Cryptosporidium parvum appears to lack a plastid genome. *Microbiology* 146 (Pt 2):315-321.

10. Ralph SA*, et al.* (2004) Tropical infectious diseases: metabolic maps and functions of the Plasmodium falciparum apicoplast. *Nature reviews. Microbiology* 2(3):203-216.

11. Parsons M, Karnataki A, & Derocher AE (2009) Evolving insights into protein trafficking to the multiple compartments of the apicomplexan plastid. *The Journal of eukaryotic microbiology* 56(3):214-220.

12. Williams RB (1998) Epidemiological aspects of the use of live anticoccidial vaccines for chickens. *International journal for parasitology* 28(7):1089-1098.

13. Lillehoj HS & Lillehoj EP (2000) Avian coccidiosis. A review of acquired intestinal immunity and vaccination strategies. *Avian diseases* 44(2):408-425.

14. Ovington KS, Alleva LM, & Kerr EA (1995) Cytokines and immunological control of Eimeria spp. *International journal for parasitology* 25(11):1331-1351.

15. Danforth HD, Watkins K, Martin A, & Dekich M (1997) Evaluation of the efficacy of Eimeria maxima oocyst immunization with different strains of day-old broiler and roaster chickens. *Avian diseases* 41(4):792-801.

16. Shirley MW, Bushell AC, Bushell JE, McDonald V, & Roberts B (1995) A live attenuated vaccine for the control of avian coccidiosis: trials in broiler breeders and replacement layer flocks in the United Kingdom. *The Veterinary record* 137(18):453-457.

17. Jenkins MC, Augustine PC, Danforth HD, & Barta JR (1991) X-irradiation of Eimeria tenella oocysts provides direct evidence that sporozoite invasion and early schizont development induce a protective immune response(s). *Infection and immunity* 59(11):4042-4048.

18. Karim MJ, Basak SC, & Trees AJ (1996) Characterization and immunoprotective properties of a monoclonal antibody against the major oocyst wall protein of Eimeria tenella. *Infection and immunity* 64(4):1227-1232.

19. Shirley MW*, et al.* (2004) The Eimeria genome projects: a sequence of events. *Trends in parasitology* 20(5):199-201.

20. Hofmann J & Raether W (1990) Improved techniques for the in vitro cultivation of Eimeria tenella in primary chick kidney cells. *Parasitology research* 76(6):479-486.

21. Wichner K (2007) Entwicklung eines *in vitro*-Kultivierung-Systems für *Eimeria falciformis*, intestinaler Parasit der Maus (*Mus musculus*). *Diploma thesis, Humboldt University Berlin*.

22. Stange J (2011) Studies on host-pathoghen interactions at mucosal barrier surfaces using the murine intestinal parasite *Eimeria falciformis*. *Dissertation, Humboldt University Berlin*.

23. Kurth M & Entzeroth R (2009) Reporter gene expression in cell culture stages and oocysts of Eimeria nieschulzi (Coccidia, Apicomplexa). *Parasitology research* 104(2):303-310.

24. Kelley GL & Youssef NN (1977) Development in cell cultures of Eimeria vermiformis Ernst, Chobotar and Hammond, 1971. *Z Parasitenkd* 53(1):23-29.

25. Kelleher M & Tomley FM (1998) Transient expression of beta-galactosidase in differentiating sporozoites of Eimeria tenella. *Molecular and biochemical parasitology* 97(1-2):21-31.

26. Hao L, Liu X, Zhou X, Li J, & Suo X (2007) Transient transfection of Eimeria tenella using yellow or red fluorescent protein as a marker. *Molecular and biochemical parasitology* 153(2):213-215.

27. Shi TY*, et al.* (2008) Transfected Eimeria tenella could complete its endogenous development in vitro. *The Journal of parasitology* 94(4):978-980.

28. Clark JD*, et al.* (2008) A toolbox facilitating stable transfection of Eimeria species. *Molecular and biochemical parasitology* 162(1):77-86.

29. Yan W*, et al.* (2009) Stable transfection of Eimeria tenella: constitutive expression of the YFP-YFP molecule throughout the life cycle. *International journal for parasitology* 39(1):109-117.

30. Wiedmer S*, et al.* (2011) New insights into the excystation process and oocyst morphology of rodent Eimeria species. *Protist* 162(4):668-678.

31. Owen D (1975) Eimeria falciformis (Eimer, 1870) in specific pathogen free and gnotobiotic mice. *Parasitology.* 71(2):293-303.

32. Haberkorn A (1970) Die Entwicklung von Eimeria falciformis (Eimer 1870) in der weißen Maus (Mus musculus). *Z. Parasitenk.* 34(1):49-67.

33. Stiff MI & Vasilakos JP (1990) Effect of in vivo T-cell depletion on the effector T-cell function of immunity to Eimeria falciformis. *Infection and immunity* 58(6):1496-1499.

34. Mesfin GM, Bellamy JE, & Stockdale PH (1978) The pathological changes caused by Eimeria falciformis var pragensis in mice. *Canadian journal of comparative medicine. Revue canadienne de medecine comparee* 42(4):496-510.

35. Stockdale PG, Stockdale MJ, Rickard MD, & Mitchell GF (1985) Mouse strain variation and effects of oocyst dose in infection of mice with Eimeria falciformis, a coccidian parasite of the large intestine. *International journal for parasitology* 15(4):447-452.

36. Lucius R & Loos-Frank B (1997) *Parasitologie* (Spektrum Akademischer Verlag).

37. Elmore SA*, et al.* (2010) Toxoplasma gondii: epidemiology, feline clinical aspects, and prevention. *Trends in parasitology* 26(4):190-196.

38. Jones JL*, et al.* (2001) Toxoplasma gondii infection in the United States: seroprevalence and risk factors. *American journal of epidemiology* 154(4):357-365.

39. Tenter AM, Heckeroth AR, & Weiss LM (2000) Toxoplasma gondii: from animals to humans. *International journal for parasitology* 30(12-13):1217-1258.

40. Meissner M, Breinich MS, Gilson PR, & Crabb BS (2007) Molecular genetic tools in Toxoplasma and Plasmodium: achievements and future needs. *Current opinion in microbiology* 10(4):349-356.

41. Soldati D & Boothroyd JC (1993) Transient transfection and expression in the obligate intracellular parasite Toxoplasma gondii. *Science* 260(5106):349-352.

42. Donald RG & Roos DS (1993) Stable molecular transformation of Toxoplasma gondii: a selectable dihydrofolate reductase-thymidylate synthase marker based on drug-resistance mutations in malaria. *Proceedings of the National Academy of Sciences of the United States of America* 90(24):11703-11707.

43. Kim K & Weiss LM (2004) Toxoplasma gondii: the model apicomplexan. *International journal for parasitology* 34(3):423-432.

44. Black MW & Boothroyd JC (2000) Lytic cycle of Toxoplasma gondii. *Microbiology and molecular biology reviews : MMBR* 64(3):607-623.

45. Keiser J, Singer BH, & Utzinger J (2005) Reducing the burden of malaria in different eco-epidemiological settings with environmental management: a systematic review. *The Lancet infectious diseases* 5(11):695-708.

46. Vanderberg JP (1981) Plasmodium berghei exoerythrocytic forms develop only in the liver. *Trans R Soc Trop Med Hyg.* 75(6):904-905.

47. Jones MK & Good MF (2006) Malaria parasites up close. *Nature medicine* 12(2):170-171.

48. Sinden RE (1983) Sexual development of malarial parasites. *Advances in parasitology* 22:153-216.

49. Billker O*, et al.* (1998) Identification of xanthurenic acid as the putative inducer of malaria development in the mosquito. *Nature* 392(6673):289-292.

50. Limenitakis J & Soldati-Favre D (2011) Functional genetics in Apicomplexa: potentials and limits. *FEBS letters* 585(11):1579-1588.

51. van Dijk MR, Waters AP, & Janse CJ (1995) Stable transfection of malaria parasite blood stages. *Science.* 268(5215):1358-1362.

52. Janse CJ, Ramesar J, & Waters AP (2006) High-efficiency transfection and drug selection of genetically transformed blood stages of the rodent malaria parasite Plasmodium berghei. *Nature protocols* 1(1):346-356.

53. O'Donnell RA*, et al.* (2002) A genetic screen for improved plasmid segregation reveals a role for Rep20 in the interaction of Plasmodium falciparum chromosomes. *The EMBO journal* 21(5):1231-1239.

54. Aravind L, Iyer LM, Wellems TE, & Miller LH (2003) Plasmodium biology: genomic gleanings. *Cell* 115(7):771-785.

55. Carvalho TG & Menard R (2005) Manipulating the Plasmodium genome. *Current issues in molecular biology* 7(1):39-55.

56. Blader IJ, Manger ID, & Boothroyd JC (2001) Microarray analysis reveals previously unknown changes in Toxoplasma gondii-infected human cells. *The Journal of biological chemistry* 276(26):24223-24231.

57. Caamano J & Hunter CA (2002) NF-kappaB family of transcription factors: central regulators of innate and adaptive immune functions. *Clinical microbiology reviews* 15(3):414-429.

58. Tato CM & Hunter CA (2002) Host-pathogen interactions: subversion and utilization of the NF-kappa B pathway during infection. *Infection and immunity* 70(7):3311-3317.

59. Caamano J, Alexander J, Craig L, Bravo R, & Hunter CA (1999) The NF-kappa B family member RelB is required for innate and adaptive immunity to Toxoplasma gondii. *J Immunol* 163(8):4453-4461.

60. Caamano J*, et al.* (2000) Identification of a role for NF-kappa B2 in the regulation of apoptosis and in maintenance of T cell-mediated immunity to Toxoplasma gondii. *J Immunol* 165(10):5720-5728.

61. Molestina RE, Payne TM, Coppens I, & Sinai AP (2003) Activation of NF-kappaB by Toxoplasma gondii correlates with increased expression of antiapoptotic genes and localization of phosphorylated IkappaB to the parasitophorous vacuole membrane. *Journal of cell science* 116(Pt 21):4359-4371.

62. Chen XM*, et al.* (2001) Cryptosporidium parvum activates nuclear factor kappaB in biliary epithelia preventing epithelial cell apoptosis. *Gastroenterology* 120(7):1774-1783.

63. Richardson PG, Hideshima T, & Anderson KC (2003) Bortezomib (PS-341): a novel, first-in-class proteasome inhibitor for the treatment of multiple myeloma and other cancers. *Cancer control : journal of the Moffitt Cancer Center* 10(5):361-369.

64. Butcher BA, Kim L, Johnson PF, & Denkers EY (2001) Toxoplasma gondii tachyzoites inhibit proinflammatory cytokine induction in infected macrophages by preventing nuclear translocation of the transcription factor NF-kappa B. *J Immunol* 167(4):2193-2201.

65. Singh AP*, et al.* (2007) Plasmodium circumsporozoite protein promotes the development of the liver stages of the parasite. *Cell* 131(3):492-504.

66. Tripathi AK, Sullivan DJ, & Stins MF (2006) Plasmodium falciparum-infected erythrocytes increase intercellular adhesion molecule 1 expression on brain endothelium through NF-kappaB. *Infection and immunity* 74(6):3262-3270.

67. Shaulian E & Karin M (2001) AP-1 in cell proliferation and survival. *Oncogene* 20(19):2390-2400.

68. Gashler A & Sukhatme VP (1995) Early growth response protein 1 (Egr-1): prototype of a zinc-finger family of transcription factors. *Progress in nucleic acid research and molecular biology* 50:191-224.

69. Ryseck RP & Bravo R (1991) c-JUN, JUN B, and JUN D differ in their binding affinities to AP-1 and CRE consensus sequences: effect of FOS proteins. *Oncogene* 6(4):533-542.

70. Chiu R, Angel P, & Karin M (1989) Jun-B differs in its biological properties from, and is a negative regulator of, c-Jun. *Cell* 59(6):979-986.

71. Hirai S, Bourachot B, & Yaniv M (1990) Both Jun and Fos contribute to transcription activation by the heterodimer. *Oncogene* 5(1):39-46.

72. Phelps ED, Sweeney KR, & Blader IJ (2008) Toxoplasma gondii Rhoptry Discharge Correlates with Activation of the Early Growth Response 2 Host Cell Transcription Factor. *Infect Immun.* 76(10):4703-4712.

73. Ihle JN (2001) The Stat family in cytokine signaling. *Current opinion in cell biology* 13(2):211-217.

74. Gavrilescu LC, Butcher BA, Del Rio L, Taylor GA, & Denkers EY (2004) STAT1 is essential for antimicrobial effector function but dispensable for gamma interferon production during Toxoplasma gondii infection. *Infection and immunity* 72(3):1257-1264.

75. Lieberman LA, Banica M, Reiner SL, & Hunter CA (2004) STAT1 plays a critical role in the regulation of antimicrobial effector mechanisms, but not in the development of Th1-type responses during toxoplasmosis. *J Immunol* 172(1):457-463.

76. Ehigiator HN, McNair N, & Mead JR (2007) Cryptosporidium parvum: the contribution of Th1-inducing pathways to the resolution of infection in mice. *Experimental parasitology* 115(2):107-113.

77. Ong YC, Reese ML, & Boothroyd JC (2010) Toxoplasma rhoptry protein 16 (ROP16) subverts host function by direct tyrosine phosphorylation of STAT6. *The Journal of biological chemistry* 285(37):28731-28740.

78. Yamamoto M*, et al.* (2009) A single polymorphic amino acid on Toxoplasma gondii kinase ROP16 determines the direct and strain-specific activation of Stat3. *The Journal of experimental medicine* 206(12):2747-2760.

79. Akira S, Uematsu S, & Takeuchi O (2006) Pathogen recognition and innate immunity. *Cell* 124(4):783-801.

80. Takeuchi O & Akira S (2010) Pattern recognition receptors and inflammation. *Cell* 140(6):805-820.

81. Kawagoe T*, et al.* (2008) Sequential control of Toll-like receptor-dependent responses by IRAK1 and IRAK2. *Nature immunology* 9(6):684-691.

82. Xia ZP*, et al.* (2009) Direct activation of protein kinases by unanchored polyubiquitin chains. *Nature* 461(7260):114-119.

83. Deng L*, et al.* (2000) Activation of the IkappaB kinase complex by TRAF6 requires a dimeric ubiquitin-conjugating enzyme complex and a unique polyubiquitin chain. *Cell* 103(2):351-361.

84. Negishi H*, et al.* (2006) Evidence for licensing of IFN-gamma-induced IFN regulatory factor 1 transcription factor by MyD88 in Toll-like receptor-dependent gene induction program. *Proceedings of the National Academy of Sciences of the United States of America* 103(41):15136-15141.

85. Schmitz F, *et al.* (2007) Interferon-regulatory-factor 1 controls Toll-like receptor 9-mediated IFN-beta production in myeloid dendritic cells. *European journal of immunology* 37(2):315-327.

86. Elinav E, Strowig T, Henao-Mejia J, & Flavell RA (2011) Regulation of the antimicrobial response by NLR proteins. *Immunity* 34(5):665-679.

87. Kanneganti TD, Lamkanfi M, & Nunez G (2007) Intracellular NOD-like receptors in host defense and disease. *Immunity* 27(4):549-559.

88. Gross O, *et al.* (2006) Card9 controls a non-TLR signalling pathway for innate anti-fungal immunity. *Nature* 442(7103):651-656.

89. van de Veerdonk FL, Netea MG, Dinarello CA, & Joosten LA (2011) Inflammasome activation and IL-1beta and IL-18 processing during infection. *Trends in immunology* 32(3):110-116.

90. Kinnebrew MA & Pamer EG (2012) Innate immune signaling in defense against intestinal microbes. *Immunological reviews* 245(1):113-131.

91. Hunter CA & Sibley LD (2012) Modulation of innate immunity by Toxoplasma gondii virulence effectors. *Nature reviews. Microbiology* 10(11):766-778.

92. Hou B, Benson A, Kuzmich L, DeFranco AL, & Yarovinsky F (2011) Critical coordination of innate immune defense against Toxoplasma gondii by dendritic cells responding via their Toll-like receptors. *Proceedings of the National Academy of Sciences of the United States of America* 108(1):278-283.

93. Yarovinsky F, *et al.* (2005) TLR11 activation of dendritic cells by a protozoan profilin-like protein. *Science* 308(5728):1626-1629.

94. Koblansky AA, *et al.* (2013) Recognition of Profilin by Toll-like Receptor 12 Is Critical for Host Resistance to Toxoplasma gondii. *Immunity* 38(1):119-130.

95. Aliberti J, *et al.* (2003) Molecular mimicry of a CCR5 binding-domain in the microbial activation of dendritic cells. *Nature immunology* 4(5):485-490.

96. Mun HS, *et al.* (2003) TLR2 as an essential molecule for protective immunity against Toxoplasma gondii infection. *International immunology* 15(9):1081-1087.

97. Debierre-Grockiego F, *et al.* (2007) Activation of TLR2 and TLR4 by glycosylphosphatidylinositols derived from Toxoplasma gondii. *J Immunol* 179(2):1129-1137.

98. Debierre-Grockiego F, *et al.* (2003) Roles of glycosylphosphatidylinositols of Toxoplasma gondii. Induction of tumor necrosis factor-alpha production in macrophages. *The Journal of biological chemistry* 278(35):32987-32993.

99. Zhou R, Gong AY, Eischeid AN, & Chen XM (2012) miR-27b targets KSRP to coordinate TLR4-mediated epithelial defense against Cryptosporidium parvum infection. *PLoS pathogens* 8(5):e1002702.

100. Krishnegowda G*, et al.* (2005) Induction of proinflammatory responses in macrophages by the glycosylphosphatidylinositols of Plasmodium falciparum: cell signaling receptors, glycosylphosphatidylinositol (GPI) structural requirement, and regulation of GPI activity. *The Journal of biological chemistry* 280(9):8606-8616.

101. Coban C*, et al.* (2005) Toll-like receptor 9 mediates innate immune activation by the malaria pigment hemozoin. *The Journal of experimental medicine* 201(1):19-25.

102. Parroche P*, et al.* (2007) Malaria hemozoin is immunologically inert but radically enhances innate responses by presenting malaria DNA to Toll-like receptor 9. *Proceedings of the National Academy of Sciences of the United States of America* 104(6):1919-1924.

103. Gowda NM, Wu X, & Gowda DC (2011) The nucleosome (histone-DNA complex) is the TLR9-specific immunostimulatory component of Plasmodium falciparum that activates DCs. *PloS one* 6(6):e20398.

104. Shaw MH*, et al.* (2009) T cell-intrinsic role of Nod2 in promoting type 1 immunity to Toxoplasma gondii. *Nature immunology* 10(12):1267-1274.

105. Caetano BC*, et al.* (2011) Intrinsic expression of Nod2 in CD4+ T lymphocytes is not necessary for the development of cell-mediated immunity and host resistance to Toxoplasma gondii. *European journal of immunology* 41(12):3627-3631.

106. Finney CA, Lu Z, LeBourhis L, Philpott DJ, & Kain KC (2009) Disruption of Nod-like receptors alters inflammatory response to infection but does not confer protection in experimental cerebral malaria. *The American journal of tropical medicine and hygiene* 80(5):718-722.

107. Dalloul RA & Lillehoj HS (2006) Poultry coccidiosis: recent advancements in control measures and vaccine development. *Expert review of vaccines* 5(1):143-163.

108. Zhang L*, et al.* (2012) Eimeria tenella: expression profiling of toll-like receptors and associated cytokines in the cecum of infected day-old and three-week old SPF chickens. *Experimental parasitology* 130(4):442-448.

109. Fetterer RH, Miska KB, Jenkins MC, & Barfield RC (2004) A conserved 19-kDa Eimeria tenella antigen is a profilin-like protein. *The Journal of parasitology* 90(6):1321-1328.

110. Rosenberg B*, et al.* (2005) Protein from intestinal Eimeria protozoan stimulates IL-12 release from dendritic cells, exhibits antitumor properties in vivo and is correlated with low intestinal tumorigenicity. *International journal of cancer. Journal international du cancer* 114(5):756-765.

111. Gazzinelli RT, Hakim FT, Hieny S, Shearer GM, & Sher A (1991) Synergistic role of CD4+ and CD8+ T lymphocytes in IFN-gamma production and protective immunity induced by an attenuated Toxoplasma gondii vaccine. *J Immunol* 146(1):286-292.

112. Denkers EY & Gazzinelli RT (1998) Regulation and function of T-cell-mediated immunity during Toxoplasma gondii infection. *Clinical microbiology reviews* 11(4):569-588.

113. Gazzinelli RT*, et al.* (1994) Parasite-induced IL-12 stimulates early IFN-gamma synthesis and resistance during acute infection with Toxoplasma gondii. *J Immunol* 153(6):2533-2543.

114. Yap G, Pesin M, & Sher A (2000) Cutting edge: IL-12 is required for the maintenance of IFN-gamma production in T cells mediating chronic resistance to the intracellular pathogen, Toxoplasma gondii. *J Immunol* 165(2):628-631.

115. Hu X & Ivashkiv LB (2009) Cross-regulation of signaling pathways by interferon-gamma: implications for immune responses and autoimmune diseases. *Immunity* 31(4):539-550.

116. Khan IA, Schwartzman JD, Matsuura T, & Kasper LH (1997) A dichotomous role for nitric oxide during acute Toxoplasma gondii infection in mice. *Proceedings of the National Academy of Sciences of the United States of America* 94(25):13955-13960.

117. Candolfi E, Hunter CA, & Remington JS (1994) Mitogen- and antigen-specific proliferation of T cells in murine toxoplasmosis is inhibited by reactive nitrogen intermediates. *Infection and immunity* 62(5):1995-2001.

118. Pfefferkorn ER, Rebhun S, & Eckel M (1986) Characterization of an indoleamine 2,3-dioxygenase induced by gamma-interferon in cultured human fibroblasts. *Journal of interferon research* 6(3):267-279.

119. Martens S*, et al.* (2005) Disruption of Toxoplasma gondii parasitophorous vacuoles by the mouse p47-resistance GTPases.Disruption of Toxoplasma gondii parasitophorous vacuoles by the mouse p47-resistance GTPases. *PLoS Pathog.* 1(3):e24.

120. Lillehoj HS (1998) Role of T lymphocytes and cytokines in coccidiosis. *International journal for parasitology* 28(7):1071-1081.

121. Smith AL & Hayday AC (1998) Genetic analysis of the essential components of the immunoprotective response to infection with Eimeria vermiformis. *International journal for parasitology* 28(7):1061-1069.

122. Rose ME, Joysey HS, Hesketh P, Grencis RK, & Wakelin D (1988) Mediation of immunity to Eimeria vermiformis in mice by L3T4+ T cells. *Infection and immunity* 56(7):1760-1765.

123. Rose ME, Hesketh P, & Wakelin D (1992) Immune control of murine coccidiosis: CD4+ and CD8+ T lymphocytes contribute differentially in resistance to primary and secondary infections. *Parasitology.* 105:349-354.

124. Smith AL & Hayday AC (2000) Genetic dissection of primary and secondary responses to a widespread natural pathogen of the gut, Eimeria vermiformis. *Infection and immunity* 68(11):6273-6280.

125. Rose ME, Wakelin D, & Hesketh P (1991) Interferon-gamma-mediated effects upon immunity to coccidial infections in the mouse. *Parasite immunology* 13(1):63-74.

126. Stange J*, et al.* (2012) IL-22 mediates host defense against an intestinal intracellular parasite in the absence of IFN-gamma at the cost of Th17-driven immunopathology. *J Immunol* 188(5):2410-2418.

127. Pogonka T*, et al.* (2010) CD8+ cells protect mice against reinfection with the intestinal parasite Eimeria falciformis. *Microbes Infect.* 12(3):218-226.

128. Harp JA, Whitmire WM, & Sacco R (1994) In vitro proliferation and production of gamma interferon by murine CD4+ cells in response to Cryptosporidium parvum antigen. *The Journal of parasitology* 80(1):67-72.

129. Tilley M, McDonald V, & Bancroft GJ (1995) Resolution of cryptosporidial infection in mice correlates with parasite-specific lymphocyte proliferation associated with both Th1 and Th2 cytokine secretion. *Parasite immunology* 17(9):459-464.

130. Ungar BL, Kao TC, Burris JA, & Finkelman FD (1991) Cryptosporidium infection in an adult mouse model. Independent roles for IFN-gamma and CD4+ T lymphocytes in protective immunity. *J Immunol* 147(3):1014-1022.

131. McDonald V, Deer R, Uni S, Iseki M, & Bancroft GJ (1992) Immune responses to Cryptosporidium muris and Cryptosporidium parvum in adult immunocompetent or immunocompromised (nude and SCID) mice. *Infection and immunity* 60(8):3325-3331.

132. Good MF & Doolan DL (1999) Immune effector mechanisms in malaria. *Current opinion in immunology* 11(4):412-419.

133. Doolan DL*, et al.* (1996) Circumventing genetic restriction of protection against malaria with multigene DNA immunization: CD8+ cell-, interferon gamma-, and nitric oxide-dependent immunity. *The Journal of experimental medicine* 183(4):1739-1746.

134. Good MF, Xu H, Wykes M, & Engwerda CR (2005) Development and regulation of cell-mediated immune responses to the blood stages of malaria: implications for vaccine research. *Annual review of immunology* 23:69-99.

135. Richards JS & Beeson JG (2009) The future for blood-stage vaccines against malaria. *Immunology and cell biology* 87(5):377-390.

136. Grau GE*, et al.* (1989) Monoclonal antibody against interferon gamma can prevent experimental cerebral malaria and its associated overproduction of tumor necrosis factor. *Proceedings of the National Academy of Sciences of the United States of America* 86(14):5572-5574.

137. Gazzinelli RT*, et al.* (1996) Role of macrophage-derived cytokines in the induction and regulation of cell-mediated immunity to Toxoplasma gondii. *Current topics in microbiology and immunology* 219:127-139.

138. Roberts CW*, et al.* (1996) Different roles for interleukin-4 during the course of Toxoplasma gondii infection. *Infection and immunity* 64(3):897-904.

139. Bratton SB, MacFarlane M, Cain K, & Cohen GM (2000) Protein complexes activate distinct caspase cascades in death receptor and stress-induced apoptosis. *Experimental cell research* 256(1):27-33.

140. Luder CG, Gross U, & Lopes MF (2001) Intracellular protozoan parasites and apoptosis: diverse strategies to modulate parasite-host interactions. *Trends in parasitology* 17(10):480-486.

141. Ziegler U & Groscurth P (2004) Morphological features of cell death. *News in physiological sciences : an international journal of physiology produced jointly by the International Union of Physiological Sciences and the American Physiological Society* 19:124-128.

142. Vaux DL & Strasser A (1996) The molecular biology of apoptosis. *Proceedings of the National Academy of Sciences of the United States of America* 93(6):2239-2244.

143. Williams GT (1994) Programmed cell death: a fundamental protective response to pathogens. *Trends in microbiology* 2(12):463-464.

144. Lang C, Gross U, & Luder CG (2007) Subversion of innate and adaptive immune responses by Toxoplasma gondii. *Parasitology research* 100(2):191-203.

145. Gavrilescu LC & Denkers EY (2001) IFN-gamma overproduction and high level apoptosis are associated with high but not low virulence Toxoplasma gondii infection. *J Immunol* 167(2):902-909.

146. Liesenfeld O, Kosek JC, & Suzuki Y (1997) Gamma interferon induces Fas-dependent apoptosis of Peyer's patch T cells in mice following peroral infection with Toxoplasma gondii. *Infection and immunity* 65(11):4682-4689.

147. Gavrilescu LC & Denkers EY (2003) Interleukin-12 p40- and Fas ligand-dependent apoptotic pathways involving STAT-1 phosphorylation are triggered during infection with a virulent strain of Toxoplasma gondii. *Infection and immunity* 71(5):2577-2583.

148. Toure-Balde A*, et al.* (1996) Plasmodium falciparum induces apoptosis in human mononuclear cells. *Infection and immunity* 64(3):744-750.

149. Kern P, Dietrich M, Hemmer C, & Wellinghausen N (2000) Increased levels of soluble Fas ligand in serum in Plasmodium falciparum malaria. *Infection and immunity* 68(5):3061-3063.

150. Helmby H, Jonsson G, & Troye-Blomberg M (2000) Cellular changes and apoptosis in the spleens and peripheral blood of mice infected with blood-stage Plasmodium chabaudi chabaudi AS. *Infection and immunity* 68(3):1485-1490.

151. Chen XM, Gores GJ, Paya CV, & LaRusso NF (1999) Cryptosporidium parvum induces apoptosis in biliary epithelia by a Fas/Fas ligand-dependent mechanism. *The American journal of physiology* 277(3 Pt 1):G599-608.

152. Laliberte J & Carruthers VB (2008) Host cell manipulation by the human pathogen Toxoplasma gondii. *Cellular and molecular life sciences : CMLS* 65(12):1900-1915.

153. Vutova P*, et al.* (2007) Toxoplasma gondii inhibits Fas/CD95-triggered cell death by inducing aberrant processing and degradation of caspase 8. *Cellular microbiology* 9(6):1556-1570.

154. Lemasters JJ*, et al.* (1999) Mitochondrial dysfunction in the pathogenesis of necrotic and apoptotic cell death. *Journal of bioenergetics and biomembranes* 31(4):305-319.

155. Carmen JC, Hardi L, & Sinai AP (2006) Toxoplasma gondii inhibits ultraviolet light-induced apoptosis through multiple interactions with the mitochondrion-dependent programmed cell death pathway. *Cellular microbiology* 8(2):301-315.

156. Keller P*, et al.* (2006) Direct inhibition of cytochrome c-induced caspase activation in vitro by Toxoplasma gondii reveals novel mechanisms of interference with host cell apoptosis. *FEMS microbiology letters* 258(2):312-319.

157. McCole DF, Eckmann L, Laurent F, & Kagnoff MF (2000) Intestinal epithelial cell apoptosis following Cryptosporidium parvum infection. *Infection and immunity* 68(3):1710-1713.

158. Suss-Toby E, Zimmerberg J, & Ward GE (1996) Toxoplasma invasion: the parasitophorous vacuole is formed from host cell plasma membrane and pinches off via a fission pore. *Proceedings of the National Academy of Sciences of the United States of America* 93(16):8413-8418.

159. Schwab JC, Beckers CJ, & Joiner KA (1994) The parasitophorous vacuole membrane surrounding intracellular Toxoplasma gondii functions as a molecular sieve. *Proceedings of the National Academy of Sciences of the United States of America* 91(2):509-513.

160. Desai SA & Rosenberg RL (1997) Pore size of the malaria parasite's nutrient channel. *Proceedings of the National Academy of Sciences of the United States of America* 94(5):2045-2049.

161. Pfefferkorn ER, Eckel M, & Rebhun S (1986) Interferon-gamma suppresses the growth of Toxoplasma gondii in human fibroblasts through starvation for tryptophan. *Molecular and biochemical parasitology* 20(3):215-224.

162. Gupta N, Zahn MM, Coppens I, Joiner KA, & Voelker DR (2005) Selective disruption of phosphatidylcholine metabolism of the intracellular parasite Toxoplasma gondii arrests its growth. *The Journal of biological chemistry* 280(16):16345-16353.

163. Plattner F & Soldati-Favre D (2008) Hijacking of host cellular functions by the Apicomplexa. *Annual review of microbiology* 62:471-487.

164. Vaidya AB (2004) Malaria parasites deck the holes in erythrocytes. *Blood* 104(13):3844.

165. Desai SA, Bezrukov SM, & Zimmerberg J (2000) A voltage-dependent channel involved in nutrient uptake by red blood cells infected with the malaria parasite. *Nature* 406(6799):1001-1005.

166. Decherf G, Egee S, Staines HM, Ellory JC, & Thomas SL (2004) Anionic channels in malaria-infected human red blood cells. *Blood cells, molecules & diseases* 32(3):366-371.

167. Lauer SA, Rathod PK, Ghori N, & Haldar K (1997) A membrane network for nutrient import in red cells infected with the malaria parasite. *Science* 276(5315):1122-1125.

168. Spycher C*, et al.* (2006) Genesis of and trafficking to the Maurer's clefts of Plasmodium falciparum-infected erythrocytes. *Molecular and cellular biology* 26(11):4074-4085.

169. Haeggstrom M*, et al.* (2004) Common trafficking pathway for variant antigens destined for the surface of the Plasmodium falciparum-infected erythrocyte. *Molecular and biochemical parasitology* 133(1):1-14.

170. Halonen SK & Weidner E (1994) Overcoating of Toxoplasma parasitophorous vacuoles with host cell vimentin type intermediate filaments. *The Journal of eukaryotic microbiology* 41(1):65-71.

171. Coppens I*, et al.* (2006) Toxoplasma gondii sequesters lysosomes from mammalian hosts in the vacuolar space. *Cell* 125(2):261-274.

172. Elliott DA & Clark DP (2000) Cryptosporidium parvum induces host cell actin accumulation at the host-parasite interface. *Infection and immunity* 68(4):2315-2322.

173. Current WL & Reese NC (1986) A comparison of endogenous development of three isolates of Cryptosporidium in suckling mice. *The Journal of protozoology* 33(1):98-108.

174. Hermosilla C*, et al.* (2008) Cytoskeletal changes in Eimeria bovis-infected host endothelial cells during first merogony. *Veterinary research communications* 32(7):521-531.

175. Cooper GM (2000) *The Cell: A Molecular Approach. (2nd ed.)* (Sunderland (MA): Sinauer Associates).

176. Nigg EA (1995) Cyclin-dependent protein kinases: key regulators of the eukaryotic cell cycle. *BioEssays : news and reviews in molecular, cellular and developmental biology* 17(6):471-480.

177. Dobbelaere DA & Kuenzi P (2004) The strategies of the Theileria parasite: a new twist in host-pathogen interactions. *Current opinion in immunology* 16(4):524-530.

178. Brunet J*, et al.* (2008) Toxoplasma gondii exploits UHRF1 and induces host cell cycle arrest at G2 to enable its proliferation. *Cellular microbiology* 10(4):908-920.

179. Molestina RE, El-Guendy N, & Sinai AP (2008) Infection with Toxoplasma gondii results in dysregulation of the host cell cycle. *Cellular microbiology* 10(5):1153-1165.

180. Schwartzman JD & Pfefferkorn ER (1982) Toxoplasma gondii: purine synthesis and salvage in mutant host cells and parasites. *Experimental parasitology* 53(1):77-86.

181. Gero AM & O'Sullivan WJ (1990) Purines and pyrimidines in malarial parasites. *Blood cells* 16(2-3):467-484; discussion 485-498.

182. Pfefferkorn ER (1984) Interferon gamma blocks the growth of Toxoplasma gondii in human fibroblasts by inducing the host cells to degrade tryptophan. *Proceedings of the National Academy of Sciences of the United States of America* 81(3):908-912.

183. Fox BA, Gigley JP, & Bzik DJ (2004) Toxoplasma gondii lacks the enzymes required for de novo arginine biosynthesis and arginine starvation triggers cyst formation. *International journal for parasitology* 34(3):323-331.

184. Gail M, Gross U, & Bohne W (2001) Transcriptional profile of Toxoplasma gondii-infected human fibroblasts as revealed by gene-array hybridization. *Molecular genetics and genomics : MGG* 265(5):905-912.

185. Sinai AP & Joiner KA (1997) Safe haven: the cell biology of nonfusogenic pathogen vacuoles. *Annual review of microbiology* 51:415-462.

186. Nelson MM*, et al.* (2008) Modulation of the host cell proteome by the intracellular apicomplexan parasite Toxoplasma gondii. *Infection and immunity* 76(2):828-844.

187. Sexton AC*, et al.* (2004) Transcriptional profiling reveals suppressed erythropoiesis, up-regulated glycolysis, and interferon-associated responses in murine malaria. *The Journal of infectious diseases* 189(7):1245-1256.

188. Coppens I, Sinai AP, & Joiner KA (2000) Toxoplasma gondii exploits host low-density lipoprotein receptor-mediated endocytosis for cholesterol acquisition. *The Journal of cell biology* 149(1):167-180.

189. Whitehead RH, VanEeden PE, Noble MD, Ataliotis P, & Jat PS (1993) Establishment of conditionally immortalized epithelial cell lines from both colon and small intestine of adult H-2Kb-tsA58 transgenic mice. *Proc Natl Acad Sci U S A.* 90(2):587-591.

190. Lackinger D & Kaina B (2000) Primary mouse fibroblasts deficient for c-Fos, p53 or for both proteins are hypersensitive to UV light and alkylating agent-induced chromosomal breakage and apoptosis. *Mutation research* 457(1-2):113-123.

191. Plattner F*, et al.* (2008) Toxoplasma profilin is essential for host cell invasion and TLR11-dependent induction of an interleukin-12 response. *Cell host & microbe* 3(2):77-87.

192. Huang da W, Sherman BT, & Lempicki RA (2009) Systematic and integrative analysis of large gene lists using DAVID bioinformatics resources. *Nat Protoc.* 4(1):44-57.

193. Stockdale PG, Stockdale MJ, Rickard MD, & Mitchell GF (1985) Mouse strain variation and effects of oocyst dose in infection of mice with Eimeria falciformis, a coccidian parasite of the large intestine. *Int J Parasitol.* 15(4):447-452.

194. Schmatz DM, Crane MS, & Murray PK (1984) Purification of Eimeria sporozoites by DE-52 anion exchange chromatography. *J Protozool.* 31(1):181-183.

195. Pellicciari R*, et al.* (2006) Modulators of the kynurenine pathway of tryptophan metabolism: synthesis and preliminary biological evaluation of (S)-4-(ethylsulfonyl)benzoylalanine, a potent and selective kynurenine aminotransferase II (KAT II) inhibitor. *ChemMedChem.* 1(5):528-531.

196. Röver S, Cesura AM, Huguenin P, Kettler R, & Szente A (1997) Synthesis and biochemical evaluation of N-(4-phenylthiazol-2-yl)benzenesulfonamides as high-affinity inhibitors of kynurenine 3-hydroxylase. *J Med Chem.* 40(26):4378-4385.

197. Mesfin GM & Bellamy JE (1978) The life cycle of Eimeria falciformis var. pragensis (Sporozoa: Coccidia) in the mouse, Mus musculus. *J Parasitol.* 64(4):696-705.

198. Huang da W, Sherman BT, & Lempicki RA (2009) Bioinformatics enrichment tools: paths toward the comprehensive functional analysis of large gene lists. *Nucleic Acids Res.* 37(1):1-13.

199. Pffefferkorn ER (1984) Interferon gamma blocks the growth of Toxoplasma gondii in human fibroblasts by inducing the host cells to degrade tryptophan. *Proc Natl Acad Sci U S A.* 81(3):908-912.

200. Byrne GI, Lehmann LK, & Landry GJ (1986) Induction of tryptophan catabolism is the mechanism for gamma-interferon-mediated inhibition of intracellular Chlamydia psittaci replication in T24 cells. *Infect Immun.* 53(2):347-351.

201. Adams O*, et al.* (2004) Inhibition of human herpes simplex virus type 2 by interferon gamma and tumor necrosis factor alpha is mediated by indoleamine 2,3-dioxygenase. *Microbes Infect.* 6(9):806-812.

202. Munn DH*, et al.* (1998) Prevention of allogeneic fetal rejection by tryptophan catabolism. *Science.* 281(5380):1191-1193.

203. Munn DH*, et al.* (1999) Inhibition of T cell proliferation by macrophage tryptophan catabolism. *J Exp Med.* 189(9):1363-1372.

204. Takikawa O, Yoshida R, Kido R, & Hayaishi O (1986) Tryptophan degradation in mice initiated by indoleamine 2,3-dioxygenase. *J Biol Chem.* 261(8):3648-3653.

205. Mellor AL & Munn DH (1999) Tryptophan catabolism and T-cell tolerance: immunosuppression by starvation? *Immunol Today.* 20(10):469-473.

206. Mellor AL & Munn DH (2003) Tryptophan catabolism and regulation of adaptive immunity. *J Immunol.* 127(12):5809-5813.

207. Zmarowski A, *et al.* (2009) Astrocyte-derived kynurenic acid modulates basal and evoked cortical acetylcholine release. *Eur J Neurosci.* 29(3):529-538.

208. Miu J, Ball HJ, Mellor AL, & Hunt NH (2009) Effect of indoleamine dioxygenase-1 deficiency and kynurenine pathway inhibition on murine cerebral malaria. *Int J Parasitol.* 39(3):363-370.

209. Stone TW & Darlington LG (2002) Endogenous kynurenines as targets for drug discovery and development. *Nat Rev Drug Discov.* 1(8):609-620.

210. Lavazec C, *et al.* (2009) Analysis of mutant Plasmodium berghei parasites lacking expression of multiple PbCCp genes. *Molecular and biochemical parasitology* 163(1):1-7.

211. Behrendt JH, Clauss W, Zahner H, & Hermosilla C (2004) Alternative mechanism of Eimeria bovis sporozoites to invade cells in vitro by breaching the plasma membrane. *The Journal of parasitology* 90(5):1163-1165.

212. Taubert A, *et al.* (2010) Microarray-based transcriptional profiling of Eimeria bovis-infected bovine endothelial host cells. *Veterinary research* 41(5):70.

213. Okomo-Adhiambo M, Beattie C, & Rink A (2006) cDNA microarray analysis of host-pathogen interactions in a porcine in vitro model for Toxoplasma gondii infection. *Infection and immunity* 74(7):4254-4265.

214. Seong JY, *et al.* (2002) Exonic splicing enhancer-dependent splicing of the gonadotropin-releasing hormone premessenger ribonucleic acid is mediated by tra2alpha, a 40-kilodalton serine/arginine-rich protein. *Mol Endocrinol* 16(11):2426-2438.

215. Makino K, *et al.* (2008) Identification and characterization of the novel centrosomal protein centlein. *Biochemical and biophysical research communications* 366(4):958-962.

216. Peng YF, *et al.* (2000) Ankycorbin: a novel actin cytoskeleton-associated protein. *Genes to cells : devoted to molecular & cellular mechanisms* 5(12):1001-1008.

217. Stossel TP, *et al.* (2001) Filamins as integrators of cell mechanics and signalling. *Nature reviews. Molecular cell biology* 2(2):138-145.

218. Siggs OM, Li X, Xia Y, & Beutler B (2012) ZBTB1 is a determinant of lymphoid development. *The Journal of experimental medicine* 209(1):19-27.

219. Fiol DF, Mak SK, & Kultz D (2007) Specific TSC22 domain transcripts are hypertonically induced and alternatively spliced to protect mouse kidney cells during osmotic stress. *The FEBS journal* 274(1):109-124.

220. Pellegrinet L, *et al.* (2011) Dll1- and dll4-mediated notch signaling are required for homeostasis of intestinal stem cells. *Gastroenterology* 140(4):1230-1240 e1231-1237.

221. Akiyama J*, et al.* (2010) Delta-like 1 expression promotes goblet cell differentiation in Notch-inactivated human colonic epithelial cells. *Biochemical and biophysical research communications* 393(4):662-667.

222. Sheng YH*, et al.* (2011) The MUC13 cell-surface mucin protects against intestinal inflammation by inhibiting epithelial cell apoptosis. *Gut* 60(12):1661-1670.

223. Meshki J, Caino MC, von Burstin VA, Griner E, & Kazanietz MG (2010) Regulation of prostate cancer cell survival by protein kinase Cepsilon involves bad phosphorylation and modulation of the TNFalpha/JNK pathway. *The Journal of biological chemistry* 285(34):26033-26040.

224. Kaczmarek K*, et al.* (2011) Overexpression of peroxisomal testis-specific 1 protein induces germ cell apoptosis and leads to infertility in male mice. *Molecular biology of the cell* 22(10):1766-1779.

225. Tomasini R*, et al.* (2001) Molecular and functional characterization of the stress-induced protein (SIP) gene and its two transcripts generated by alternative splicing. SIP induced by stress and promotes cell death. *The Journal of biological chemistry* 276(47):44185-44192.

226. Yeh WC*, et al.* (2000) Requirement for Casper (c-FLIP) in regulation of death receptor-induced apoptosis and embryonic development. *Immunity* 12(6):633-642.

227. Boatright KM, Deis C, Denault JB, Sutherlin DP, & Salvesen GS (2004) Activation of caspases-8 and -10 by FLIP(L). *The Biochemical journal* 382(Pt 2):651-657.

228. Small GW*, et al.* (2004) Evidence that mitogen-activated protein kinase phosphatase-1 induction by proteasome inhibitors plays an antiapoptotic role. *Molecular pharmacology* 66(6):1478-1490.

229. Liu YX*, et al.* (2008) DUSP1 is controlled by p53 during the cellular response to oxidative stress. *Mol Cancer Res.* 6(4):624-633.

230. Liu X, Lu R, Xia Y, & Sun J (2010) Global analysis of the eukaryotic pathways and networks regulated by Salmonella typhimurium in mouse intestinal infection in vivo. *BMC genomics* 11:722.

231. Jenner RG & Young RA (2005) Insights into host responses against pathogens from transcriptional profiling. *Nature reviews. Microbiology* 3(4):281-294.

232. Korhonen R*, et al.* (2011) Attenuation of the acute inflammatory response by dual specificity phosphatase 1 by inhibition of p38 MAP kinase. *Molecular immunology* 48(15-16):2059-2068.

233. Zhang Y*, et al.* (2004) Regulation of innate and adaptive immune responses by MAP kinase phosphatase 5. *Nature.* 430(7001):793-797.

234. Bogdan C (2000) The function of type I interferons in antimicrobial immunity. *Current opinion in immunology* 12(4):419-424.

235. Fitzgerald KA (2011) The interferon inducible gene: Viperin. *Journal of interferon & cytokine research : the official journal of the International Society for Interferon and Cytokine Research* 31(1):131-135.

236. Dent AL, Shaffer AL, Yu X, Allman D, & Staudt LM (1997) Control of inflammation, cytokine expression, and germinal center formation by BCL-6. *Science* 276(5312):589-592.

237. Willecke K*, et al.* (2002) Structural and functional diversity of connexin genes in the mouse and human genome. *Biological chemistry* 383(5):725-737.

238. Hernandez MC*, et al.* (1997) ENC-1: a novel mammalian kelch-related gene specifically expressed in the nervous system encodes an actin-binding protein. *The Journal of neuroscience : the official journal of the Society for Neuroscience* 17(9):3038-3051.

239. Kosaki R, Watanabe K, & Yamaguchi Y (1999) Overproduction of hyaluronan by expression of the hyaluronan synthase Has2 enhances anchorage-independent growth and tumorigenicity. *Cancer research* 59(5):1141-1145.

240. Durand M*, et al.* (2007) The OXR domain defines a conserved family of eukaryotic oxidation resistance proteins. *BMC cell biology* 8:13.

241. Chen B, Zhang D, & Pollard JW (2003) Progesterone regulation of the mammalian ortholog of methylcitrate dehydratase (immune response gene 1) in the uterine epithelium during implantation through the protein kinase C pathway. *Mol Endocrinol* 17(11):2340-2354.

242. Peixoto L*, et al.* (2010) Integrative genomic approaches highlight a family of parasite-specific kinases that regulate host responses. *Cell host & microbe* 8(2):208-218.

243. Bradley PJ & Sibley LD (2007) Rhoptries: an arsenal of secreted virulence factors. *Current opinion in microbiology* 10(6):582-587.

244. Boothroyd JC & Dubremetz JF (2008) Kiss and spit: the dual roles of Toxoplasma rhoptries. *Nature reviews. Microbiology* 6(1):79-88.

245. Johnston WT, Shirley MW, Smith AL, & Gravenor MB (2001) Modelling host cell availability and the crowding effect in Eimeria infections. *International journal for parasitology* 31(10):1070-1081.

246. Belli SI*, et al.* (2002) Biochemical characterisation of the 56 and 82 kDa immunodominant gametocyte antigens from Eimeria maxima. *International journal for parasitology* 32(7):805-816.

247. Belli SI*, et al.* (2009) Conservation of proteins involved in oocyst wall formation in Eimeria maxima, Eimeria tenella and Eimeria acervulina. *Int J Parasitol.* 39(10):1063-1070.

248. Min W, *et al.* (2003) Profiling local gene expression changes associated with Eimeria maxima and Eimeria acervulina using cDNA microarray. *Applied microbiology and biotechnology* 62(4):392-399.

249. Kim DK, *et al.* (2011) Comparative microarray analysis of intestinal lymphocytes following Eimeria acervulina, E. maxima, or E. tenella infection in the chicken. *PloS one* 6(11):e27712.

250. Degrandi D, *et al.* (2007) Extensive characterization of IFN-induced GTPases mGBP1 to mGBP10 involved in host defense. *J Immunol* 179(11):7729-7740.

251. Steinfeldt T, *et al.* (2010) Phosphorylation of mouse immunity-related GTPase (IRG) resistance proteins is an evasion strategy for virulent Toxoplasma gondii. *PLoS Biol.* 8(12):e1000576.

252. Schmid M, Lehmann MJ, Lucius R, & Gupta N (2012) Apicomplexan parasite, Eimeria falciformis, co-opts host tryptophan catabolism for life cycle progression in mouse. *The Journal of biological chemistry* 287(24):20197-20207.

253. Qiao D, Yang X, Meyer K, & Friedl A (2008) Glypican-1 regulates anaphase promoting complex/cyclosome substrates and cell cycle progression in endothelial cells. *Molecular biology of the cell* 19(7):2789-2801.

254. Hu Y, *et al.* (2007) MAGI-2 Inhibits cell migration and proliferation via PTEN in human hepatocarcinoma cells. *Archives of biochemistry and biophysics* 467(1):1-9.

255. Imai T, *et al.* (2008) Epigenetic inactivation of RASSF2 in oral squamous cell carcinoma. *Cancer science* 99(5):958-966.

256. Nakayama K, Hara T, Hibi M, Hirano T, & Miyajima A (1999) A novel oncostatin M-inducible gene OIG37 forms a gene family with MyD118 and GADD45 and negatively regulates cell growth. *The Journal of biological chemistry* 274(35):24766-24772.

257. Garcia-Domingo D, *et al.* (1999) DIO-1 is a gene involved in onset of apoptosis in vitro, whose misexpression disrupts limb development. *Proceedings of the National Academy of Sciences of the United States of America* 96(14):7992-7997.

258. Weidemann W, *et al.* (2010) Lessons from GNE-deficient embryonic stem cells: sialic acid biosynthesis is involved in proliferation and gene expression. *Glycobiology* 20(1):107-117.

259. Xu H, *et al.* (2010) MS4a4B, a CD20 homologue in T cells, inhibits T cell propagation by modulation of cell cycle. *PLoS One.* 5(11):e13780.

260. Cubas R, Zhang S, Li M, Chen C, & Yao Q (2010) Trop2 expression contributes to tumor pathogenesis by activating the ERK MAPK pathway. *Molecular cancer* 9:253.

261. Lan Y, *et al.* (2008) Aberrant expression of Cks1 and Cks2 contributes to prostate tumorigenesis by promoting proliferation and inhibiting programmed cell death. *International journal of cancer. Journal international du cancer* 123(3):543-551.

262. Tian XY, *et al.* (2012) Bone morphogenic protein-4 induces endothelial cell apoptosis through oxidative stress-dependent p38MAPK and JNK pathway. *Journal of molecular and cellular cardiology* 52(1):237-244.

263. Wada T, *et al.* (2007) A crucial role of plasma membrane-associated sialidase in the survival of human cancer cells. *Oncogene* 26(17):2483-2490.

264. Mori S, Nishikawa SI, & Yokota Y (2000) Lactation defect in mice lacking the helix-loop-helix inhibitor Id2. *The EMBO journal* 19(21):5772-5781.

265. Vairapandi M, Balliet AG, Hoffman B, & Liebermann DA (2002) GADD45b and GADD45g are cdc2/cyclinB1 kinase inhibitors with a role in S and G2/M cell cycle checkpoints induced by genotoxic stress. *Journal of cellular physiology* 192(3):327-338.

266. Cho HJ, *et al.* (2010) Gadd45b mediates Fas-induced apoptosis by enhancing the interaction between p38 and retinoblastoma tumor suppressor. *The Journal of biological chemistry* 285(33):25500-25505.

267. Bernatchez PN, *et al.* (2007) Myoferlin regulates vascular endothelial growth factor receptor-2 stability and function. *The Journal of biological chemistry* 282(42):30745-30753.

268. Billiard F, *et al.* (2011) Ongoing Dll4-Notch signaling is required for T-cell homeostasis in the adult thymus. *European journal of immunology* 41(8):2207-2216.

269. Harris JE, Green JA, Elkington PT, & Friedland JS (2007) Monocytes infected with Mycobacterium tuberculosis regulate MAP kinase-dependent astrocyte MMP-9 secretion. *Journal of leukocyte biology* 81(2):548-556.

270. Green JA, *et al.* (2010) Mycobacterium tuberculosis upregulates microglial matrix metalloproteinase-1 and -3 expression and secretion via NF-kappaB- and Activator Protein-1-dependent monocyte networks. *J Immunol* 184(11):6492-6503.

271. Samten B, *et al.* (2008) CREB, ATF, and AP-1 transcription factors regulate IFN-gamma secretion by human T cells in response to mycobacterial antigen. *J Immunol* 181(3):2056-2064.

272. Passegué E & Wagner EF (2000) JunB suppresses cell proliferation by transcriptional activation of p16(INK4a) expression. *EMBO J.* 19(12):2969-2979.

273. Bakiri L, Lallemand D, Bossy-Wetzel E, & Yaniv M (2000) Cell cycle-dependent variations in c-Jun and JunB phosphorylation: a role in the control of cyclin D1 expression. *EMBO J.* 19(9):2056-2068.

274. Andrecht S, Kolbus A, Hartenstein B, Angel P, & Schorpp-Kistner M (2002) Cell cycle promoting activity of JunB through cyclin A activation. *J Biol Chem.* 27(39):35961-35968.

275. Passegue E & Wagner EF (2000) JunB suppresses cell proliferation by transcriptional activation of p16(INK4a) expression. *The EMBO journal* 19(12):2969-2979.

276. Ding SZ*, et al.* (2008) Helicobacter pylori and mitogen-activated protein kinases mediate activator protein-1 (AP-1) subcomponent protein expression and DNA-binding activity in gastric epithelial cells. *FEMS immunology and medical microbiology* 53(3):385-394.

277. Malnou CE*, et al.* (2007) Heterodimerization with Jun family members regulates c-Fos nucleocytoplasmic traffic. *J Biol Chem.* 282(42):31046-31059.

278. Yoo YG & Lee MO (2004) Hepatitis B virus X protein induces expression of Fas ligand gene through enhancing transcriptional activity of early growth response factor. *J Biol Chem.* 279(35):36242-36249.

279. Shin EC, J.S. S, Park JH, Kim H, & Kim SJ (1999) Expression of Fas ligand in human hepatoma cell lines: Role of hepatitis-B virus X (HBX) in induction of Fas ligand. *Int J Cancer.* 82(4):587-591.

280. Liu D, Evans I, Britton G, & Zachary I (2008) The zinc-finger transcription factor, early growth response 3, mediates VEGF-induced angiogenesis. *Oncogene.* 27(21):2989-2998.

281. Stutz A, Kessler H, Kaschel ME, Meissner M, & Dalpke AH (2012) Cell invasion and strain dependent induction of suppressor of cytokine signaling-1 by Toxoplasma gondii. *Immunobiology.* 217(1):28-36.

282. Tourtellotte WG, Nagarajan R, Auyeung A, Mueller C, & Milbrandt J (1999) Infertility associated with incomplete spermatogenic arrest and oligozoospermia in Egr4-deficient mice. *Development.* 126(22):5061-5071.

283. Wieland GD*, et al.* (2005) Early growth response proteins EGR-4 and EGR-3 interact with immune inflammatory mediators NF-kappaB p50 and p65. *J Cell Sci.* 118(Pt 14):3203-3212.

284. Platanias LC (2005) Mechanisms of type-I- and type-II-interferon-mediated signalling. *Nature reviews. Immunology* 5(5):375-386.

285. Saeij JP*, et al.* (2007) Toxoplasma co-opts host gene expression by injection of a polymorphic kinase homologue. *Nature* 445(7125):324-327.

286. Stark GR, Kerr IM, Williams BR, Silverman RH, & Schreiber RD (1998) How cells respond to interferons. *Annual review of biochemistry* 67:227-264.

287. Johnson DR & Pober JS (1994) HLA class I heavy-chain gene promoter elements mediating synergy between tumor necrosis factor and interferons. *Molecular and cellular biology* 14(2):1322-1332.

288. Kaplan MH, Sun YL, Hoey T, & Grusby MJ (1996) Impaired IL-12 responses and enhanced development of Th2 cells in Stat4-deficient mice. *Nature* 382(6587):174-177.

289. Takeda K*, et al.* (1996) Essential role of Stat6 in IL-4 signalling. *Nature* 380(6575):627-630.

290. Shimoda K*, et al.* (1996) Lack of IL-4-induced Th2 response and IgE class switching in mice with disrupted Stat6 gene. *Nature* 380(6575):630-633.

291. Schneider A*, et al.* (2004) Restriction-mediated differential display (RMDD) identifies pip92 as a pro-apoptotic gene product induced during focal cerebral ischemia. *J Cereb Blood Flow Metab.* 24(2):224-236.

292. Brès V, Yoh SM, & Jones KA (2008) The multi-tasking P-TEFb complex. *Curr Opin Cell Biol.* 20(3):334-340.

293. Michels AA*, et al.* (2004) Binding of the 7SK snRNA turns the HEXIM1 protein into a P-TEFb (CDK9/cyclin T) inhibitor. *EMBO J.* 23(13):2608-2619.

294. Martinez-Morales PL, Quiroga AC, Barbas JA, & Morales AV (2010) SOX5 controls cell cycle progression in neural progenitors by interfering with the WNT–β-catenin pathway. *EMBO Rep.* 11(6):466-472.

295. Thein DC*, et al.* (2010) The closely related transcription factors Sox4 and Sox11 function as survival factors during spinal cord development. *J Neurochem.* 115(1):131-141.

296. Conrotto P, Andréasson U, Kuci V, Borrebaeck CA, & Ek S (2011) Knock-down of SOX11 induces autotaxin-dependent increase in proliferation in vitro and more aggressive tumors in vivo. *Mol Oncol.* 5(6):527-537.

297. Hsieh MJ, Yao YL, Lai IL, & Yang WM (2006) Transcriptional repression activity of PAX3 is modulated by competition between corepressor KAP1 and heterochromatin protein 1. *Biochem Biophys Res Commun.* 349(2):573-581.

298. Akimova T, Beier UH, Wang L, Levine MH, & Hancock WW (2011) Helios expression is a marker of T cell activation and proliferation. *PLoS One.* 6(8):e24226.

299. Narni-Mancinelli E*, et al.* (2012) Tuning of natural killer cell reactivity by NKp46 and Helios calibrates T cell responses. *Science.* 335(6066):344-348.

300. Thimmulappa RK*, et al.* (2006) Nrf2 is a critical regulator of the innate immune response and survival during experimental sepsis. *The Journal of clinical investigation* 116(4):984-995.

301. Khor TO*, et al.* (2006) Nrf2-deficient mice have an increased susceptibility to dextran sulfate sodium-induced colitis. *Cancer research* 66(24):11580-11584.

302. Hayashi F*, et al.* (2001) The innate immune response to bacterial flagellin is mediated by Toll-like receptor 5. *Nature* 410(6832):1099-1103.

303. Hoshino K*, et al.* (1999) Cutting edge: Toll-like receptor 4 (TLR4)-deficient mice are hyporesponsive to lipopolysaccharide: evidence for TLR4 as the Lps gene product. *J Immunol* 162(7):3749-3752.

304. Oliveira AC, *et al.* (2004) Expression of functional TLR4 confers proinflammatory responsiveness to Trypanosoma cruzi glycoinositolphospholipids and higher resistance to infection with T. cruzi. *J Immunol* 173(9):5688-5696.

305. Alexopoulou L, Holt AC, Medzhitov R, & Flavell RA (2001) Recognition of double-stranded RNA and activation of NF-kappaB by Toll-like receptor 3. *Nature* 413(6857):732-738.

306. Diebold SS, Kaisho T, Hemmi H, Akira S, & Reis e Sousa C (2004) Innate antiviral responses by means of TLR7-mediated recognition of single-stranded RNA. *Science* 303(5663):1529-1531.

307. Melo MB, *et al.* (2010) UNC93B1 mediates host resistance to infection with Toxoplasma gondii. *PLoS pathogens* 6(8):e1001071.

308. Saijo S, *et al.* (2007) Dectin-1 is required for host defense against Pneumocystis carinii but not against Candida albicans. *Nature immunology* 8(1):39-46.

309. Rothfuchs AG, *et al.* (2007) Dectin-1 interaction with Mycobacterium tuberculosis leads to enhanced IL-12p40 production by splenic dendritic cells. *J Immunol* 179(6):3463-3471.

310. Aoki N, *et al.* (2009) Expression and functional role of MDL-1 (CLEC5A) in mouse myeloid lineage cells. *Journal of leukocyte biology* 85(3):508-517.

311. Behler F, *et al.* (2012) Role of Mincle in alveolar macrophage-dependent innate immunity against mycobacterial infections in mice. *J Immunol* 189(6):3121-3129.

312. Saijo S, *et al.* (2010) Dectin-2 recognition of alpha-mannans and induction of Th17 cell differentiation is essential for host defense against Candida albicans. *Immunity* 32(5):681-691.

313. Fujikado N, *et al.* (2008) Dcir deficiency causes development of autoimmune diseases in mice due to excess expansion of dendritic cells. *Nature medicine* 14(2):176-180.

314. Bottazzi B, Doni A, Garlanda C, & Mantovani A (2010) An integrated view of humoral innate immunity: pentraxins as a paradigm. *Annu Rev Immunol.* 28:157-183.

315. Garlanda C, *et al.* (2002) Non-redundant role of the long pentraxin PTX3 in anti-fungal innate immune response. *Nature.* 420(6912):182-186.

316. Dias AA, *et al.* (2001) TSG-14 transgenic mice have improved survival to endotoxemia and to CLP-induced sepsis. *J Leukoc Biol.* 69(6):928-936.

317. Lang R, Hammer M, & Mages J (2006) DUSP meet immunology: dual specificity MAPK phosphatases in control of the inflammatory response. *J Immunol* 177(11):7497-7504.

318. Chi H, *et al.* (2006) Dynamic regulation of pro- and anti-inflammatory cytokines by MAPK phosphatase 1 (MKP-1) in innate immune responses. *Proceedings of the National Academy of Sciences of the United States of America* 103(7):2274-2279.

319. Al-Mutairi MS*, et al.* (2010) MAP kinase phosphatase-2 plays a critical role in response to infection by Leishmania mexicana. *PLoS pathogens* 6(11):e1001192.

320. Zhang Y*, et al.* (2004) Regulation of innate and adaptive immune responses by MAP kinase phosphatase 5. *Nature* 430(7001):793-797.

321. Srivastava N, Sudan R, & Saha B (2011) CD40-modulated dual-specificity phosphatases MAPK phosphatase (MKP)-1 and MKP-3 reciprocally regulate Leishmania major infection. *J Immunol* 186(10):5863-5872.

322. Grumont RJ, Rasko JE, Strasser A, & Gerondakis S (1996) Activation of the mitogen-activated protein kinase pathway induces transcription of the PAC-1 phosphatase gene. *Mol Cell Biol.* 16(6):2913-2921.

323. Rohan PJ*, et al.* (1993) PAC-1: a mitogen-induced nuclear protein tyrosine phosphatase. *Science.* 259(5102):1763-1766.

324. Jeffrey KL*, et al.* (2006) Positive regulation of immune cell function and inflammatory responses by phosphatase PAC-1. *Nat Immunol.* 7(3):274-283.

325. Yin Y, Liu YX, Jin YJ, Hall EJ, & Barrett JC (2003) PAC1 phosphatase is a transcription target of p53 in signalling apoptosis and growth suppression. *Nature.* 422(6931):527-531.

326. Loetscher M*, et al.* (1996) Chemokine receptor specific for IP10 and mig: structure, function, and expression in activated T-lymphocytes. *The Journal of experimental medicine* 184(3):963-969.

327. Qin S*, et al.* (1998) The chemokine receptors CXCR3 and CCR5 mark subsets of T cells associated with certain inflammatory reactions. *The Journal of clinical investigation* 101(4):746-754.

328. Khan IA*, et al.* (2000) IP-10 is critical for effector T cell trafficking and host survival in Toxoplasma gondii infection. *Immunity* 12(5):483-494.

329. Hardison JL, Wrightsman RA, Carpenter PM, Lane TE, & Manning JE (2006) The chemokines CXCL9 and CXCL10 promote a protective immune response but do not contribute to cardiac inflammation following infection with Trypanosoma cruzi. *Infection and immunity* 74(1):125-134.

330. Heyn I (2011) Influence of IFN-γ regulated host factors on the development of Eimeria falciformis in the mouse. *Bachelor Thesis, Humboldt University Berlin*.

331. Huang S, Paulauskis JD, Godleski JJ, & Kobzik L (1992) Expression of macrophage inflammatory protein-2 and KC mRNA in pulmonary inflammation. *Am J Pathol.* 141(4):981-988.

332. Lin Q*, et al.* (2011) Impaired wound healing with defective expression of chemokines and recruitment of myeloid cells in TLR3-deficient mice. *J Immunol.* 186(6):3710-3717.

333. Kollmar O, Junker B, Rupertus K, Menger MD, & Schilling MK (2007) Studies on MIP-2 and CXCR2 expression in a mouse model of extrahepatic colorectal metastasis. *Eur J Surg Oncol.* 33(6):803-811.

334. Bolitho C, Hahn MA, Baxter RC, & Marsh DJ (2010) The chemokine CXCL1 induces proliferation in epithelial ovarian cancer cells by transactivation of the epidermal growth factor receptor. *Endocr Relat Cancer.* 17(4):929-940.

335. Liu J, *et al.* (2011) Tumor-associated macrophages recruit CCR6+ regulatory T cells and promote the development of colorectal cancer via enhancing CCL20 production in mice. *PLoS One.* 6(4):e19495.

336. Salazar-Gonzalez RM, *et al.* (2006) CCR6-mediated dendritic cell activation of pathogen-specific T cells in Peyer's patches. *Immunity* 24(5):623-632.

337. Di Sabatino A, Calarota SA, Vidali F, Macdonald TT, & Corazza GR (2011) Role of IL-15 in immune-mediated and infectious diseases. *Cytokine & growth factor reviews* 22(1):19-33.

338. Biet F, Locht C, & Kremer L (2002) Immunoregulatory functions of interleukin 18 and its role in defense against bacterial pathogens. *J Mol Med (Berl)* 80(3):147-162.

339. Pestka S, *et al.* (2004) Interleukin-10 and related cytokines and receptors. *Annual review of immunology* 22:929-979.

340. Braat H, *et al.* (2006) A phase I trial with transgenic bacteria expressing interleukin-10 in Crohn's disease. *Clinical gastroenterology and hepatology : the official clinical practice journal of the American Gastroenterological Association* 4(6):754-759.

341. Sokol CL, Barton GM, Farr AG, & Medzhitov R (2008) A mechanism for the initiation of allergen-induced T helper type 2 responses. *Nature immunology* 9(3):310-318.

342. Cruikshank WW, Kornfeld H, & Center DM (2000) Interleukin-16. *Journal of leukocyte biology* 67(6):757-766.

343. Czuprynski CJ & Brown JF (1987) Recombinant murine interleukin-1 alpha enhancement of nonspecific antibacterial resistance. *Infection and immunity* 55(9):2061-2065.

344. Miller LS, *et al.* (2007) Inflammasome-mediated production of IL-1beta is required for neutrophil recruitment against Staphylococcus aureus in vivo. *J Immunol* 179(10):6933-6942.

345. Gonzalez-Navajas JM, *et al.* (2010) Interleukin 1 receptor signaling regulates DUBA expression and facilitates Toll-like receptor 9-driven antiinflammatory cytokine production. *The Journal of experimental medicine* 207(13):2799-2807.

346. Lebeis SL, Powell KR, Merlin D, Sherman MA, & Kalman D (2009) Interleukin-1 receptor signaling protects mice from lethal intestinal damage caused by the attaching and effacing pathogen Citrobacter rodentium. *Infection and immunity* 77(2):604-614.

347. Pelloux H*, et al.* (1996) Influence of cytokines on Toxoplasma gondii growth in human astrocytoma-derived cells. *Parasitology research* 82(7):598-603.

348. Zhou L*, et al.* (2007) IL-6 programs T(H)-17 cell differentiation by promoting sequential engagement of the IL-21 and IL-23 pathways. *Nature immunology* 8(9):967-974.

349. Wei L, Laurence A, Elias KM, & O'Shea JJ (2007) IL-21 is produced by Th17 cells and drives IL-17 production in a STAT3-dependent manner. *The Journal of biological chemistry* 282(48):34605-34610.

350. Sonkodi S, Abraham G, & Mohacsi G (1990) Effects of nephrectomy on hypertension, renin activity and total renal function in patients with chronic renal artery occlusion. *Journal of human hypertension* 4(3):277-279.

351. Harrington LE*, et al.* (2005) Interleukin 17-producing CD4+ effector T cells develop via a lineage distinct from the T helper type 1 and 2 lineages. *Nature immunology* 6(11):1123-1132.

352. Alexander WS*, et al.* (1999) SOCS1 is a critical inhibitor of interferon gamma signaling and prevents the potentially fatal neonatal actions of this cytokine. *Cell* 98(5):597-608.

353. Zimmermann S, Murray PJ, Heeg K, & Dalpke AH (2006) Induction of suppressor of cytokine signaling-1 by Toxoplasma gondii contributes to immune evasion in macrophages by blocking IFN-gamma signaling. *J Immunol.* 176(3):1840-1847.

354. Alexander WS*, et al.* (1999) Suppressors of cytokine signaling (SOCS): negative regulators of signal transduction. *Journal of leukocyte biology* 66(4):588-592.

355. Chen Z*, et al.* (2006) Selective regulatory function of Socs3 in the formation of IL-17-secreting T cells. *Proceedings of the National Academy of Sciences of the United States of America* 103(21):8137-8142.

356. Machado FS*, et al.* (2006) Anti-inflammatory actions of lipoxin A4 and aspirin-triggered lipoxin are SOCS-2 dependent. *Nat Med.* 12(3):330-334.

357. Sato K*, et al.* (2012) Osteopontin is critical to determine symptom severity of influenza through the regulation of NK cell population. *Biochemical and biophysical research communications* 417(1):274-279.

358. Ashkar S*, et al.* (2000) Eta-1 (osteopontin): an early component of type-1 (cell-mediated) immunity. *Science* 287(5454):860-864.

359. Galli SJ, Tsai M, Gordon JR, Geissler EN, & Wershil BK (1992) Analyzing mast cell development and function using mice carrying mutations at W/c-kit or Sl/MGF (SCF) loci. . *Ann N Y Acad Sci.* 664:69-88.

360. Reber L, Da Silva CA, & Frossard N (2006) Stem cell factor and its receptor c-Kit as targets for inflammatory diseases. *Eur J Pharmacol.* 533(1-3):327-340.

361. Dzitko K*, et al.* (2012) Inhibitory effect of prolactin on Toxoplasma proliferation in peripheral blood mononuclear cells from patients with hyperprolactinemia. *Parasite Immunol.* 34(6):302-311.

362. Filipin Mdel V*, et al.* (2011) Prolactin: does it exert an up-modulation of the immune response in Trypanosoma cruzi-infected rats? *Vet Parasitol.* 181(2-4):139-145.

363. Frare EO*, et al.* (2010) Growth hormones therapy in immune response against Trypanosoma cruzi. *Res Vet Sci.* 88(2):273-278.

364. Stolen CM*, et al.* (2005) Absence of the Endothelial Oxidase AOC3 Leads to Abnormal Leukocyte Traffic In Vivo. *Immunity.* 22(1):105-115.

365. Jalkanen S & Salmi M (2001) Cell surface monoamine oxidases: enzymes in search of a function. *EMBO J.* 20(15):3893-3901.

366. Stone JR & Yang S (2006) Hydrogen peroxide: a signaling messenger. . *Antioxid Redox Signal.* 8(3-4):243-270.

367. de Fougerolles AR, Stacker SA, Schwarting R, & Springer TA (1991) Characterization of ICAM-2 and evidence for a third counter-receptor for LFA-1. *J Exp Med.* 174(1):253-267.

368. de Beer MC*, et al.* (1995) Characterization of constitutive human serum amyloid A protein (SAA4) as an apolipoprotein. *J Lipid Res.* 36(3):526-534.

369. Badolato R*, et al.* (1994) Serum amyloid A is a chemoattractant: induction of migration, adhesion, and tissue infiltration of monocytes and polymorphonuclear leukocytes. *J Exp Med.* 180(1):203-209.

370. Jijon HB, Madsen KL, Walker JW, Allard B, & Jobin C (2005) Serum amyloid A activates NF-kappaB and proinflammatory gene expression in human and murine intestinal epithelial cells. *Eur J Immunol.* 35(3):718-726.

371. Migita K*, et al.* (1998) Serum amyloid A protein induces production of matrix metalloproteinases by human synovial fibroblasts. *Lab Invest.* 78(5):535-539.

372. Medina C & Radomski MW (2006) Role of matrix metalloproteinases in intestinal inflammation. *The Journal of pharmacology and experimental therapeutics* 318(3):933-938.

373. Mott JD & Werb Z (2004) Regulation of matrix biology by matrix metalloproteinases. *Current opinion in cell biology* 16(5):558-564.

374. Elkington P*, et al.* (2011) MMP-1 drives immunopathology in human tuberculosis and transgenic mice. *The Journal of clinical investigation* 121(5):1827-1833.

375. Cauwe B & Opdenakker G (2010) Intracellular substrate cleavage: a novel dimension in the biochemistry, biology and pathology of matrix metalloproteinases. *Critical reviews in biochemistry and molecular biology* 45(5):351-423.

376. Ayabe T, *et al.* (2002) Activation of Paneth cell alpha-defensins in mouse small intestine. *The Journal of biological chemistry* 277(7):5219-5228.

377. Wilson CL, *et al.* (1999) Regulation of intestinal alpha-defensin activation by the metalloproteinase matrilysin in innate host defense. *Science* 286(5437):113-117.

378. Li CK, *et al.* (2004) Impaired immunity to intestinal bacterial infection in stromelysin-1 (matrix metalloproteinase-3)-deficient mice. *J Immunol* 173(8):5171-5179.

379. Butcher BA, *et al.* (2005) p47 GTPases regulate Toxoplasma gondii survival in activated macrophages. *Infect Immun.* 73(6):3278-3286.

380. Taylor GA, Feng CG, & Sher A (2004) p47 GTPases: regulators of immunity to intracellular pathogens. *Nat Rev Immunol.* 4(2):100-109.

381. Santiago HC, *et al.* (2005) Mice deficient in LRG-47 display enhanced susceptibility to Trypanosoma cruzi infection associated with defective hemopoiesis and intracellular control of parasite growth. *J Immunol.* 175(12):8165-8172.

382. Collazo CM, *et al.* (2001) Inactivation of LRG-47 and IRG-47 reveals a family of interferon gamma-inducible genes with essential, pathogen-specific roles in resistance to infection. *J Exp Med.* 194(2):181-188.

383. MacMicking JD, Taylor GA, & McKinney JD (2003) Immune control of tuberculosis by IFN-gamma-inducible LRG-47. *Science.* 302(5645):654-659.

384. Taylor GA, *et al.* (2000) Pathogen-specific loss of host resistance in mice lacking the IFN-gamma-inducible gene IGTP. *Proc Natl Acad Sci U S A.* 97(2):751-755.

385. de Souza AP, *et al.* (2003) Absence of interferon-gamma-inducible gene IGTP does not significantly alter the development of chagasic cardiomyopathy in mice infected with Trypanosoma cruzi (Brazil strain). *J Parasitol.* 89(6):1237-1239.

386. Liesenfeld O, *et al.* (2011) The IFN-γ-inducible GTPase, Irga6, protects mice against Toxoplasma gondii but not against Plasmodium berghei and some other intracellular pathogens. *PLoS One.* 6(6):e20568.

387. Kim BH, *et al.* (2011) A family of IFN-gamma-inducible 65-kD GTPases protects against bacterial infection. *Science* 332(6030):717-721.

388. Boehm U, *et al.* (1998) Two families of GTPases dominate the complex cellular response to IFN-gamma. *J Immunol* 161(12):6715-6723.

389. Selleck EM, *et al.* (2013) Guanylate-binding protein 1 (Gbp1) contributes to cell-autonomous immunity against Toxoplasma gondii. *PLoS pathogens* 9(4):e1003320.

390. Yamamoto M, *et al.* (2012) A cluster of interferon-gamma-inducible p65 GTPases plays a critical role in host defense against Toxoplasma gondii. *Immunity* 37(2):302-313.

391. Riedl SJ & Salvesen GS (2007) The apoptosome: signalling platform of cell death. *Nature reviews. Molecular cell biology* 8(5):405-413.

392. Atkinson EA*, et al.* (1998) Cytotoxic T lymphocyte-assisted suicide. Caspase 3 activation is primarily the result of the direct action of granzyme B. *The Journal of biological chemistry* 273(33):21261-21266.

393. Heussler VT, Kuenzi P, & Rottenberg S (2001) Inhibition of apoptosis by intracellular protozoan parasites. *International journal for parasitology* 31(11):1166-1176.

394. Varfolomeev E & Vucic D (2008) (Un)expected roles of c-IAPs in apoptotic and NFkappaB signaling pathways. *Cell Cycle* 7(11):1511-1521.

395. Marsters SA*, et al.* (1996) Apo-3, a new member of the tumor necrosis factor receptor family, contains a death domain and activates apoptosis and NF-kappa B. *Curr Biol.* 6(12):1669-1676.

396. Huard B, Gaulard P, Faure F, Hercend T, & Triebel F (1994) Cellular expression and tissue distribution of the human LAG-3-encoded protein, an MHC class II ligand. . *Immunogenetics.* 39(3):213-217.

397. Huard B, Prigent P, Tournier M, Bruniquel D, & Triebel F (1995) CD4/major histocompatibility complex class II interaction analyzed with CD4- and lymphocyte activation gene-3 (LAG-3)-Ig fusion proteins. *Eur J Immunol.* 25(9):2718-2721.

398. Butler NS*, et al.* (2011) Therapeutic blockade of PD-L1 and LAG-3 rapidly clears established blood-stage Plasmodium infection. *Nat Immunol.* 13(2):188-195.

399. Rössig L*, et al.* (2002) Angiotensin II-induced upregulation of MAP kinase phosphatase-3 mRNA levels mediates endothelial cell apoptosis. *Basic Res Cardiol.* 97(1):1-8.

400. Evdokiou A & Cowled PA (1998) Growth-regulatory activity of the growth arrest-specific gene, GAS1, in NIH3T3 fibroblasts. *Exp Cell Res.* 240(2):359-367.

401. Zamorano A, Lamas M, Vergara P, Naranjo JR, & Segovia J (2003) Transcriptionally mediated gene targeting of gas1 to glioma cells elicits growth arrest and apoptosis. *J Neurosci Res.* 71(2):256-263.

402. Sjöström M*, et al.* (2007) SIK1 is part of a cell sodium-sensing network that regulates active sodium transport through a calcium-dependent process. *Proc Natl Acad Sci U S A.* 104(43):16922-16927.

403. Cheng H*, et al.* (2009) SIK1 couples LKB1 to p53-dependent anoikis and suppresses metastasis. *Sci Signal.* 2(80):ra35.

404. Varfolomeev E*, et al.* (2012) Characterization of ML-IAP protein stability and physiological role in vivo. *The Biochemical journal* 447(3):427-436.

405. Graumann K, Hippe D, Gross U, & Luder CG (2009) Mammalian apoptotic signalling pathways: multiple targets of protozoan parasites to activate or deactivate host cell death. *Microbes and infection / Institut Pasteur* 11(13):1079-1087.

406. Boatright KM*, et al.* (2003) A unified model for apical caspase activation. *Molecular cell* 11(2):529-541.

407. Hashimoto M, Nakajima-Shimada J, & Aoki T (2005) Trypanosoma cruzi posttranscriptionally up-regulates and exploits cellular FLIP for inhibition of death-inducing signal. *Molecular biology of the cell* 16(8):3521-3528.

408. Kuenzi P, Schneider P, & Dobbelaere DA (2003) Theileria parva-transformed T cells show enhanced resistance to Fas/Fas ligand-induced apoptosis. *J Immunol* 171(3):1224-1231.

409. Abud HE, Watson N, & Heath JK (2005) Growth of intestinal epithelium in organ culture is dependent on EGF signalling. *Experimental cell research* 303(2):252-262.

410. Cottle DL*, et al.* (2009) SLIMMER (FHL1B/KyoT3) interacts with the proapoptotic protein Siva-1 (CD27BP) and delays skeletal myoblast apoptosis. *The Journal of biological chemistry* 284(39):26964-26977.

411. Culjkovic B*, et al.* (2008) The eIF4E RNA regulon promotes the Akt signaling pathway. *J Cell Biol.* 181(1):51-63.

412. Kreuger J, Spillmann D, Li JP, & Lindahl U (2006) Interactions between heparan sulfate and proteins: the concept of specificity. *J Cell Biol.* 174(3):323-327.

413. Reijmers RM*, et al.* (2010) Targeting EXT1 reveals a crucial role for heparan sulfate in the growth of multiple myeloma. *Blood.* 115(3):601-604.

414. Ohkawa Y*, et al.* (2011) Wisp2/CCN5 up-regulated in the central nervous system of GM3-only mice facilitates neurite formation in Neuro2a cells via integrin-Akt signaling. *Biochem Biophys Res Commun.* 411(3):483-489.

415. Banerjee S*, et al.* (2003) WISP-2 gene in human breast cancer: estrogen and progesterone inducible expression and regulation of tumor cell proliferation. *Neoplasia.* 5(1):63-73.

416. Zhao C*, et al.* (2001) Charcot-Marie-Tooth disease type 2A caused by mutation in a microtubule motor KIF1Bbeta. *Cell.* 105(5):587-597.

417. Michaeli A*, et al.* (2008) Serum amyloid A enhances plasminogen activation: implication for a role in colon cancer. *Biochem Biophys Res Commun.* 368(2):368-373.

418. Ghosh AK, Coppens I, Gårdsvoll H, Ploug M, & Jacobs-Lorena M (2011) Plasmodium ookinetes coopt mammalian plasminogen to invade the mosquito midgut. *Proc Natl Acad Sci U S A.* 108(41):17153-17158.

419. Ferguson DA, *et al.* (2005) Selective identification of secreted and transmembrane breast cancer markers using Escherichia coli ampicillin secretion trap. *Cancer Res.* 65(18):8209-8217.

420. Fischer H, Stenling R, Rubio C, & Lindblom A (2001) Colorectal carcinogenesis is associated with stromal expression of COL11A1 and COL5A2. *Carcinogenesis.* 22(6):875-878.

421. Kubota K, *et al.* (1999) Ca(2+)-independent cell-adhesion activity of claudins, a family of integral membrane proteins localized at tight junctions. *Curr Biol.* 9(18):1035-1038.

422. Evans MJ, *et al.* (2007) Claudin-1 is a hepatitis C virus co-receptor required for a late step in entry. *Nature.* 446(7137):801-805.

423. Liu S, *et al.* (2009) Tight junction proteins claudin-1 and occludin control hepatitis C virus entry and are downregulated during infection to prevent superinfection. *J Virol.* 83(4):2011-2014.

424. Fabry B, Klemm AH, Kienle S, Schäffer TE, & Goldmann WH (2011) Focal adhesion kinase stabilizes the cytoskeleton. *Biophys J* 101(9):2131-2138.

425. Schlaepfer DD, Mitra SK, & Ilic D (2004) Control of motile and invasive cell phenotypes by focal adhesion kinase. *Biochimica et biophysica acta* 1692(2-3):77-102.

426. Owen KA, Abshire MY, Tilghman RW, Casanova JE, & Bouton AH (2011) FAK regulates intestinal epithelial cell survival and proliferation during mucosal wound healing. *PLoS One.* 6(8):e23123.

427. Ussar S, *et al.* (2008) Loss of Kindlin-1 causes skin atrophy and lethal neonatal intestinal epithelial dysfunction. *PLoS Genet.* 4(12):e1000289.

428. Zhu W, Chan EK, Li J, Hemmerich P, & Tan EM (2001) Transcription activating property of autoantigen SG2NA and modulating effect of WD-40 repeats. *Exp Cell Res.* 269(2):312-321.

429. Xu B, *et al.* (2000) WNK1, a novel mammalian serine/threonine protein kinase lacking the catalytic lysine in subdomain II. *J Biol Chem.* 275(22):16795-16801.

430. Tu SW, Bugde A, Luby-Phelps K, & Cobb MH (2011) WNK1 is required for mitosis and abscission. *Proc Natl Acad Sci U S A.* 108(4):1385-1390.

431. Sun X, Gao L, Yu RK, & Zeng G (2006) Down-regulation of WNK1 protein kinase in neural progenitor cells suppresses cell proliferation and migration. *J Neurochem.* 99(4):1114-1121.

432. Guibal FC, *et al.* (2002) ASB-2 Inhibits Growth and Promotes Commitment in Myeloid Leukemia Cells. *J Biol Chem.* 277(1):218-224.

433. McDaneld TG, Hannon K, & Moody DE (2006) Ankyrin repeat and SOCS box protein 15 regulates protein synthesis in skeletal muscle. *Am J Physiol Regul Integr Comp Physiol.* 290(6):1672-1682.

434. Wang HQ, Xu ML, Ma J, Zhang Y, & Xie CH (2012) Frizzled-8 as a putative therapeutic target in human lung cancer. *Biochem Biophys Res Commun.* 417(1):62-66.

435. Asiedu M, Wu D, Matsumura F, & Wei Q (2009) Centrosome/spindle pole-asssociated protein regulates cytokinesis via promoting the recruitment of MyoGEF to the central spindle. *Mol Biol Cell.* 20(5):1428-1441.

436. Blangy A*, et al.* (1995) Phosphorylation by p34cdc2 regulates spindle association of human Eg5, a kinesin-related motor essential for bipolar spindle formation in vivo. *Cell.* 83(7):1159-1169.

437. Patzke S*, et al.* (2005) Identification of a novel centrosome/microtubule-associated coiled-coil protein involved in cell-cycle progression and spindle organization. *Oncogene.* 24(7):1159-1173.

438. Yu C*, et al.* (2011) Myoferlin gene silencing decreases Tie-2 expression in vitro and angiogenesis in vivo. *Vascul Pharmacol.* 55(1-3):26-33.

439. Draheim KM*, et al.* (2010) ARRDC3 suppresses breast cancer progression by negatively regulating integrin β4. *Oncogene.* 29(36):5032-5047.

440. Villalonga P, Guasch RM, Riento K, & Ridley AJ (2004) RhoE Inhibits Cell Cycle Progression and Ras-Induced Transformation. *Mol Cell Biol.* 24(18):7829-7840.

441. Arnaud-Dabernat S, Yadav D, & Sarvetnick N (2008) FGFR3 contributes to intestinal crypt cell growth arrest. *J Cell Physiol.* 216(1):261-268.

442. Han SH*, et al.* (2003) VDUP1 upregulated by TGF-beta1 and 1,25-dihydorxyvitamin D3 inhibits tumor cell growth by blocking cell-cycle progression. *Oncogene.* 22(26):4035-4046.

443. Kwon HJ*, et al.* (2012) Vitamin D3 upregulated protein 1 deficiency promotes N-methyl-N-nitrosourea and Helicobacter pylori-induced gastric carcinogenesis in mice. *Gut.* 61(1):53-63.

444. Nishiyama A*, et al.* (1999) Identification of thioredoxin-binding protein-2/vitamin D (3) up-regulated protein 1 as a negative regulator of thioredoxin function and expression. *J Biol Chem.* 274(31):21645-21650.

445. Bourne HR, Sanders DA, & McCormick F (1991) The GTPase superfamily: conserved structure and molecular mechanism. *Nature.* 349(6305):117-127.

446. Finlin BS*, et al.* (2001) RERG Is a Novel ras-related, Estrogen-regulated and Growth-inhibitory Gene in Breast Cancer. *J Biol Chem.* 276(45):42259-42267.

447. Albig AR & Schiemann WP (2005) Identification and characterization of regulator of G protein signaling 4 (RGS4) as a novel inhibitor of tubulogenesis: RGS4 inhibits mitogen-activated protein kinases and vascular endothelial growth factor signaling. *Mol Biol Cell.* 16(2):609-625.

448. Koul D*, et al.* (1998) p202 prevents apoptosis in murine AKR-2B fibroblasts. *Biochemical and biophysical research communications* 247(2):379-382.

449. Min W, Ghosh S, & Lengyel P (1996) The interferon-inducible p202 protein as a modulator of transcription: inhibition of NF-kappa B, c-Fos, and c-Jun activities. *Molecular and cellular biology* 16(1):359-368.

450. Blaustein MP & Lederer WJ (1999) Sodium/calcium exchange: its physiological implications. *Physiol Rev.* 79(3):763-854.

451. Philipson KD & Nicoll DA (2000) Sodium-calcium exchange: a molecular perspective. *Annu Rev Physiol.* 62:111-133.

452. Husain M*, et al.* (1997) Regulation of vascular smooth muscle cell proliferation by plasma membrane Ca(2+)-ATPase. *Am J Physiol.* 272(6 Pt 1):C1947-1959.

453. Béguin P*, et al.* (2001) Regulation of Ca2+ channel expression at the cell surface by the small G-protein kir/Gem. *Nature.* 411(6838):701-706.

454. Chien AJ*, et al.* (1995) Roles of a membrane-localized beta subunit in the formation and targeting of functional L-type Ca2+ channels. *J Biol Chem.* 270(50):30036-30044.

455. Hou J, Renigunta A, Yang J, & Waldegger S (2010) Claudin-4 forms paracellular chloride channel in the kidney and requires claudin-8 for tight junction localization. *Proceedings of the National Academy of Sciences of the United States of America* 107(42):18010-18015.

456. Preston P*, et al.* (2010) Disruption of the K+ channel beta-subunit KCNE3 reveals an important role in intestinal and tracheal Cl- transport. *The Journal of biological chemistry* 285(10):7165-7175.

457. Bear CE*, et al.* (1992) Purification and functional reconstitution of the cystic fibrosis transmembrane conductance regulator (CFTR). *Cell* 68(4):809-818.

458. Raychowdhury R, Niles JL, McCluskey RT, & Smith JA (1989) Autoimmune target in Heymann nephritis is a glycoprotein with homology to the LDL receptor. *Science.* 244(4909):1163-1165.

459. Christensen EI & Birn H (2002) Megalin and cubilin: multifunctional endocytic receptors. *Nat Rev Mol Cell Biol.* 3(4):256-266.

460. Fernández E*, et al.* (2002) rBAT-b(0,+)AT heterodimer is the main apical reabsorption system for cystine in the kidney. *Am J Physiol Renal Physiol.* 283(3):540-548.

461. Pompella A, Visvikis A, Paolicchi A, De Tata V, & Casini AF (2003) The changing faces of glutathione, a cellular protagonist. *Biochem Pharmacol.* 66(8):1499-1503.

462. Bröer A*, et al.* (2011) Impaired nutrient signaling and body weight control in a Na+ neutral amino acid cotransporter (Slc6a19)-deficient mouse. *J Biol Chem.* 286(30):26638-26651.

463. Mackness MI, Arrol S, Abbott C, & Durrington PN (1993) Protection of low-density lipoprotein against oxidative modification by high-density lipoprotein associated paraoxonase. *Atherosclerosis.* 104(1-2):129-135.

464. Bhasin KK*, et al.* (2006) Trypanosoma congolense: paraoxonase 1 prolongs survival of infected mice. *Exp Parasitol.* 114(3):240-245.

465. Glomset JA (1968) The plasma lecithin:cholesterol acyltransferase reaction. *J Lipid Res.* 9(2):155-167.

466. Taylor JM, Borthwick F, Bartholomew C, & Graham A (2010) Overexpression of steroidogenic acute regulatory protein increases macrophage cholesterol efflux to apolipoprotein AI. *Cardiovasc Res.* 86(3):526-534.

467. Coppens I, Sinai AP, & Joiner KA (2000) Toxoplasma gondii exploits host low-density lipoprotein receptor-mediated endocytosis for cholesterol acquisition. *J Cell Biol.* 149(1):167-180.

468. Sonda S*, et al.* (2001) Cholesterol esterification by host and parasite is essential for optimal proliferation of Toxoplasma gondii. *J Biol Chem.* 276(37):34434-34440.

469. Nishikawa Y*, et al.* (2005) Host cell lipids control cholesteryl ester synthesis and storage in intracellular Toxoplasma. *Cell Microbiol.* 7(6):849-867.

470. Karlsson EA, Wang S, Shi Q, Coleman RA, & Beck MA (2009) Glycerol-3-phosphate acyltransferase 1 is essential for the immune response to infection with coxsackievirus B3 in mice. *The Journal of nutrition* 139(4):779-783.

471. Hammond LE*, et al.* (2007) Increased oxidative stress is associated with balanced increases in hepatocyte apoptosis and proliferation in glycerol-3-phosphate acyltransferase-1 deficient mice. *Experimental and molecular pathology* 82(2):210-219.

472. Hunt MC, Siponen MI, & Alexson SE (2012) The emerging role of acyl-CoA thioesterases and acyltransferases in regulating peroxisomal lipid metabolism. *Biochim Biophys Acta.* Epub ahead of print.

473. Takahashi S, Kawarabayasi Y, Nakai T, Sakai J, & Yamamoto T (1992) Rabbit very low density lipoprotein receptor: a low density lipoprotein receptor-like protein with distinct ligand specificity. *Proc Natl Acad Sci U S A.* 89(19):9252-9256.

474. Angel P & Karin M (1991) The role of Jun, Fos and the AP-1 complex in cell-proliferation and transformation. *Biochim Biophys Acta.* 1072(2-3):129-157.

475. McGivern DR & Lemon SM (2011) Virus-specific mechanisms of carcinogenesis in hepatitis C virus associated liver cancer. *Oncogene.* 30(17):1969-1983.

476. Maruyama K, Sano G, Ray N, Takada Y, & Matsuo K (2007) c-Fos-deficient mice are susceptible to Salmonella enterica serovar Typhimurium infection. *Infect Immun.* 75(3):1520-1523.

477. Contreras I*, et al.* (2010) Leishmania-induced inactivation of the macrophage transcription factor AP-1 is mediated by the parasite metalloprotease GP63. *PLoS Pathog.* 6(10):e1001148.

478. Foletta VC, Segal DH, & Cohen DR (1998) Transcriptional regulation in the immune system: all roads lead to AP-1. *J Leukoc Biol.* 63(2):139-152.

479. Kang SM*, et al.* (2011) c-Fos regulates hepatitis C virus propagation. *FEBS Lett.* 585(20):3236-3244.

480. Herrmann KM & Weaver LM (1999) The Shikimate Pathway. *Annual review of plant physiology and plant molecular biology* 50:473-503.

481. Roberts CW*, et al.* (2002) The shikimate pathway and its branches in apicomplexan parasites. *The Journal of infectious diseases* 185 Suppl 1:S25-36.

482. Roberts F*, et al.* (1998) Evidence for the shikimate pathway in apicomplexan parasites. *Nature* 393(6687):801-805.

483. McConkey GA (1999) Targeting the shikimate pathway in the malaria parasite Plasmodium falciparum. *Antimicrobial agents and chemotherapy* 43(1):175-177.

484. Bender DA (1983) Biochemistry of tryptophan in health and disease. *Molecular aspects of medicine* 6(2):101-197.

485. Peters JC (1991) Tryptophan nutrition and metabolism: an overview. *Adv Exp Med Biol.* 294:345-358.

486. Young SN, St-Arnaud-McKenzie D, & Sourkes TL (1978) Importance of tryptophan pyrrolase and aromatic amino acid decarboxylase in the catabolism of tryptophan. *Biochem Pharmacol.* 27(5):763-767.

487. Babcock TA & Carlin JM (2000) Transcriptional activation of indoleamine dioxygenase by interleukin 1 and tumor necrosis factor alpha in interferon-treated epithelial cells. *Cytokine.* 12(6):588-594.

488. Robinson CM, Shirey KA, & Carlin JM (2003) Synergistic transcriptional activation of indoleamine dioxygenase by IFN-gamma and tumor necrosis factor-alpha. *J Interferon Cytokine Res.* 23(8):413-421.

489. Jung ID*, et al.* (2007) Differential regulation of indoleamine 2,3-dioxygenase by lipopolysaccharide and interferon gamma in murine bone marrow derived dendritic cells. *FEBS Lett.* 581(7):1449-1456.

490. Grohmann U*, et al.* (2002) CTLA-4-Ig regulates tryptophan catabolism in vivo. *Nat Immunol.* 3(11):1097-1101.

491. Shi YF, Mahrt JL, & Mogil RJ (1989) Kinetics of murine delayed-type hypersensitivity response to Eimeria falciformis (Apicomplexa: Eimeriidae). *Infect Immun.* 57(1):146-151.

492. Rose ME, Hesketh, P., Wakelin, D. (1992) Immune control of murine coccidiosis: CD4+ and CD8+ T lymphocytes contribute differentially in resistance to primary and secondary infections. *Parasitology.* 105:349-354.

493. Rose ME, Wakelin, D., Hesketh, P. (1991) Interferon-gamma-mediated effects upon immunity to coccidial infections in the mouse. *Parasite Immunol.* 13(1):63-74.

494. Ball HJ*, et al.* (2007) Characterization of an indoleamine 2,3-dioxygenase-like protein found in humans and mice. *Gene.* 396(1):203-213.

495. Rossi F, Schwarcz R, & Rizzi M (2008) Curiosity to kill the KAT (kynurenine aminotransferase): structural insights into brain kynurenic acid synthesis. *Current opinion in structural biology* 18(6):748-755.

496. Okuno E, Nakamura M, & Schwarcz R (1991) Two kynurenine aminotransferases in human brain. *Brain research* 542(2):307-312.

497. Guidetti P, Okuno E, & Schwarcz R (1997) Characterization of rat brain kynurenine aminotransferases I and II. *Journal of neuroscience research* 50(3):457-465.

498. Taylor MW & Feng GS (1991) Relationship between interferon-gamma, indoleamine 2,3-dioxygenase, and tryptophan catabolism. *FASEB J.* 5(11):2516-2522.

499. Bodaghi B*, et al.* (1999) Role of IFN-gamma-induced indoleamine 2,3 dioxygenase and inducible nitric oxide synthase in the replication of human cytomegalovirus in retinal pigment epithelial cells. *J Immunol.* 162(2):957-964.

500. MacKenzie CR*, et al.* (1999) Growth inhibition of multiresistant enterococci by interferon-gamma-activated human uro-epithelial cells. *J Med Microbiol.* 48(10):935-941.

501. Thomas SM*, et al.* (1993) IFN-gamma-mediated antimicrobial response. Indoleamine 2,3-dioxygenase-deficient mutant host cells no longer inhibit intracellular Chlamydia spp. or Toxoplasma growth. *J Immunol.* 150(12):5529-5534.

502. Divanovic S*, et al.* (2011) Opposing Biological Functions of Tryptophan Catabolizing Enzymes During Intracellular Infection. *J Infect Dis.* 205(1):152-161.

503. Knubel CP*, et al.* (2010) Indoleamine 2,3-dioxigenase (IDO) is critical for host resistance against Trypanosoma cruzi. *FASEB J.* 24(8):2689-2701.

504. Bozza S*, et al.* (2005) A crucial role for tryptophan catabolism at the host/Candida albicans interface. *J Immunol.* 174(5):2910-2918.

505. Bell LV, Else, K.J. (2011) Regulation of colonic epithelial cell turnover by IDO contributes to the innate susceptibility of SCID mice to Trichuris muris infection. *Parasite Immunol.* 33(4):244-249.

506. Harrington L*, et al.* (2008) Deficiency of indoleamine 2,3-dioxygenase enhances commensal-induced antibody responses and protects against Citrobacter rodentium-induced colitis. *Infect Immun.* 76(7):3045-3053.

507. Hoshi M*, et al.* (2010) The absence of IDO upregulates type I IFN production, resulting in suppression of viral replication in the retrovirus-infected mouse. *J Immunol.* 185(6):3305-3312.

508. Adams O*, et al.* (2004) Role of indoleamine-2,3-dioxygenase in alpha/beta and gamma interferon-mediated antiviral effects against herpes simplex virus infections. *J Virol.* 78(5):2632-2636.

509. Mellor AL, Keskin DB, Johnson T, Chandler P, & Munn DH (2002) Cells expressing indoleamine 2,3-dioxygenase inhibit T cell responses. *J Immunol.* 168(8):3771-3776.

510. Hwu P*, et al.* (2000) Indoleamine 2,3-dioxygenase production by human dendritic cells results in the inhibition of T cell proliferation. *J Immunol.* 164(7):3596-3599.

511. Fallarino F*, et al.* (2002) T cell apoptosis by tryptophan catabolism. *Cell Death Differ.* 9(10):1069-1077.

512. Frumento G*, et al.* (2002) Tryptophan-derived catabolites are responsible for inhibition of T and natural killer cell proliferation induced by indoleamine 2,3-dioxygenase. *J Exp Med.* 196(4):459-468.

513. Terness P*, et al.* (2002) Inhibition of allogeneic T cell proliferation by indoleamine 2,3-dioxygenase-expressing dendritic cells: mediation of suppression by tryptophan metabolites. *J Exp Med.* 196(4):447-457.

514. Okuda S, Nishiyama N, Saito H, & Katsuki H (1996) Hydrogen peroxide-mediated neuronal cell death induced by an endogenous neurotoxin, 3-hydroxykynurenine. *Proc Natl Acad Sci U S A.* 93(22):12553-12558.

515. Wei H*, et al.* (2000) Neuronal apoptosis induced by pharmacological concentrations of 3-hydroxykynurenine: characterization and protection by dantrolene and Bcl-2 overexpression. *J Neurochem.* 75(1):81-90.

516. Bender DA, Njagi EN, & Danielian PS (1990) Tryptophan metabolism in vitamin B6-deficient mice. *Br J Nutr.* 63(1):27-36.

517. Li J, Beerntsen BT, & James AA (1999) Oxidation of 3-hydroxykynurenine to produce xanthommatin for eye pigmentation: a major branch pathway of tryptophan catabolism during pupal development in the yellow fever mosquito, Aedes aegypti. *Insect biochemistry and molecular biology* 29(4):329-338.

518. Chiou SJ*, et al.* (1998) Purification of toxic compounds from larvae of the gray fleshfly: the identification of paralysins. *Biochemical and biophysical research communications* 246(2):457-462.

519. Paglino A, Lombardo F, Arca B, Rizzi M, & Rossi F (2008) Purification and biochemical characterization of a recombinant Anopheles gambiae tryptophan 2,3-

dioxygenase expressed in Escherichia coli. *Insect biochemistry and molecular biology* 38(9):871-876.

520. Carter R & Nijhout MM (1977) Control of gamete formation (exflagellation) in malaria parasites. *Science.* 195(4276):407-409.

521. Nijhout MM (1979) Plasmodium gallinaceum: exflagellation stimulated by a mosquito factor. *Exp Parasitol.* 48(1):75-80.

522. Billker O, Shaw MK, Margos G, & Sinden RE (1997) The roles of temperature, pH and mosquito factors as triggers of male and female gametogenesis of Plasmodium berghei in vitro. *Parasitology.* 115(1):1-7.

523. Billker O, Miller AJ, & Sinden RE (2000) Determination of mosquito bloodmeal pH in situ by ion-selective microelectrode measurement: implications for the regulation of malarial gametogenesis. *Parasitology* 120 (Pt 6):547-551.

524. Billker O*, et al.* (2004) Calcium and a calcium-dependent protein kinase regulate gamete formation and mosquito transmission in a malaria parasite. *Cell* 117(4):503-514.

525. Raabe AC, Wengelnik K, Billker O, & Vial HJ (2011) Multiple roles for Plasmodium berghei phosphoinositide-specific phospholipase C in regulating gametocyte activation and differentiation. *Cellular microbiology* 13(7):955-966.

526. Bens M*, et al.* (1996) Transimmortalized mouse intestinal cells (m-ICc12) that maintain a crypt phenotype. *The American journal of physiology* 270(6 Pt 1):C1666-1674.

527. Lee SL, Tourtellotte LC, Wesselschmidt RL, & Milbrandt J (1995) Growth and differentiation proceeds normally in cells deficient in the immediate early gene NGFI-A. *The Journal of biological chemistry* 270(17):9971-9977.

528. Tourtellotte WG & Milbrandt J (1998) Sensory ataxia and muscle spindle agenesis in mice lacking the transcription factor Egr3. *Nature genetics* 20(1):87-91.

529. Tourtellotte WG, Nagarajan R, Auyeung A, Mueller C, & Milbrandt J (1999) Infertility associated with incomplete spermatogenic arrest and oligozoospermia in Egr4-deficient mice. *Development* 126(22):5061-5071.

530. Tourtellotte WG, Nagarajan R, Bartke A, & Milbrandt J (2000) Functional compensation by Egr4 in Egr1-dependent luteinizing hormone regulation and Leydig cell steroidogenesis. *Molecular and cellular biology* 20(14):5261-5268.

531. Droin NM, Pinkoski MJ, Dejardin E, & Green DR (2003) Egr family members regulate nonlymphoid expression of Fas ligand, TRAIL, and tumor necrosis factor during immune responses. *Molecular and cellular biology* 23(21):7638-7647.

532. Johnson RS, Spiegelman BM, & Papaioannou V (1992) Pleiotropic effects of a null mutation in the c-fos proto-oncogene. *Cell* 71(4):577-586.

533. Wu JJ & Bennett AM (2005) Essential role for mitogen-activated protein (MAP) kinase phosphatase-1 in stress-responsive MAP kinase and cell survival signaling. *The Journal of biological chemistry* 280(16):16461-16466.

534. Jeffrey KL, *et al.* (2006) Positive regulation of immune cell function and inflammatory responses by phosphatase PAC-1. *Nature immunology* 7(3):274-283.

535. Maillet M, *et al.* (2008) DUSP6 (MKP3) null mice show enhanced ERK1/2 phosphorylation at baseline and increased myocyte proliferation in the heart affecting disease susceptibility. *The Journal of biological chemistry* 283(45):31246-31255.

536. Jeffrey KL, Camps M, Rommel C, & Mackay CR (2007) Targeting dual-specificity phosphatases: manipulating MAP kinase signalling and immune responses. *Nature reviews. Drug discovery* 6(5):391-403.

537. Panzer U, *et al.* (2007) Chemokine receptor CXCR3 mediates T cell recruitment and tissue injury in nephrotoxic nephritis in mice. *Journal of the American Society of Nephrology : JASN* 18(7):2071-2084.

538. Kuziel WA, *et al.* (2003) CCR5 deficiency is not protective in the early stages of atherogenesis in apoE knockout mice. *Atherosclerosis* 167(1):25-32.

539. Liu Z, *et al.* (2011) Chemokine CXCL11 links microbial stimuli to intestinal inflammation. *Clinical and experimental immunology* 164(3):396-406.

540. Liaw L, *et al.* (1998) Altered wound healing in mice lacking a functional osteopontin gene (spp1). *The Journal of clinical investigation* 101(7):1468-1478.

541. Koller FL, *et al.* (2012) Lack of MMP10 exacerbates experimental colitis and promotes development of inflammation-associated colonic dysplasia. *Laboratory investigation; a journal of technical methods and pathology* 92(12):1749-1759.

542. Little CB, *et al.* (2009) Matrix metalloproteinase 13-deficient mice are resistant to osteoarthritic cartilage erosion but not chondrocyte hypertrophy or osteophyte development. *Arthritis and rheumatism* 60(12):3723-3733.

543. Yu P, *et al.* (2004) Biochemical and phenotypic abnormalities in kynurenine aminotransferase II-deficient mice. *Molecular and cellular biology* 24(16):6919-6930.

544. Truscott RJ & Elderfield AJ (1995) Relationship between serum tryptophan and tryptophan metabolite levels after tryptophan ingestion in normal subjects and age-related cataract patients. *Clin Sci (Lond)* 89(6):591-599.

545. Williams SA, Monti JA, Boots LR, & Cornwell PE (1984) Quantitation of xanthurenic acid in rabbit serum using high performance liquid chromatography. *The American journal of clinical nutrition* 40(1):159-167.

546. Billker O, *et al.* (1998) Identification of xanthurenic acid as the putative inducer of malaria development in the mosquito. *Nature* 392(6673):289-292.

547. Dessens JT, Sinden RE, & Claudianos C (2004) LCCL proteins of apicomplexan parasites. *Trends in parasitology* 20(3):102-108.

List of Publications and Presentations

Publications written in the course of this work

Schmid M, Lehmann MJ, Lucius R, Gupta N "Apicomplexan parasite, *Eimeria falciformis*, co-opts host tryptophan catabolism for life cycle progression in mouse" Journal of Biological Biochemistry 287 (24): 20197-207 (2012)

Schmid M, Heitlinger E, Spork S, Mollenkopf HJ, Lucius R, Gupta N "*Eimeria falciformis* infection of the mouse caecum identifies opposing roles of IFNγ-regulated host pathways for the parasite development" Mucosal Immunology, *accepted*

Other work

Schmid M, Sollwedel A, Thuere C, Zenclussen ML, Wafula PO, Mueller DN, Gratze P, Wociechowsky C, Volk HD, Zenclussen AC "Murine pre-eclampsia induced by unspecific activation of the immune system correlates with alterations in the eNOS and AT1 receptor expression in the kidneys and placenta" Placenta 28 (7): 688-700 (2007)

Presentations

Oral presentation at the European Congress on Protistology (ECOP), 2011, Berlin, Germany "The Apicomplexan Parasite *Eimeria falciformis* Co-Opts Host Indoleamine 2, 3-Dioxygenase for its Life Cycle Progression"

Poster presentation at the Gordon Research Conference "Biology of Host-Parasite Interaction", 2010, Newport, Rhode Island, USA "*Ex vivo* Transcriptomics of *Eimeria*-infected Mouse Caecum Cells Identifies Indoleamine 2,3-Dioxygenase and Major Immune Determinants of the *in vivo* Parasite Development"

Oral presentation at the PhD Symposium "Life under (Re)construction, 2010, Berlin, Germany "Investigation of the Local Host Response to an Obligate Intracellular Parasite *Eimeria falciformis* by *ex vivo* Transcriptomics"

Poster presentation at the Joint Meeting of the German Societies of Parasitology and Protozoology (DGP), 2010, Düsseldorf, Germany "Deduction of the Mouse Enteric Immune Response to an obligate Intracellular Pathogen *Eimeria falciformis* by *ex vivo* Transcriptomics"

Berlin, den 7.01.2014 Manuela Schmid

Selbständigkeitserklärung

Hiermit erkläre ich an Eides statt, die vorliegende Dissertation selbständig angefertigt und keine anderen als die angegeben Quellen und Hilfsmittel benutzt zu haben.

Berlin, den 7.01.2014 Manuela Schmid